MAGYAR ÁLLAMI
EÖTVÖS LORÁND
GEOFIZIKAI INTÉZET

GEOFIZIKAI
KÖZLEMÉNYEK

ВЕНГЕРСКИЙ
ГЕОФИЗИЧЕСКИЙ
ИНСТИТУТ
ИМ Л. ЭТВЕША

ГЕОФИЗИЧЕСКИЙ
БЮЛЛЕТЕНЬ

BUDAPEST

EÖTVÖS LORÁND
GEOPHYSICAL INSTITUTE
OF HUNGARY

GEOPHYSICAL TRANSACTIONS

CONTENTS

VOL. 36. NO. 3–4. SEPT. 1991 (ISSN 0016–7177)

TARTALOMJEGYZÉK

СОДЕРЖАНИЕ

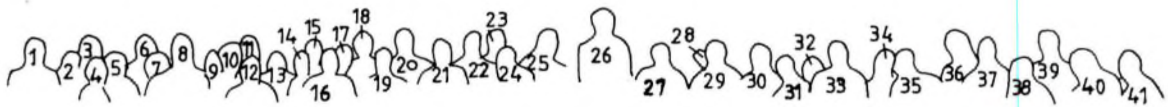

1 - Arthur W. Green 2 - Mioara Alexandrescu 3 - Ivan Hrvoic 4 - Leone Gilbert 5 - Magdolna Váczy 6 - László Hegymegi 7 - Daniel Gilbert 8 - Ole Rasmussen 9 - Michel Menvielle 10 - Yu. A. Burtsev 11 - V. O. Papitashvili 12 - N. Y. Bagdasarova 13 - Kari Pajunpaa 14 - Johannes Kultima 15 - Christian Sucksdorff 16 - Richard Coles 17 - Etelka Aczél 18 - Lasse Häkkinen 19 - Francois-Xavier Lalanne 20 - Günter Schulz 21 - Zoltán Szabó 22 - Viktor Wesztergom 23 - Róbert Stomfai 24 - Ákos Wallner 25 - József Verő 26 - Jan Raagaard Petersen 27 - Zoltán Vörös 28 - Gábor Kövesi 29 - Volker Auster Sr. 30 - Hans-Ulrich Auster Jr 31 - Alexander Lichopoj 32 - János Kiss 33 - Tomasz Ernst 34 - B. A. Belov 35 - Jacques Bitterly 36 - A. I. Ivanitza 37 - Jean Rasson 38 - Jozef Podsklan 39 - Jansen van Beek 40 - Andre Bourtenbourg 41 - Jean-Michel Cantin

OPENING ADDRESS OF THE WORKSHOP BY TAMÁS BODOKY *

Ladies and gentlemen,

I have the honour to welcome you on behalf of the Association of Hungarian Geophysicists to the third Workshop on magnetic observatory instruments in Tihany.

Since the Meeting of the International Union of Geodesy and Geophysics held in Hamburg in 1983, where the concept of the Workshop originated, a great deal has done in the field of observatory instrumentation and on that of the handling and processing of observatory data. Digital data acquisiton systems have replaced the classical methods and the satellite based INTERMAGNET program has brought a dramatic change in magnetic observatory work, opening new perspectives for the applications of geomagnetic data. But I would think that all of this is much better known by you and will certainly be discussed in detail later. Instead therefore would you allow me to say some words about the place and the institute where we are now.

Tihany has to thank its birth to late tertiary volcanism. Tihany's volcanic hills have been inhabited, as archeological evidence has shown us, since the stone age and, in spite of its apparent tranquility the peninsula has seen some rather restless times. After the peaceful Roman period the region was a transit station of moving peoples of the great migration. For example, Theodoric the Great, the Goth who conquered ancient Italy, was born here. Later, in the years when William the Conqueror crossed the Channel, one of the first Hungarian kings—Endre the First—founded an abbey on the eastern side, from which a chapel can be seen even today under the present church, with the grave of the king. The Latin text of the founding document contains the first written fragments of our language, it is therefore one of our national treasures.

In the thirteenth century a not entirely friendly visit of the Mongolians of Genghis Khan resulted in the abbey being converted into a fortress. That stronghold of Tihany played an important role later when, for one and a

* President of the Association of Hungarian Geophysicists

half centuries Lake Balaton was the border of the Moslem Empire of the Turks. I believe that that was the only period in Hungarian history when we had a navy and fought naval battles. In bygone ages the ice of the Lake also served as a scence of famous duels.

However, not only has the winter ice of the Lake played its part in the history of our people but in that of geophysics as well. At the end of the last century baron Loránd Eötvös, a professor of Budapest University, who was concerned with the shape and rotation of the Earth, invented the torsion balance as a means of measuring the horizontal gradient and the curvature of the gravitational field. He recognized the possibility of utilizing his invention in a practical way too. During the winter of 1902-1903 he performed torsion balance measurements on a grid on the frozen Lake Balaton thus eliminating problems relating to terrain corrections.

The exploratory torsion balance measurements in the years 1915-1916 seeking hydrocarbons on what were to become the oil fields of Egbell are now of science-historical significance: from this time on we can speak of applied geophysics in hydrocarbon explorations.

After the death of Eötvös in 1919, his colleagues founded the Eötvös Loránd Geophysical Institute. This Institute has wide ranging activities both in the pure and the applied areas of geophysics. The Geomagnetic Observatory in Tihany was founded in 1954 as a part of the Institute's Earth Physics Department.

Now, after the very succesful Ottawa and Nurmijärvi Workshops, you are here in that Observatory, and I do hope that your third Workshop will result in very wortwhile achievements too. I offer my best wishes for your successful endeavour and wish you a very pleasant time.

INTRODUCTION

Alpár Körmendi and László Hegymegi *

1. Tihany Geophysical Observatory and the Workshop

Readers are kindly invited to recall Ron Niblett's words in the 'Foreword' to the Proceedings of the International Workshop on Magnetic Observatory Instruments, Ottawa, 1986: 'the concept of a working workshop... originated in discussion between W. F. Stuart and C. G. Sucksdorff, at the time of the IUGG meeting in Hamburg in 1983'. An international scientific team worked on the preparation of the first workshop for three years. Another three years passed between the first Workshop and the second one (Nurmijärvi, 1989). The question might arise as to why should the third workshop be organized so close to the previous one? The two main reasons are as follows:

The development of the instrumentation and data processing technique has been accelerated between the two workshops and we could expect that the workshop in Nurmijrävi would give it a push again. But this development involves the risk of separating the geomagnetic observatories into two groups: the first one equipped with fluxgate sensors, Overhauser proton magnetometers, highly intelligent data acquisition systems; the other one having less sensitive (but maybe more stable in the long term) quartz variometers and old fashioned loggers .

These phenomena might well cause difficulties in data exchange and difficulties because of the difference in the quality of the collected data. Bill Stuart underlined in both of his papers in the Proceedings of the Ottawa Workshop that 'the observing community is very isolated'. His statement is true in an increased degree for scientists living in the former COMECON countries (mainly as a consequence of COCOM), or in the Third World because of a shortage of money. Those who participated in the Nurmijärvi Workshop agreed that a new workshop should be arranged within three

* Eötvös Loránd Geophysical Institute of Hungary P.O.B. 35, H-1440 Budapest, Hungary

years and it ought to give a greater chance of testing those instruments missing from Ottawa and Nurmijärvi. Tihany Observatory (especially with regard to the Eötvös L. Geophysical Institute as its background) seemed to have all the facilities needed for the next workshop.

Spring 1991 seemed to be an optimal choice for a Workshop but it had to be rejected in consequence of the General Assembly of IAGA in Vienna in the same year. The year 1992 was considered as being too late. The risk in organizing the Workshop in 1990 was that manufacturers who produced new instruments for the Nurmijärvi Workshop would not come. The hesitation was ended by Bill Green's telex upholding the Workshop in the autumn of 1990. Events proved him right. (Has he some kind of seer's power ?). The dramatic political changes and the collapse of the economy in the central-east European countries could have stopped the Workshop in 1991 or 1992.

The Workshop would not have been possible without
— the financial support of the IAGA Division V
— the technical and financial support of ELGI
— the hard work done by the staff of Tihany Observatory and the Earth Physics Department and a group from the Seismic Department
— the local organizing committee
— Daniel Gilbert's selfless work.

We are immensely grateful to the institutions and individuals for their support.

The venue of this Workshop was Tihany Geophysical Observatory which belongs to the Eötvös Loránd Geophysical Institute located on the Tihany Peninsula at Lake Balaton. The main buildings are in the village and the recording/measuring houses are on hill called Cser hegy among vineyards. The distance between the main buildings and the measuring site is about 1 m.

The Tihany Peninsula was built by Pliocene volcanic and postvolcanic activity: the pleasant cone-shaped hills are monuments of one-time geysers. Because of geysiric limestone the main part of the Peninsula is free from magnetic anomalies. The spatial fluctuation of the magnetic field in the grounds of the observatory is less than +/-20nT.

Tihany Geophysical Observatory is the fourth geomagnetic observatory in Hungary. The first observatory was founded in Buda in 1871 and closed in 1889 when the increased industrial activity of the town hindered its proper functioning. The second one was established in Ogyalla (in German and in English papers this is written as O Gyalla) in 1893 in the framework of the Royal Hungarian Meteorological Institute. Today it belongs to the Slovakian Academy of Sciences under the name Hurbanovo Geophysical Observatory. The third Hungarian geomagnetic observatory worked as a provisional substitute of the lost Ogyalla Observatory in Budakeszi near Budapest between 1949 and 1955.

In the early fifties Tihany Peninsula became a protected area and it was expected to have an isolated nature far from the railway and industrial disturbances. It was in view of this that the Hungarian geophysical observatory was constructed in Tihany. Unfortunately as tourism increased it demanded more and more electric power so bigger transformer stations were built in the area after 1970. Later a UHF transmitting station and the ever widening use of CB radios started to disturb the proton magnetometers. The electrification of the railway on the southern shore of Lake Balaton was carried out in 1989.

Main events in the functioning of the observatory:

1953 The observatory was founded by the Eötvös Loránd Geophysical Institute. It was designed by Professor Gy. Barta.

1954 Magnetic recording was started. Instrumentation: La Cour variometers for *D, H, Z* components, Matting-Wiesenberg magnetic theodolite, Askania earth-inductor, QHMs and BMZs for base-line evaluation.

1956 The first yearbook was published.

1960 Rapid-run recording for pulsation was started.

1965 Earth tide registration started with an Askania gravity meter. Experiments with a home-made protonmagnetometer.

1972 Periodical whistler recording and analysis. Rapid-run magnetic recording was finished.

1979 Change in instrumentation: new Bobrov type quartz variometers and ELSEC vector protonmagnetometer. Digital recording of one-minute data on punched tape.

1982 Starting with DIMARS automatic data acquisition system. Moving of earth tide recording to a cave in the Buda-hills.

1986 New instrument for absolute measurements: EDA DIM-100

1987 Study of disturbing effects caused by electric railway started.

For a certain period we had the feeling that we would have to close the observatory because of the disturbing effect of the electrified railway but we subsequently learnt that the method used by the Hungarian Railways minimizes disturbances. We therefore proceeded with the development of our recording system and decided to join INTERMAGNET.

The idea of a worldwide geomagnetic observatory system with observatories linked to each other by satellite was presented by A.W. Green at the Workshop on Magnetic Observatory Instruments in Ottawa (1986). Initially the plan was to realize an equatorial observatory network organized and operated by the U. S. Geological Survey. The idea was later discussed in Chambon La Foret, and in Vancouver in August 1987 and it was proposed that automatic digital observatories be used with satellite communications everywhere and that a worldwide observatory network be elaborated which can produce real-time magnetic data for the users.

To organize the network the INTERMAGNET program was formed; Intermagnet is headed by an Executive Council (R. L. Coles, A.W. Green, J. L. LeMouel and W. F. Stuart). The program determined the compatible equipment which is technically of a high level but not necessarily expensive. This equipment should measure the components of the magnetic field every second and should then calculate the means for five seconds and one minute. The data for twelve minutes would then be transmitted via satellite. The participating countries and institutions with their own instruments would be able to join the network and transmit their data to the regional geomagnetic information nodes (GIN) by a weather satellite network or by other means, using standard INTERMAGNET formats. The GIN would be able to exchange data and data products globally as rapidly as appropriate, and would maintain data files for all contributing observatories. It would be for the Executive Council to decide on the media and formats for the collected data and these data would be available for the scientific community.

The intention is to establish and maintain observatories in remote areas where local support is lacking and to encourage this activity in developing countries with the involvement and enhancement of local expertise.

With such a network we can hope to have global geomagnetic data and production of indices in close to real-time. These data are needed for monitoring current geomagnetic conditions and forecasting future conditions, as well as giving the possibility of investigating the physical processes of solar-terrestrial interactions and the Earth's deep interior.

The quality of these data is strongly depends on the instruments used in the network and it is therefore very important to measure the characteristics and performance of the instruments. This is one of the reasons for organizing workshops and carrying out measurement tests.

Although not all of our aims achieved and an INTERMAGNET station in operation could not be demonstrated, we believe that a lot of useful information was collected and exchanged during the workshop. We have tried to summarize the most important results of comparative recordings and to publish them together with papers presented or submitted by participants.

The Eötvös Loránd Geophysical Institute (ELGI) has given an invaluable aid in finishing the Workshop — it will be completed by publication of the proceedings — by offering to publish the proceedings as a Special Issue of the Geophysical Transactions of ELGI. We are extremely grateful to our colleagues for the final lay-out of this volume.

For various reasons a number of would-be participants could not attend the workshop, or instruments could not be presented; however their papers or the results of the tests of the instruments carried out in Tihany at another time were obviously of general interest to the participants so we included them in the proceedings.

2. Technical preparation

In the variation house of the observatory there are four pillars built for the La-Cour system. This allows eight up- to-date sensors to be placed. On the basis of preliminary reporting 14 sets of equipment could be expected. It was therefore planned to set up four to six further sets of equipment in the absolute house and to build temporary pillars for the vector proton magnetometers far from the other equipment. A stable pillar was built outside the house, for the absolute measurements. Three large caravans were placed in the garden of the observatory for the electronic units. Because of topographical differences we could not place them within 50 m of the variation house where the sensors were put (we did not want to get nearer because of the metal in the caravans).

An efficient survey was carried out in order to discover the magnetic bodies and to remove them. The disturbances originated primarily from electric cables (iron conducting/strengthening fibre, iron protective screening) and from iron pieces thrown away during construction. The location map of the absolute house and of the variation one is shown in *Fig.1.*

2.1. The workshop

Fewer participants and less equipment arrived than was expected on the basis of preliminary reports (at that time in the USA and in Canada the newspapers were pursuing a violent campaign against government offices who were said to be squandering the money of the taxpayers; consequently, the demonstration of the station INTERMAGNET did not take place). Finally 10 variation stations arrived. Among them the GEOMAG (IPG), which was awaited with great interest, arrived 6 days after the planned time. This upset the strict time schedule of the workshop: the variation house had to be opened in the middle of the heating period and the GEOMAG sensor had to be set up. A small camping caravan had to be placed near to the variation house, for the electronics of GEOMAG. These two interventions caused much more trouble than was expected and made the data processing much more difficult.

2.2. Location of the equipment

The location of the equipment is shown in *Fig.2.* Some of the sensors and electronic units (amplifiers, power supplies) were connected with short cables to the sensors. The electronic units were located in three places depending on the cable length:

a. in the same room as the sensors
b. in the loft of the variation house
c. in caravans.

Within the electronic units there was no thermometer so the temperature dependence of the electronic units could not be tested.

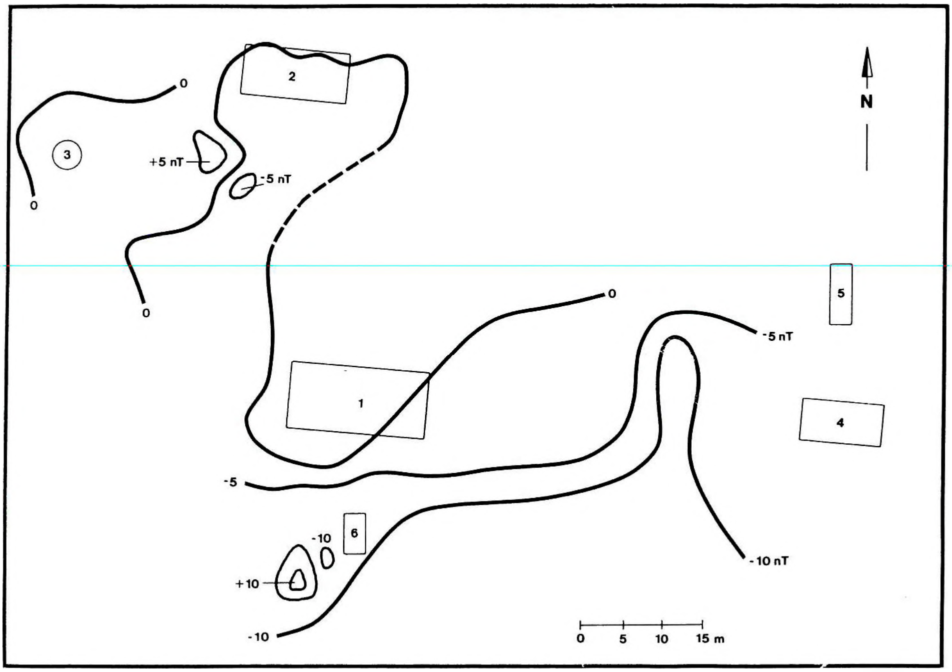

Fig. 1. Tihany Geophysical Observatory. Houses and isolines of the magnetic anomalies (nT)
1) Variation House 2) Absolute House 3) Rubidium Vector Magnetometer (RVM) 4) Palaeomagnetic Laboratory 5) Caravan for electronics 6) Small caravan for GEOMAG

1. ábra. Tihanyi Obszervatórium. Észlelőházak helye és a mágneses anomáliák
1) variációs ház 2) abszolút ház 3) rubídium vektor-magnetométer 4) paleomágneses mérőház 5) lakókocsi a regisztrálóműszerek számára 6) kis lakókocsi a GEOMAG számára

Рис. 1. Здания Тиханьской Геофизической обсефватории и изолинии магнитных аномалий (нт)
1) Dом вариаций 2) Dом абсолютный 3) Рубидиевый векторный магнитометр 4) Палеомагнитная лаборатория 5) Вагончик для записывающих приборов 6) Вагончик для GEOMAG

2.3. The data format

One of basic experiences of the Ottawa workshop was: if each participant applies different format, then the data processing needs much more work than the data acquisition. The prescribed format for the Nurmijärvi workshop worked very well so we wanted to use it. Unfortunately, only

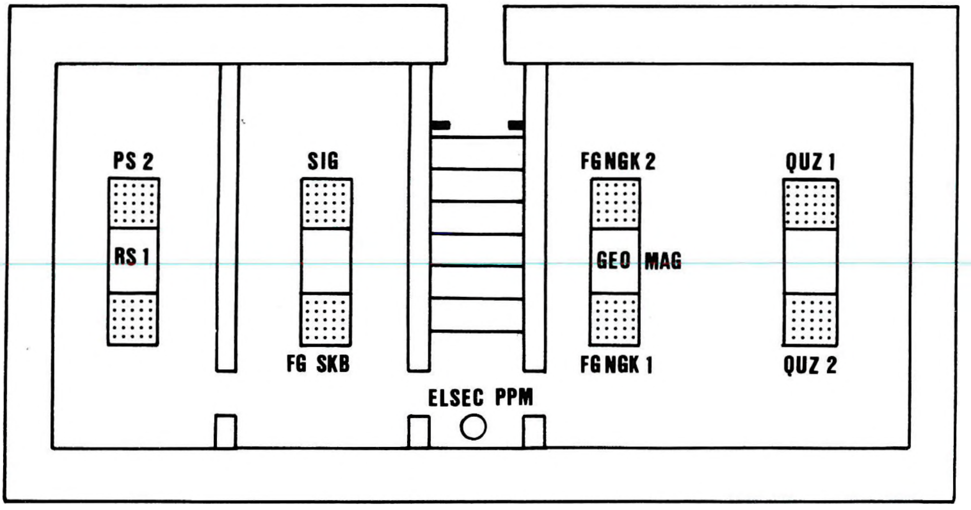

Fig. 2. Instruments in the Variation House

2. ábra. A műszerek elhelyezése a variációs házban

Рис. 2. Размещение приборов в Доме вариаций

two participants gave the data in this format so the processing work was very much increased.

2.4. Data processing

During the workshop six personal computers, printers and plotters were available for quick visual representation of data. FORTRAN and BASIC programs were written partly because of the great variety of data formats. Later, the high level scientific and technical programming language ASYST was used because of its many advantages.

2.5. Disturbances making the data processing difficult

The majority of data provided by the participants was very noisy; the data series had to be smoothed. It was very inconvenient that several pieces of equipment added clock signals of varying amplitude to the useful signals. The setting up of the GEOMAG equipment in the middle of the measuring period resulted in jumps of varying extent. Simultaneously a magnetic source (at that time unknown) caused a jump on the recording of the FGSKB instrument. After the workshop we managed to find this source by repeated checking of the variation house. That part of the variation house not used in normal operation had for ages been closed off by a plastic door. After demolishing the door we saw that within the door there was an iron rod of about 50 cm length and 10 mm diameter. It was turned from N-S to E-W direction on opening the door and back to N-S on closing it.

2.6. Test of equipments beyond the workshop

In 1989 and 1990, before the workshop several Soviet made magnetic variation stations and data loggers were tested in Tihany: this equipment consisted of CMVS-2, CMVS-6, CAIS manufactured by SKB, and the fluxgate magnetometer produced by the technicians of the Ukranian Academy of Sciences. The constructers had intended to participate in the workshop, but they did not manage to arrive. Originally we wanted to enclose the test results on the material of the workshop as two short appendices. During the data processing it would have become clear, however, that several phenomena can better be understood just on the basis of these measurements. This means that they relate more closely to the materials of the workshop so they are expounded among the data of the workshop.

3. Production and interpretation of difference curves

3.1. Choice of references

Visual comparison of field strength components registered by different items of equipment shows the rough deviations only. For quantitative comparison a standard or reference system is needed. The standard system in Tihany possesses orientation errors; this was indicated at the Nurmijärvi workshop. The origin of the errors is the quartz fibre since this does not coincide with the geometric (symmetric) axis of the sensor. Should we use common platforms this error cannot be eliminated, it can be corrected only by calculation. Efforts were made to determine the parameters of the sensors to such an extent that after correction our data could be used for reference purposes. During the workshop three events occurred the consequences of which were hardly reparable. The first was the setting up of the GEOMAG equipment, the second related to the iron pieces in the plastic door (they were mentioned earlier). The third event was a repair: the THY reference remained on a concrete pillar covered by glass plate. On 13th September it was removed by Soviet experts (in order to eliminate the occasional disturbances arising from the mechanical stresses of the glass). As it was mentioned only later, there was nothing that could be done. The baselines jumped, the sensitivities changed. From the beginning of the common recording the THY reference was practically of no use.

The reference necessary for comparison was produced artificially on the basis of recordings of several quartz variometers, using the data of absolute measurements, of the comparison with RVM and of nonlinear estimation of parameters referred to GSM (RVM was not included in the temperature test; at the same time, it possessed a very stable baseline: the average deviation was 4 " in *D* and 10 " in *I*).

3.2. How the data were obtained and their continuity

Disturbances originating from setting up the GEOMAG and on 16th September from turning the door containing magnetic material could not be corrected equally well for every piece of equipment.Therefore some of the data were omitted. Time series were assembled in such a way that the temperature monotonically increased *(Fig. 3)*. In the disturbed sections there was no heating nor was there cooling. Each data array contains 5580 data per component *(X, Y, Z, F, t)*. Digested data are stored in the special ASYST format and they can easily be transformed into ASCII files. Of course, the original recorded data were preserved too.

Recordings of two instruments (PS1 and QUZ1) were not continuous because of internal electronic errors; one further one (FGNGK2) had no *Z* component and on the records of FGNGK1 there were unexplainable jumps on 18th September. Recording from FGNGK1 was extremely noisy, presumably because of the noises collected by the long cable connected to the asymmetric output.

3.3. Smoothing; computation of the correction coefficients

Application of smoothing or procedures of least squares usually requires commands of 1-2 words in the ASYST programming language . Smoothing means optimum-filtration: the convolution of noisy data with the inverse Fourier transformation of the Blackman window.

Two methods were applied to determine the correction coefficients: a linear one using the reference and a nonlinear one using the *F* data

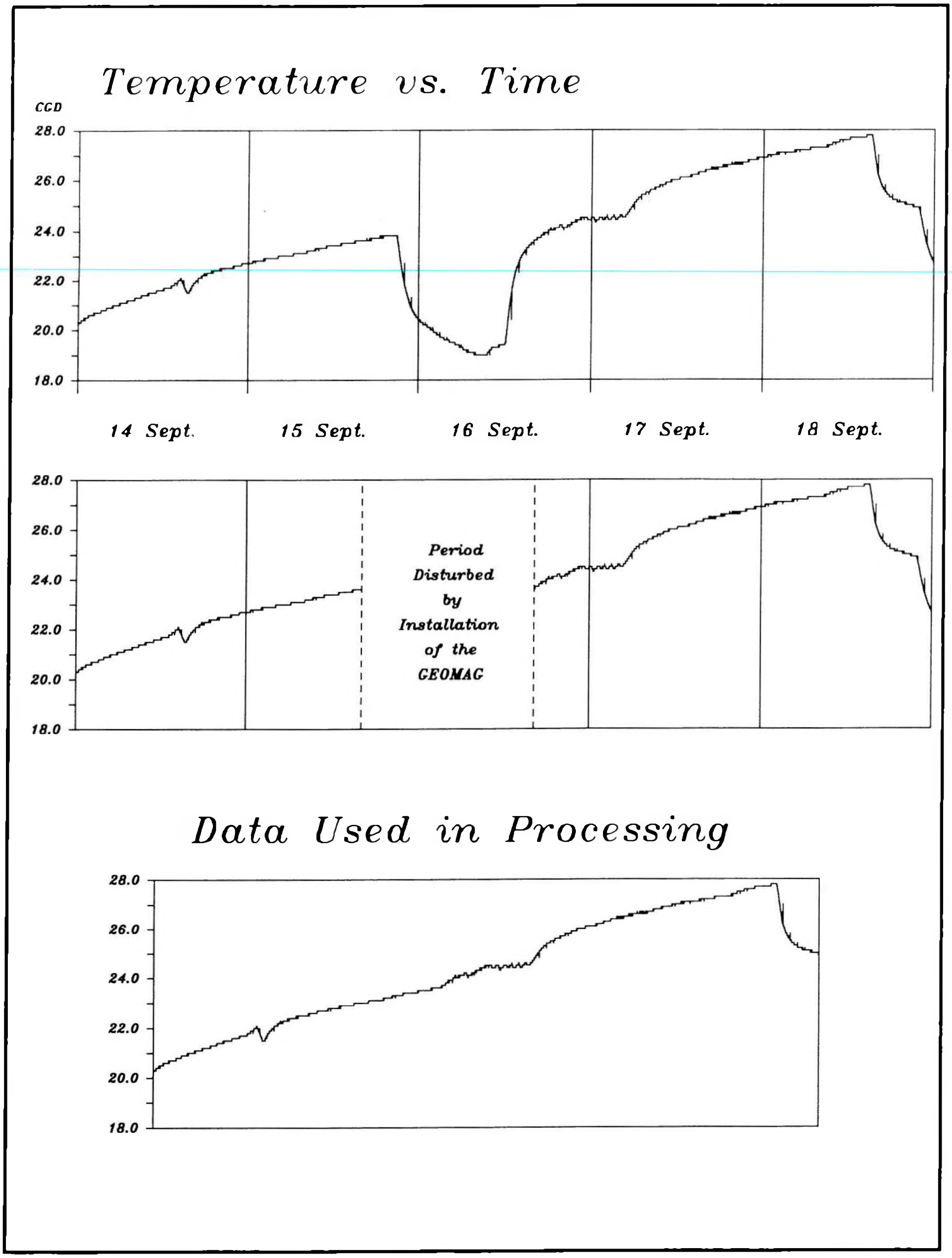

Fig. 3. Temperature change in the variation house during the Workshop

3. ábra. Hőmérsékletváltozás a variációs házban aWorkshop ideje alatt

Рис. 3. Изменение температуры в Доме вариаций во время рабочей встречи

(GSM-19). The two procedures use different input data and give slightly different results. For both methods the whole data array containing 5580 data in one minute steps was used.

Similarly to the procedure applied in Nurmijärvi a multilinear regression algorithm was applied to determine the sensitivity, orientation and temperature coefficient of the field components. In vector form:

$$\begin{bmatrix} X \\ Y \\ Z \end{bmatrix}_{corr} = \begin{bmatrix} C_{xx} & C_{xy} & C_{xz} & C_{xt} \\ C_{yx} & C_{yy} & C_{yz} & C_{yt} \\ C_{zx} & C_{zy} & C_{zz} & C_{zt} \end{bmatrix} \cdot \begin{bmatrix} X \\ Y \\ Z \\ Z \end{bmatrix}_{rec}$$

The computation of the C_{ij} coefficients can be carried out finding the minimum of the function

$$\sum_{k=1}^{5580} (C_{xx}X + C_{xy}Y + C_{xz}Z + C_{xt}t - X_{corr})^2$$

(and two formulae for Y and Z such as for X)

The baseline values were modified so that at 0 hour on 14th September the minute values should be the same. Later the baseline of the reference was subtracted in order to form the variations necessary for the calculation.

For nonlinear estimations of parameters the original variations were used, the baselines could considerably differ each from other. As a starting point, the following supposition was used: F measured by the proton precession magnetometer and F computed from the components should be the same. This supposition is usually not fulfilled, however the correction coefficients can be computed, assuming systematic errors. Unfortunately, the result of the computation is not unambiguous, it slightly depends on the chosen algorithm. For reasons not detailed here, the so called HILL algorithm was used (1).

The components given in vector form again:

$$\begin{bmatrix} X \\ Y \\ Z \end{bmatrix} = \begin{bmatrix} X_B \\ Y_B \\ Z_B \end{bmatrix} + \begin{bmatrix} b_{x0} \\ b_{y0} \\ b_{z0} \end{bmatrix} + \begin{bmatrix} b_{xx} & b_{xy} & b_{xz} \\ b_{yx} & b_{yy} & b_{yz} \\ b_{zx} & b_{zy} & b_{zz} \end{bmatrix} \cdot \begin{bmatrix} X \\ Y \\ Z \end{bmatrix}$$

where X_B, Y_B, Z_B are the baseline values.

The task is to find the minimum of the function.

$$\sum_{k=1}^{5580} (\sqrt{X^2 + Y^2 + Z^2} - F)^2$$

Two special cases:

a) IPG GEOMAG. According to verbal information from X. F. Lalane, the application possibility of the equipment on satellites was tested in August 1990. Returning from holiday he saw that equipment (the sensor?) had become seriously damaged during the test. At first he thought repair to be hopeless and cancelled the participation. Later he tried to repair the instrument and in Chambon la Foret it seemed to be successful. As a matter of interest he brought the equipment to Tihany, although late. Unfortunately, during transport further contact errors occurred and they could not be repaired in Tihany. The recording fractions carried out are unsuitable for comparison therefore they are not included in the volume.

b) RVM and RVM(M). For a detailed description of RVM operating on the ASMO principle see this volume, (farther back). Originally the instrument was designed to measure *F, D* and *I.* The results contained very strange systematic errors, especially in component *Z.* The *F* values measured by RVM were compared with the same values measured by GSM 19. The different of data series reflects a daily periodicity *(Fig.4.)* In our opinion this periodicity is connected with the changes of the network frequency (50 Hz nominal). Hungary produces and at the same time imports electric energy from the Soviet Union and from Austria and the 'tolerance limits' of these networks is different. The period time of the network may differ from 20 ms by -0.1 to +0.15 ms, due to the national load distribution. It can be seen well: the above changes coincide partly with the daily main work time (GMT 4 to 12 hour) and partly with the working day-holiday change: there are fewer disturbances on Saturday and Sunday than on Monday. In order to verify our idea, on a winter Monday the changes of reciprocal of the network frequency were measured for comparison. The shape of the curve is similar: there is a steep increase at the start of work, and after finishing the working day there is no monotonic decrease but a further increase according to the early nightfall (about 16 hour).

We have no hypotesis as to how the noise could get into the RVM. A startling resemblance of noises was observed during the test of the Ukranian

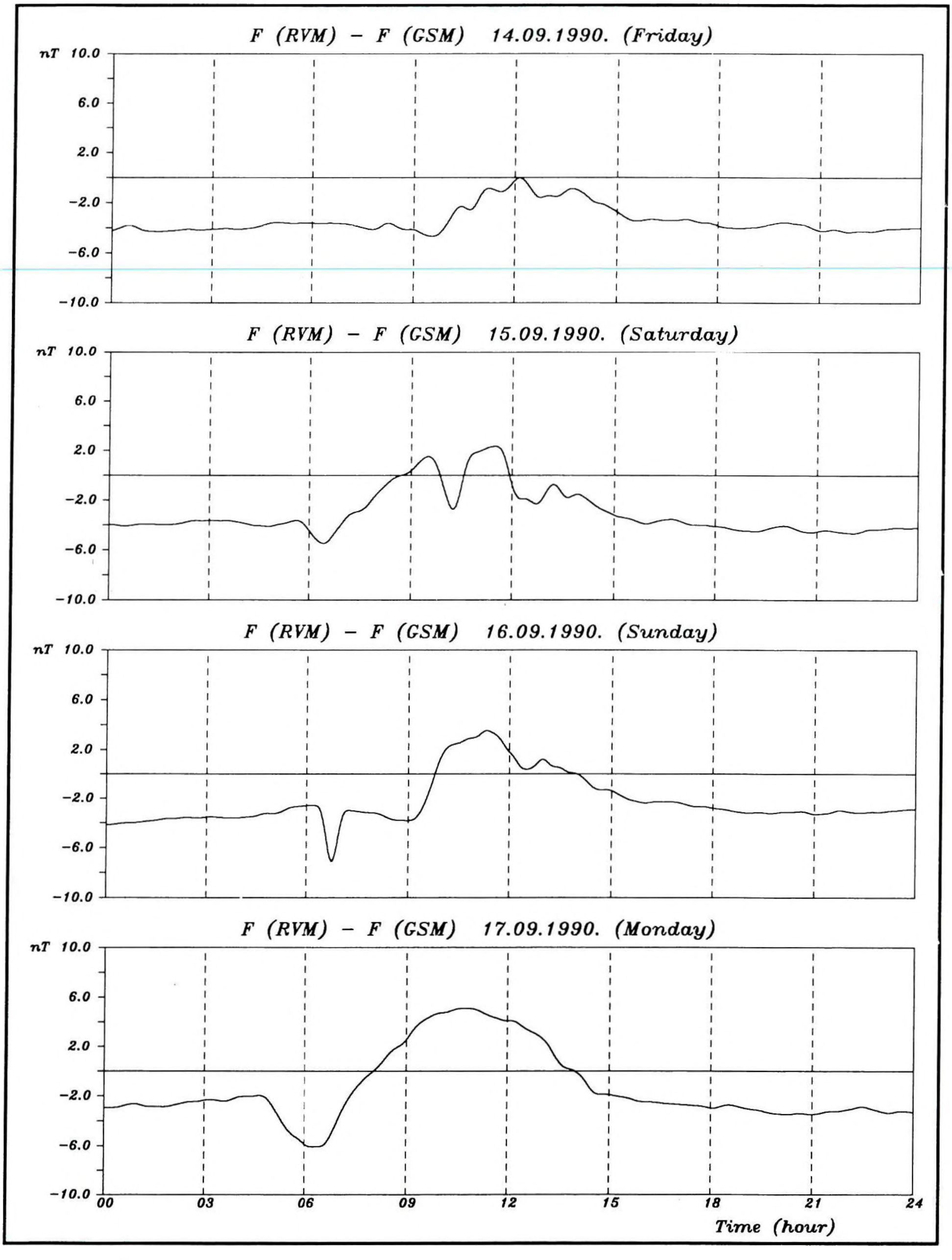

Fig. 4. Differences between the measured values by RVM and GSM

4.ábra. RVM és GSM műszerek adatai közti különbség

Рис. 4. Разница между показаниями приборов RVM и GSM fluxgate magnetometers (FGASU) in spite of the fact that both their working principle and the electronic realization strongly differ from the RVM.

The error of measuring the period time did not affect the angle measurements (I and D) in an unambiguously detectable way. Therefore an X, Y, Z data series was constructed where F was taken from the proton precession magnetometer GSM 19, I and D — from the RVM. This was called RVM(M): RVM-modified.

3.4. The temperature in the variation house

During the workshop (in September) the temperature in the underground rooms of the variation house was about 18 to 20 °C, and the outside temperature was about the same, therefore the rooms could not be cooled by ventilation. The starting temperature was 20 °C and the highest was 30°C. The difference of 10°C was reached in four days, so the daily change was small. Therefore the time series for the four days are illustrated together.

3.5. Description of Figures 5–33

The following parameters are illustrated for each piece of equipment and each component:

a. variation of component
b. variation of temperature
c. difference from the reference without correction
d. difference from the reference after correction
e. correction coefficients obtained by multilinear regression.

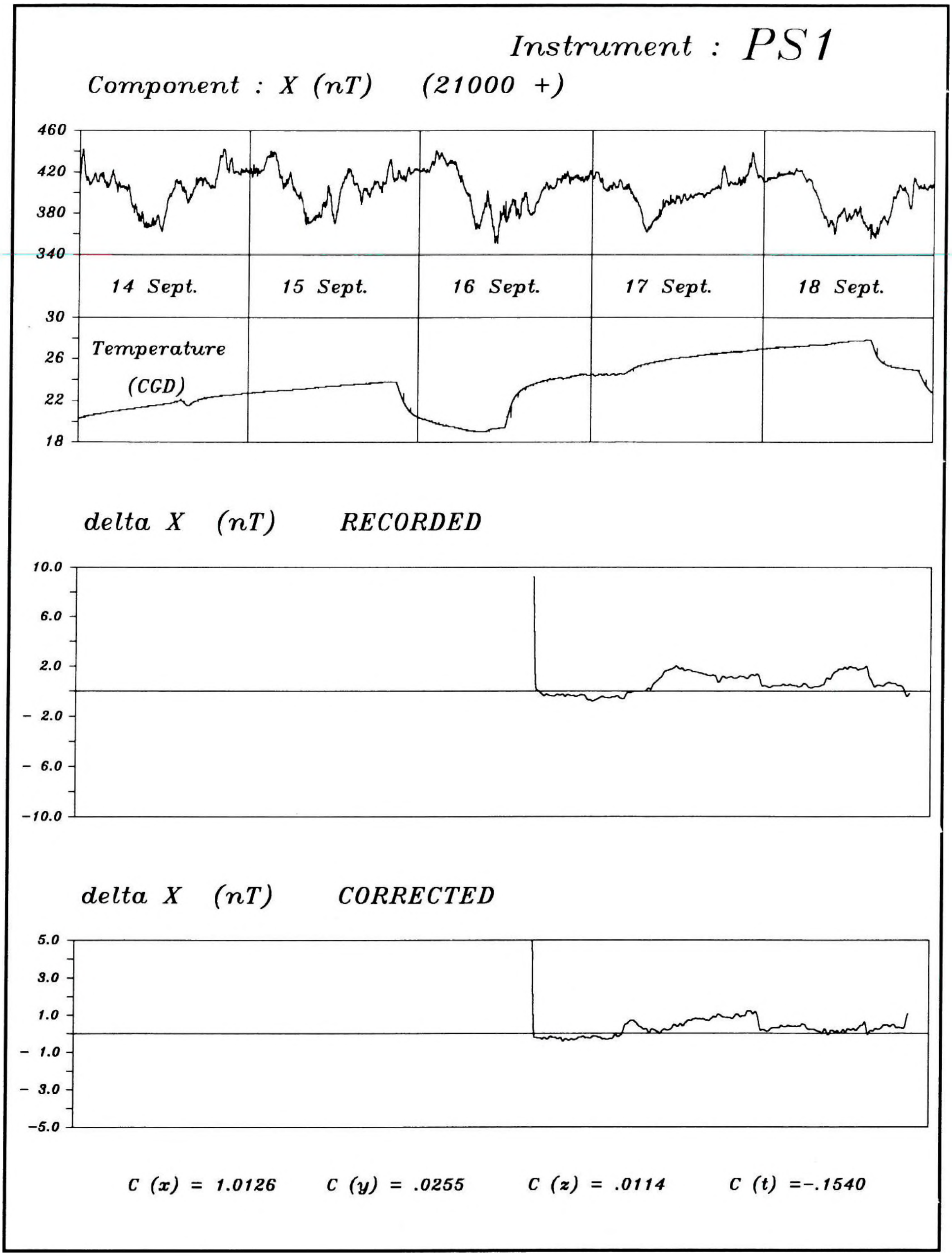

Instrument : PS1
Component : X (nT) (21000 +)
460
420
380
340
14 Sept.
15 Sept.
16 Sept.
17 Sept.
18 Sept.
30
26
22
18
Temperature
(CGD)
delta X (nT) RECORDED
10.0
6.0
2.0
− 2.0
− 6.0
−10.0
delta X (nT) CORRECTED
5.0
3.0
1.0
− 1.0
− 3.0
−5.0
C (x) = 1.0126
C (y) = .0255
C (z) = .0114
C (t) =−.1540

Fig.5.

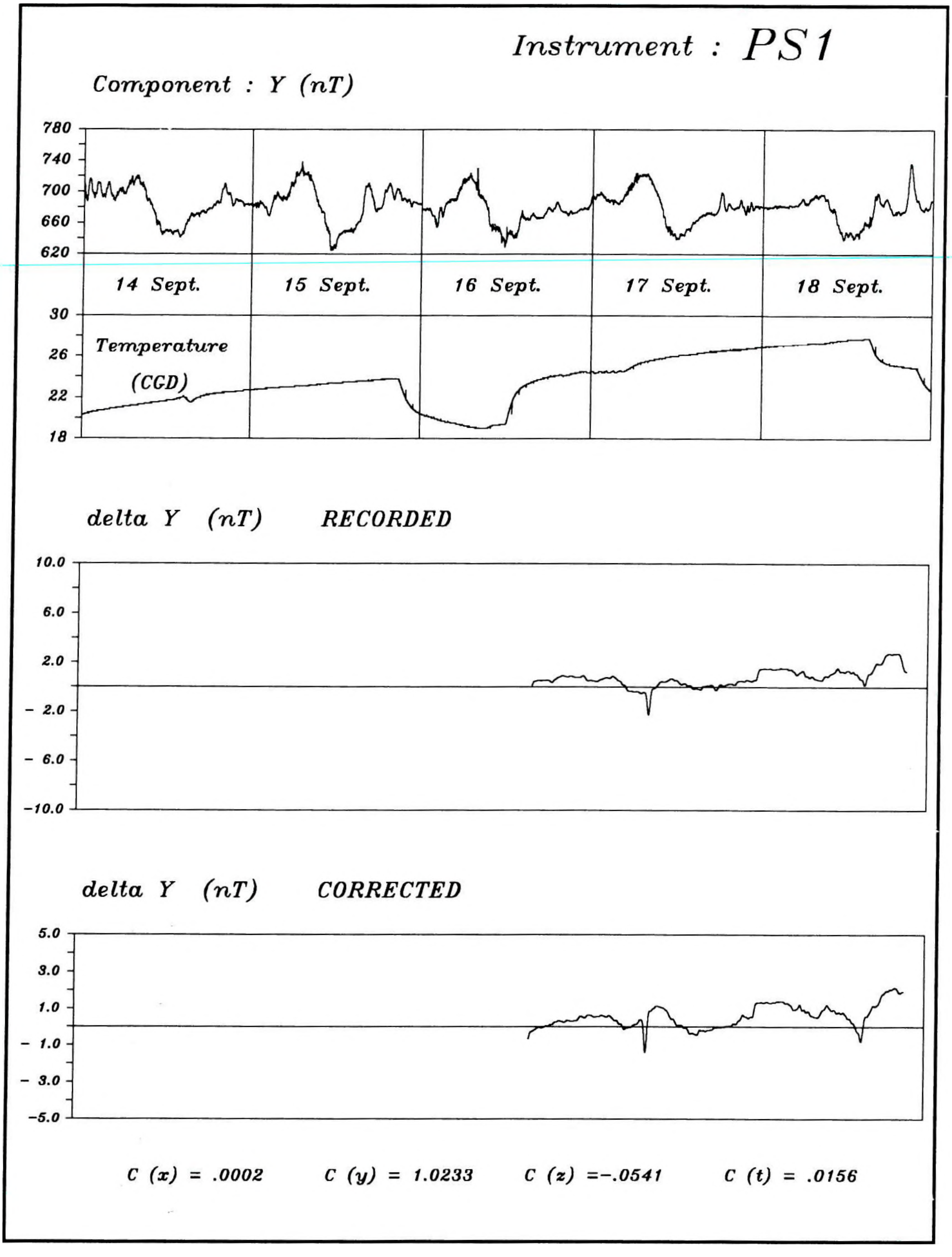
Instrument : PS1
Component : Y (nT)
780
740
700
660
620
14 Sept.
15 Sept.
16 Sept.
17 Sept.
18 Sept.
30
26
22
18
Temperature
(CGD)
delta Y (nT) RECORDED
10.0
6.0
2.0
- 2.0
- 6.0
-10.0
delta Y (nT) CORRECTED
5.0
3.0
1.0
- 1.0
- 3.0
-5.0
C (x) = .0002
C (y) = 1.0233
C (z) =-.0541
C (t) = .0156

Fig.6.

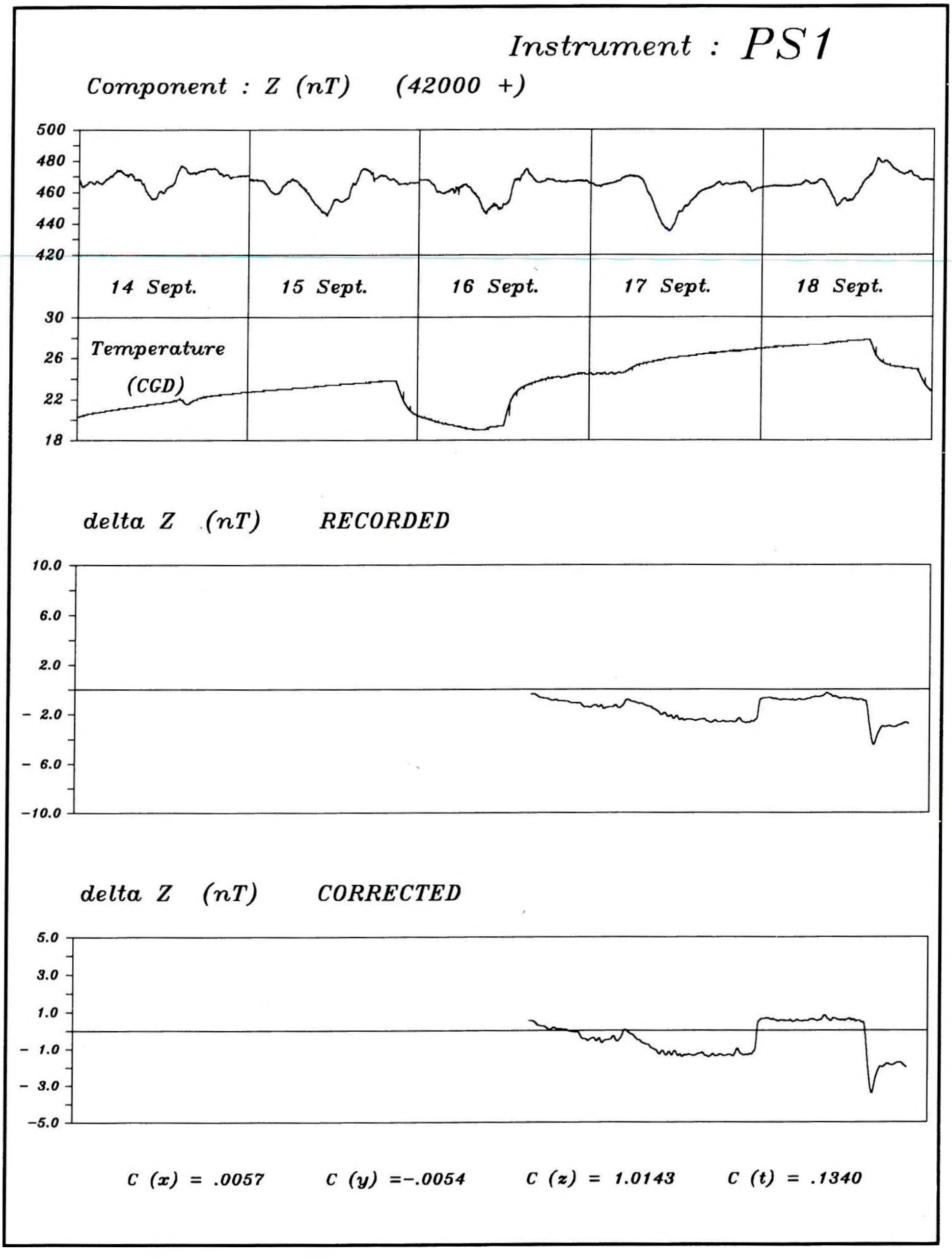
Instrument : PS1
Component : Z (nT) (42000 +)
500
480
460
440
420
14 Sept.
15 Sept.
16 Sept.
17 Sept.
18 Sept.
30
26
22
18
Temperature
(CGD)
delta Z (nT) RECORDED
10.0
6.0
2.0
- 2.0
- 6.0
-10.0
delta Z (nT) CORRECTED
5.0
3.0
1.0
- 1.0
- 3.0
-5.0
C (x) = .0057
C (y) =-.0054
C (z) = 1.0143
C (t) = .1340

Fig. 7.

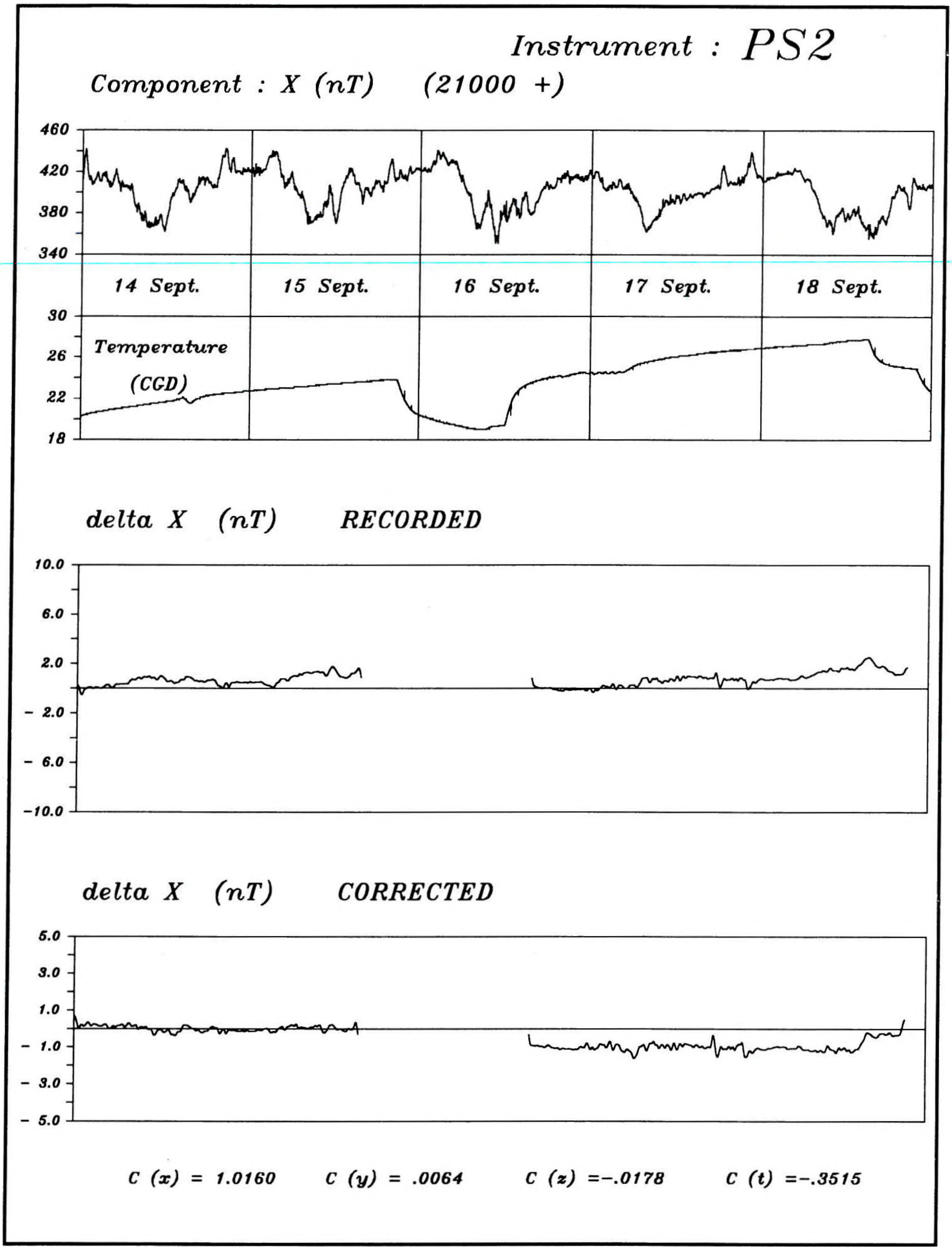
Instrument : PS2
Component : X (nT) (21000 +)
460
420
380
340
14 Sept.
15 Sept.
16 Sept.
17 Sept.
18 Sept.
30
26
22
18
Temperature
(CGD)
delta X (nT) RECORDED
10.0
6.0
2.0
- 2.0
- 6.0
-10.0
delta X (nT) CORRECTED
5.0
3.0
1.0
- 1.0
- 3.0
- 5.0
C (x) = 1.0160
C (y) = .0064
C (z) =-.0178
C (t) =-.3515

Fig.8.

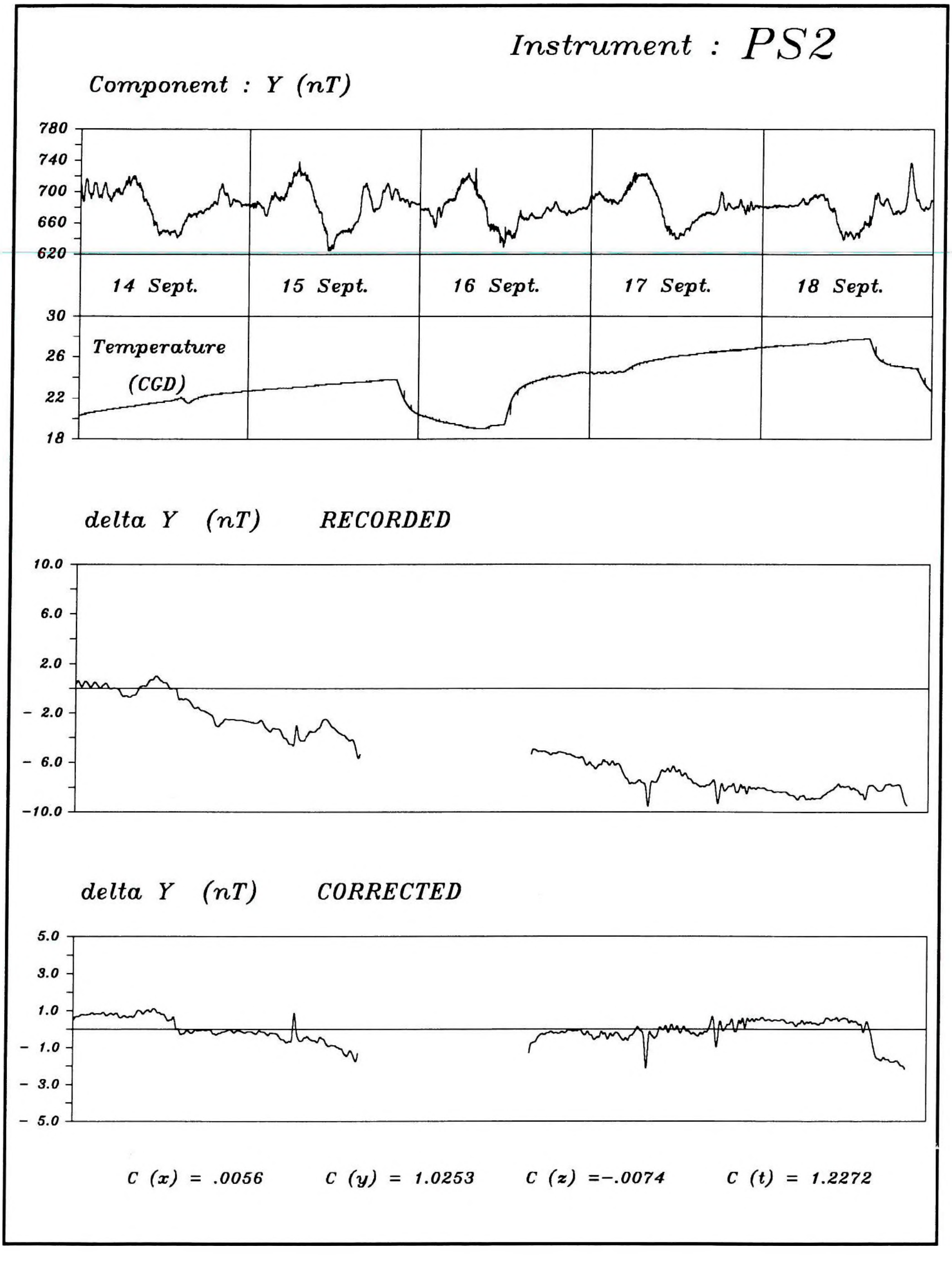

Instrument : PS2
Component : Y (nT)
780
740
700
660
620
14 Sept.
15 Sept.
16 Sept.
17 Sept.
18 Sept.
30
26
22
18
Temperature
(CGD)
delta Y (nT) RECORDED
10.0
6.0
2.0
- 2.0
- 6.0
-10.0
delta Y (nT) CORRECTED
5.0
3.0
1.0
- 1.0
- 3.0
- 5.0
C (x) = .0056
C (y) = 1.0253
C (z) =-.0074
C (t) = 1.2272

Fig. 9.

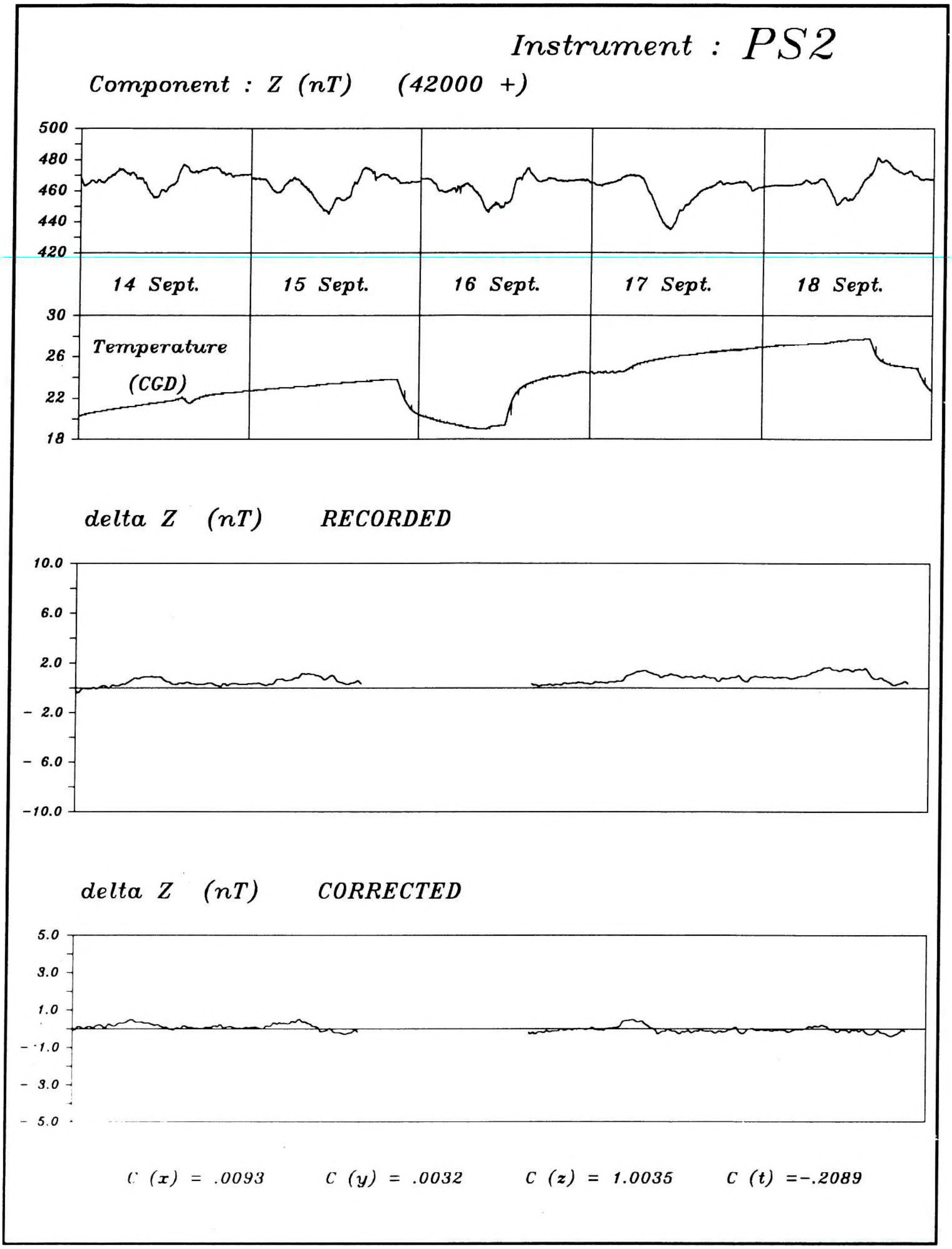

Instrument : PS2
Component : Z (nT) (42000 +)
500
480
460
440
420
14 Sept.
15 Sept.
16 Sept.
17 Sept.
18 Sept.
30
26
22
18
Temperature
(CGD)
delta Z (nT) RECORDED
10.0
6.0
2.0
- 2.0
- 6.0
-10.0
delta Z (nT) CORRECTED
5.0
3.0
1.0
-1.0
- 3.0
- 5.0
C (x) = .0093
C (y) = .0032
C (z) = 1.0035
C (t) =-.2089

Fig.10.

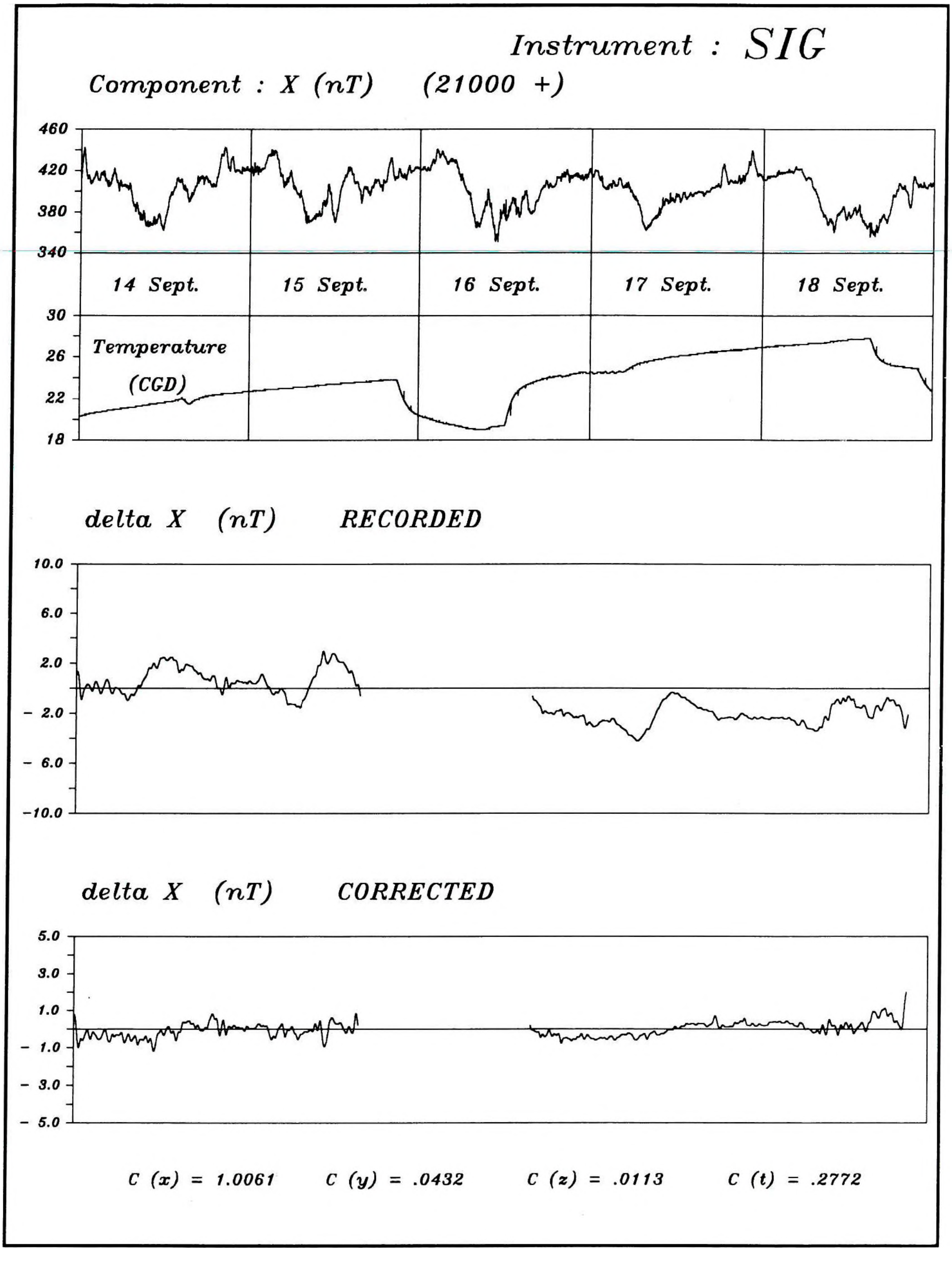

Instrument : SIG
Component : X (nT) (21000 +)
460
420
380
340
14 Sept.
15 Sept.
16 Sept.
17 Sept.
18 Sept.
30
26
22
18
Temperature
(CGD)
delta X (nT) RECORDED
10.0
6.0
2.0
− 2.0
− 6.0
−10.0
delta X (nT) CORRECTED
5.0
3.0
1.0
− 1.0
− 3.0
− 5.0
C (x) = 1.0061 C (y) = .0432 C (z) = .0113 C (t) = .2772

Fig.11.

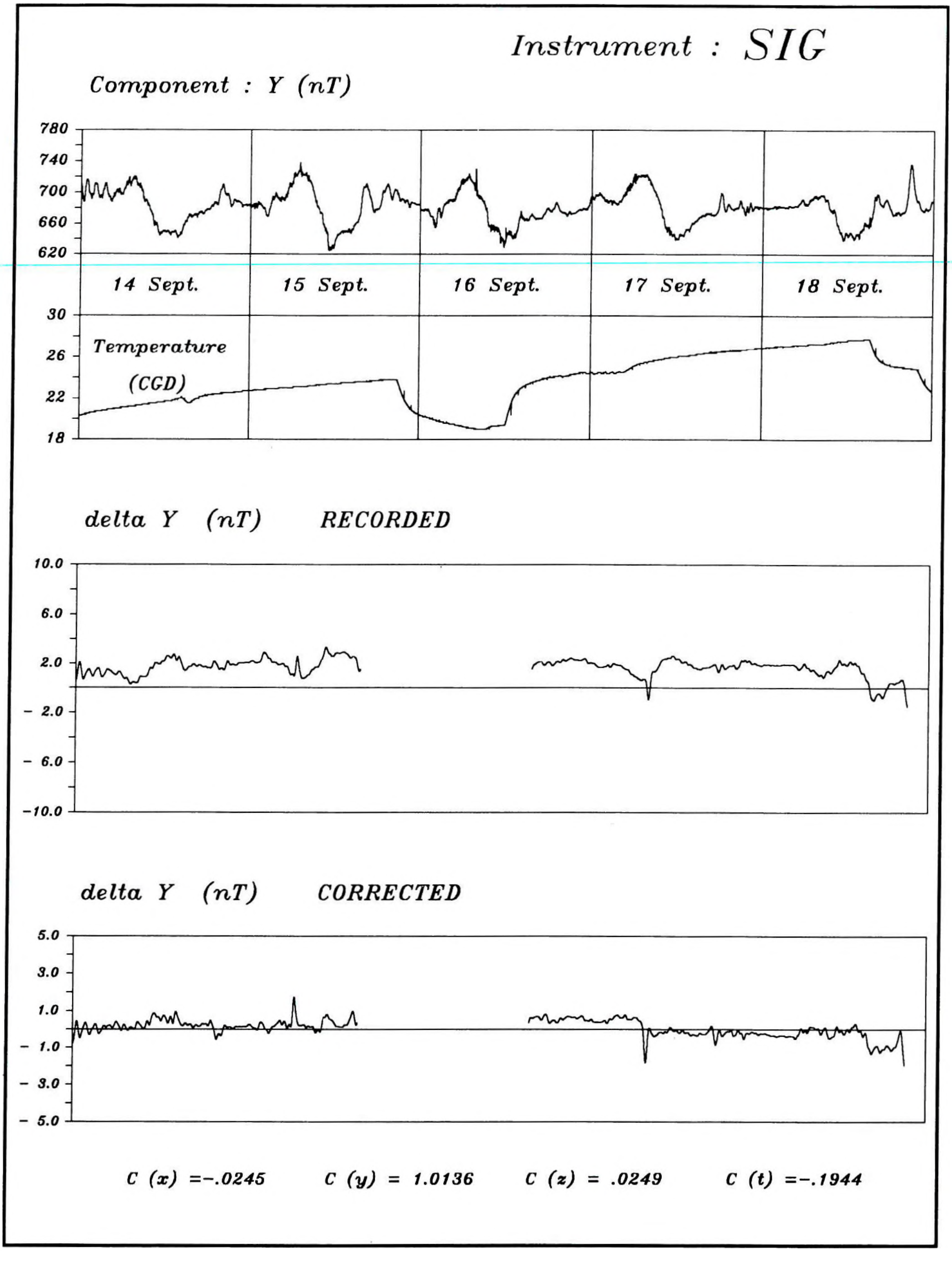
Instrument : SIG
Component : Y (nT)
780
740
700
660
620
14 Sept.
15 Sept.
16 Sept.
17 Sept.
18 Sept.
30
26
22
18
Temperature
(CGD)
delta Y (nT) RECORDED
10.0
6.0
2.0
- 2.0
- 6.0
-10.0
delta Y (nT) CORRECTED
5.0
3.0
1.0
- 1.0
- 3.0
- 5.0
C (x) =-.0245
C (y) = 1.0136
C (z) = .0249
C (t) =-.1944

Fig. 12.

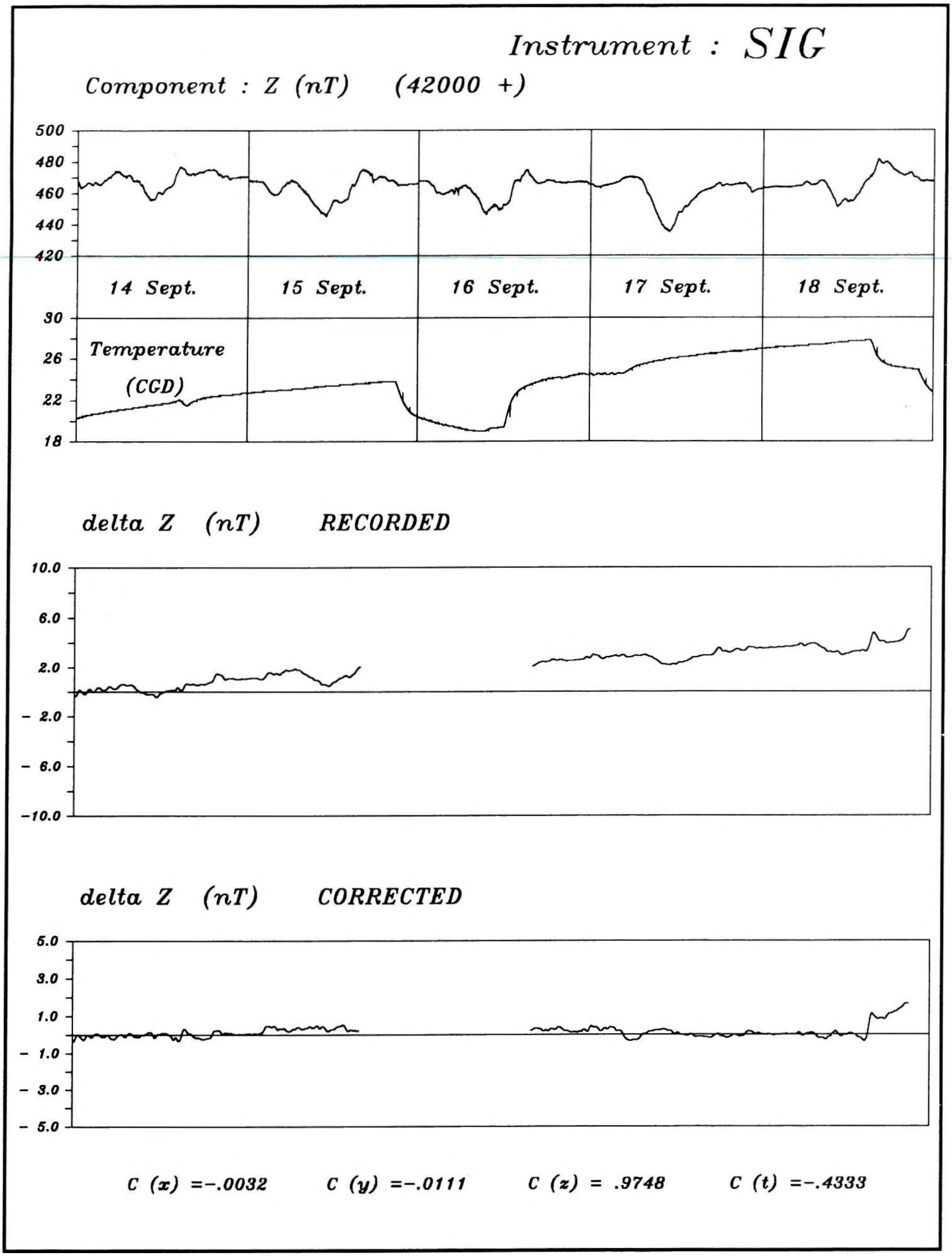
Instrument : SIG
Component : Z (nT) (42000 +)
500
480
460
440
420
14 Sept.
15 Sept.
16 Sept.
17 Sept.
18 Sept.
30
26
22
18
Temperature
(CGD)
delta Z (nT) RECORDED
10.0
6.0
2.0
- 2.0
- 6.0
-10.0
delta Z (nT) CORRECTED
5.0
3.0
1.0
- 1.0
- 3.0
- 5.0
C (x) =-.0032
C (y) =-.0111
C (z) = .9748
C (t) =-.4333

Fig. 13.

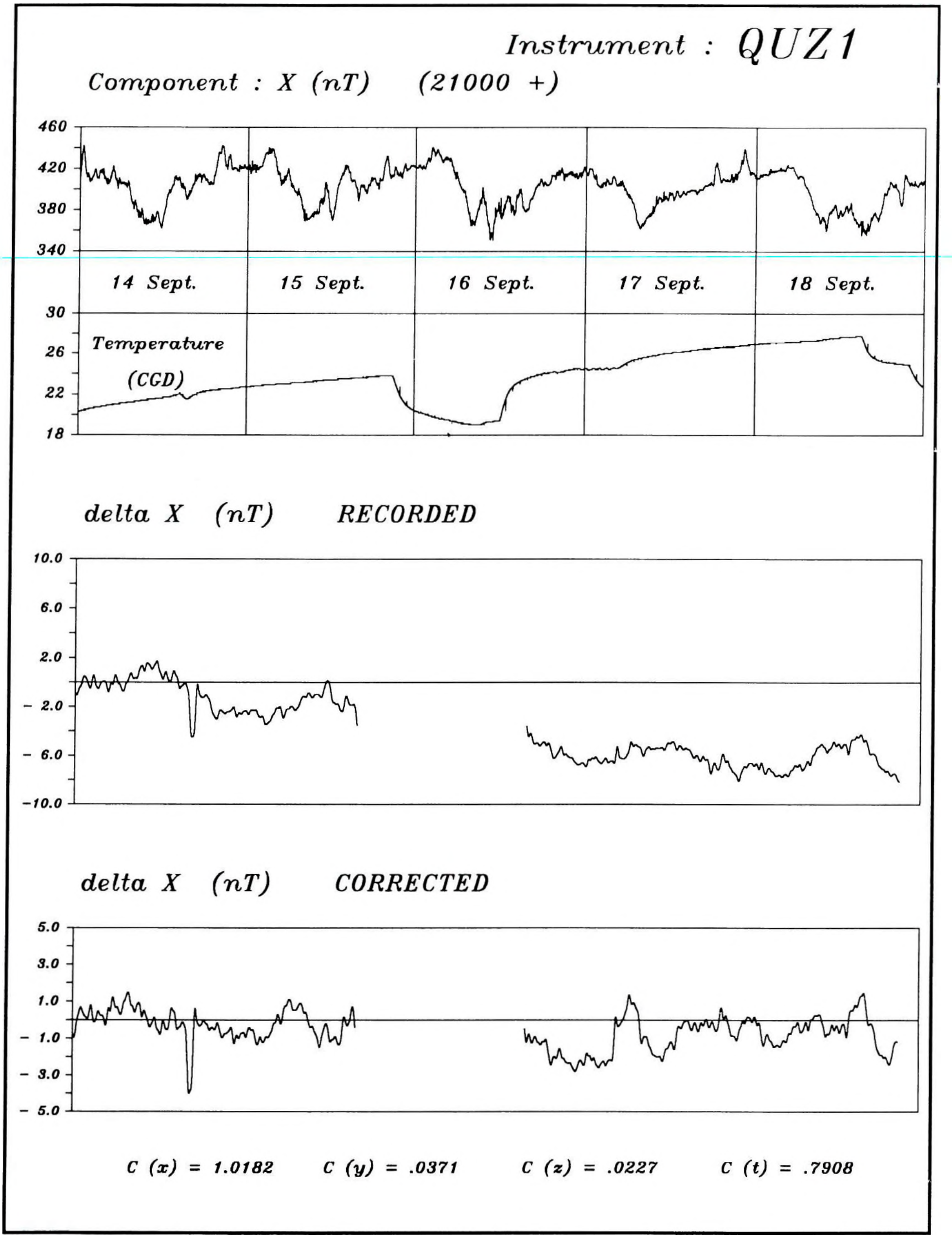
Instrument : QUZ1
Component : X (nT) (21000 +)
460
420
380
340
14 Sept.
15 Sept.
16 Sept.
17 Sept.
18 Sept.
30
26
22
18
Temperature
(CGD)
delta X (nT) RECORDED
10.0
6.0
2.0
- 2.0
- 6.0
-10.0
delta X (nT) CORRECTED
5.0
3.0
1.0
- 1.0
- 3.0
- 5.0
C (x) = 1.0182
C (y) = .0371
C (z) = .0227
C (t) = .7908

Fig. 14.

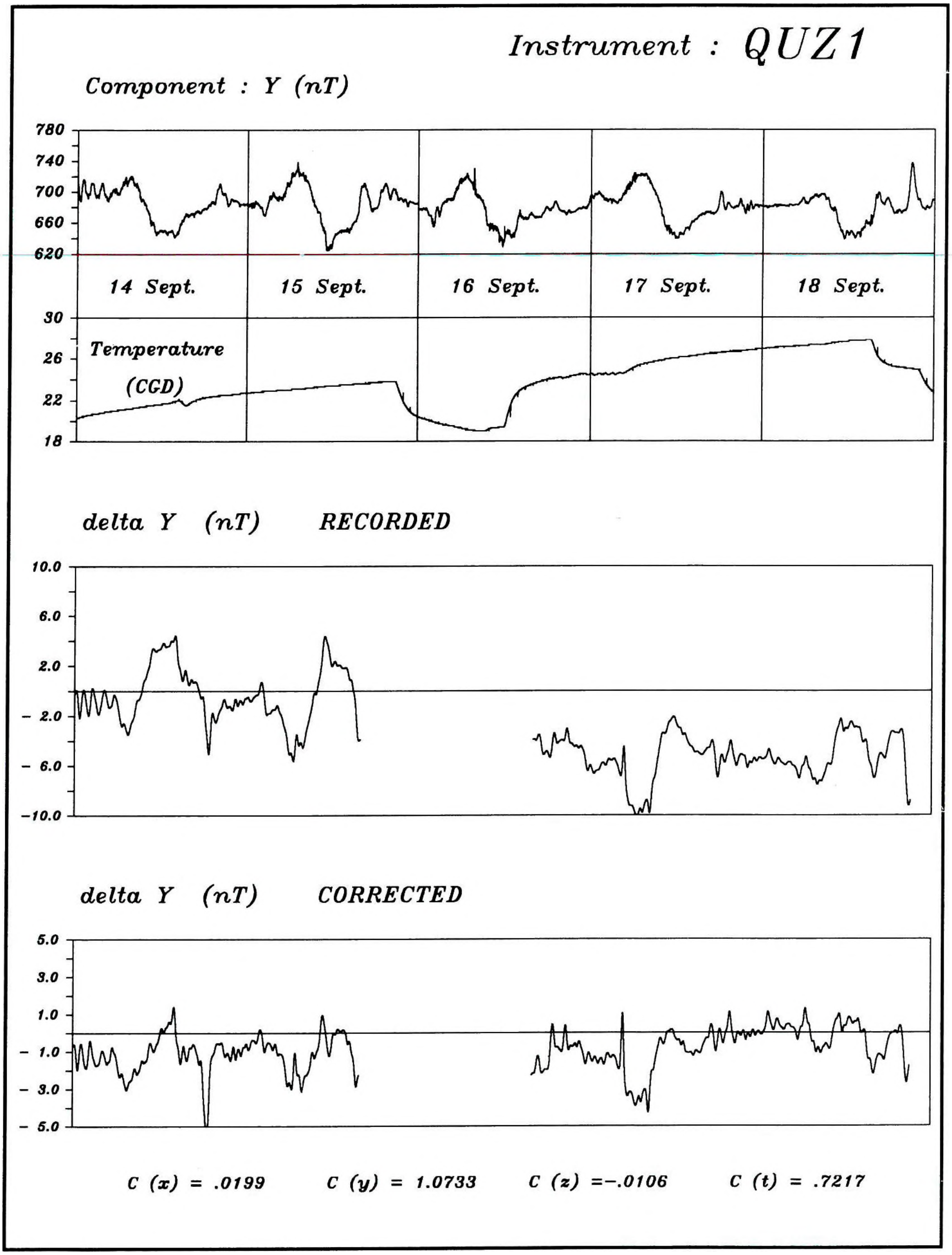
Instrument : QUZ1
Component : Y (nT)
780
740
700
660
620
14 Sept.
15 Sept.
16 Sept.
17 Sept.
18 Sept.
30
26
22
18
Temperature
(CGD)
delta Y (nT) RECORDED
10.0
6.0
2.0
- 2.0
- 6.0
-10.0
delta Y (nT) CORRECTED
5.0
3.0
1.0
- 1.0
- 3.0
- 5.0
C (x) = .0199
C (y) = 1.0733
C (z) =-.0106
C (t) = .7217

Fig. 15.

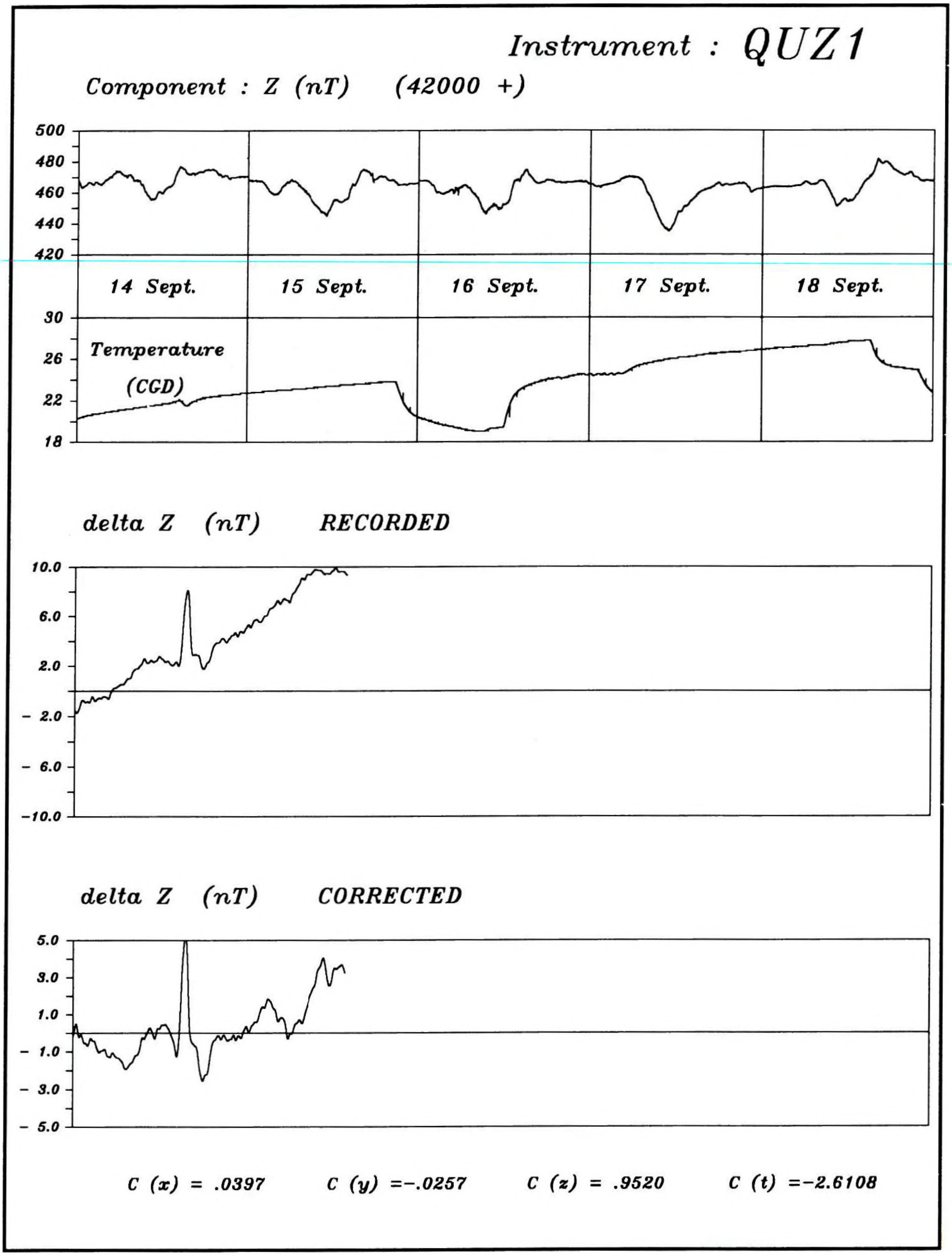
Instrument : QUZ1
Component : Z (nT) (42000 +)
500
480
460
440
420
14 Sept.
15 Sept.
16 Sept.
17 Sept.
18 Sept.
30
26
22
18
Temperature
(CGD)
delta Z (nT) RECORDED
10.0
6.0
2.0
- 2.0
- 6.0
-10.0
delta Z (nT) CORRECTED
5.0
3.0
1.0
- 1.0
- 3.0
- 5.0
C (x) = .0397
C (y) =-.0257
C (z) = .9520
C (t) =-2.6108

Fig.16.

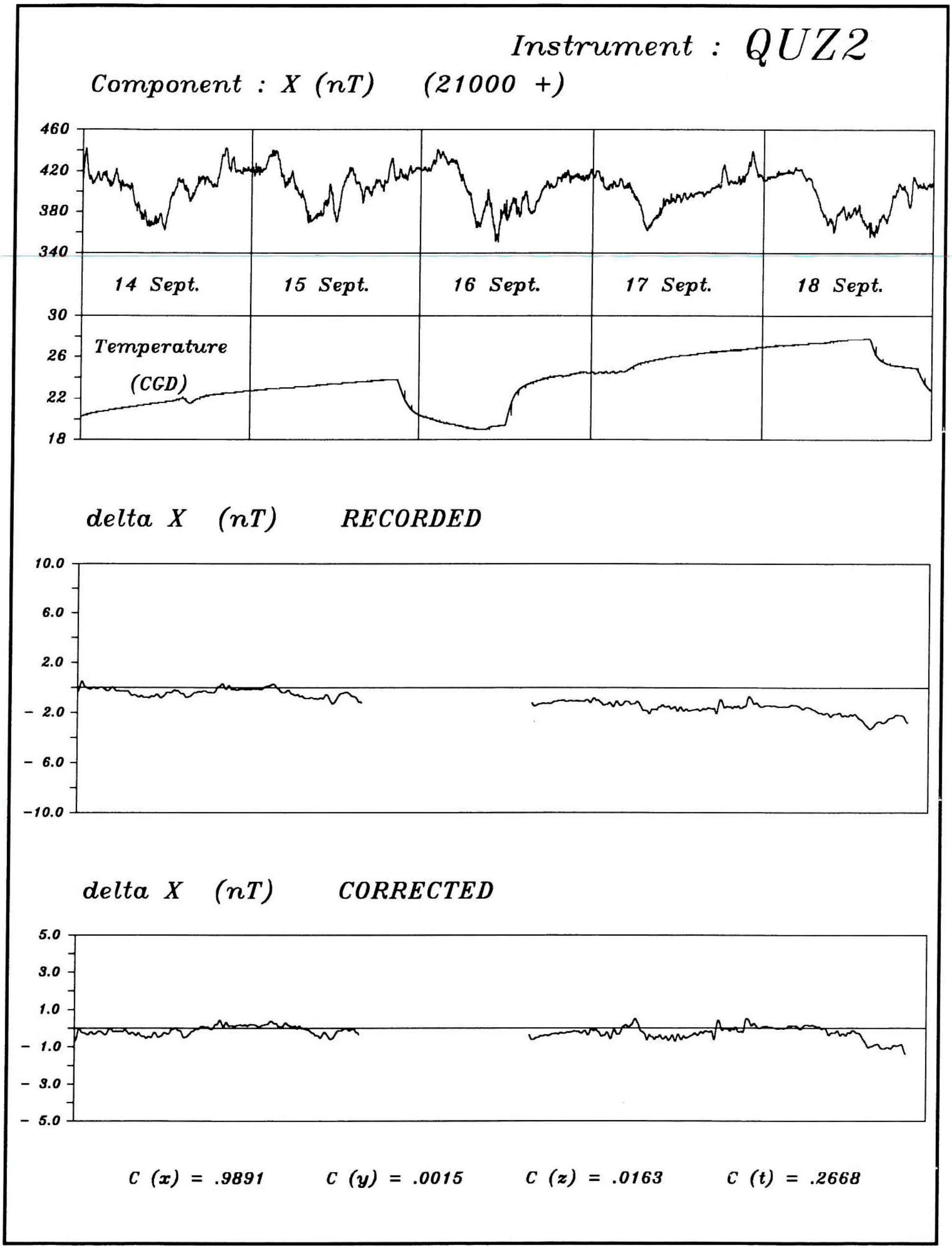
Instrument : QUZ2
Component : X (nT) (21000 +)
460
420
380
340
14 Sept.
15 Sept.
16 Sept.
17 Sept.
18 Sept.
30
26
22
18
Temperature
(CGD)
delta X (nT) RECORDED
10.0
6.0
2.0
- 2.0
- 6.0
-10.0
delta X (nT) CORRECTED
5.0
3.0
1.0
- 1.0
- 3.0
- 5.0
C (x) = .9891
C (y) = .0015
C (z) = .0163
C (t) = .2668

Fig. 17.

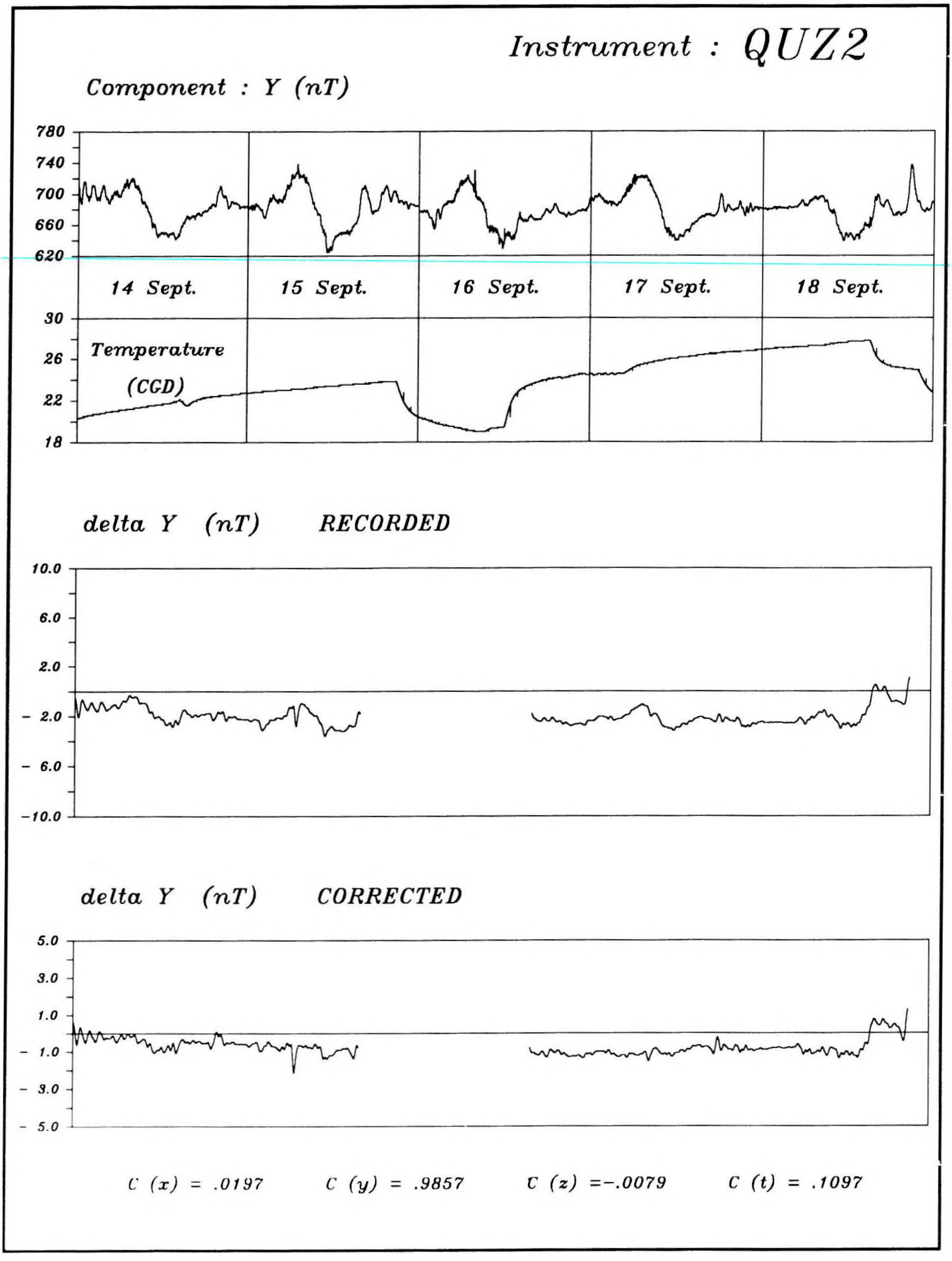
Instrument : QUZ2
Component : Y (nT)
780
740
700
660
620
14 Sept.
15 Sept.
16 Sept.
17 Sept.
18 Sept.
30
26
22
18
Temperature
(CGD)
delta Y (nT) RECORDED
10.0
6.0
2.0
- 2.0
- 6.0
-10.0
delta Y (nT) CORRECTED
5.0
3.0
1.0
- 1.0
- 3.0
- 5.0
C (x) = .0197
C (y) = .9857
C (z) =-.0079
C (t) = .1097

Fig. 18.

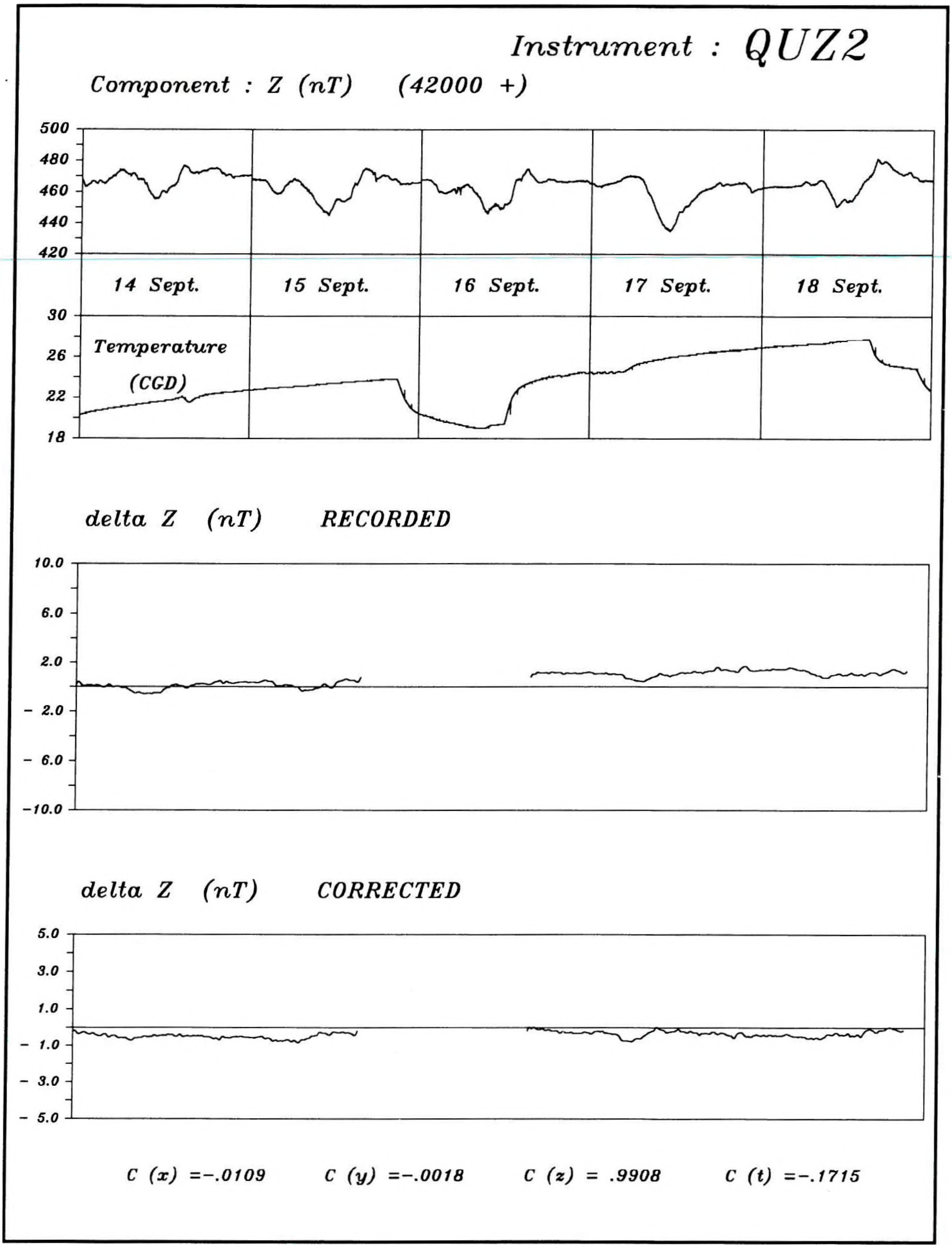
Instrument : QUZ2
Component : Z (nT) (42000 +)
500
480
460
440
420
14 Sept.
15 Sept.
16 Sept.
17 Sept.
18 Sept.
30
26
22
18
Temperature
(CGD)
delta Z (nT) RECORDED
10.0
6.0
2.0
- 2.0
- 6.0
-10.0
delta Z (nT) CORRECTED
5.0
3.0
1.0
- 1.0
- 3.0
- 5.0
C (x) =-.0109
C (y) =-.0018
C (z) = .9908
C (t) =-.1715

Fig.19.

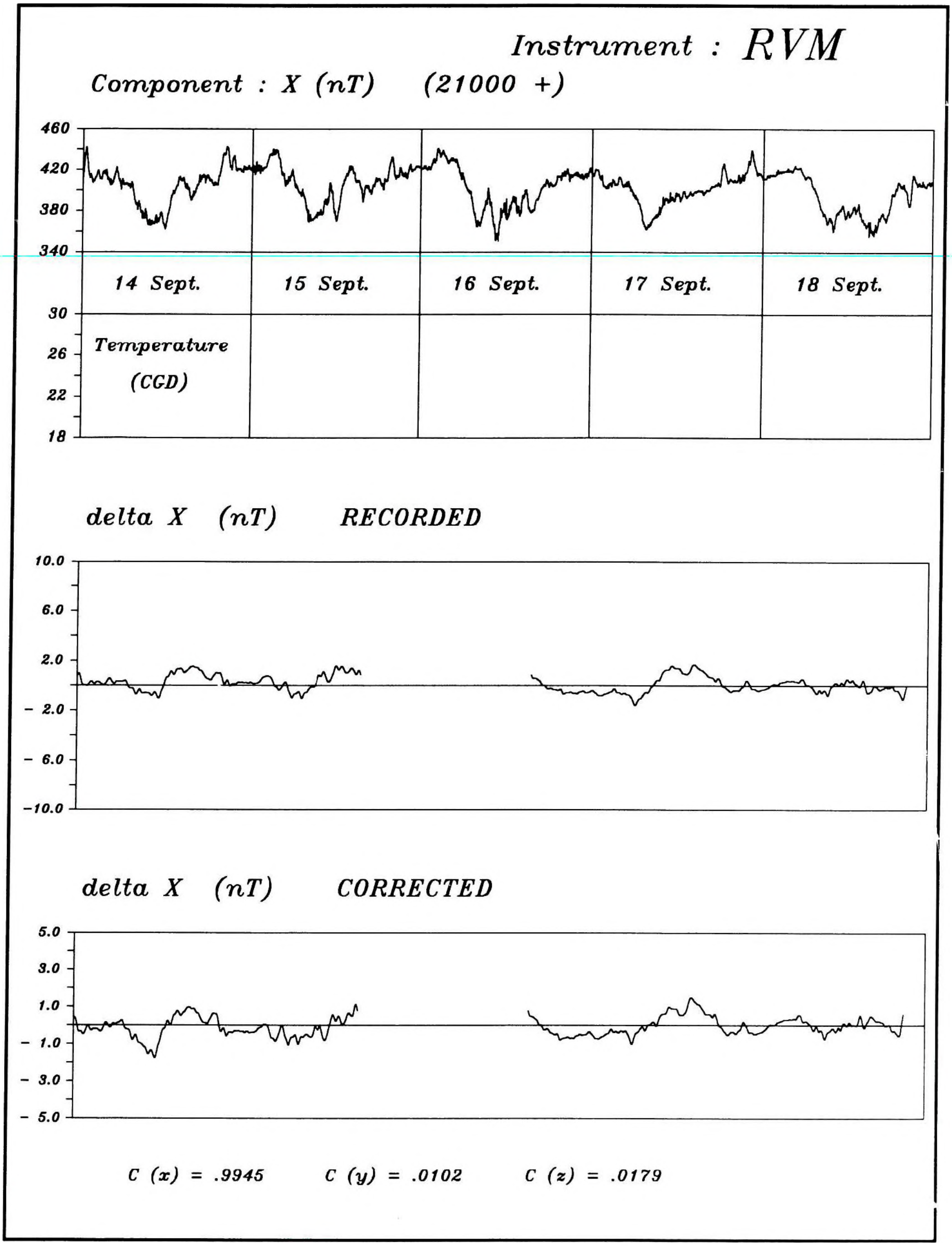
Instrument : RVM
Component : X (nT) (21000 +)
460
420
380
340
14 Sept.
15 Sept.
16 Sept.
17 Sept.
18 Sept.
30
26
22
18
Temperature
(CGD)
delta X (nT) RECORDED
10.0
6.0
2.0
- 2.0
- 6.0
-10.0
delta X (nT) CORRECTED
5.0
3.0
1.0
- 1.0
- 3.0
- 5.0
C (x) = .9945
C (y) = .0102
C (z) = .0179

Fig.20.

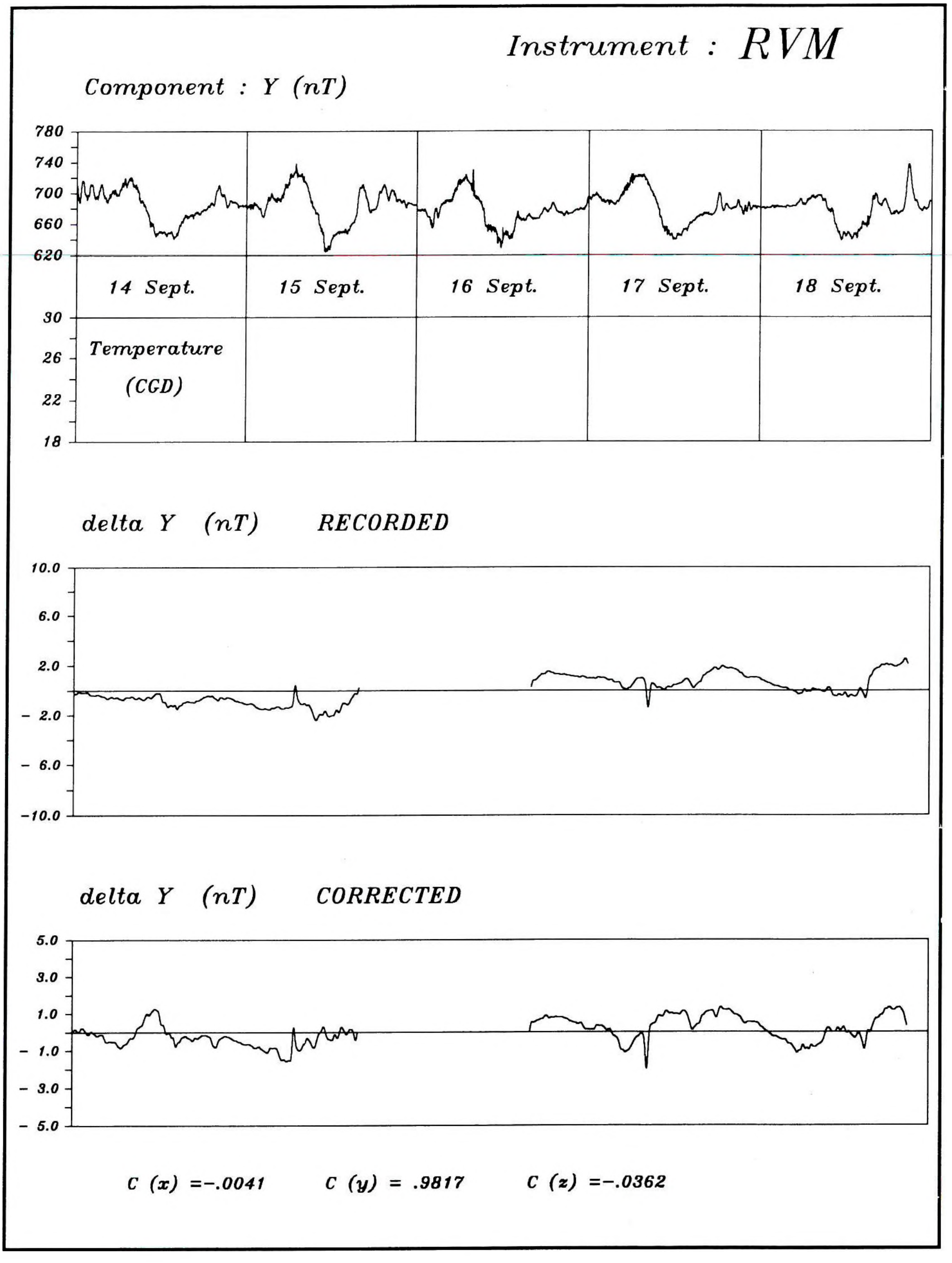
Instrument : RVM
Component : Y (nT)
780
740
700
660
620
14 Sept.
15 Sept.
16 Sept.
17 Sept.
18 Sept.
30
26
22
18
Temperature
(CGD)
delta Y (nT) RECORDED
10.0
6.0
2.0
- 2.0
- 6.0
-10.0
delta Y (nT) CORRECTED
5.0
3.0
1.0
- 1.0
- 3.0
- 5.0
C (x) =-.0041
C (y) = .9817
C (z) =-.0362

Fig.21.

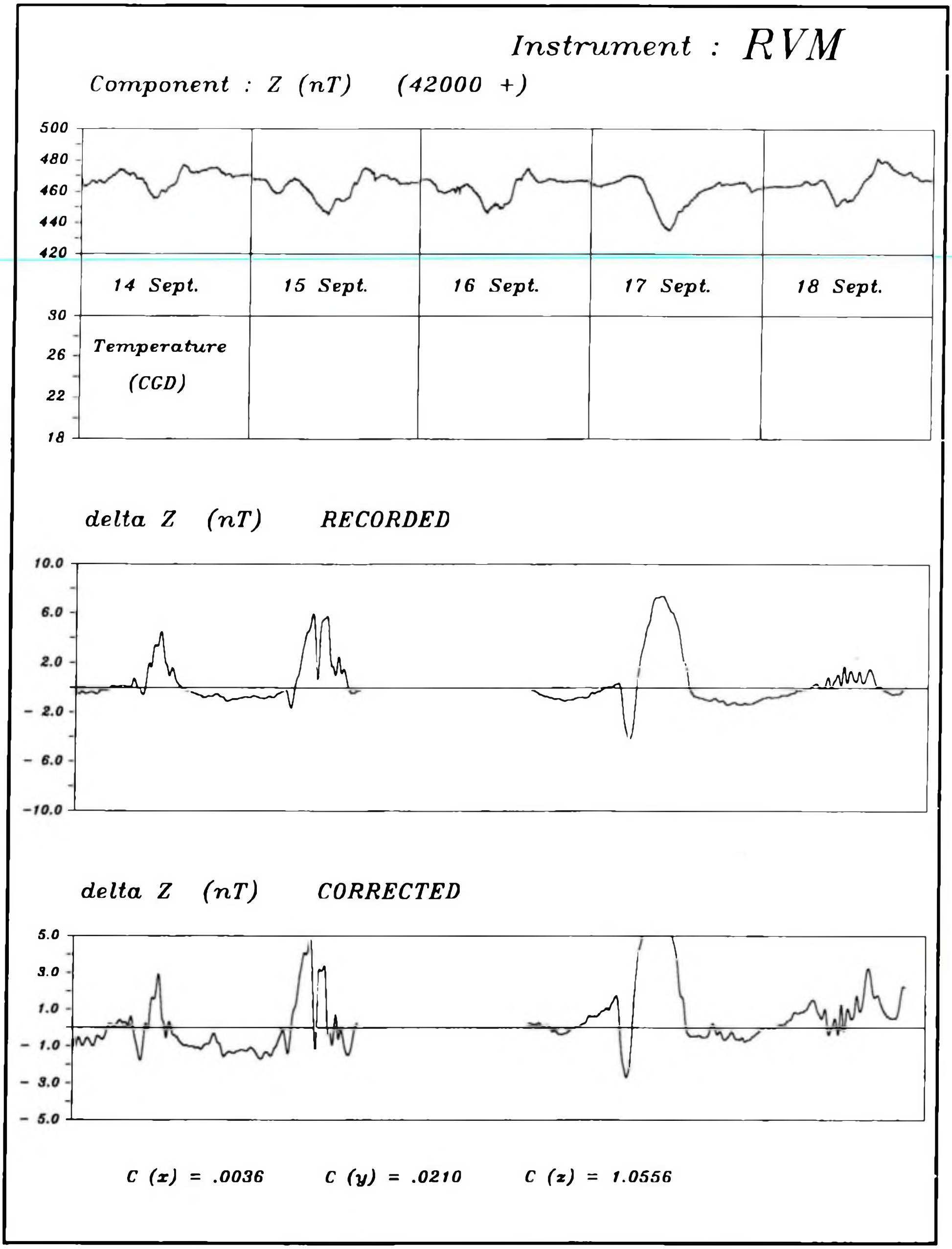
Instrument : RVM
Component : Z (nT) (42000 +)
500
480
460
440
420
14 Sept.
15 Sept.
16 Sept.
17 Sept.
18 Sept.
30
26
22
18
Temperature
(CCD)
delta Z (nT) RECORDED
10.0
6.0
2.0
- 2.0
- 6.0
-10.0
delta Z (nT) CORRECTED
5.0
3.0
1.0
- 1.0
- 3.0
- 5.0
C (x) = .0036
C (y) = .0210
C (z) = 1.0556

Fig.22.

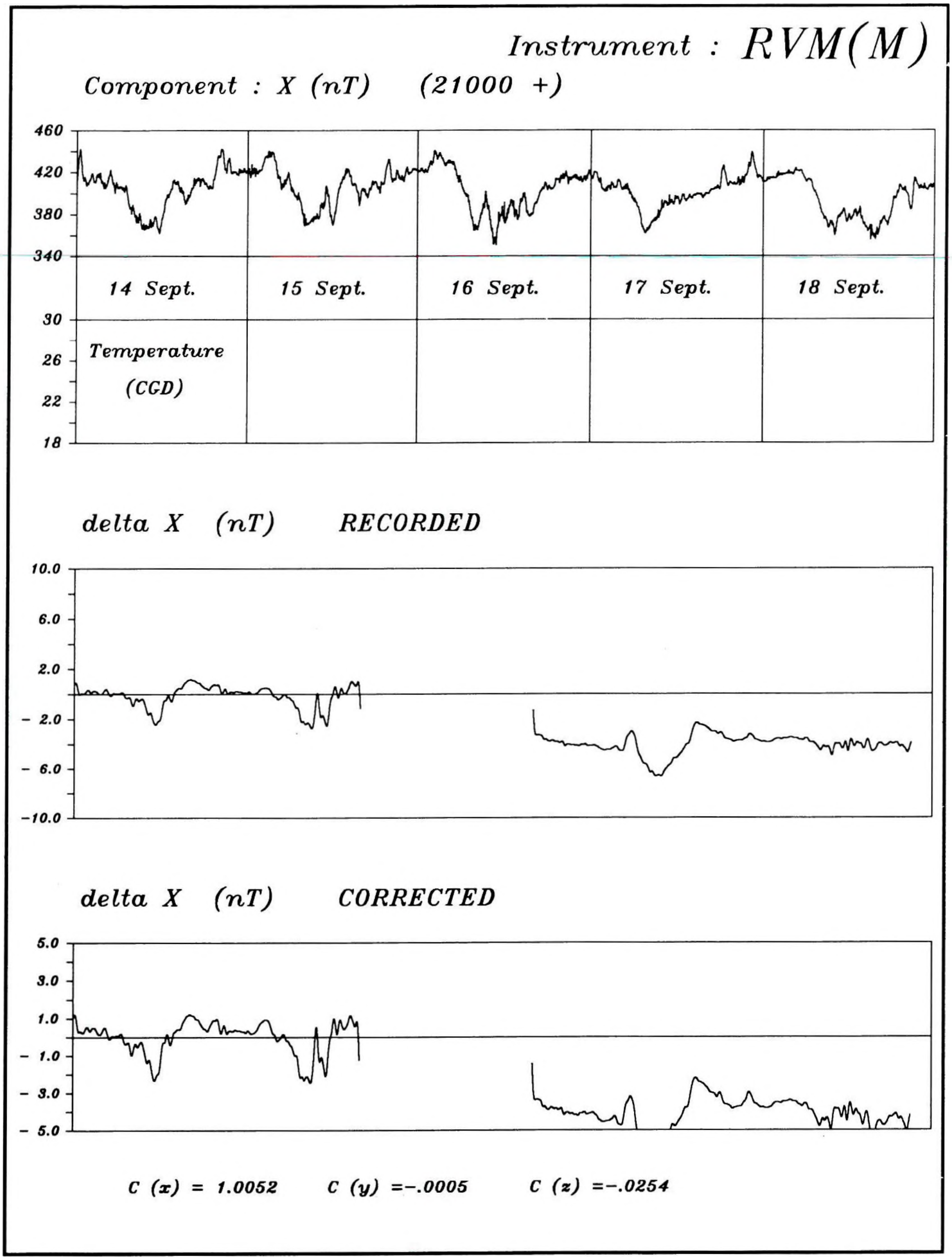
Instrument : RVM(M)
Component : X (nT) (21000 +)
460
420
380
340
14 Sept.
15 Sept.
16 Sept.
17 Sept.
18 Sept.
30
26
22
18
Temperature
(CGD)
delta X (nT) RECORDED
10.0
6.0
2.0
- 2.0
- 6.0
-10.0
delta X (nT) CORRECTED
5.0
3.0
1.0
- 1.0
- 3.0
- 5.0
C (x) = 1.0052
C (y) =-.0005
C (z) =-.0254

Fig.23.

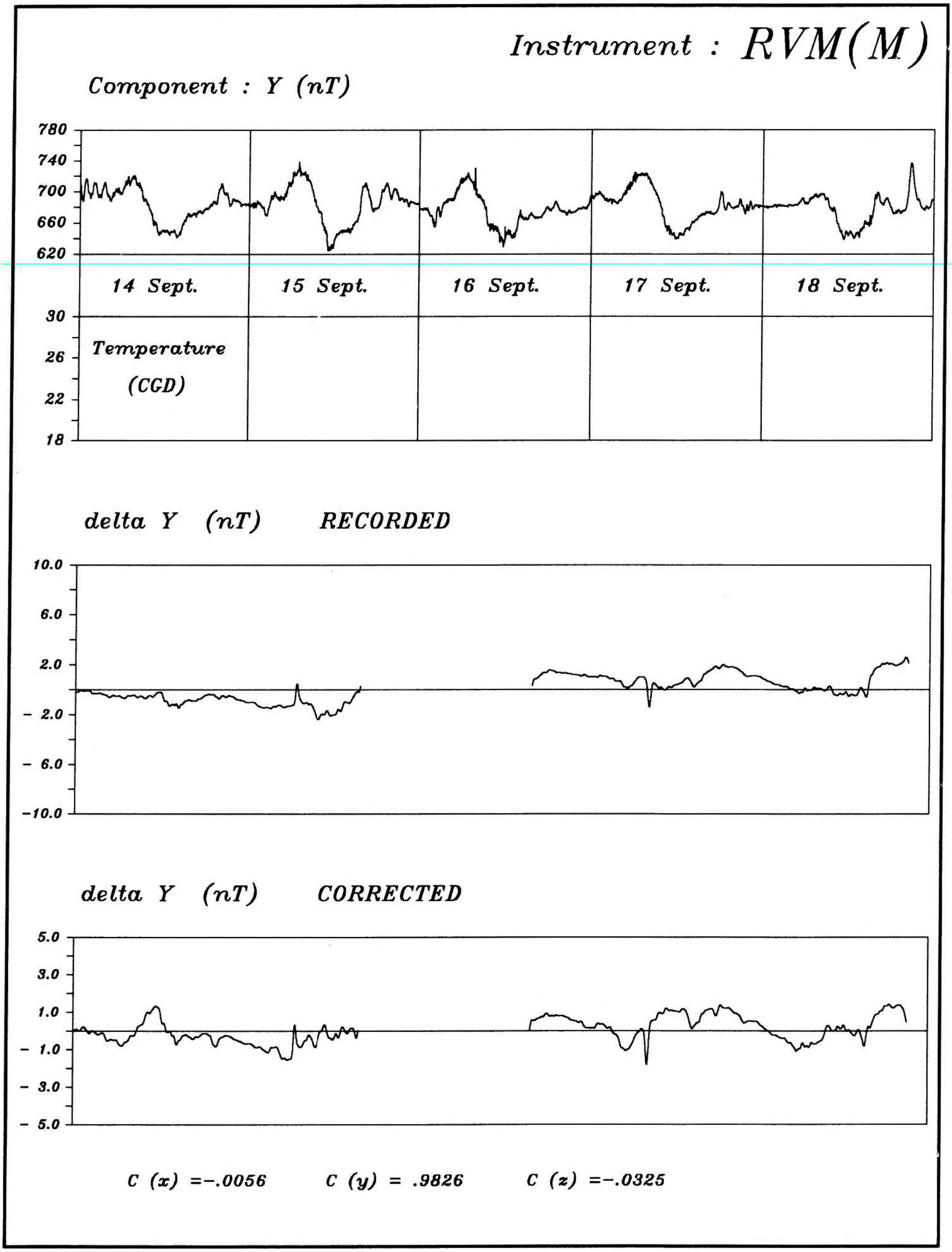
Instrument : RVM(M)
Component : Y (nT)
780
740
700
660
620
14 Sept.
15 Sept.
16 Sept.
17 Sept.
18 Sept.
30
26
22
18
Temperature
(CGD)
delta Y (nT) RECORDED
10.0
6.0
2.0
- 2.0
- 6.0
-10.0
delta Y (nT) CORRECTED
5.0
3.0
1.0
- 1.0
- 3.0
- 5.0
C (x) =-.0056
C (y) = .9826
C (z) =-.0325

Fig.24.

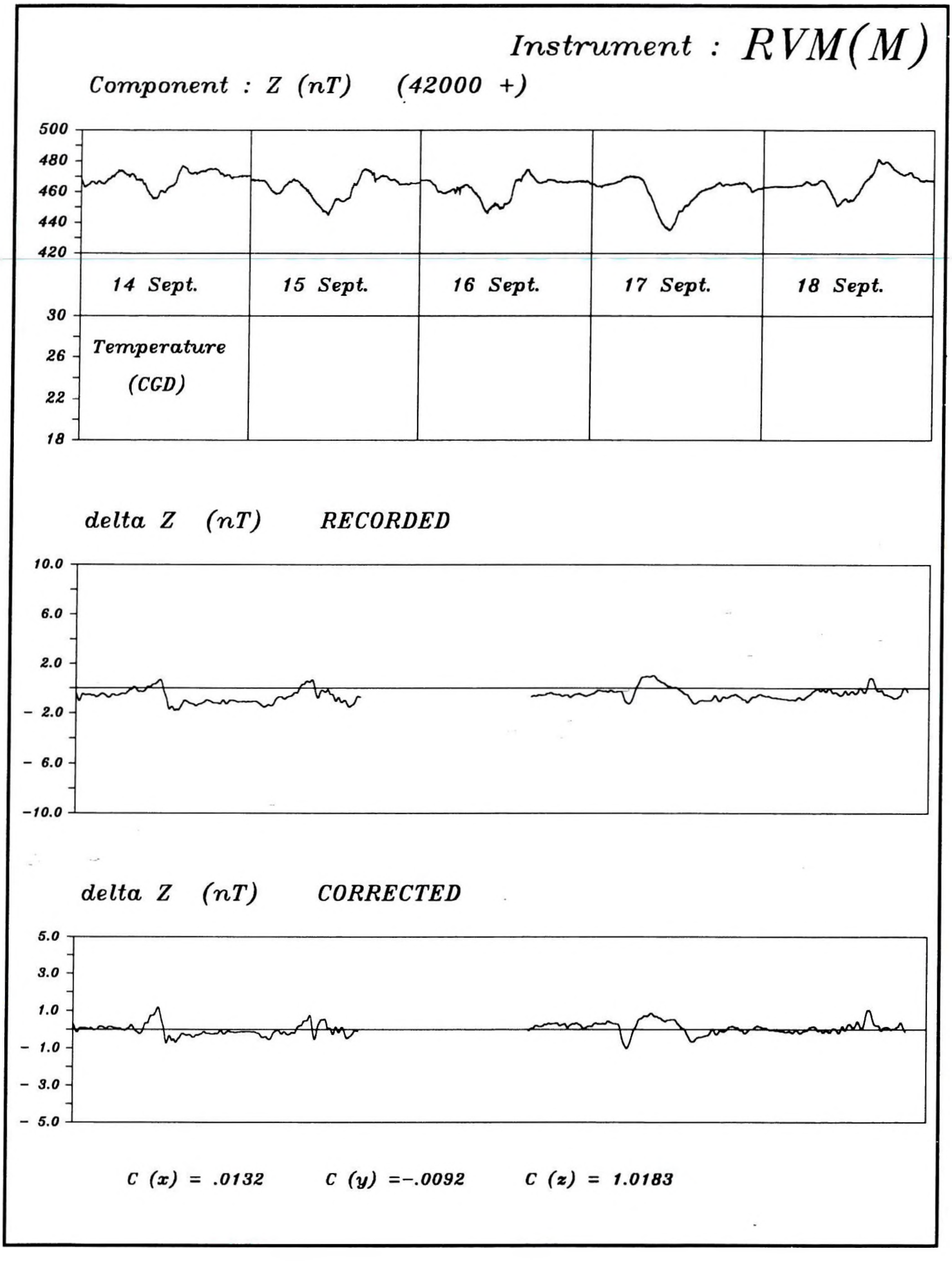
Instrument : RVM(M)
Component : Z (nT) (42000 +)
500
480
460
440
420
14 Sept.
15 Sept.
16 Sept.
17 Sept.
18 Sept.
30
26
22
18
Temperature
(CGD)
delta Z (nT) RECORDED
10.0
6.0
2.0
- 2.0
- 6.0
-10.0
delta Z (nT) CORRECTED
5.0
3.0
1.0
- 1.0
- 3.0
- 5.0
C (x) = .0132
C (y) =-.0092
C (z) = 1.0183

Fig.25.

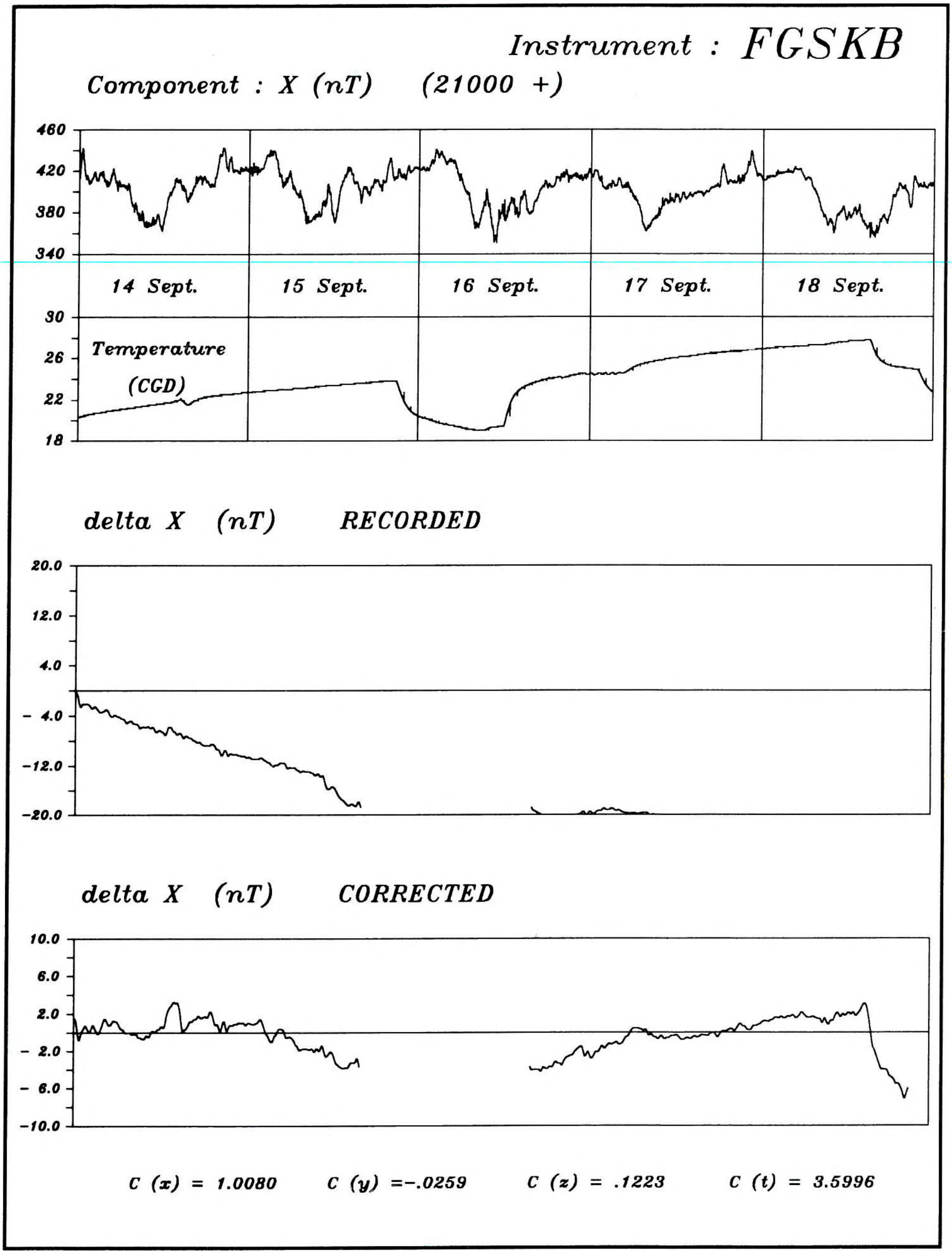
Instrument : FGSKB
Component : X (nT) (21000 +)
460
420
380
340
14 Sept.
15 Sept.
16 Sept.
17 Sept.
18 Sept.
30
26
22
18
Temperature
(CGD)
delta X (nT) RECORDED
20.0
12.0
4.0
- 4.0
-12.0
-20.0
delta X (nT) CORRECTED
10.0
6.0
2.0
- 2.0
- 6.0
-10.0
C (x) = 1.0080
C (y) =-.0259
C (z) = .1223
C (t) = 3.5996

Fig.26.

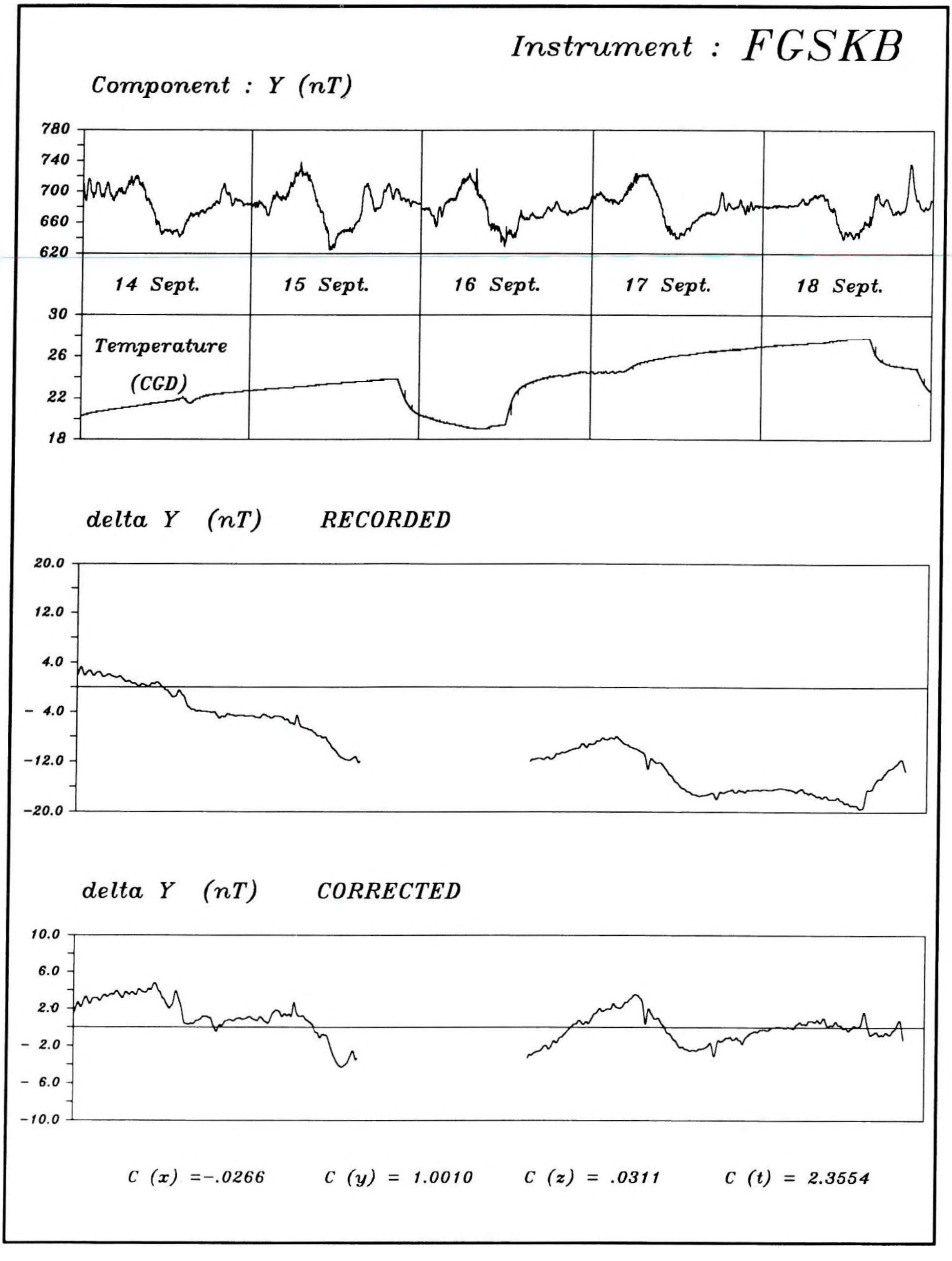
Instrument : FGSKB
Component : Y (nT)
780
740
700
660
620
14 Sept.
15 Sept.
16 Sept.
17 Sept.
18 Sept.
30
26
22
18
Temperature
(CGD)
delta Y (nT) RECORDED
20.0
12.0
4.0
- 4.0
-12.0
-20.0
delta Y (nT) CORRECTED
10.0
6.0
2.0
- 2.0
- 6.0
-10.0
C (x) =-.0266
C (y) = 1.0010
C (z) = .0311
C (t) = 2.3554

Fig. 27.

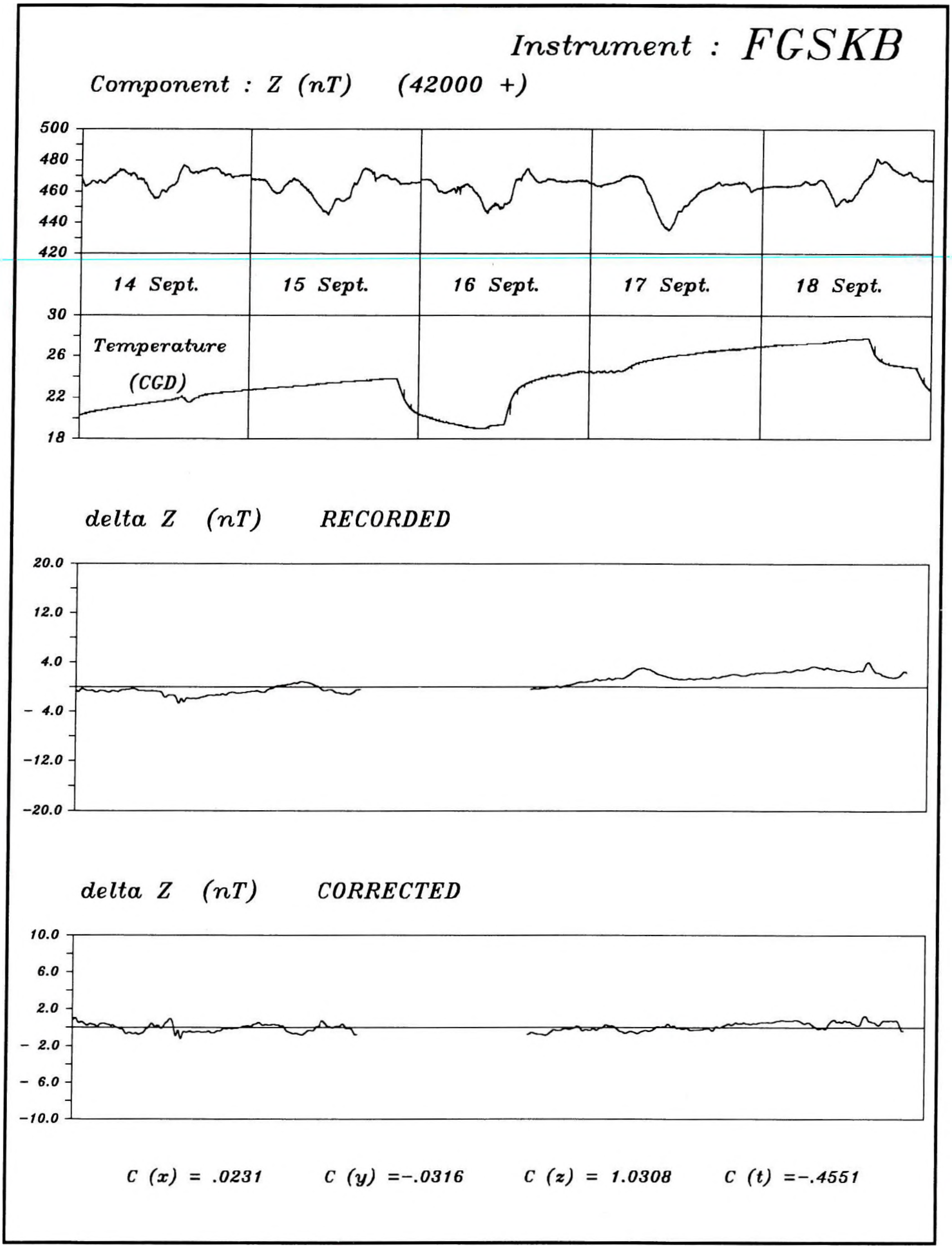
Instrument : FGSKB
Component : Z (nT) (42000 +)
500
480
460
440
420
14 Sept.
15 Sept.
16 Sept.
17 Sept.
18 Sept.
30
26
22
18
Temperature
(CGD)
delta Z (nT) RECORDED
20.0
12.0
4.0
- 4.0
-12.0
-20.0
delta Z (nT) CORRECTED
10.0
6.0
2.0
- 2.0
- 6.0
-10.0
C (x) = .0231
C (y) =-.0316
C (z) = 1.0308
C (t) =-.4551

Fig.28.

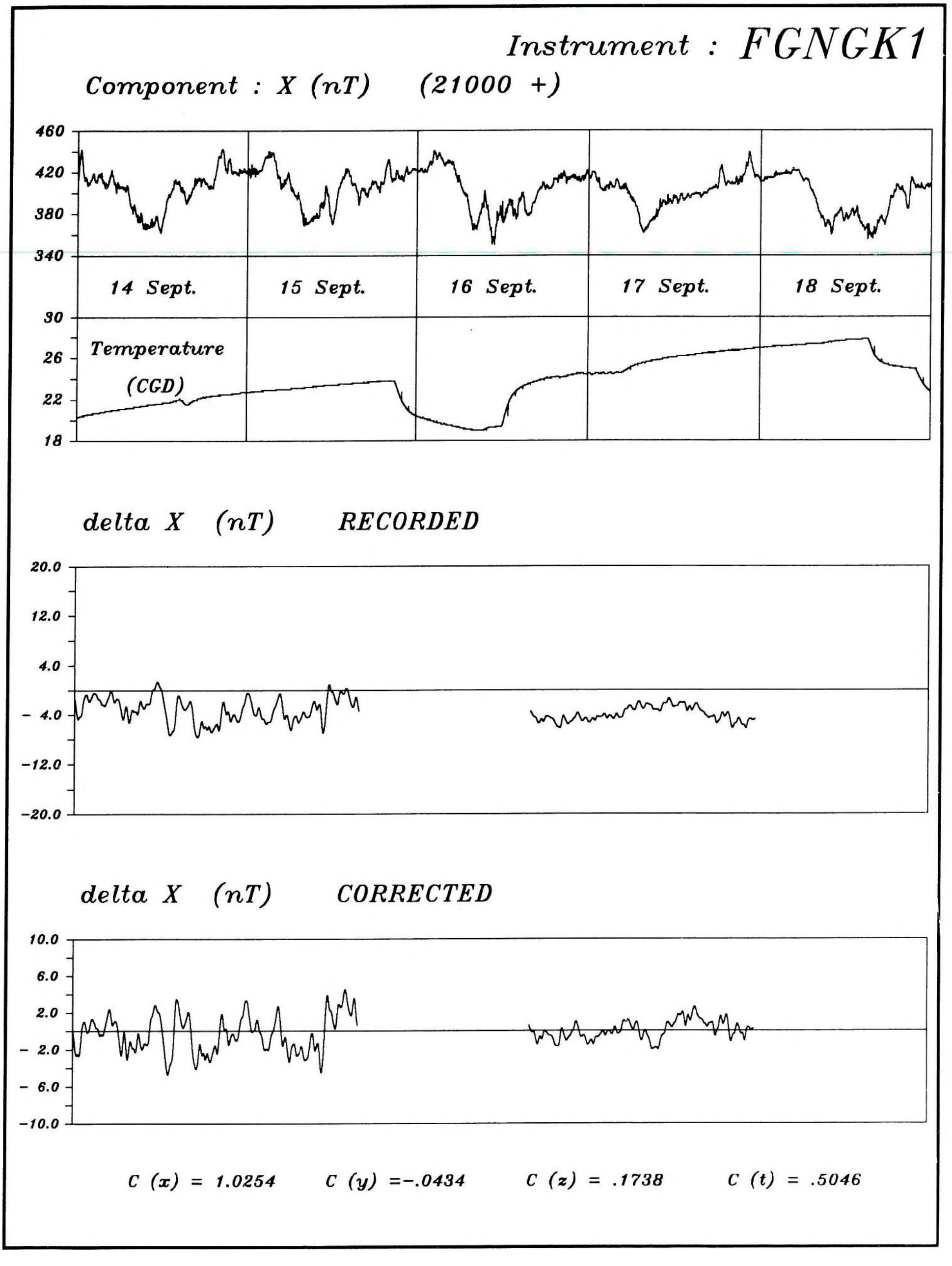

Instrument : FGNGK1
Component : X (nT) (21000 +)
460
420
380
340
14 Sept.
15 Sept.
16 Sept.
17 Sept.
18 Sept.
30
26
22
18
Temperature
(CGD)
delta X (nT) RECORDED
20.0
12.0
4.0
- 4.0
-12.0
-20.0
delta X (nT) CORRECTED
10.0
6.0
2.0
- 2.0
- 6.0
-10.0
C (x) = 1.0254
C (y) =-.0434
C (z) = .1738
C (t) = .5046

Fig.29.

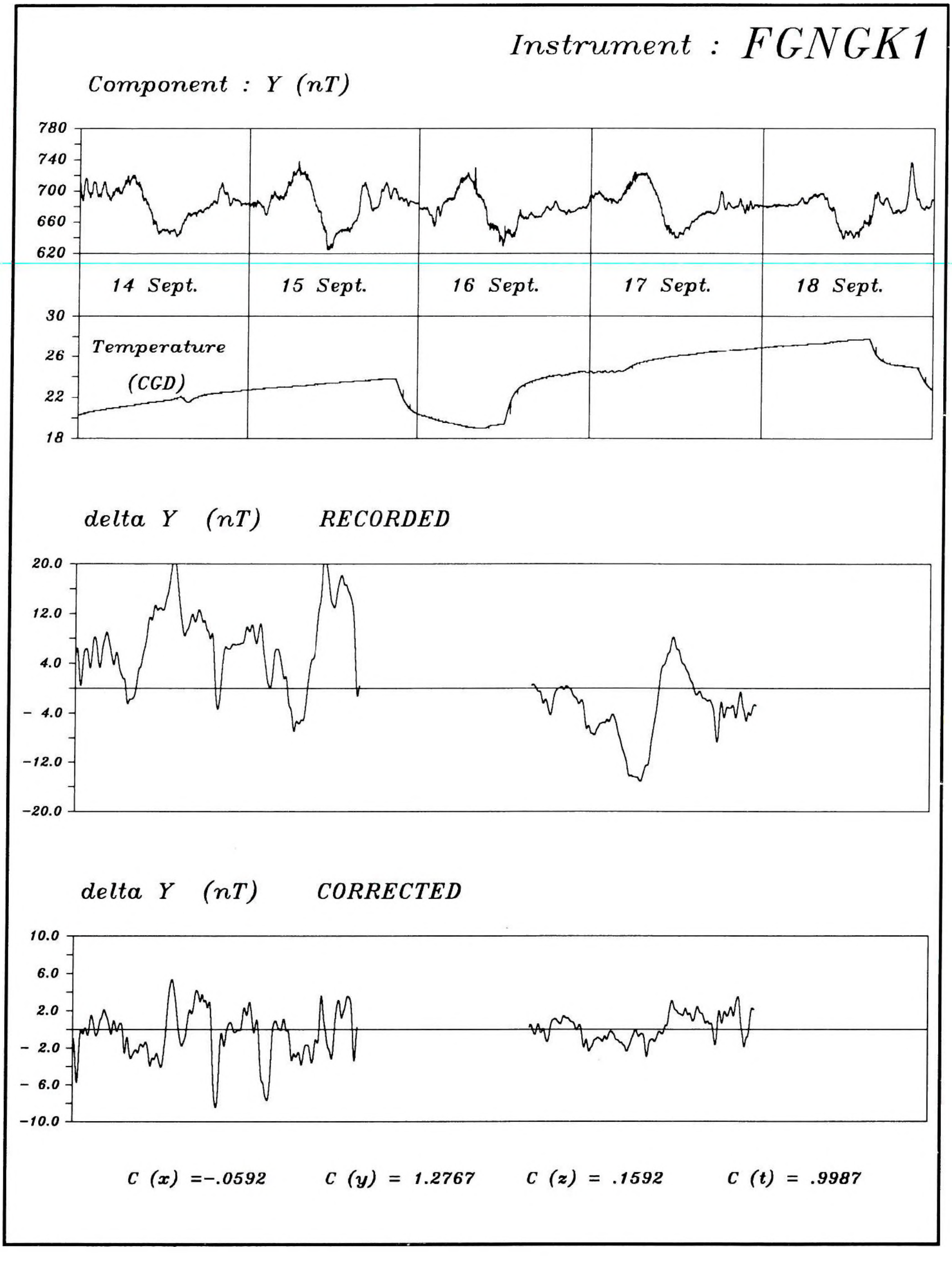
Instrument : FGNGK1
Component : Y (nT)
780
740
700
660
620
14 Sept.
15 Sept.
16 Sept.
17 Sept.
18 Sept.
30
26
22
18
Temperature
(CGD)
delta Y (nT) RECORDED
20.0
12.0
4.0
- 4.0
-12.0
-20.0
delta Y (nT) CORRECTED
10.0
6.0
2.0
- 2.0
- 6.0
-10.0
C (x) =-.0592
C (y) = 1.2767
C (z) = .1592
C (t) = .9987

Fig.30.

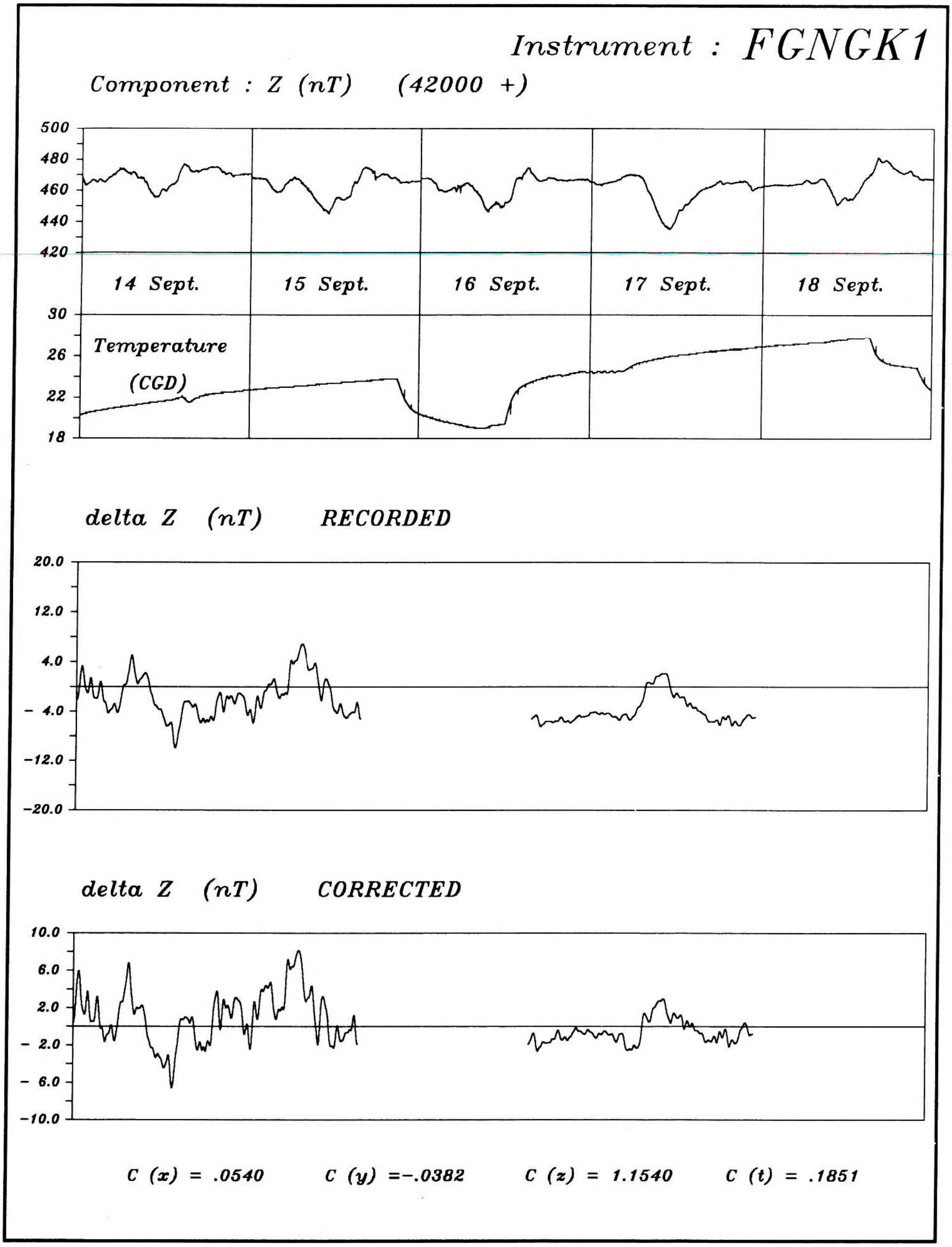

Instrument : FGNGK1
Component : Z (nT) (42000 +)
500
480
460
440
420
14 Sept.
15 Sept.
16 Sept.
17 Sept.
18 Sept.
30
26
22
18
Temperature
(CGD)
delta Z (nT) RECORDED
20.0
12.0
4.0
- 4.0
-12.0
-20.0
delta Z (nT) CORRECTED
10.0
6.0
2.0
- 2.0
- 6.0
-10.0
C (x) = .0540
C (y) =-.0382
C (z) = 1.1540
C (t) = .1851

Fig.31.

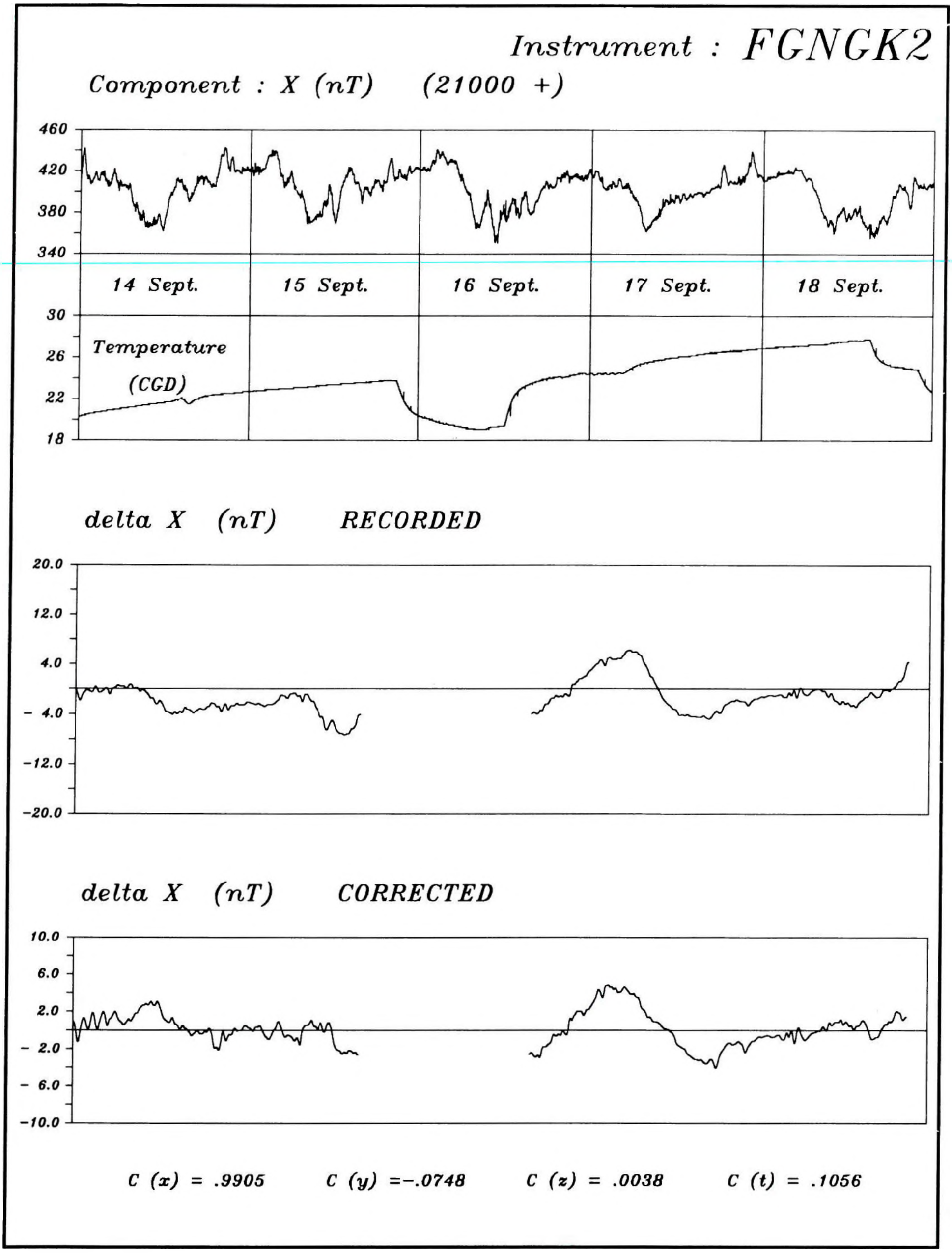
Instrument : FGNGK2
Component : X (nT) (21000 +)
460
420
380
340
14 Sept.
15 Sept.
16 Sept.
17 Sept.
18 Sept.
30
26
22
18
Temperature
(CGD)
delta X (nT) RECORDED
20.0
12.0
4.0
- 4.0
-12.0
-20.0
delta X (nT) CORRECTED
10.0
6.0
2.0
- 2.0
- 6.0
-10.0
C (x) = .9905
C (y) =-.0748
C (z) = .0038
C (t) = .1056

Fig.32.

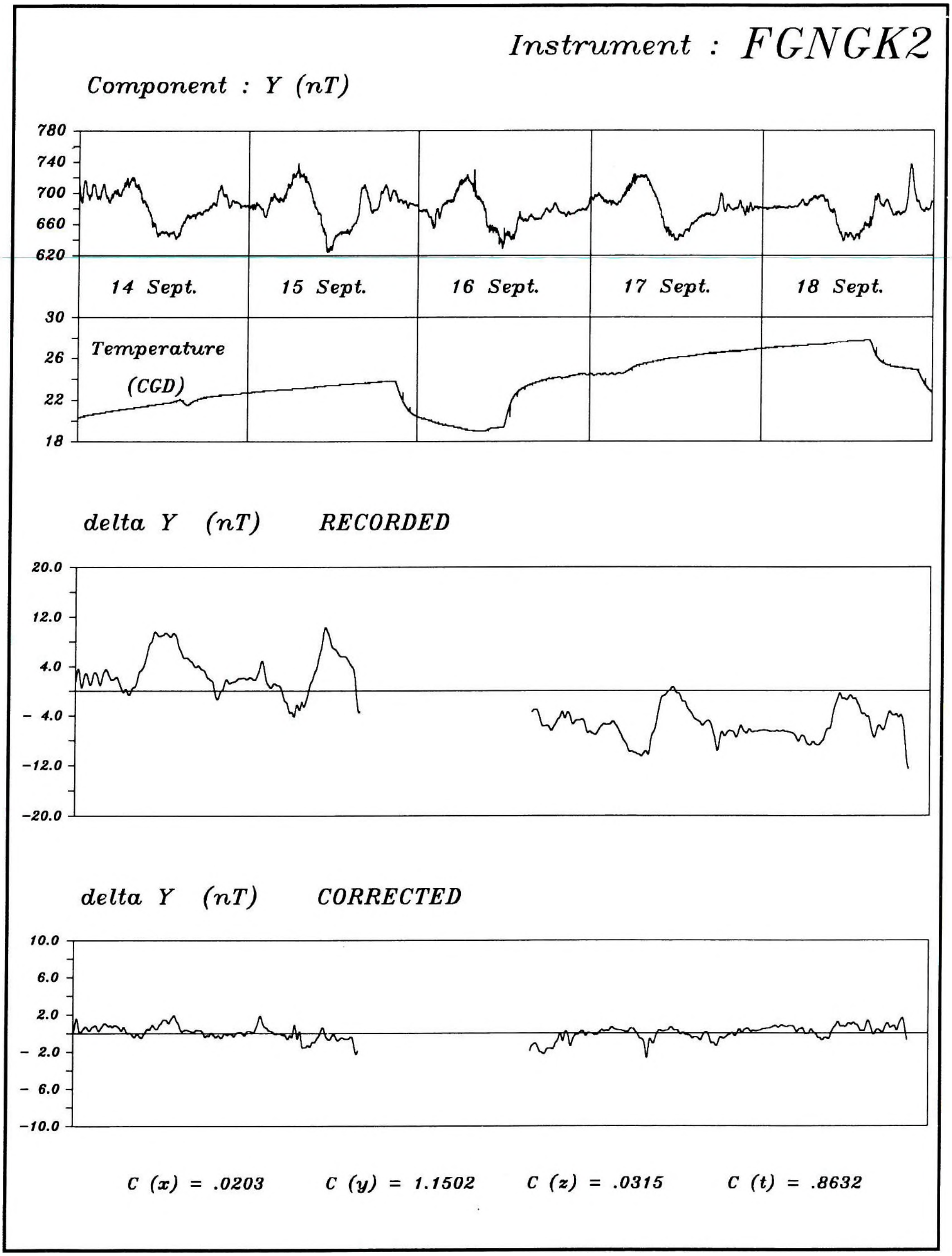
Instrument : FGNGK2
Component : Y (nT)
780
740
700
660
620
14 Sept.
15 Sept.
16 Sept.
17 Sept.
18 Sept.
30
26
22
18
Temperature
(CGD)
delta Y (nT) RECORDED
20.0
12.0
4.0
- 4.0
-12.0
-20.0
delta Y (nT) CORRECTED
10.0
6.0
2.0
- 2.0
- 6.0
-10.0
C (x) = .0203
C (y) = 1.1502
C (z) = .0315
C (t) = .8632

Fig.33.

The differences ($F_{measured} - F_{computed}$) before correction and after two kinds of correction are illustrated for three quartz variometers and for two fluxgate magnetometers in *Fig. 34–38.*

The coefficient matrices of PS2, SIG, QUZ2 variometers characterizing the sensitivities and orthogonality obtained by multilinear regression (C_{ij}) and by nonlinear parameter estimation (b_{ij}) are given for comparison.

C b

PS2

$$\begin{bmatrix} 1.0160 & 0.0064 & -0.0178 \\ 0.0056 & 1.0253 & -0.0074 \\ 0.0093 & 0.0032 & 1.0035 \end{bmatrix} \qquad \begin{bmatrix} 1.0068 & -0.0003 & 0.0048 \\ 0.0061 & 1.0001 & -0.0009 \\ 0.0084 & 0.0021 & 0.9930 \end{bmatrix}$$

SIG

$$\begin{bmatrix} 1.0061 & 0.0432 & 0.0113 \\ -0.0245 & 1.0136 & 0.0249 \\ -0.0032 & -0.0111 & 0.9743 \end{bmatrix} \qquad \begin{bmatrix} 1.0207 & -0.0070 & 0.0000 \\ -0.0024 & 0.9678 & 0.0012 \\ -0.0260 & 0.0075 & 0.9715 \end{bmatrix}$$

QUZ2

$$\begin{bmatrix} 0.9891 & 0.0015 & 0.0163 \\ 0.0197 & 0.9857 & -0.0079 \\ -0.0109 & -0.0018 & 0.9908 \end{bmatrix} \qquad \begin{bmatrix} 0.9689 & -0.0036 & 0.0041 \\ -0.0137 & 1.0015 & -0.0125 \\ -0.0093 & -0.0005 & 0.9981 \end{bmatrix}$$

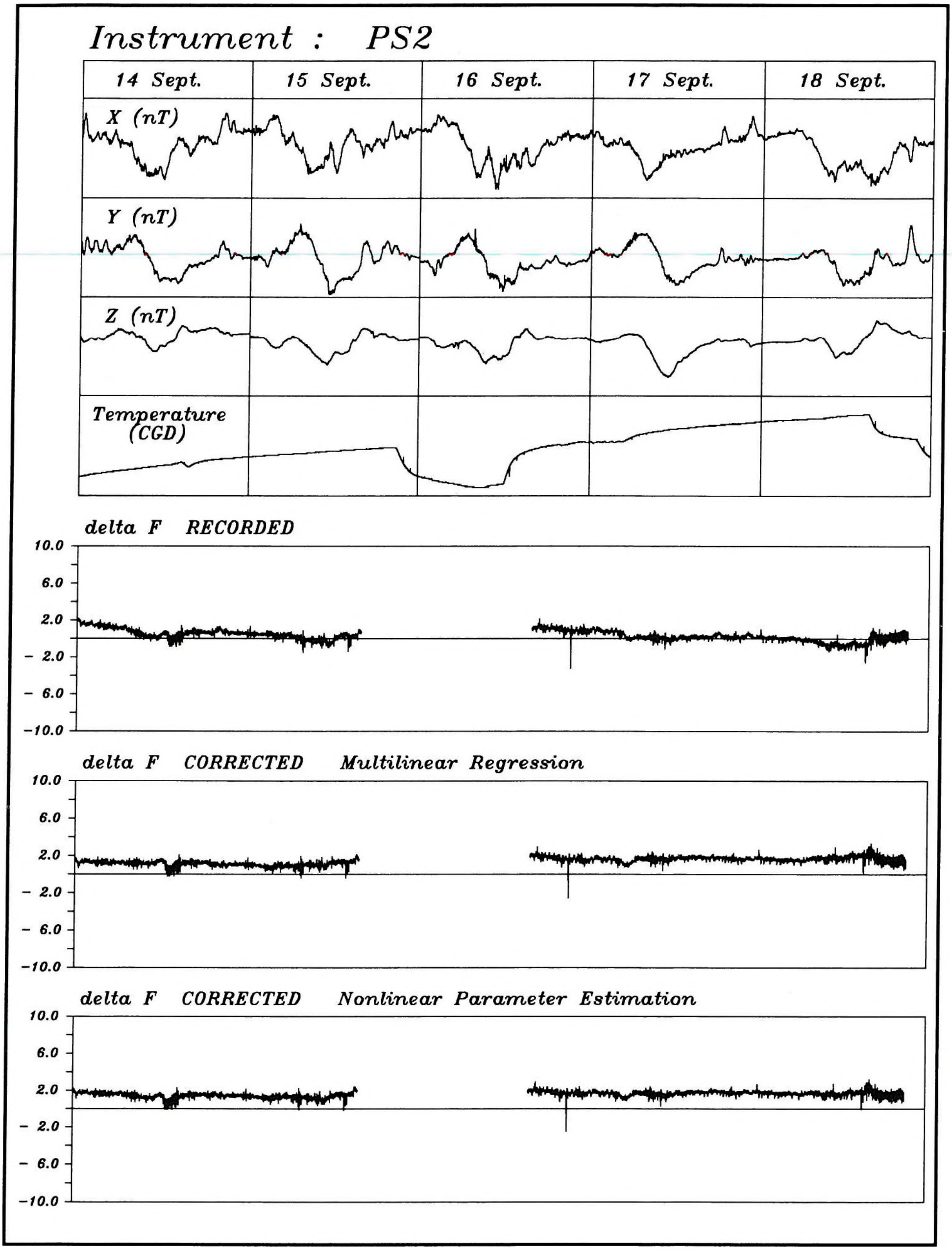
Instrument : PS2
14 Sept.
15 Sept.
16 Sept.
17 Sept.
18 Sept.
X (nT)
Y (nT)
Z (nT)
Temperature (CGD)
delta F RECORDED
10.0
6.0
2.0
- 2.0
- 6.0
-10.0
delta F CORRECTED Multilinear Regression
10.0
6.0
2.0
- 2.0
- 6.0
-10.0
delta F CORRECTED Nonlinear Parameter Estimation
10.0
6.0
2.0
- 2.0
- 6.0
-10.0

Fig.34.

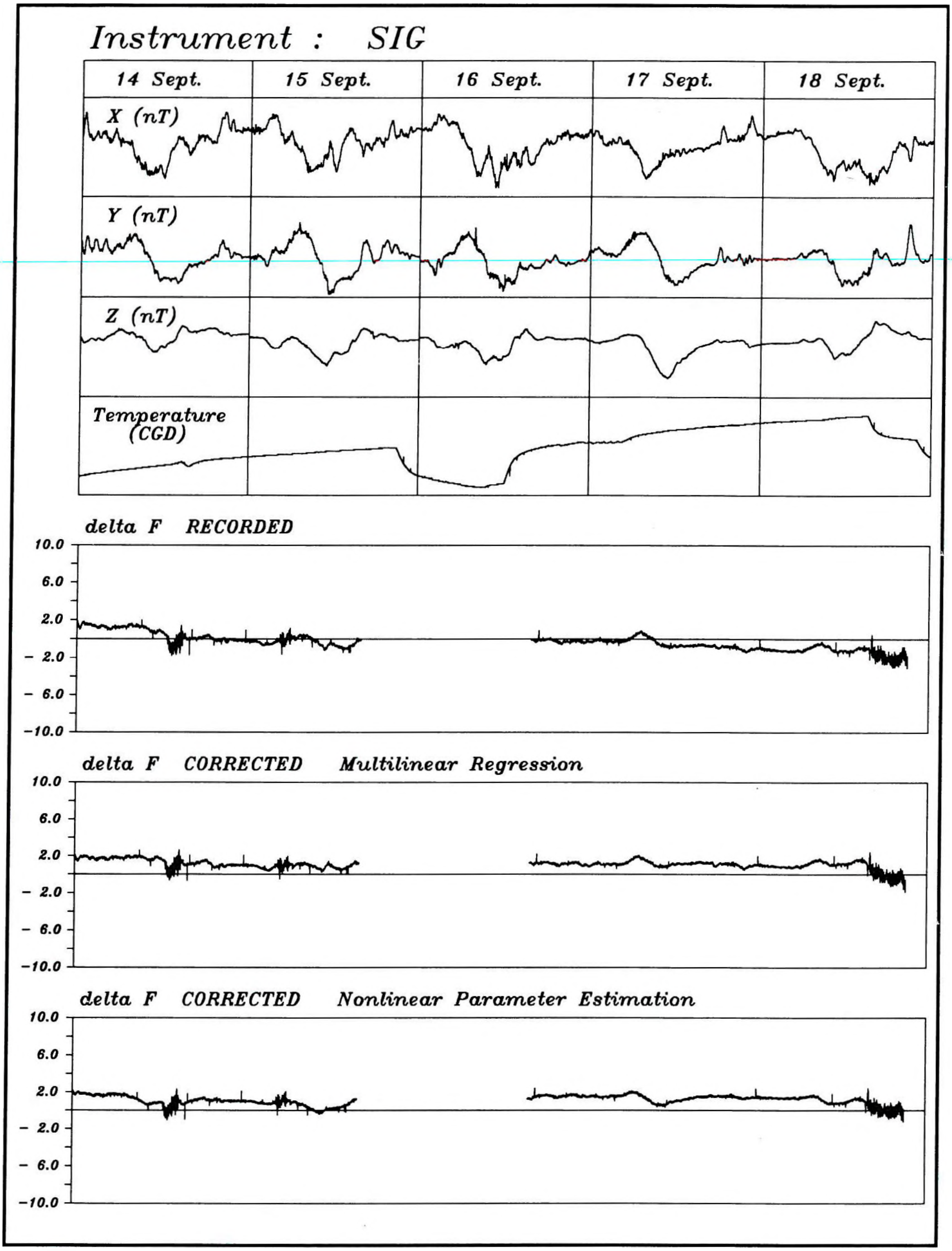
Instrument : SIG
14 Sept.
15 Sept.
16 Sept.
17 Sept.
18 Sept.
X (nT)
Y (nT)
Z (nT)
Temperature (CGD)
delta F RECORDED
10.0
6.0
2.0
- 2.0
- 6.0
-10.0
delta F CORRECTED Multilinear Regression
delta F CORRECTED Nonlinear Parameter Estimation

Fig.35.

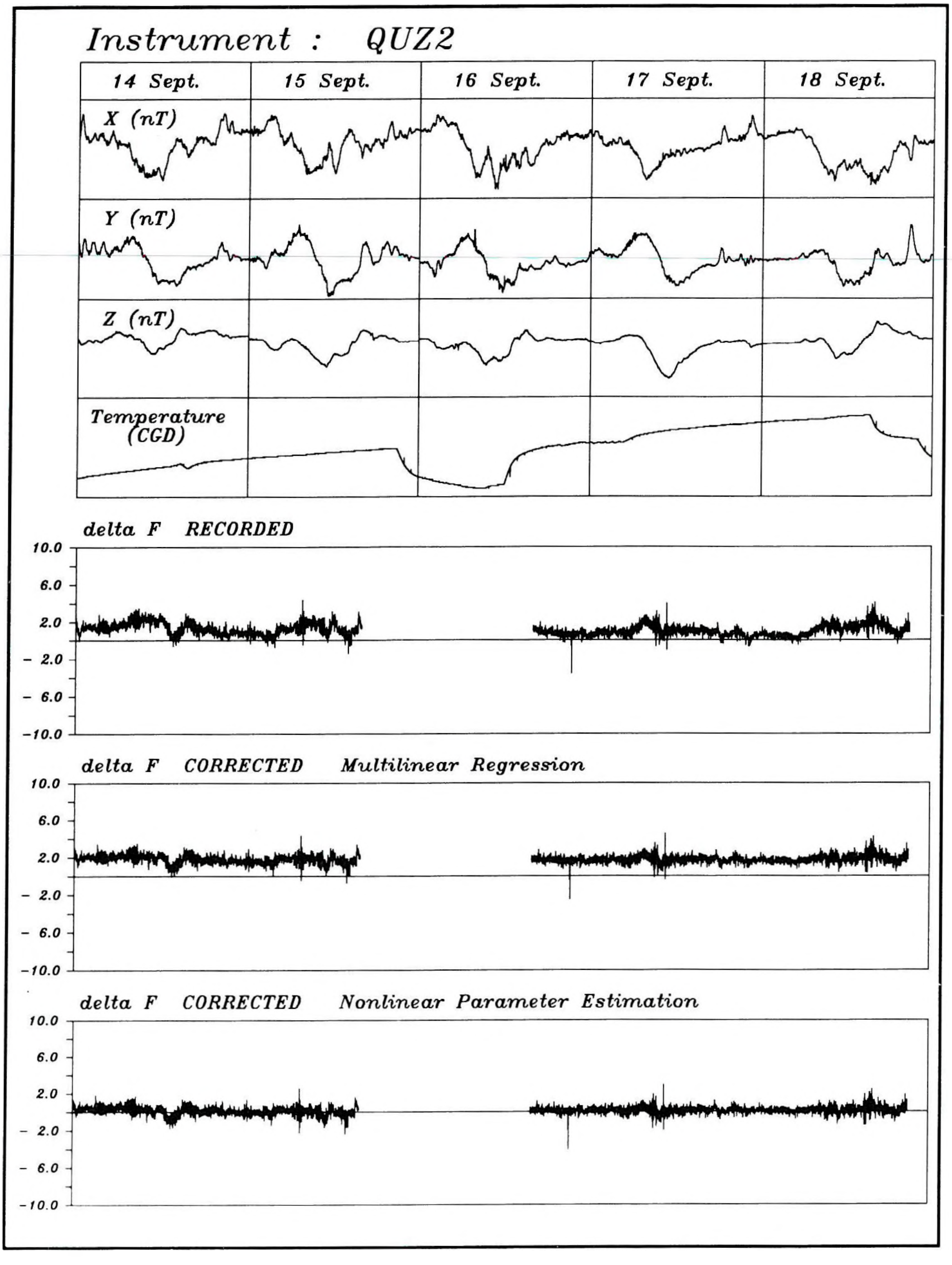
Instrument : QUZ2
14 Sept.
15 Sept.
16 Sept.
17 Sept.
18 Sept.
X (nT)
Y (nT)
Z (nT)
Temperature (CGD)
delta F RECORDED
delta F CORRECTED Multilinear Regression
delta F CORRECTED Nonlinear Parameter Estimation
10.0
6.0
2.0
- 2.0
- 6.0
-10.0

Fig. 36.

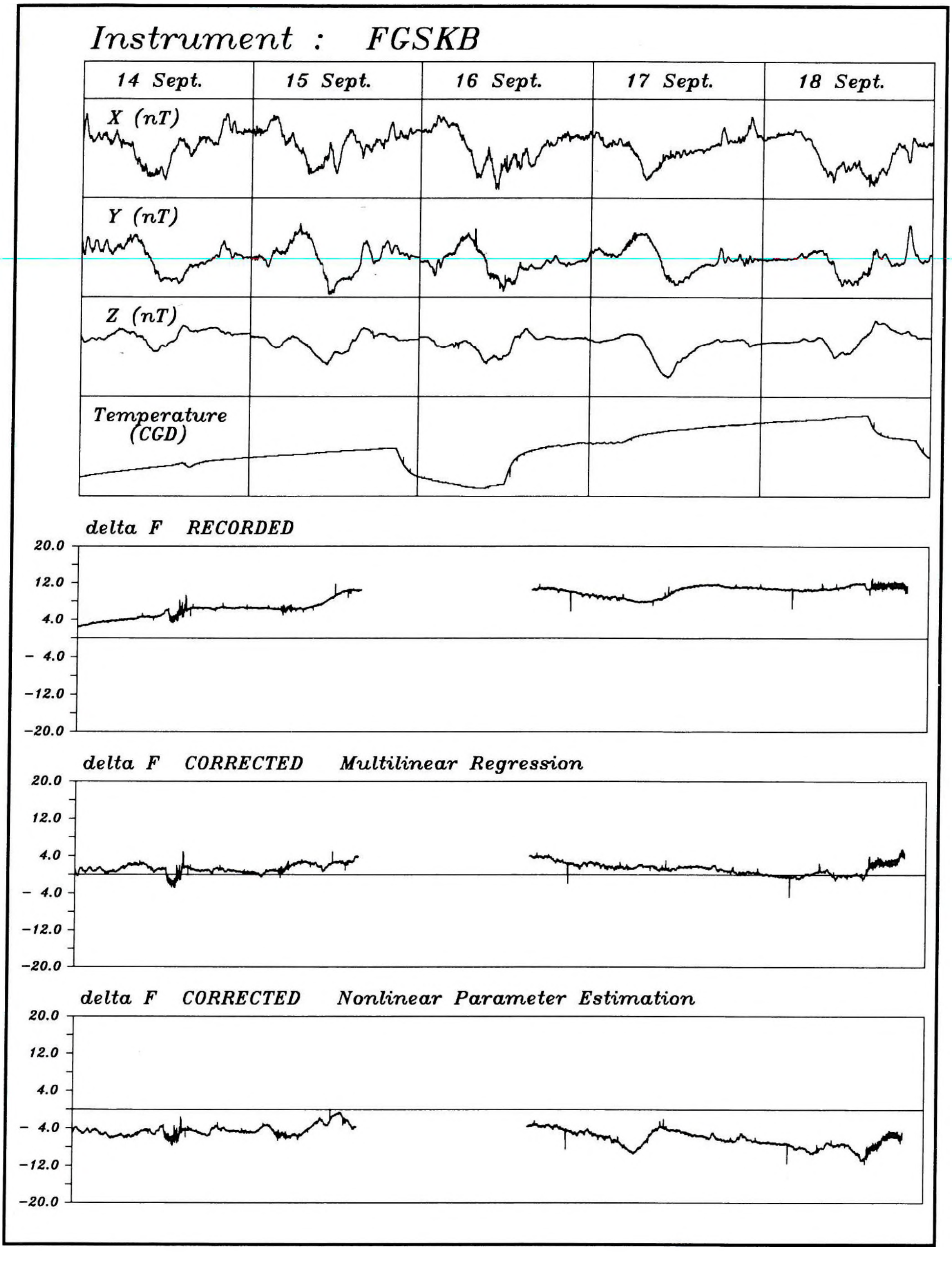
Instrument : FGSKB
14 Sept.
15 Sept.
16 Sept.
17 Sept.
18 Sept.
X (nT)
Y (nT)
Z (nT)
Temperature (CGD)
delta F RECORDED
20.0
12.0
4.0
- 4.0
-12.0
-20.0
delta F CORRECTED Multilinear Regression
20.0
12.0
4.0
- 4.0
-12.0
-20.0
delta F CORRECTED Nonlinear Parameter Estimation
20.0
12.0
4.0
- 4.0
-12.0
-20.0

Fig.37.

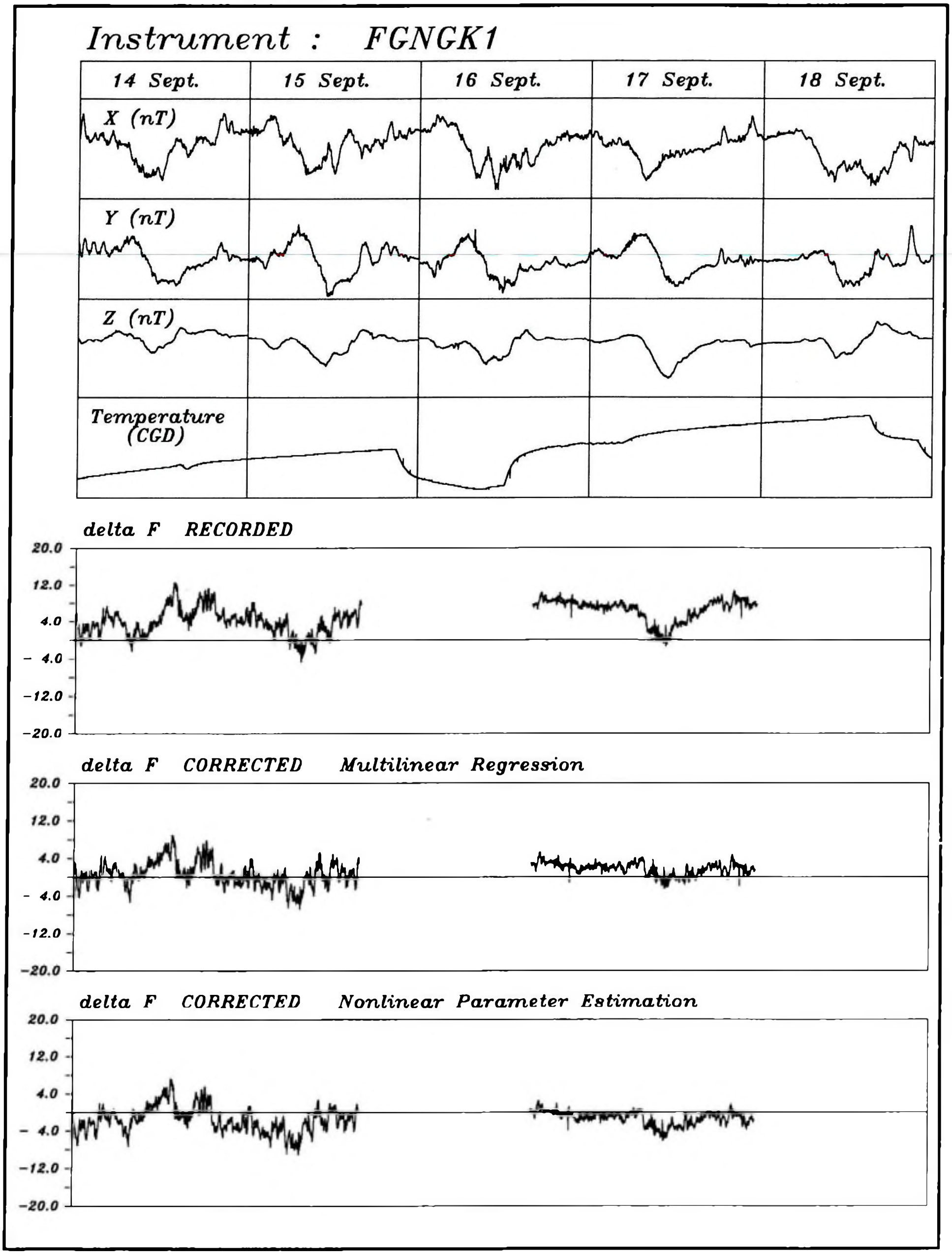
Instrument : FGNGK1
14 Sept.
15 Sept.
16 Sept.
17 Sept.
18 Sept.
X (nT)
Y (nT)
Z (nT)
Temperature (CGD)
delta F RECORDED
20.0
12.0
4.0
- 4.0
-12.0
-20.0
delta F CORRECTED Multilinear Regression
20.0
12.0
4.0
- 4.0
-12.0
-20.0
delta F CORRECTED Nonlinear Parameter Estimation
20.0
12.0
4.0
- 4.0
-12.0
-20.0

Fig. 38.

4. Test of quartz variometers during the time elapsed between the Nurmijärvi and Tihany Workshops.

The Hurbanovo Geomagnetic Observatory was equipped with a complete digital variation system CMVS-2 made by SKB (Soviet Union) in 1982. Quartz variometers originally belonging to a CMVS-2 system were installed in Tihany Geophysical Observatory in 1985. (They are connected to a DIMARS data acquisition unit.) Periodically, manufacturers compare their new instruments and the systems installed earlier in both observatories. The original intention of the authors of the Introduction was to give a report on the comparative recording made by CMVS-6 and CAIS in Hurbanovo and in Tihany as a supplement to this proceedings. But in view of the manuscript of V. Odintsov the Editors suggested that the description of instruments should be omitted (covered more exactly by him in this volume) thus the authors have tried to summarize the main results.

4.1. Hurbanovo, 4–16 June 1989

The CMVS-2 variometers of the HUR observatory are kept at a constant temperature. The sensors for the CMVS-6 and CAIS of SKB were installed on piers for transitory use in the garden of the observatory. The temperature dependence of the CMVS-6 was determined using the CMVS-2 HUR as a reference:

CMVS-6 (SKB)	D < 0.1 nT / CGD
	H < 0.2 nT / CGD
	Z < 0.1 nT/CGD

By analysing the records of both systems the following relationship was found:

$$D_{CMVS\text{-}6} + 0.047 \; Z_{CMVS\text{-}6} = 0.97 \; D_{CMVS\text{-}6}$$

$$H_{CMVS\text{-}6} + 0.2 \; t = 0.98 \; H_{CMVS\text{-}6}$$

$$Z_{CMVS\text{-}6} - 0.0375 \; D_{CMVS\text{-}6} = 0.965 \; Z_{CMVS\text{-}6}$$

The base-line values of the instruments installed in the garden changed as a consequence of a heavy rainfall. The authors supposed the real cause of the change in the baseline values to be the tilting of the piers. Therefore the influence of tilting has been tested and the results are given for the CMVS-6 (in nT/arc min)

tilting to axis	component D	H	Z
X	-	-1.5	-3.75
Y	-2.5	-	-1.25

The hypothesis of the manufacturers is that the slow shift in baseline of quartz variometers is mainly caused by the tilting of the piers.

4.2. Tihany, 17 – 26 June 1989

With regard to the possibilities at Tihany Observatory we focused on the spectral analysis of CAIS and on application of nonlinear parameter estimation. For visual comparison the differences between the total field calculated from components (F_{calc}) and the same measured by a proton magnetometer (F_{meas}) are given for CMVS-6 and CMVS-2 and (THY) in *Fig. 39.* The coefficients for sensitivities and directions obtained by the HILL algorithm are as follows

CMVS-6 (SKB)			CMVS-2 (THY)		
0.9782	-0.0045	-0.0150	1.0588	0.0110	0.1114
-0.0193	0.9629	-0.0181	0.0031	1.0001	-0.0089
-0.0085	-0.0316	1.0322	0.0521	0.0131	1.0368

4.3. Test of the fluxgate magnetometer of the Academy Science of the Ukraine (FGASU) in February 1991

The FGASU was preregistered at the Tihany workshop but it was tested later for administrative reasons. This has meant two advantages:

— we had the experiences gained during the workshop

— we carry out the temperature test in the range 0–30 C°.

The FGASU magnetometer is installed in the absolute house, and the quartz variometers of the Tihany Observatory (kept at constant temperature) were used as a reference. The temperature dependence of the sensor and that of electronics were tested separately.

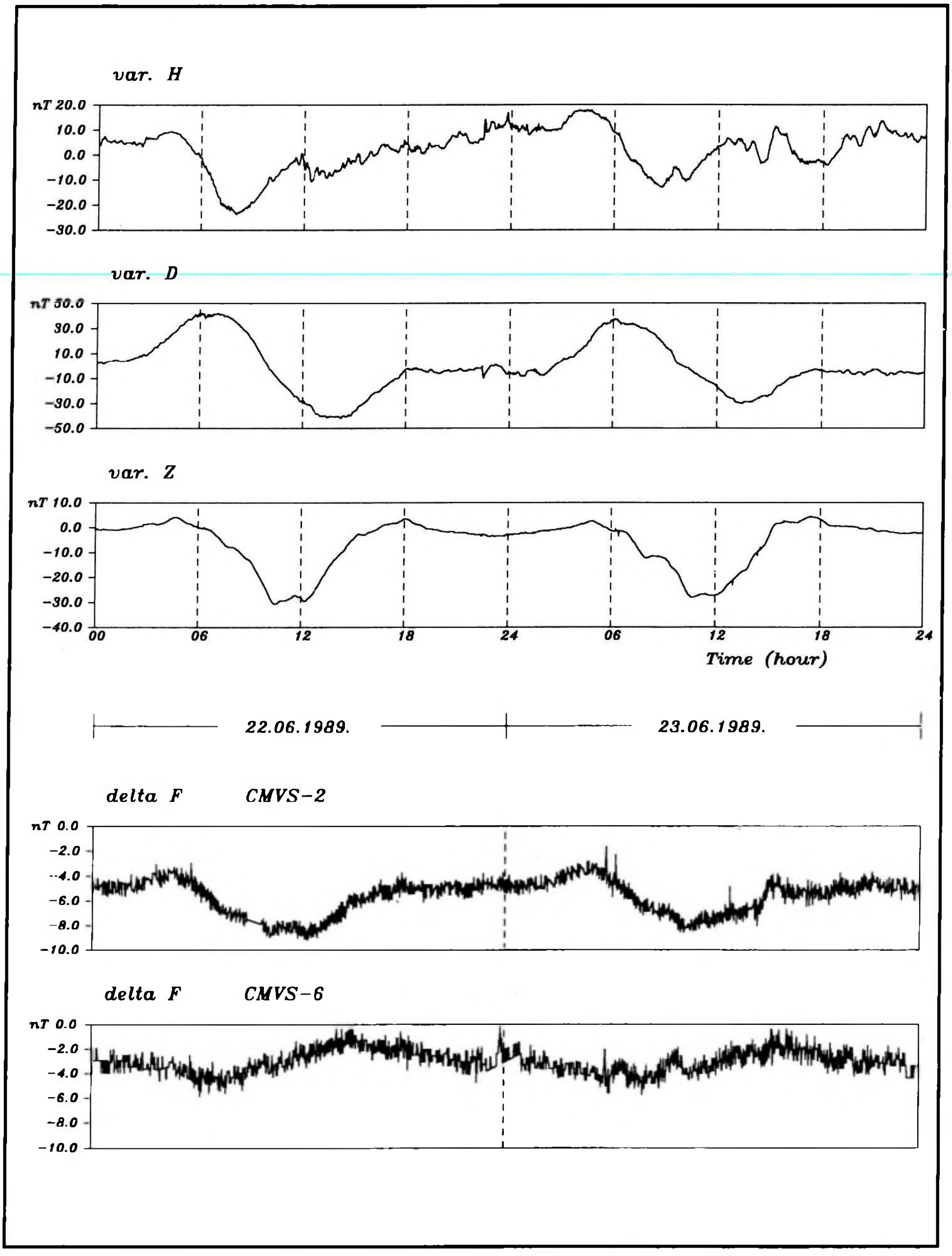
var. H
nT 20.0
10.0
0.0
-10.0
-20.0
-30.0
var. D
nT 50.0
30.0
10.0
-10.0
-30.0
-50.0
var. Z
nT 10.0
0.0
-10.0
-20.0
-30.0
-40.0
00
06
12
18
24
06
12
18
24
Time (hour)
22.06.1989.
23.06.1989.
delta F CMVS-2
nT 0.0
-2.0
-4.0
-6.0
-8.0
-10.0
delta F CMVS-6
nT 0.0
-2.0
-4.0
-6.0
-8.0
-10.0

Fig.39.

The temperature coefficients for the sensor:

D	< 0.1 nT / °C
H	< 0.3 nT / °C
Z	= 0.65 nT / °C
for electronics (every channel)	
	3.5 nT / °C

The orientation in the horizontal plane of FGASU and QUZ THY was slightly different . The difference in the *Z* component and in the temperature versus time is given in *Fig.40.*

5. List of Recording Instrumets

Instrument	Manufacturer	Code in this volume
TPM	Belsk Geophys.Observatory	PS1 PS2
Quartz	IZMIRAN	QUZ1 QUZ2
SIGMA	SKB	SIG
FM - 2	SKB	FG SKB
IKF	Interkosmos Forschung	FG NGK1 FG NGK2
GEOMAG	GEOMAG	GEOMAG
RVM		RVM RVM (M)
GSM 19	GEM Sistem	GSM-19
	Instruments tested before or after the workshop	
CMVS-2 (DMVS-2)	SKB	CMVS-2
CMVS-6 (DMVS-6	SKB	CMVS-6
CAIS (DAIS)	SKB	CAIS
	Acad.Sci.Ukraina	FG ASU

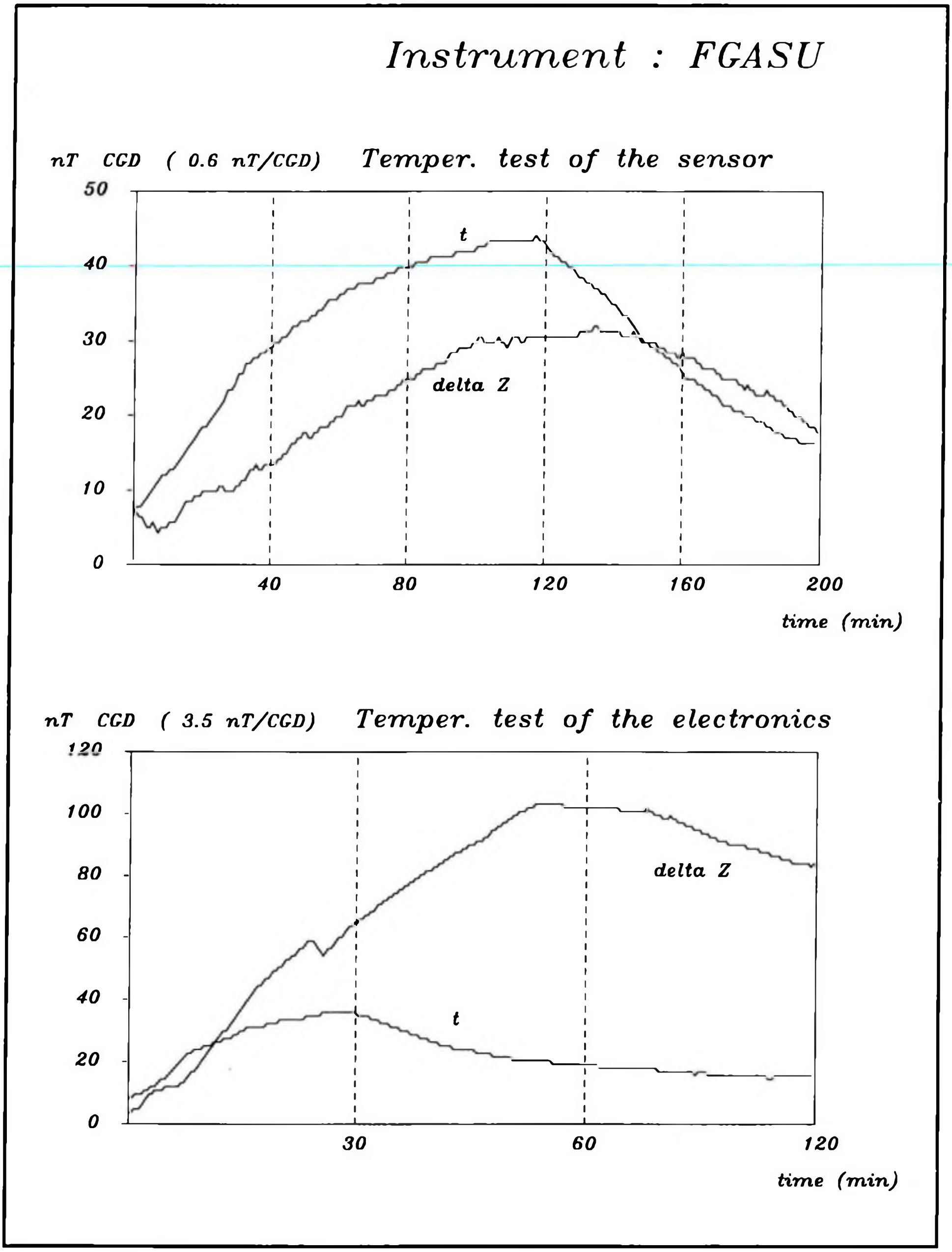
Instrument : FGASU
nT CGD (0.6 nT/CGD) Temper. test of the sensor
50
40
30
20
10
0
40
80
120
160
200
time (min)
t
delta Z
nT CGD (3.5 nT/CGD) Temper. test of the electronics
120
100
80
60
40
20
0
30
60
120
time (min)
delta Z
t

Fig.40.

PS 1 and PS 2

Quartz variometers with photoelectric converters connected to a digital data logger for use in the observatory and in the field. A detailed description is given by [MARIANUK 1977], [MARIANUK et al. 1978], [JANKOWSKY et al. 1984]. The instrument was tested in Ottawa [TUREWICZ at al. 1988], and it works in the Nurmijarvi observatory as the standard system of the observatory [(eds.) KAURISTIE et al. 1990].

Quartz 1 and Quartz 2

Quartz variometers with photoelectric transducers giving an analog (voltage) output. The instruments were connected to the DIMARS intelligent data acquisition system. A detailed description is given by [PAPITASHVILI 1990]

SIGMA

A stand-alone geophysical measuring station. The system is aimed at measuring the variation of the magnetic components of the Earth's electromagnetic field in the observatory or in the field. The intelligent system can run either built-in programs or user-developed programs. (Assembler, BASIC.)

Specifications

Measuring range:	
—magnetic induction, nT	-3200-: +3200
—voltage, V	-8-: +8
Value of LSB:	
—magnetic induction, nT	0.1
—voltage, mV	0.25
Dynamic range, dB	96
Relative error of measurement	0.001
Temperature drift of crystal sensors, nT/ °C	0.5
—with temperature corrections	0.1

Supply:

—mains supply (220-+ 22V, 50-+ 1 Hz)

—accumulator battery (24-+ 2.4 V or 12-+ 1.2 V)

Power consumption, V.A	-< 15

FM-2

Fluxgate magnetometer

The FM-2 is developed to measure the three components of the geomagnetic field on board a satellite but it can be used on the Earth's surface too. The instrument has a modular structure. This makes it possible to reduce the measuring range and increase the resolution and accuracy by surface application. The distance between the sensor and control electronics is max. 10 m. Part of specification:

On board a satellite :	
dynamic range	-65500 -: 65500 nT
resolution (LSB)	1 nT
main absolute error	15 nT
bandpass	DC to 1 Hz
orthogonality error	less than 30 min. of arc.
operating temperature	-60 -: 60 °C (sensor only)
power consumption	8 W (typical)
By surface application:	
dynamic range	-1024 -: 1024 nT
bandpass	DC to 10 Hz

GEOMAG Automatic Magnetic Observatory

It is mentioned that GEOMAG is a French company and its automatic magnetic observatory differs from the GEOMAG 1 fluxgate magnetometers of Dowty Ltd. Since 1986, the department of geomagnetism of the Institut de Physique du Globe de Paris (IPGP) has been involved in a program named Observatoire Magnetique Planetaire (OMP), a worldwide project of fifteen to twenty automatic magnetic observatories. The development of the vector magnetometer for the OMP project was carried out by a team of engineers from IPGP and Thomson-Sintra ASM, a major French company dealing with applications in electronics and magnetics. The scalar magnetometer for this equipment was developed by GEM SYSTEMS, a Canadian company specialized in Overhauser Effect Magnetometers. Each automatic observatory is tested and certified by Institut de Physique du Globe de Paris at the Chambon la Foret Magnetic Observatory.

GEOMAG vector magnetometer

3 components fluxgate magnetometer.
Orthogonality error of axis: <0.5 minutes of arc.
Perfect long term and thermal stability of axis alignment.
Resolution: 0.1 nT.
Dynamic range: -11,800/+64,800 nT
Band pass: software flexible from D.C. to 3.5 Hz.
Noise: 0.05 nT rms.
Long term stability: <3 nT/year
Sampling rate: software flexible from 1 min to 20 Hz.
Simultaneous sampling of the three components.
Temperature measurement on sensor: range +/-100°C, resolution 0.1°C.
Temperature coefficient of sensor: <0.1 nT/ °C
Temperature coefficient of electronic console: .0.1 nT/ °C

GEOMAG scalar magnetometer

Overhauser Effect proton magnetometer.
Resolution: 0.01 nT.
Dynamic range: 20,000/120,000 nT, automatic tuning.
Absolute accuracy: 0.2 nT.
Long term stability: 0.05 nT/year.
Sampling rate: 3 sec. minimum interval.

General Information

NEC V40 MS-DOS PC compatible micro computer.
RS232 serial output.
Large (250 x 81 mm) LCD graphic display (optional).

Time base stability: 3 s/year
stability over operating temperature <1 ppm
aging less than 1ppm/year.
GOES, GMS or METEOSAT satellite data collection platform available (INTERMAGNET project)
100 x 160 mm Eurocard design.
Size
Scalar sensor: Cylinder diameter: 70 mm, length: 150 mm.
Vector sensor: Cylinder diameter: 180 mm, height: 180 mm without suspension; 300 mm with suspension systems (EMR Canada License).
Electronic console: 19″ standard, rack 3U height (optional fibreglass waterproof packaging).
Weight:29 kg. Power requirements: 12 V D.C. 15 W.
Operating temperature: -40 to +60°C.
MTBF: 3 years.
MTTR: 1 hour.

Rubidium Vector Magnetometer

A detailed description is given by J. Rasson in this volume.

Three-component fluxgate magnetometers made in Germany at the Niemegk Geomagnetic Observatory.

Two versions of the magnetometer were tested during the workshop: one with analog (voltage) output, the other with built-in digital data-logger. Unfortunately the editors have not received any technical data or description of the instruments.

GSM-19 Overhauser memory magnetometer gradiometer of GEM SYSTEMS

The GSM-19 is a versatile high sensitivity Overhauser effect (proton) magnetometer designed for operation in the field and in the observatory.
Summary of features and advantages:
1. Increased survey productivity. At each station the operator depresses One key to take and store a reading of magnetic field with coordinates, date and time and up to 3 VLF stations.
2. True 0.1 nT sensitivity, 0.2 nT absolute accuracy ensures highest quality

ground surveys.
3. Full synchronization of the mobile and base station makes the data free of diurnal variations even during magnetically active days, eliminating down time and allowing for better planning and execution of surveys.
4. Computer compatibility facilitates and greatly speeds up automated data processing and interpretation thus further increasing productivity.
5. High absolute accuracy and long term stability make GSM-19 a primary standard for measurement of the Earth's magnetic field, suitable for any long term monitoring of the field and calibration of other instruments such as fluxgates (for component measurement) and other proton or alkali vapour magnetometers.
6. Very flexible hardware/software design allows for quick mods for any special measurements of magnetic field of the Earth.

Resolution:	0.01 nt (0.01 gamma)
Absolute accuracy:	0.2 nT
Range:	20,000-120,000 nt, autotuning, manual override
Gradient tolerance:	up to 10,000 nT/m
Operating modes:	
manual:	automatic storage of label, time and date, magnetic field, 3 sec. minimum interval
base station:	3 to 60 sec. intervals standard, others optional, time, date, magnetic field stored
remote control:	the same as manual but controlled through
RS232C interface	
Storage capacity:	
manual operation:	3,800 standard, 30,000 optional; with 3 VLF stations 1,850 standard, 3,700 optional
base station:	21,800 standard, 174,000 optional (24 hr operation at 0.5 sec interval)
gradiometer:	3,200 standard, 26,000 optional; with 3 VLF stations 1,700 standard, 3,400 optional

Power consumption:	2 Ws per reading, up to 0.5 W standby, less than 0.4 mW when off.
Power source:	12 V 1.9 Ah sealed lead acid battery standard, others optional
Operating temperature:	-40 to +60° C
input/output:	6 pin weatherprof connector, rs-232c, and (optional) analog output.

CMVS-2 Quartz variometers

The oldest version of the digital systems for recording the variation of the geomagnetic field developed by the Special Constructing Bureau (SKB) of the Acad. Sci. of the Soviet Union in the late 70's. A description is given by [PODSKLAN et al 1984].

CMVS-6

A digital magnetometer with quartz sensors was developed for use in unmanned stations in the near-polar region. A sophisticated system using all experiences gained with CMVS-2 stations. Its special hardware and data-format make it possible to store one-minute data over 400 days on a C-120 audio tape cassette. A description is given by [AMIANTOV et al. 1990].

CAIS

A stand-alone digital measuring system has been developed to record the variation of the Earth's electromagnetic field. Equipped with quartz variometers having new structure, and with programmed timer it is suitable for studying global magnetohydrodynamic phenomena in combination with powerful pulsed sources. A deep analysis of the system is given by Odintsov in this volume.

Specifications

Measurement range:

—magnetic induction, nT	from -1310 to 1310
—voltage, mW	

from -131 to 131

Nominal ADC resolution:	
—magnetic induction, nT	0.01
—voltage, mkV	1
Number of measuring channels	6
Dynamic range of measuring channels, dB	108
Frequency range, Hz	0 - 15
Sampling rate, sec	0.01
Power consumption, V.A, max	20
Power source voltage, V	24

6. Absolute measurements.

Participants and Instruments.

D. Gilbert	DI - fluxgate
G. v. Beek	DI - fluxgate
G. Schulz	DI - fluxgate
K. Pajunpaa	DI - fluxgate
J. Kultima	DI - fluxgate
O. Rasmussen	DI - fluxgate
J. Rasson	DI - fluxgate
J. Marianuk / J. Reda	QHM
M. Alexandrescu	QHM
V. Auster	Miniaturized Vector Proton m
V. Belov	Miniaturized Vector Proton m.

The number of instruments classified by their operating principle:

Workshop	DI-fluxgate	QHM	Other
Ottawa , 1986	6	2	1
Nurmijärvi ,1989	7	4	2
Tihany , 1990	7	2	2

We did not mention in the chronicle of the Workshop that Daniel Gilbert visited the observatory in July 1990 and he offered to make absolute measurements in the period of the workshop. His rigorous work started on 9th September and finished on 21st September, making it possible to check the baseline values of the Tihany recording system before and after the common recordings. Reference pier No.1 in the absolute house has been rebuilt and a new pier has been erected in the garden of the observatory in front of the workshop. The reference marks of the observatory are the towers of the abbey church. Let us illustrate by example how precisely Daniel Gilbert did his observations. The two piers combined with the two towers give four sets of determinations of declination. He checked the true azimuth by sun-shot nearly every day. On analysing his four series of measurements he found a difference in order of magnitude of 5 arc seconds. Daniel was convinced that it must be a systematic error. In view of this he searched for the cause. He observed the angular difference between the two towers every ten minutes from sunrise till noon. He demonstrated that the difference increased continuously by 7 arc seconds from sunrise to noon due to the thermal dilatation of the towers.

7. Remarks and conclusions

Most of the recording instruments tested during the workshop in Tihany were not tested in Ottawa or in Nurmijärvi. There were quite ‘old’ (such as the PS1 and PS2 quartz variometers developed in 1976) but very stable, and quite new (such as GEOMAG developed in 1990) representing the highest technology among them. One of the paradoxes of the workshop was that the old model surpassed the latest one.

The manufacturers followed three independent ways of developing magnetometers:

— magnets suspended on a torsion wire with electro-optical transducer (quartz variometer),

— having a saturable-core as a sensing element (ringcore fluxgate magnetometer),

— optically pumped vector magnetometer (RVM).

In spite of the three different principles of operation the parameters of the instruments are similar. The records of the quartz variometers were unambiguously better than the records of the fluxgate sensors tested in Tihany. The rubidium vector magnetometer is really attractive for its high resolution and wide frequency range but these are compensated by its relatively short span of life and its price.

The manufacturers of instruments tested in Tihany have to focus (at least) on two topics in the near future:

— to improve the signal/noise ratio,

— to avoid the big power supply and electronics boxes connected by a short cable to the sensors.

Many quartz variometers have a calibration error 1-4%. This probably comes from their very simple technique for calibration: a single circular turn around the variometer-body. It is recommended to calibrate the variometers in Helmholtz coils.

The two general conclusions correspond to the conclusions drawn in Nurmijärvi: — 'the recordings still seem not to be enough for an accuracy of one nanotesla,

— the series of Workshops started in Ottawa needs to be continued'.

REFERENCES

AMIANTOV A. S., ZAITSEV A. N., ODINTSOV V. I. 1990: The unmanned geophysical data collecting platform based on the digital magnetometer CMVS-6. Physics of the Earth and Planet. Int. **59**, pp. 61-65

JANKOWSKI J., MARIANUK J., RUTA A., SUCKSDORFF C., KIVINEN A. 1984: Long-term stability of a torque balance variometer with photoelectric converters in observatory practice. Geophysical Survey **6**, pp. 367-380 (eds.) KAURISTIE K. SUCKSDORFF C., NEVANLINNA H. 1990: PSM as Nurmijärvi standard. Proc. of the Internat. Workshop on Geomagn. Observatory Data Acquisition and Processing. pp. 26-27

MARIANUK J. 1977: Photoelectric converters for recording the geomagnetic field elements: construction and principle of operation. Publ. Inst. Geoph. Pol. Acad. Sci. C-4 (114)

MARIANUK J., GNOINSKI A., SZYMANSKI A. 1978: Recording of geomagnetic field elements with a photoelectric magnetometer. Publ. Inst. Geoph. Pol. Acad. Sci. C-5 (125)

PAPITASHVILI V. 1990: IZMIRAN quartz photoelectric variometer QPEV

PODSKLAN J., KOVAC I. 1984: One year experience with CMVS-2 magnetic variation station. Geophzsical Survey 6, pp. 317-322

TUREWICZ W., SUCKSDORFF C., HÄKKINEN L. 1988:Magnetometre photoelectique a torsion mpt. (Compte Rendu d'Atelier International sur les Instruments d'Observatoire Magnetique) Comission Geologique du Canada. Etude 88-17

GEOPHYSICAL TRANSACTION 1991
Vol. 36. No. 3-4. pp 187-194

RUBIDIUM VAPOUR VECTOR MAGNETOMETER

Jean RASSON*

The paper deals with a rubidium vapour vector magnetometer attached to an IBM PC. This applies a new polarization technique and fast high resolution frequency measurement in order to increase accuracy. It recalls how a RVM (rubidium vector magnetometer) was installed in Tihany during the Workshop and it comments on the recorded data.

Keywords: rubidium vector magnetometer

1. Introduction

The triaxial magnetometer uses the mechanical design of the ASMO system developed by Alldredge in the sixties [ALLDREDGE and SALDUKAS 1964] and constructed by Varian for the USCGS (type 4980A). It is basically a DI Helmoltz coil system (22″ diameter/42 turns) allowing homogeneous bias fields (26000 nT) to be applied on an optical pumping total field magnetometer. By making five successive measurements on the Larmor frequency using the appropriate coil polarizations, the total field F and the variations of the D and I angular components of the geomagnetic field vector can be extracted [BACON 1955]. The optical pumping magnetometer is a Varian type 49-538A which claims a useful resolution of 0.005 nT.

Hence the novelty in this magnetometer consists in the new data acquisition and management system, new polarization technique and fast high resolution frequency measurement resulting in improved overall accuracy.

* Institute Royal Météorologique, Centre De Physique du Globe, B-5670 Dourbes Belgique

The design goal was:

— to obtain one complete vector *(D, I, F)* measurement every second in time with a useful resolution of about one second of arc or one tenth of a nanotesla;

— to compute from this data minute means and store them on an IBM PC compatible 720 kilobytes diskette;

— to save the non-averaged instantaneous second data in a separate file on a contact closure, in the event of an absolute measurement occurring for baseline determination.

The instantaneous second data should also be capable of being used to generate an *H* component analog record with 0.01 nT resolution for micropulsation studies. Operations such as clock adjustment or diskette exchange should not interrupt the data acquisition. The display of the most recent data, both instantaneous and minute means, should be given on a graphic screen.

2. The data acquisition system

The Magnetometer has been provided with an IBM PC compatible computer equipped with real time clock, with one 360 kilobytes 5 1/2″ and one 3 1/4″ 720 kilobytes disk drive but without a hard disk. There is also a Hercules graphic card and a digital 48 lines I/O card. The high resolution counter (Guide Technology 200) is also an IBM PC compatible card installed inside the computer case.

A constant current source delivering approximately 120 mA is switched by two low power transistor *H*-bridges to provide the alternating polarizing currents to the ASMO coils. These currents are allowed to stabilize for 50 ms before an actual frequency measurement is taken on the Larmor frequency. The frequency measurement proper is made in exactly 20 ms. All the timing is clocked by the PC and the mains frequency, which is derived by way of a transformer and a 4046 CMOS phase-locked loop. This is necessary to remove the almost always present 50 Hz mains pollution of the magnetic field. Other time domain filtering on the Larmor signal is difficult. The polarization and measurement are initiated by the PC through a single pulse sent over the parallel interface.

3. Scale values

One of the advantages of this Bacon type variometer is that the scale values can be computed by data given by the instrument itself, provided that the rubidium vapour magnetometer is correctly calibrated. This latter means that one has determined the constants of the 'head equation', relating the Larmor frequency with the magnetic field. It has been empirically ascertained that for observatory use a linear relationship is sufficiently accurate:

$$F\,(\mathrm{nT}) = A\,(\mathrm{nT/Hz}) \cdot f\,(\mathrm{Hz}) + B\,(\mathrm{nT}) \qquad (1)$$

where F is the total field, f is the Larmor frequency, and A and B are the constants of this head equation. The constants are computed after a sufficient number of absolute total field measurements have become available for a least squares adjustment. The constant B may contain any dF due to spatial gradient between the reference absolute pillar and the RVM.

The scale value J in degrees per Hertz for the D component is given by [ALLDREDGE and SALDUKAS 1964]:

$$J = (180/\pi) \cdot (E \cdot A \cdot F_o)/H_o\,, \qquad (2)$$

the scale value K in degrees per Hertz for the I component is:

$$K = (180/\pi) \cdot E \cdot A \qquad (3)$$

A is the sensitivity of the rubidium magnetometer appearing in (1), F_o is the mean total field value, H_o is the mean horizontal component and E is given by

$$E\,[\mathrm{nT}^{-1}] = (F_+ + F_-)\,/(\,4\,B\,F_0\,)\,, \qquad (4)$$

where

$$B\,[\mathrm{nT}] = \sqrt{(F_+^2 + F_-^2 - 2\,F_o^2)/2} \qquad (5)$$

F_+ and F_- are the mean total fields measured by the rubidium head when the currents in either direction are present in the polarization Helmoltz coils. They are of course different for the *D* and *I* components. A special purpose subprogram allows measurement of these quantities when necessary.

4. Measurements in Tihany with the RVM

The RVM was installed in Tihany geophysical observatory from 11 September to 18 September 1990 and recorded the geomagnetic field vector successfully during that period of time. Because of the presence of a perturbing field due to the polarization currents in the Helmoltz coils, the instrument could not be located in the recording vault of the observatory with the other variometers participating in the intercomparison session. The RVM was placed instead on a gypsum pillar in a small double-walled hut on the top of a hill at a distance of about 50 m from the recording room. The pillar rested on a concrete floor and was completed on 9 September 1990. There was no temperature control inside this building. The installation proved nevertheless to be entirely satisfactory. The PC and control electronics were located at a distance of about 120 m—near the entrance of the observatory.

In order to calibrate the rubidium magnetometer, absolute *F* measurements were made in Tihany with various proton magnetometers. Of these, some were working rather erratically at that time. To get a head equation using a least squares fit, I had to reject some *F* measurements and keep others arbitrarily and in this process errors were probably introduced. I estimate errors in *F* to be less than +/-5 nT.

Absolute *D* and *I* measurements for baseline determination were made using a non-magnetic Zeiss 010B theodolite equipped with a DImag88 fluxgate magnetometer from IPG Strasbourg featuring an amorphous sensor. *Figures 1* and 2 summarize those measurements. Baseline drift for *D* is about 20″ from 13/9 to 18/9; scatter is at the +/-7″ level. For *I* there is no obvious drift and scatter is +/-6″.

No measurements are available of the temperature of the RVM during the intercomparison session. There could be an effect on the *I* component as one sees that the afternoon baseline determinations are always too high

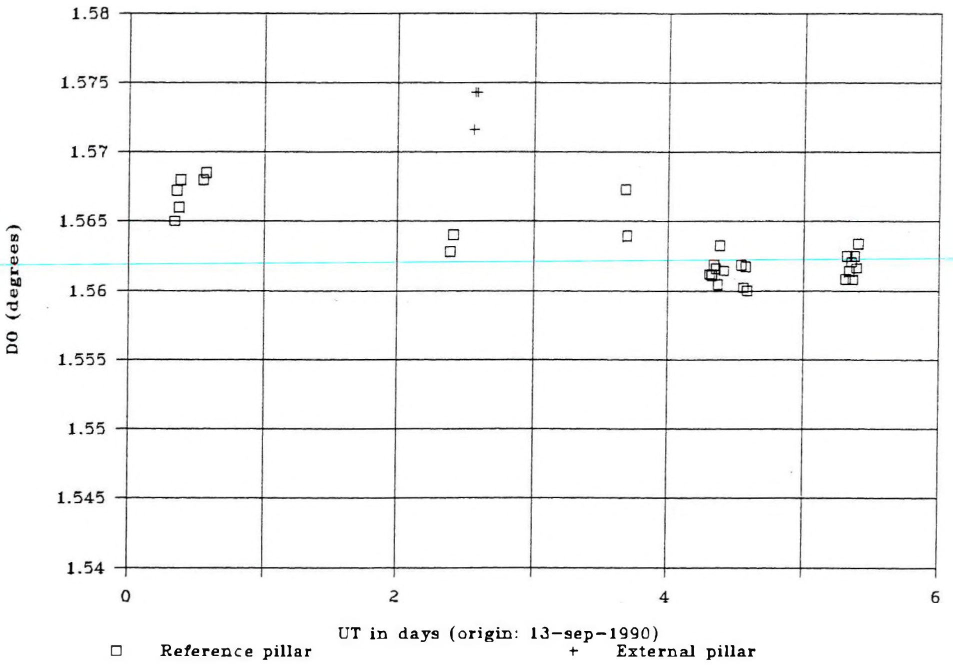

Fig. 1. Declination baseline measurements during the Tihany workshop. Note that .01 degree = 36″. Sightings from the external pillar were made on East tower of Tihany church and reduced with an azimuth of 4.000 degrees

1.ábra. Rubidium Vektor Magnetométer deklináció bázisvonala. A tihanyi mérés idején .01°=36″. A külső pillértől az irányitást a tihanyi templom keleti tornyára célozták és 4,000 fok azimuttal csökkentették

Рис. 1. Опорная линия наклонений рубидиевого векторного магнитометра. Во время измерений в Тихани .01°=36″ Визиры были нацелены со столба на восточную башню тиханьского костела и уменьшены на 4,00 градуса по

by say ten seconds of arc. Bearing in mind a diurnal temperature wave of 5°C amplitude, this could give a tentative temperature coefficient of 2″/°C for the inclination. The *D* component does not seem to have this defect.

Data were reduced with a constant mean base for *D* (1.5628°) and *I* (63.1886°). Scale values were 0.0002945°/unit for *D* and 0.0001411°/unit for *I*. *A*=0.22531 nT/Hz and *B*=-2494.9 nT in the head equation. Taking a variable base to give a better fit to the baseline determinations could result in a slight improvement. *Fig. 3* gives an example of the data.

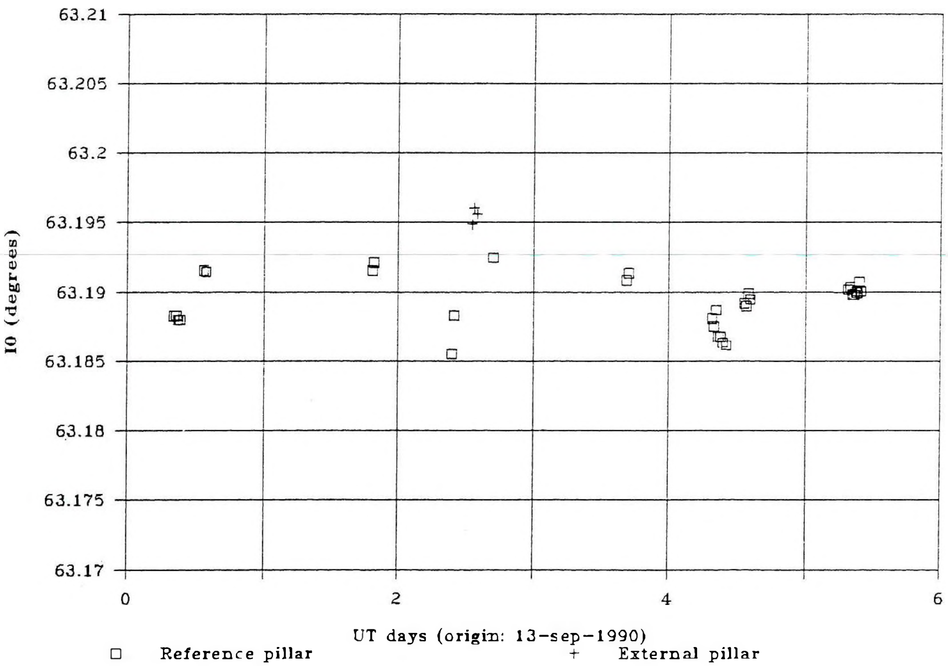

Fig. 2. Inclination baseline measurements

2.ábra. Rubidium Vektor Magnetométer inklináció bázisvonala

Рис. 2. Опорная линия склонений рубидиевого векторного магнитометра

5. Conclusion

One sees that Bacon's idea and Alldredge's ASMO scheme can still be valuable for the collection of digital geomagnetic data, especially if modern electronics is switched in. Big advantages come from the use of a PC equipped with a high resolution counter card allowing compactness and low cost for the data acquisition. The superb performance of the optical pumping magnetometer allows measurement at a fast rate and high sensitivity without the need to manipulate submicrovolt signals. The scale values

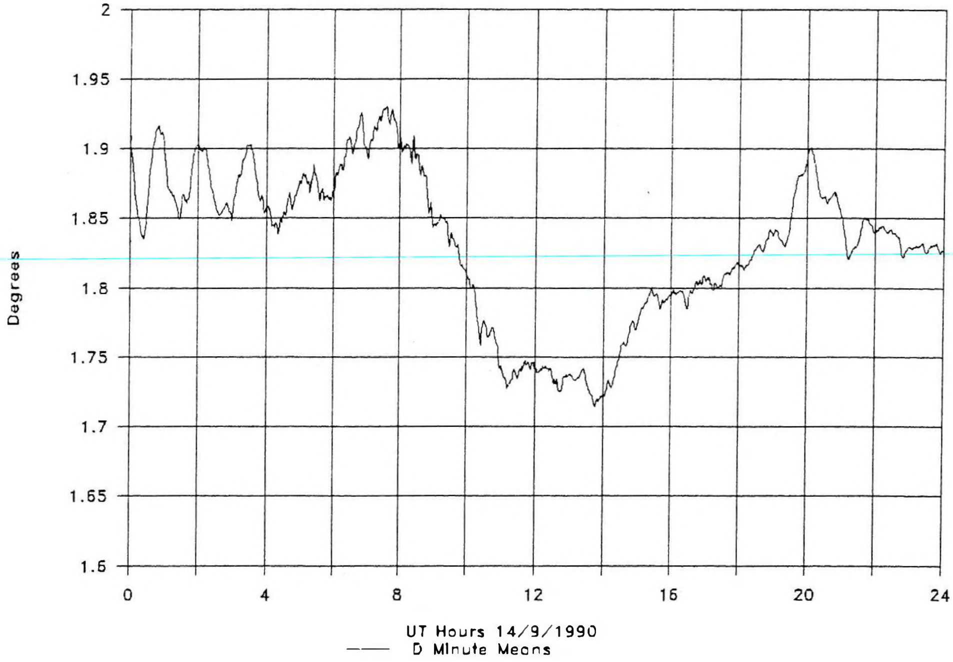

Fig. 3. Geomagnetic declination for 14 September 1990 in Tihany as recorded by the rubidium vector magnetometer

3.ábra. Rubidium Vektor Magnetométerrel észlelt földmágneses deklináció 1990 szeptember 14-én

Рис. 3. Средние по минутам рубидиевого векторного магнитометра

need not be determined by an external calibration device. The baseline stability is satisfactory and the temperature coefficient should not be a problem if modest temperature control is provided for the recording room. The installation is quite simple by orienting the coils on *H* and there is no need to locate geographic north. Finally I consider it an advantage to measure the same components for the variometers as for the absolute measurements.

Acknowledgements

Many thanks go to Alpár Körmendi, Daniel Gilbert and André Bourtembourg for assistance during the Tihany workshop.

REFERENCES

ALLDREDGE, L.R. and SALDUKAS, I. 1964: An automatic standard magnetic observatory. J. Geophys. Res. **69 (10),** pp. 1963-1970.

BACON, F.W. 1955: Adaptation of a free precession magnetometer to measurements of declination. Master's Thesis, U.S. Naval Postgraduate School, Monterey, California.

RUBÍDIUM VEKTOR MAGNETOMÉTER

Jean RASSON

IBM-PC-hez kapcsolt új optikai gerjesztésű rubídium vektor magnetométert ismertet a szerző, mely új technikát használ a polarizálásra és a frekvenciamérésre a pontosság növelése céljából. Megadja a Workshop alatti mérés helyszínrajzát és megjegyzéseket fűz a mérési eredményekhez.

РУБИИДЕВИЙ ВЕКТОРНЫЙ МАГНИТОМЕТР

Йан РАССОН

Автором дается характеристика нового рубидиевого векторного магнитометра с оптическим возбуждением, подключенного к компъютеру IBM, в котором для увеличения точности применяется новая техника поляризации и измерения частот. Приводится план ситуации производства измерений во время рабочей встречи (Workshop) и комментарии к результатм измерений.

GEOPHYSICAL TRANSACTIONS 1991
Vol. 36. No. 3-4. pp. 195-213

A DEVELOPMENT OF WIDE RANGE LOW NOISE QUARTZ TORSION MAGNETOMETERS

V. I. ODINTSOV*

The noise level associated with strong negative feedback in torsion quartz variometers with photoelectric converters was analysed. The results of optimization of the movable magnet suspended on an elastic thread by maximizing the magnetic moment with reference to moment of inertia has been obtained. The theoretical and experimental appreciation was made for two magnetic materials—'Samcomag' $SmCo_5$ and Fe-Co-Cr. It has been shown that the frequency range of 'Samcomag' variometers should be restricted to below 16 Hz (Fe-Co-Cr— to 4 Hz) within the bounds of maximum permissible noise of a magnetometer equal to 3.2 pT p-p. These frequencies probably are the limiting ones for torsion quartz variometers with photoelectric converter.

Keywords: quartz torsion magnetometer, noise

1. Introduction

Opto-mechanical quartz variometers are widely used nowadays [BOBROV 1961]. Angular displacements of the variometer are transformed into electric signals by opto-electronic converters. This — together with strong negative feedback — allows the wide-spread use of quartz variometer based magnetometers together with other types of instrument, in measuring the components of the magnetic induction in geomagnetic observatories [JANKOWSKI et al. 1984, HEGYMEGI et al. 1986]. On the basis of detailed analysis of characteristics of variometers with negative feedback, basic relationships have been obtained for calculating the met-

* Institute of Terrestrial Magnetism, Ionosphere and Radio Wave Propagation (IZMIRAN) 142092, Troitsk, Moscow region, USSR

rologic characteristics of the variometer [MARIANIUK 1977]. It is shown that in the case of strong amplification and strong negative feedback the instabilities of opto-electronic converter have neglibigle effects on the parameters of the variometer.

At the same time, the effects of the strong negative feedback on the threshold sensitivity have not been analysed in detail. There is no method available to estimate the limiting values of the parameters of the variometer, depending on the degree of the negative feedback and on the required frequency range of the magnetometer.

2. Basic relations for calculating the parameters of the quartz magnetometer

The opto-mechanical quartz variometer with negative feedback (the quartz magnetometer) is a linear system with automatic control and can be illustrated by a block diagram. The units of the diagram *(Fig.1.)* are: the variometer itself, the opto-electronic converter converting the angular displacements of the variometer into electric signals, and the negative feedback circuit.

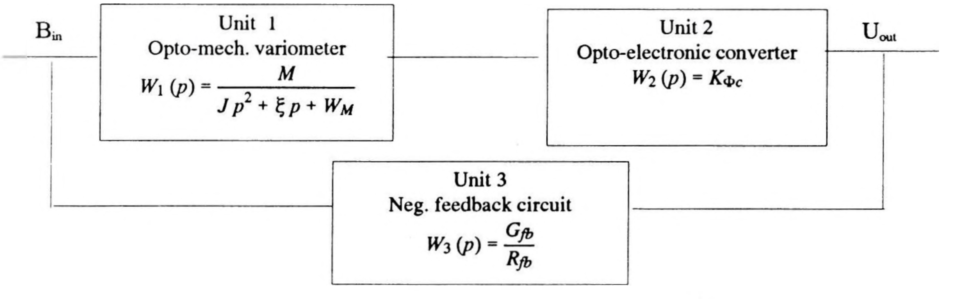

Fig.1. Block diagram of opto-mechanical variometer with negative feedback

1. ábra. Negatív visszacsatolással ellátott optikai (kvarc) variométer blokkvázlata

Рис. 1. Структурная схема оптико-механического вариометра с отрицательной обратной связью

The main feature of the magnetometer is a moving magnet with a small mirror. The magnet is hung on quartz thread and is located in the centre of a coil arranged to provide negative feedback. Angular displacements of the magnet with mirror are converted by the opto-electronic converter into output current. This current will be fed to the feedback coil, where the current produces a compensating magnetic field. This magnetic field holds the ray of light reflected from the moving mirror of the variometer in a strictly fixed position as compared to the photo-sensors of the opto-electronic converter. In this way, the value of the feed-back current will be adjusted proportionally to the magnetic field to be measured.

The movement of the magnet can be described with a linear differential equation of second order [AFANASIEV et al. 1972]:

$$J \frac{d^2\theta}{dt^2} + \xi \frac{d\theta}{dt} + W_M \theta = M \; \delta B, \qquad \text{where} \qquad (1)$$

J — is the moment of inertia of the moving part of the variometer (kg/ m2);
ξ — is the damping coefficient (N ms/rad);
θ — is the angular displacement of the moving part of the variometer (rad);
W_M — is the total torsion coefficient of the variometer, $W_M = C$ or $W_M = C + M B$ (N m/rad)
C — is the torsion coefficient of the quartz thread (N m/rad);
M — is the magnetic moment of the magnet (A m^2);
B — is the magnetic field component parallel to the magnetic moment of the magnet (T);
δ B — is the change of magnetic field turning the magnet to an angle θ from the condition of equilibrium.

$$W_1(p) = \frac{\theta(p)}{\delta B(p)} = \frac{M}{Jp^2 + \xi p + W_M}, \qquad \text{where} \qquad (2)$$

The following transfer function corresponds to the differential equation (1) of the variometer:
p — is the Laplace operator.

The dynamic characteristics of the variometer are completely determined by the operating characteristics: by the damped natural frequency ω_{ov} or period T_{ov} of the variometer, by the damping factor β_{ov} and by the

$$\omega^2 = \frac{W_M}{J}; \quad T_{ov} = \frac{2\pi}{\omega_{ov}}; \quad \beta_{ov} = \xi / (2\sqrt{W_M J}); \quad W_1(0) = \frac{M}{W_M} \tag{3}$$

sensitivity $W_1(0)$ of the variometer in normal mode of operation. They are described by the following expressions:

$$W_1(p) = \frac{M}{W_M} \frac{1}{p^2/\omega_{ov}^2 + 2\beta_{ov} \, p/\omega_{ov} + 1} \tag{4}$$

Taking (3) into consideration, the transfer function (2) can be written in the form:

In order to simplify the subsequent analysis we will consider that the opto-electronic converter possesses no inertia as compared to the variometer, $K_{\Phi c}$ is the conversion coefficient from the angular position of the mirror to a proportional output current (A/rad), and the negative feedback circuit consists only of the resistor R_{fb} (Ω) and the feedback coil converting

$$W_2(p) = K_{\Phi c} \tag{5}$$

$$W_3(p) = \frac{G_{fb}}{R_{fb}} \tag{6}$$

the current into magnetic field with a conversion coefficient G_{fb} (T/A). Their transfer functions are:

$$W_{fb}(p) = \frac{W_1(p) \; W_2(p)}{1 + W_1(p) \; W_2(p) \; W_3(p)}$$

With feedback connected the transfer function of the variometer can be determined by the expression [KLUIEV 1973]:

$$W_{fb}(p) = \frac{U_{out}(p)}{\delta B(p)} = \frac{R_{fb}}{G_{fb}} \frac{M \; K_{\Phi c} \, (G_{fb}/R_{fb})}{J \; p^2 + \xi \, p + W_M + M \, K_{\Phi c} \; (G_{fb}/R_{fb})} \tag{7}$$

After substitution of expressions for transfer functions of the units in Figure 1 and proper transformations we will obtain the following equation: where $M \; K_{\Phi c} \; (G_{fb}/R_{fb})$ is an additional torsion coefficient which effects the moving part of the variometer due to the negative feedback. It can be

$$W_{EM} = M\, K_{\Phi c}\, \frac{G_{fb}}{R_{fb}} \tag{8}$$

called the electromagnetic torsion coefficient W_{EM}:

$$W_{fb}(p) = \frac{R_{fb}}{G_{fb}}\, \frac{W_{EM}}{J p^2 + \xi p + W_M + W_{EM}} \tag{9}$$

and equation (7) can be written in the form

The increase of the torsion coefficient acting on the moving part of the variometer with feedback, as compared to the same moment of an independent variometer, determines a certain value of γ_0 which can be called the

$$\gamma_0 = \frac{W_M}{W_M + W_{EM}}$$

stability of the magnetometer:

On the analogy of the characteristics of an independent reference

$$\omega_0^2 = \frac{W_M + W_{EM}}{J} = \frac{\omega_{ov}^2}{\gamma_0}; \qquad T_0 = T_{ov}\, \sqrt{\gamma_0}\ ;$$

$$\beta_0 = \frac{\xi}{2\sqrt{J\,(W_M + W_{EM})}} = \beta_{ov}\, \sqrt{\gamma_0}\ ; \tag{10}$$

$$W_{fb}(0) = \frac{M\, K_{\Phi c}}{W_M + W_{EM}} = \frac{R_{fb}}{G_{fb}}\,(1 - \gamma_0)\ ,$$

variometer:

where:

ω_0 is the natural frequency of the variometer with feedback;

β_0 is the damping factor of the variometer with feedback;

$W_{fb}(0)$ is the sensitivity of the magnetometer in normal mode of operation (V/T).

Taking (10) into account, the final expression will be obtained:

$$W_{fb}(p) = \frac{R_{fb}}{G_{fb}} \frac{1 - \gamma_0}{p^2/\omega_0^2 + 2\beta_0 p/\omega_0 + 1} \tag{11}$$

3. Noise passing through the magnetometer

If the noise characteristics $P(n)$ are known, then the potential change at the output of the magnetometer $\Delta U(p)$ induced by noise arriving at arbitrary point in the block diagram can be written with the following formula [RABINOVICH 1972]:

$$\Delta U(p) = P_n(p) \prod_{i=j}^{n} W_i(p) \frac{1}{1 + W_1(p) \cdot W_2(p) \cdot W_3(p)}, \quad \text{where}$$

$\prod_{i=j}^{n}$ is the product of the transfer functions of the units from the place of noise input to the output of the magnetometer.

In the particular case when the noise effects the input of unit 2:

$$\frac{\Delta U(p)}{P_n(p)} = \frac{W_2(p)}{1 + W_1(p)\ W_2(p)\ W_3(p)} = \frac{W_{fb}(p)}{W_1(p)} \tag{12}$$

The relative value of the noise characteristics at the output of the magnetometer can be obtained using the expression $U_{nom} = B_{nom}(1 - \gamma_0) R_{fb}/G_{fb}$ where B_{nom} and U_{nom} are the nominal values of the magnetic induction at the input of the magnetometer and that of the voltage at the output of the magnetometer, respectively, in normal mode of operation:

$$\frac{\Delta U(p)}{U_{nom}} = \frac{P_n(p)}{B_{nom}(1 - \gamma_0)} \frac{G_{fb}}{R_{fb}} \frac{W_{fb}(p)}{W_1(p)}$$

After substitution of values of $W(p)$ and $W_{fb}(p)$ from (4) and (11) and after proper reductions we get

$$\frac{\Delta U(p)}{U_{nom}} = \frac{P_n(p)}{B_{nom}} \frac{W_M}{M} \frac{p^2/\omega_{ov}^2 + 2\beta_{ov}\ p/\omega_{ov} + 1}{p^2/\omega_0^2 + 2\beta_0\ p/\omega_0 + 1} \tag{13}$$

If the signal to noise ratio at the output of the magnetometer is considered to be 1, then in case of known noise $P_n\ (p)$ the limiting value of the threshold sensitivity $B_{nom}(p)$ of the magnetometer will be:

$$B_{nom}(p) = P_n(p)\,\frac{W_M}{M}\,\frac{p^2/\omega_{ov}^2 + 2\beta_{ov}\, p/\omega_{ov} + 1}{p^2/\omega_0^2 + 2\,\beta_0\ p/\omega_0 + 1} \tag{14}$$

It follows from expression (14) that the limiting value of the threshold sensitivity $B_{nom}(p)$ of the magnetometer is not constant for the whole frequency range and depends on both the frequency features of the noise and the natural frequency of the variometer.

4. The effect of the opto-electronic converter on the threshold sensitivity of the magnetometer

Noise referred to the input of the optoelectronic converter of angular displacements can be induced by fluctuation of illumination intensity, shot noise of photosensors, mechanical movement of elements of the optoelectronic converter or to changes of parameters of the surrounding medium.

Let us suppose that the noise $P_n\ (p)$ (we consider only the shot noise of the photosensors, for the sake of certainty) makes a disturbance with amplitude P_n which is uniformly distributed in the operating frequency range of the magnetometer. Then the frequency dependence of threshold sensitivity $B_{nom}\ (\omega)$ of the magnetometer can be described with the expression:

$$B_{nom}(\omega) = P_n\,\frac{W_M}{M}\sqrt{\frac{(1 - \omega^2/\omega_{ov}^2)^2 + \beta_{ov}^2\omega^2/\omega_{ov}^2}{(1 - \omega^2/\omega_o^2)^2 + 4\,\beta_0^2\,\omega^2/\omega_0^2}} \tag{15}$$

Expression (15) shows that at low frequencies ($\omega << \omega_{ov}$) the threshold sensitivity of the magnetometer does not depend on the frequency and equals $P_n \; W_M/M$. With increasing frequency both the threshold sensitivity B_{nom} and the amplitude of noise at the output of the magnetometer increase.

Fig.2. shows the frequency dependence of the threshold sensitivity of the magnetometer in the case of a fixed damping factor of the magnetometer β_0 = 0.82; parameters of the curves are the different values of damping factor β_{ov} of the initial variometer.

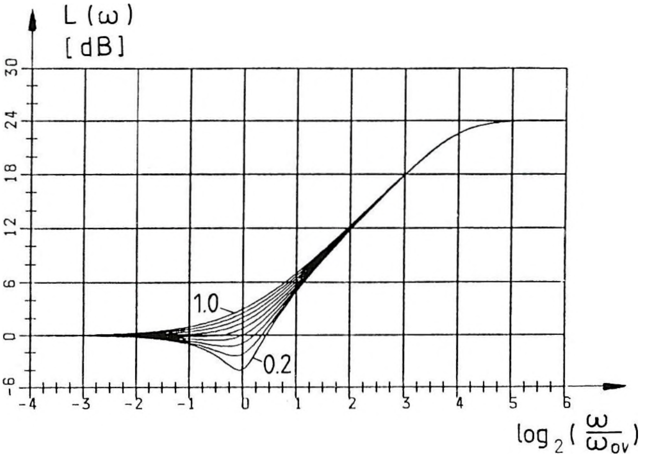

Fig.2. Logarithmic amplitude-frequency characteristics versus the noise of the magnetometer, at different values of damping factor β_{ov} from 0.2 to 1.

2. ábra. A magnetométer zajának logaritmikus amplitudó-frekvencia karakterisztikája a β_{ov} csillapitási tényező különböző értékeire 0.2-től 1-ig

Рис. 2. Логарифмические амплитудно-частотные характеристики относительного шума магнитометра при значениях степени затухания β_{ov} от 0,2 до 1

For the sake of descriptiveness the frequency dependence is illustrated using a logarithmic scale. The value $B_{nom}(0) = P_n \; W_M/M$ was taken as the initial noise level. The logarithmic amplitude-frequency characteristics of the threshold sensitivity of the magnetometer in dB (as compared to the initial noise level) can be obtained from expression (15):

$$L(\omega) = 10\lg\frac{B_{nom}(\omega)}{B_{nom}(0)} =$$

$$= 10\lg\sqrt{(1-\omega^2/\omega_{ov}^2)^2 + 4\beta_{ov}^2\,\omega^2/\omega_{ov}^2} - \\ - 10\lg\sqrt{(1-\omega^2/\omega_0^2)^2 + 4\beta_0^2\,\omega^2/\omega_0^2} \tag{16}$$

In the initial part of the characteristics, where $\omega << \omega_{ov}$, the logarithmic amplitude-frequency characteristics of the threshold sensitivity of the magnetometer is a straight line coinciding with the axis of abscissae. At high frequencies ($\omega > \omega_0$), the logarithmic amplitude-frequency charac-

$$L(\omega) = 10\lg(\omega_0^2/\omega^2) = -10\lg\gamma_0$$

teristics is also a straight line parallel to the axis of abscissae running at a

$$L(\omega) = 10\lg(\omega^2/\omega_{ov}^2) = 20\lg(\omega/\omega_{ov})$$

distance from this axis

At frequencies $\omega_{ov} < \omega < \omega_0$ the characteristic is a straight line with a slope 6 dB/octave, crossing the axis of abscissae at $\omega/\omega_{ov} = 1$, and the high frequency straight line at $\omega/\omega_0 = 1$.

The most interesting part of the frequency characteristic is the frequency range about $\omega \approx \omega_{ov}$. Fig. 2. shows that in case $0.4 < \beta_{ov} < 0.7$ the real logarithmic amplitude-frequency characteristic of the noise of the magnetometer can be substituted by an approximate characteristic; the error is less than 3 dB. For other values of damping factor the noise amplitude can be estimated with the help of curve series (*Fig.3*). On the basis of the curve series, corrections for the approximate (asymptotic) logarithmic amplitude-frequency characteristics can be calculated.

In order to obtain a low level of noise at the output of the magnetometer, the cutoff frequency ω_{ov} of the initial variometer should be increased up to values about the upper limiting frequency of the magnetometer.

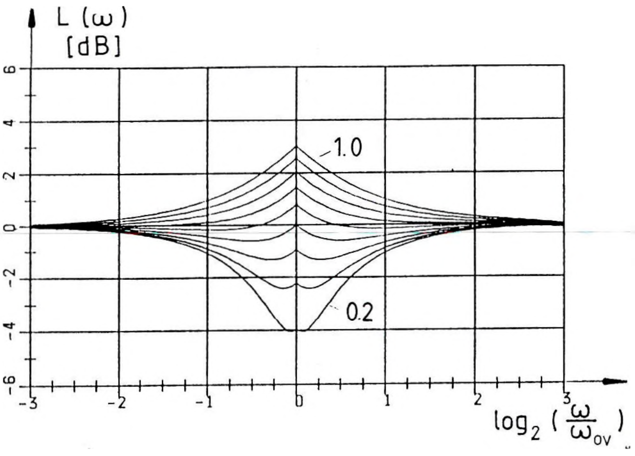

Fig.3. Correction curves for approximation of the two straight lines of logarithmic amplitude-frequency characteristics versus the noise of the magnetometer, at different values of damping factor β_{ov} from 0.2 to 1.

3. ábra. Korrekciós görbék arra az esetre, ha a magnetométer log-log zajfeszültség-frekvencia karakterisztikáját két egyenes szakasszal közelítik, a β_{ov} csillapítási tényező különböző értékeire 0.2-től 1-ig

Рис. 3. Поправочные кривые к аппроксимированной двумя прямыми ЛАХЧ относительного шума магнитометра при значениях степени затухания β_{ov} от 0,2 до 1

5. Dependence of the noise of the magnetometer on the construction features of the variometer

In order to obtain the relationship between the logarithmic amplitudef-requency characteristics of the threshold sensitivity of the magnetometer and the characteristics of the initial variometer and the opto-electronic converter, let us express the value W_M/M in expression (15) with the help of the construction parameters of the variometer — the magnetic moment M and moment of inertia J of the moving magnet with a small mirror —, combining them with the natural frequency of the magnetic system of the variometer. From expression (3) follows:

$$f_{ov} = \frac{1}{T_{ov}} = \frac{\omega_{ov}}{2\pi} = \frac{1}{2\pi}\sqrt{(M/J)\ (W_M/M)} = \frac{1}{2\pi}\sqrt{(M/J)\ (1/W_1(0))}$$

For the sake of practical application it is convenient to define the 'quality coefficient' Q of the magnetic system of the variometer which is the product of the conversion coefficient (rad/T) of the variometer in normal operation and the second power of the natural frequency of the variometer:

$$Q = f_{ov}^2\ W(0) = \frac{1}{4\pi^2}\ \frac{M}{J}$$

On the basis of experimental study of many quartz variometers and computer-calculated results aimed at optimization of the form and dimensions of the magnets from the point of view of maximizing the ratio M/J, the following mean 'quality coefficient' values can be obtained depending on the material:

$Q_{sc} = 2 \cdot 10^6\ \mathrm{Hz}^2\ \mathrm{rad/T}$ for samarium-cobalt and

$Q_v = 0.125 \cdot 10^6\ \mathrm{Hz}^2\ \mathrm{rad/T}$ for vicalloy.

The value of Q could be significantly increased using new, samarium-cobalt type magnetic materials for making the moving magnet. This could be achieved due to the fact that samarium-cobalt is able to preserve a large enough remanent magnetization even in the case of a very high demagnetization coefficient. Consequently, the dimensions of the magnet perpendicular to the axis of rotation can be reduced so that the magnetic moment will preserve its previous value and the moment of inertia of the moving part of the magnet can be reduced.

Fig.4. shows the dependence of conversion coefficient upon the natural frequency for vicalloy based (line 1) and samarium-cobalt based (line 2) quartz variometers. If the conversion coefficient W_1 is $0.125 \cdot 10$ rad/nT, then the natural frequency of a samarium-cobalt based variometer is about 4 Hz, and that of a vicalloy based one is 1 Hz. If the angular sensitivity P_n of the photo-converter equals $0.5 \cdot 10^{-7}$ rad, then the sensitivity of the magnetometer is constant in the frequency range from DC to the natural frequency of the variometer and its value is $B_{nom} = P_n\ W_M/M = 0.4$ pT (this is shown in Fig. 4 by the straight line

running at a distance of 0.4 pT from the frequency axis). At frequencies higher than the natural frequency the noise amplitude increases (the threshold sensitivity of the magnetometer increases) with a speed of 6 dB/octave according to the characteristics of the variometers (straight lines marked by 1 or 2).

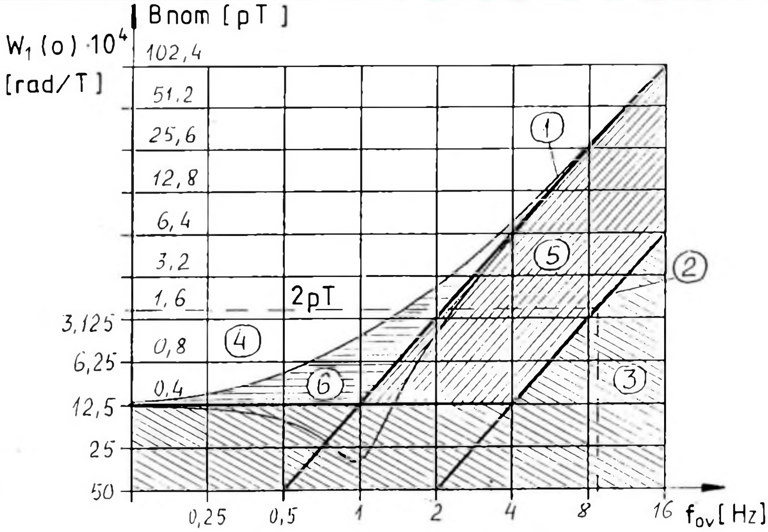

Fig.4. The own frequency versus conversion coefficient for vicalloy based (1) and samarium-cobalt based (2) variometer and the corresponding noise levels at the output of the magnetometer.

4. ábra. A variométer saját frekvenciája az átalakítási tényező függvényében és a megfelelő kimeneti zajfeszültség (1) vicalloy, (2) samarium-kobalt mágnes esetén.

Рис. 4. Зависимости собственной частоты от коэффициента преобразования вариометров на основе викаллоя (1) и самарий-кобальта (2) и соответствующие им уровни шума на выходе магнитометра

The above straight lines determine a range characterizing the noise distribution of the sensors versus frequency (hatched area marked by 3 in Fig. 4). If the conversion coefficient of the vario- meter decreases down to $W_1(0) = 0.25 \cdot 10^5$ rad/T, its natural frequency increases up to 9 Hz (for samarium-cobalt) and the threshold sensitivity of the magnetometer decreases down to $B_{nom} = 2$ pT (dotted line in Fig.4).

In this case the range characterizing the noise of the sensors will be limited from above by the level 2 pT. This means the noise of the sensor increases up to the non-hatched area marked by 4 in Fig. 4. which is especially important for low frequencies.

If the variometer is made from vicalloy (line marked by 1), then its noise level is significantly higher in the frequency range from DC to 16 Hz than that of the samarium-cobalt based variometer (the difference is the area marked 5 in Fig. 4). This is because in the case of equal conversion coefficients the own frequency of the samarium-cobalt based variometer is four times higher than that of the vicalloy based variometer.

Finally, in the case of the samarium-cobalt variometer the amplitude of noise components at frequency 16 Hz is 6.4 pT while in the case of the vicalloy variometer it is 102.4 pT. Consequently, if the threshold sensitivity is fixed about 1 pT, then the pass band of magnetometers with vicalloy based sensors should be limited from DC to a frequency of about 1.6 Hz.

The damping factor of the magnetic system is of great importance from point of view of obtaining good noise characteristics of the magnetometer. This is because the angular frequency ω_{dec} of the decaying vibrations is always less than the natural frequency ω_{ov} of a variometer without damping. The relation of the two frequencies is:

$$\omega_{dec} = \omega_{ov}\sqrt{1 - \beta_{ov}^2}$$

Fig. 5. shows the frequency of decaying vibrations ω_{dec}/ω_{ov} (in relative units) versus the damping factor β_{ov} .

It can be seen from the figure that if the damping factor changes from 0.4 to 0.7, then the natural frequency of the variometer changes a little only

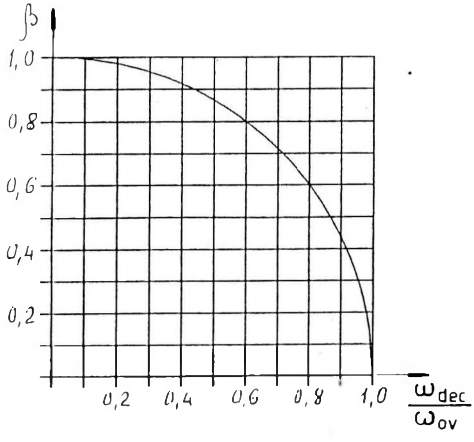

Fig.5. Frequency of decreasing vibrations of the variometer versus damping factor

5. ábra. A variométer rezgési frekvenciájának csökkenése a csillapítás függvényében

Рис. 5. Зависимость частоты затухающих колебаний вариометра от степени затухания and is between 0.95 ω_{ov} and 0.7 ω_{ov} . For higher damping factors the natural frequency of the variometer abruptly decreases: at β_{ov} = 0.85 it is only half of the initial natural frequency .

This results in the increase of the noise of the magnetometer at frequencies about the natural frequency of the variometer (area marked by 6 in Fig. 4). Consequently, it is not practical to enhance the damping factor of the variometer over 0.82. On the other hand, reduction of damping of the variometer results in an increase of noise level related to seismic vibrations of the variometer. The optimal value of the damping factor β_{ov} is between 0.6 and 0.82. In this case the natural frequency of the variometer reaches 0.6- 0.8 ω_{ov}.

6. Results of experimental tests of quartz magnetometers

The experimental tests of quartz magnetometers were carried out using the digital automatic measuring station CAIS [ASKEROV et al. 1989]. The noise characteristics were investigated with a spectrum analyzer type FFT CF-300 made by the firm ONO SOKKI (Japan). The measurements were carried out in June 1989 under real operating circumstances at the geomagnetic observatory Tihany (Hungary) in two frequency ranges: from 0.1 to 15 Hz and from 0.1 to 5 Hz. *Fig. 6 (a—c)* shows the obtained noise spectra of the sensors for the first frequency range and *Fig. 7 (a—c)* — for the second one.

During estimation of noise at the output of the quartz magnetometers the following settings of the spectrum analyzer were used:

— instrument scale: 0—1 mV_{pp} (0—4 pT_{pp});

— frequency range of the analysis: 0.1 to 20 Hz;

— number of spectrum lines : 200.

As a result of the analysis the following peak-to-peak values were obtained as noise level at the output of the sensors:
in the first frequency range — B_x = 7 pT, B_y = 11 pT, B_z = 6 pT;
in the second one — B_x = 3.5 pT, B_y = 4 pT, B_z = 2 pT.
These results agree well with calculated values of output noise level of the quartz magnetometers.

In order to compare the noise levels of magnetometers with variometers made from different materials, *Fig. 8* shows the real spectrum of signals

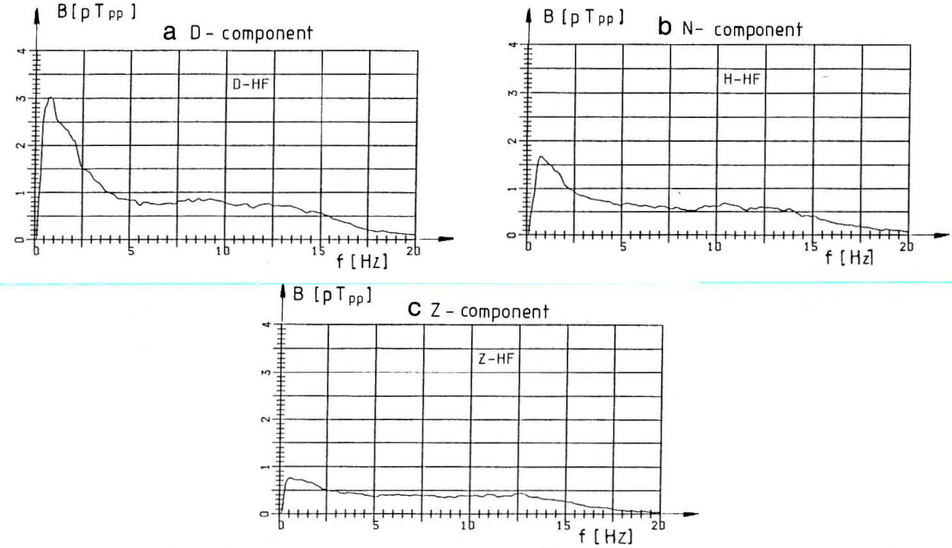

Fig.6. Spectra of signals at the output of quartz sensors type CAIS in the frequency range from 0.1 to 15 Hz, without geomagnetic perturbation.
a—component D; b—component N; c—component Z.

6. *ábra.* CAIS kvarc variométerek kimenő jelének spektruma 0.1 - 15 Hz-es tartományban normál mágneses tevékenység esetén

Рис. 6. Спектры сигналов на выходах кварцевых датчиков ЦАИС в условиях отсутствия геомагнитной возмущенности в диапазоне частот от 0,1 до 15 гц

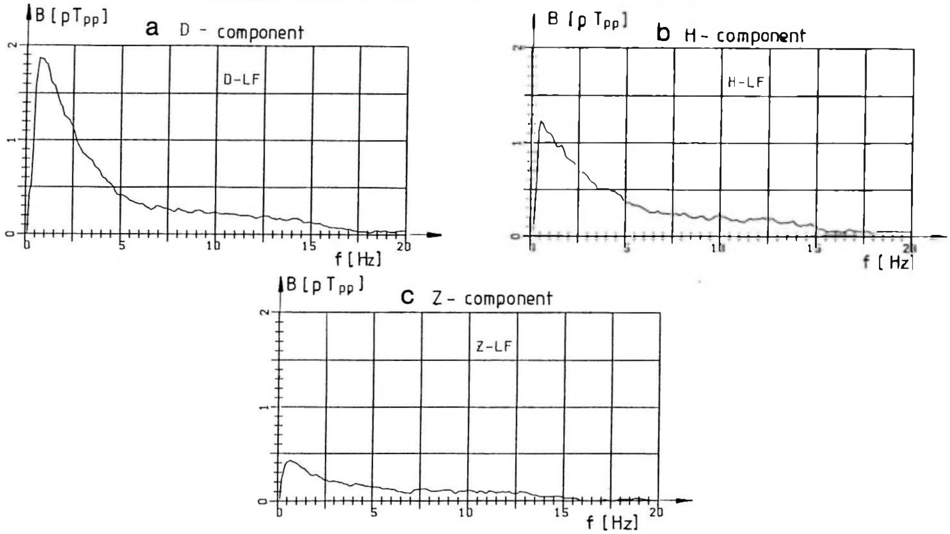

Fig. 7. Spectra of signals at the output of quartz sensors type CAIS in the frequency range from 0.1 to 5 Hz, without geomagnetic perturbation.
a—component D; b —component N; c—component Z.

7. *ábra.* CAIS kvarc variométerek kimenő jelének spektruma 0.1 - 5 Hz-es tartományban normál mágneses tevékenység esetén

Рис. 7. Спектры сигналов на выходах кварцевых датчиков ЦАИС в условиях отсутствия геомагнитной возмущенности в диапазоне частот от 0,1 до 5 гц at the output of the vicalloy based (a) and samarium-cobalt based (b) variometers in the frequency range from 1 to 20 Hz. It can be seen in the figures that the graphs of noise amplitude versus frequency are similar for the examined variometers. The noise amplitude, however, begins to increase at lower frequencies (below 3 Hz) and the amplitude maximum reaches 40 pT for vicalloy variometers, while in the case of samarium-cobalt these values are about 8 Hz and 1.1 pT, respectively.

In order to compare the experimental graphs of frequency distribution of noises at the output of the quartz magnetometers with curves characte-

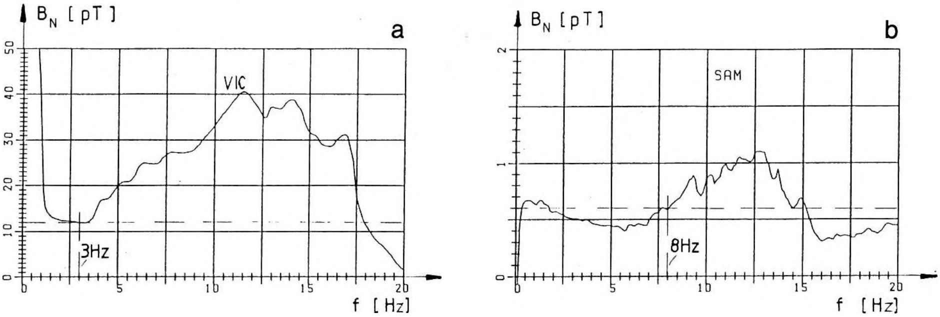

Fig.8.. Noise spectrum at the output of quartz sensor made (a):from vicalloy (W_1 (0) = 18.5 · 10^3 rad/nT ;(b):from samarium-cobalt ($W_1(0)$=31.2 · 10^3 rad/T).The frequency range from 1 to 20 Hz.

8. ábra. Vicalloyból (a) illetve szamárium-kobaltból (b) készült kvarc variométer kimeneti zajfeszültségének spektruma 0.1-20 Hz frekvencia tartományban (a): $W_1(0)$= 18.5 · 10^3rad/T, (b): $W_1(0)$= 31.2 · 10^3 rad/T)

Рис. 8. Спектр шума на выходе кварцевого датчика из викаллоя (a):W1(0)=18.5 · 10^3 рад/тл, (b):W1(0)=31.2 · 10^3рад/тл.) В частотном диапазоне от 1 до 20 гц

rizing the features of magnetic materials (Fig. 4), *Fig. 9* shows the spectrum of signals (Fig. 8) in logarithmic scale. The slope of approximate straight lines in Fig.8 equals 6 dB/octave which corresponds to the characteristics of materials shown in Fig. 4. This supports the conclusions drawn on the nature of noises at the output of quartz magnetometers.

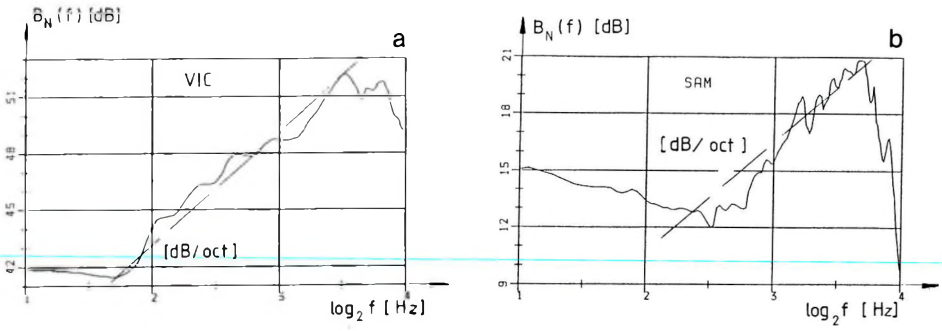

Fig. 9. Noise spectrum at the output of quartz sensor made (a):from vicalloy ($W_1(0)$ = 18.5 · 10^3 rad/nT ; (b):from samarium-cobalt ($W_1(0)$=31.2 · 10^3 rad/T).The frequency range from 1 to 20 Hz (in logarithmic scale)

9. ábra. Vicalloyból (a) illetve szamárium-kobaltból (b) készült kvarc variométer kimeneti zajfeszültségének spektruma 0.1-20 Hz frekvencia tartományban (a): $W_1(0)$= 18.5 · 10^3rad/T, (b): $W_1(0)$= 31.2 · 10^3 rad/T) logaritmikus léptékben

Рис. 9. Спектр шума на выходе кварцевого датчика из викаллоя (a):$W_1(0)$=18.5 · 10^3 рад/тл, (b):$W_1(0)$=31.2 · 10^3рад/тл.) В частотном диапазоне от 1 до 20 гц (в логарифмическом масштабе)

7. Conclusions

The results presented show that opto-electronic converters of angular displacements possess the lowest threshold sensitivity. If adjusted carefully, this angular sensitivity may reach 0.25 · 10^{-7} rad. It means if the conversion coefficient of the variometer is taken as 0.125 · 10^6 rad/T, then — at a threshold sensitivity of 0.2 pT — the natural frequency of the magnetometer with the vicalloy-based variometer is about 1 Hz, and in the case of the samarium-cobalt it is about 4 Hz. If the allowed noise level of the magnetometer is 3.2 pT_{pp}, then the frequency range of the magnetometer with the vicalloy-based variometer will be limited to 4 Hz, in the case of samarium-cobalt — to 16 Hz. These estimations are the limiting values of parameters of quartz vario meters with opto-electronic converters.

REFERENCES

AFANASIEV YU. V., STUDENOV N. V., SHCHELKIN A. P. 1972: Converters, instruments and equipments with magnetometer. Publ. H. Energia, Moscow

ASKEROV E. N., BAGDASAROVA N. Yu., ODINTSOV V. I. et al 1989: The CAIS digital automatic station. Geofizicheskaya Apparatura, **91**, pp. 3-12

BOBROV V. N. 1961: Universal high-stability sensitive element with 0 temperature coefficient for magnetometers, variometers and microvariometers recording any component of the Earth's magnetic field. Trudy Instituta Zemnogo Magnetisma i Radivoln **18**, (28), pp. 55-67

HEGYMEGI L., DRIMUSZ L, KÖRÖS Z. 1986: Eötvös institute DIMARS Quartz Magnetometer. Proceedings of the International Workshop on Magnetic Observatory Instruments, Ottawa, Canada, 30 July - 9 August 1986, pp. 25-26

JANKOWSKI J., MARIANUK J., RUTA A., SUCKSDORFF C., KIVINEN M. 1984: Long-term stability of a torque-balance variometer with photoelectric converters in observatory practice. Geophysical Surveys **6**, 3-4, pp. 367-380

KLIUIEV A. S. 1973: Automatic control. Publ. H. Energia, Moscow, 391 p.

MARIANIUK J. 1977: Photoelectric converter for recording the geomagnetic field elements: construction and principles of operation. Publ. Inst. Geophys. Pol. Acad. Sc., C-4, 114 p.

RABINOVICH S. G. 1972: Galvanometric autocompensating instruments. Publ. H. of standards, Moscow, pp. 36-40

ALACSONY ZAJSZINTŰ KVARC TORZIÓS MAGNETOMÉTEREK FEJLESZTÉSE

V. I. ODINCOV

A szerzők a fotoelektromos konverterrel ellátottkvarc magnetométerek erős negatív visszacsatolásából eredő zajszintet elemzik. A rugalmas szálakra felfüggesztett mozgatható mágnes optimalizálásának eredményeit a mágneses momentumnak a tehetetlenségi momentumhoz viszonyított maximalizálásával érik el. Az elméleti és kísérleti becslést két mágneses anyagra - 'Samcomag' $SmCo_5$ és Fe-Co-Cr-ra végezték el. Bemutatják, hogy a 'Samcomag' variométer frekvenciatartományát 16 Hz (az Fe-Co-Cr-ét 4 Hz) alá kell szorítani a magnetométerek maximálisan megengedhető 3,2 pT pp zaj határán belül. Ezek a frekvenciák valószínü a határértékeket jelentik a fotoelektronos konverterrel ellátott torziós kvarc variométereknek.

РЕЗУЛЬТАТЫ ИССЛЕDОВАНИЙ НИЗКОПОРОГОВЫХ ШИРОКОПОЛОСНЫХ КВАРЦЕВЫХ МАГНИТОМЕТРОВ

ОДИНЦОВ В.И.

Dан анализ механизма влияния отрицателяной обратной связи на порог чувствительности оптико-механического кварцевого вариометра с оптико-электронным преобразователем угловых перемещений Определены критерии оптимизации разрмеров и формы магнитов изготовленных из различных магнитных материалов по условию максимума отношения магнитного момента к моменту инерции Dаны теоретические и экспериментальные оценки уровня шума магнитометров на основании викаллоя и самарий-кобальта Показано что при заданном предельно допустимом уровне шума магнитометра равном 3, птл от пика до пика частотный диапазон магнитометра с вариометром на основе викаллоя будет ограничен сверху частотой гц самарий-кобальта - 1 гц Эти частоты повидимому являются предельными для кварцевых вариометров с оптико-электронным преобразователем.

GEOPHYSICAL TRANSACTIONS 1991
Vol. 36. No. 3-4. pp. 215-226

THE DIGITAL QUARTZ TORSION MAGNETOMETER WITH CHARGE-BALANCING INTEGRATION

V. I. ODINTSOV*

The paper describes a new way for the digital-to-analog conversion of the quartz torsion magnetometer output signal voltage by means of insertion of a charge-balancing A/D converter in the strong negative feedback loop of the quartz torsion variometer with photoelectronic system which converts the deflection of the variometer's magnet into electric voltage changes. The main expressions of the transfer functions for the automatic control circuit units and the transfer function of the magnetometer as a whole are deduced. The results of experimental testing of the digital magnetic variation station CMVS-6 based on the digital torsion magnetometer with charge-balancing integration are presented.

Keywords: digital quartz magnetometer, torsion, charge-balance

1. Introduction

The requirements for the accuracy of magnetic measurements have been increased, in connection with the widespread use of magnetometers based on opto-mechanical quartz variometers in geomagnetic observatories [KAURISTIE et al. 1989, ODINTSOV 1991] and with the speedy development of digital data processing in magnetometry. Since the opto-mechanical quartz variometer is an oscillating unit with a rather large time constant, practically every known method of A/D conversion produces additional errors during the process of coding its output signal. Their origin may be the uncertain connection to the moment of reading of the actual value of the quantity to be measured in time, the effect of random noises superposed

* Institute of Terrestrial Magnetism, Ionosphere and Radio Wave Propagation (IZMIRAN) 142092, Troitsk, Moscow Region, USSR

onto the process under examination, the limited dynamic range or the zero level shift of the A/D converter. A possible method for decreasing the errors of the A/D conversion is to insert the converter into the negative feedback circuit of the magnetometer. One of the variants of technical realization of this method will be studied in this example of a digital magnetovariation converter with opto-mechanical quartz variometer.

2. Structural scheme of the converter

Fig. 1 shows the structural scheme of the digital magnetovariation converter with integration. In contrast to the quartz magnetometer [ODINTSOV 1991], the digital magnetovariation converter additionally includes a charge-balancing A/D converter [KIME 1973] which is inserted between the output of the opto-electronic converter of the variometer and

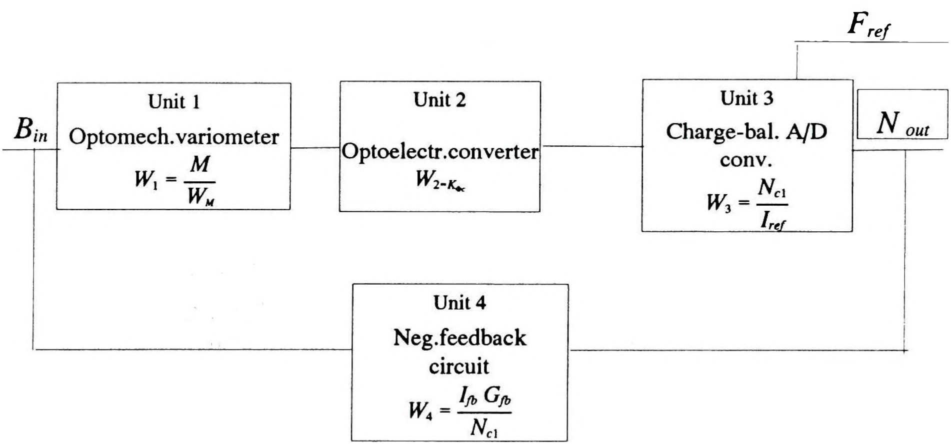

Fig. 1. Block diagram of the digital magnetovariation converter with integration

1.ábra. Az integrálóval ellátott digitális magnetovariációs konverter blokk-vázlata

Рис 1. Структурная схема цифрового магнитовариационного преобразователя интегрирующего типа the input of the negative feedback unit. The strong negative feedback allows the 'null-detection' operation of the variometer, where the indicator magnet practically does not change its position at an arbitrary value (within the measuring range) of magnetic induction at the input of the magnetovariation converter.

Mathematics for the transfer functions W_1 of the variometer and W_2 of the opto-electronic converter are described in detail in [ODINTSOV 1991] and need no explanation here. In the normal mode of operation of the magnetometer these expressions have the following form:

$$W_1 = \frac{M}{W_M}$$

$$W_2 = K_{\Phi c} \qquad \text{where}$$

W_M is the total torsion coefficient of the variometer,
$W_M = C$ or $W_M = C + MB$ (Nm/rad);
C is the torsion coefficient of the quartz thread (Nm/rad);
M is the magnetic moment of the magnet (Am^2);
B is the magnetic field component parallel to the magnetic moment of the magnet (T);
$K_{\Phi c}$ is the conversion coefficient from the angular position of the mirror to the proportional value of output current (A/rad).

Let us deal in detail with transfer functions W_3 of charge-balancing A/D converter and W_4 of negative feedback unit.

3. Transfer functions of the charge-balancing A/D converter and of the negative feedback

The structural scheme of the charge-balancing A/D converter can be seen in *Fig.2.* It includes an integrator, a threshold detector, a clock unit and a reference current source with switch. The converter is characterized by the final value of charge accumulated during a complete integration cycle being zero. The charge absorbed by the integrator during the process when the input current flows will be compared to the output charge of the integrator during its discharge by reference current pulses of strictly fixed and stable duration. In the normal mode of operation the number of

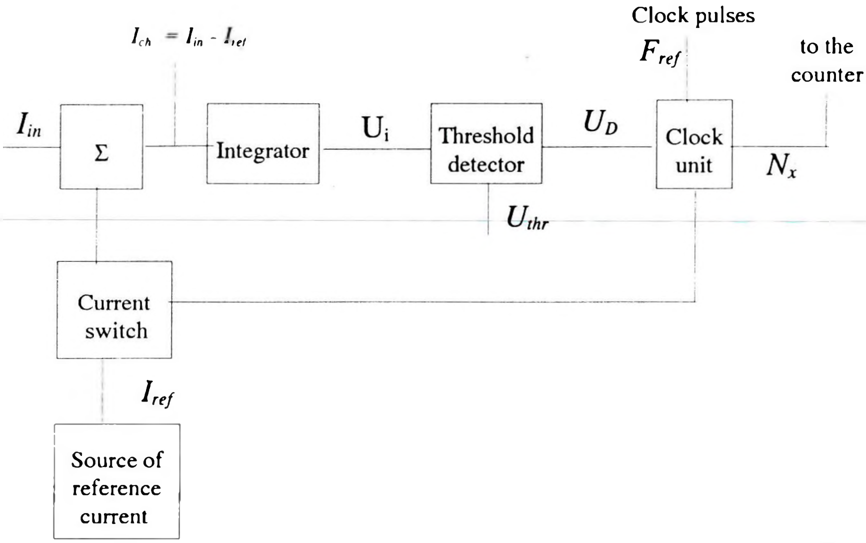

Fig.2. Block diagram of the charge-balancing A/D converter

2.ábra. A töltés-kiegyenlítő A/D konverter blokkvázlata

Рис. 2. Структурная схема АЦП с уравновешиванием заряда

discharge pulses is proportional to the integral of the input current. The integration process is continuous in character and may take an unlimited long time because discharge pulses will be formed at each time when the output voltage exceeds a certain threshold level.

At the start, the current switch turns off and only the input current I_{in} will reach to the input of the integrator. The integrator consists of an inverting operational amplifier and a capacitor, so the time diagram of the voltage U at the output of the integrator is a straight line with negative slope. Its tilt angle is proportional to the value of input current I_{in} :

$$U_{integr} = I_{in} \frac{T_{ch}}{C} , \quad \text{where} \qquad (1)$$

T_{ch} is the charging time of the capacitor C by the input current of the integrator.

The C capacitor will be charged until the voltage at the input of the threshold detector exceeds the level U_{thr}, being equal to the comparison voltage of the threshold detector. Comparison in the threshold detector allows the switching of the clock unit at the arrival of the next clock pulse. At the same time, the current switch will be closed and subtraction of the stable reference current I_{ref} from the input current of the integrator begins. The reference current is chosen higher than any allowed value of the input current. Therefore subtraction of the reference current I_{ref} from the input current I_{in} results in a polarity change of the current I_{ch} at the input of the integrator and the slope of linear voltage U_{integr} at the output of the integrator will be change to positive.

During this part of the integration cycle the clock pulses at the output of the clock unit will be collected by a pulse counter. When the potential U_{integr} reaches the level U_{thr} again (but now from the other side), on arrival of the next clock pulse the clock unit turns the current switch off. So a discharge pulse will get to the input of the integrator. The duration of the pulse is equal to the period or several periods of the clock pulses, while its amplitude is the value of the reference current.

The discharging process of the integrator can be described by the equation

$$- U_{integr} = (I_{in} - I_{ref}) \frac{T_{disch}}{C} \quad , \quad \text{where} \qquad (2)$$

$T_{disch} = N/F_{ref}$ is the time of discharge of condenser C by current I_{ref};
N is the number of clock pulses at the output of the clock unit;
F_{ref} is the frequency of clock pulses.

In the normal mode of operation the total change of voltage at the output of the integrator for one cycle equals zero; the common solution of equations (1) and (2) gives

$$I_{ref}\, T_{disch} = I_{in} \; (T_{ch} + T_{disch}) \qquad (3)$$

Since the integration cycle T_{integr} equals the sum of charging and discharging times of capacitor C, i.e. $T_{integr} = T_{ch} + T_{disch}$, so—taking into account that $T_{disch} = N/F_{ref}$ —the number of pulses N at the output of the clock unit during one integration cycle can be determined from equation (3):

$$N = \frac{I_{in}}{I_{ref}} F_{ref}\ T_{integr} \tag{4}$$

The converter has no external synchronization, so the integration cycles will be repeated continuously until the conversion period is completed. The duration of the conversion period T_{conv} is determined by the number of clock pulses N_{c1} arriving at the digital converter, i.e.

$$T_{conv} = \frac{N_{c1}}{F_{ref}} \tag{5}$$

The value of N_{c1} is a constant for a given converter and is chosen when planning the converter. The number of clock pulses N_x collected by the counter during one conversion period is a variable quantity directly proportional to the input current of the converter. The value N_x actually is the digital output signal of the converter:

$$N_x = \frac{I_{in}}{I_{ref}} F_{ref}\, T_{conv} = N_{c1} \frac{I_{in}}{I_{ref}} \tag{6}$$

From equation (6) the final form of the transfer function of the charge-balancing A/D converter in the normal mode of operation can be obtained:

$$W_3 = \frac{N_x}{I_{in}} = \frac{N_{c1}}{I_{ref}} \qquad [\text{ imp/A }] \tag{7}$$

It can be seen from equation (7) that the conversion coefficient of the input current I_{in} into the digital code N_x depends neither on capacitance C of the integrator, nor on comparison level U_{thr} of the threshold detector, nor on frequency of clock pulses F_{ref} , and consequently does not depend on their stability.

The negative feedback circuit includes the stabilized source of feedback current I_{fb} with current switch and the feedback coil converting the current into magnetic field with conversion coefficient G_{fb} . The clock unit of the charge-balancing A/D converter controls the feedback current switch. This switch connects the feedback coil to the feedback current source for the duration of the current pulse discharging the integrator of the A/D converter. The current form in the feedback coil is periodically repeated pulses with constant amplitude; the pulse duration equals the period or several periods of the clock pulses. The mean value of the magnetic field in the feedback coil can be obtained through the integration features of the quartz variometer under the circumstances when the natural frequency of the variometer is much less (about 3-4 orders) than that of the feedback current pulses. The increase of the digital code ΔN_x at the output of the charge-balancing A/D converter during the conversion period T_{conv} results in the increase of magnetic field in the feedback coil:

$$\Delta B_{fb} = I_{fb}\ G_{fb}\ \frac{\Delta T}{T_{conv}} = I_{fb}\ G_{fb}\ \frac{\Delta N_x}{N_{c1}}\ , \qquad \text{where}$$

$\Delta T = \Delta N_x / F_{ref}$; $T_{conv} = N_{c1} / F_{ref}$. So the transfer function of the feedback unit in the normal mode of operation can be given by the expression:

$$W_4 = \frac{\Delta B_{fb}}{\Delta N_x} = \frac{I_{fb}\ G_{fb}}{N_{c1}} \qquad \text{[T/imp.].} \qquad (9)$$

In the case of feedback, the transfer function of the variometer can be determined by the expression [KLINIEV 1973]:

$$W_{fb} = \frac{W_1\ W_2\ W_3}{1 + W_1\ W_2\ W_3\ W_4} \qquad (10)$$

After substitution of expressions for the transfer functions of the units and transformation of expression (10) we can obtain the equation of the digital magnetovariation converter with integration which expresses the conversion coefficient of the magnetic field to digital code:

$$W_{fb} = \frac{\dfrac{M}{W_M}\ K_{\Phi c}\ \dfrac{N_{c1}}{I_{ref}}}{1 + \dfrac{M}{W_M}\ K_{\Phi c}\ \dfrac{I_{fb}}{I_{ref}}\ G_{fb}} \qquad \text{[imp/T].} \qquad (11)$$

Here the expression $MK_{\Phi c}\ (I_{fb}/I_{ref})\ G_{fb} = W_{EM}$ is an additional torsion moment, the so called electromagnetic torsion [ODINTSOV 1991] which effects the moving part of the variometer due to the negative feedback. So the equation (11) can be written in the form

$$W_{fb} = \frac{N_{c1}}{I_{fb}\ G_{fb}}\ \frac{W_M}{W_M + W_{EM}} = \frac{N_{c1}}{I_{fb}\ G_{fb}}\ (1 - \gamma_0) \qquad \text{[imp/T],} \qquad (12)$$

where $\gamma_0 = W_M / (W_M + W_{EM})$ is the stability of the converter.

Analysis of expression (12) shows that the conversion error is determined by errors in the conversion coefficient of the feedback coil G_{fb} , by the stability of the source of feedback current I_{fb} , but does not depend on errors of the integrator and threshold detector and on instability of the frequency of the reference generator.

4. Principle of the digital magnetovariation converter with integration

The principle of the digital magnetovariation converter with integration based on the opto-mechanical quartz variometer [ZAITSEV et al. 1990] is shown in *Fig. 3*.

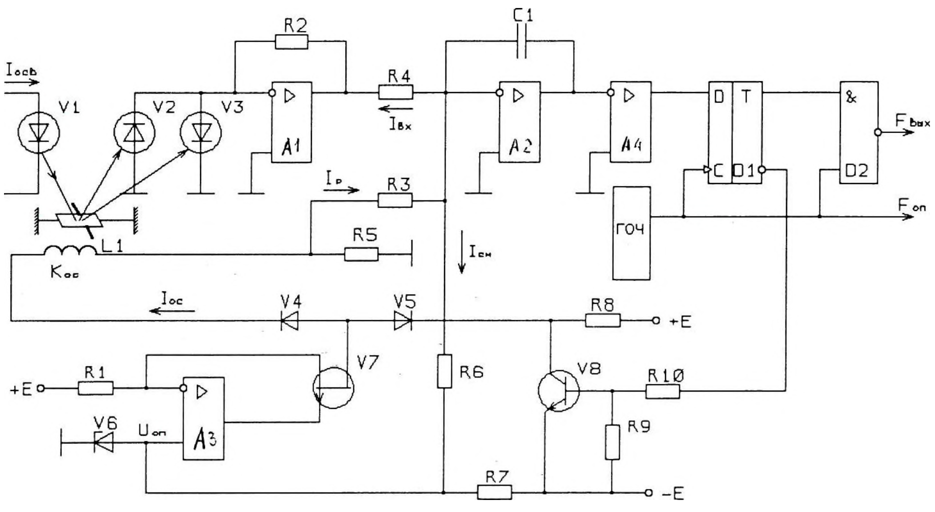

Fig.3. Principle of the digital magnetovariation converter with integration

3. ábra. Az integrálóval ellátott digitális magnetovariációs konverter működésének elvi vázlata

Рис. 3. Принципиальная схема цифрового магнитовариационного преобразователя интегрирующего типа .

It contains a variometer with feedback coil *L1* and opto-electronic converter with led *V1* and photodiodes *V2*–*V3*, current amplifier *A1*, integrator *A2*, threshold detector *A4*, clock unit *D1*, source of feedback current *A3*, *V6*, *V7* with diodic current switch *V4*, *V5*, *V8*.

The output current of the photoconverter will be converted to the input current I_{in} of the integrator by current amplifier consisting of an operational amplifier *A1* and resistors *R2* and *R4*. The general conversion coefficient of the variometer with photoconverter and amplifier can be written in the form

$$K_{MKV} = W_1\, W_2 \frac{R2}{R4} = \frac{M}{W_M} K_{\Phi c} \frac{R2}{R4} \qquad [\mathrm{A/T}] \qquad (13)$$

where $W_1 = M/W_M$ is the conversion coefficient of the opto-mechanical quartz variometer (rad/T);
$W_2 = K_{\Phi c}$ is the conversion coefficient of the opto-electronic variometer (A/rad);
$R2$ is the feedback resistor of the current amplifier (Ω);
$R4$ is the input resistor of the integrator (Ω).

The pulses of discharge current I_{ref} are formed from the feedback current I_{fb} by current divider consisting of resistors $R3$ and $R5$. The feedback current is produced by the source of reference current consisting of operational amplifier *A3* and field effect transistor *V7*.

Standard resistor *R1* and Zener dioda *V6* with output voltage U_{ref} are used as basic elements for the source of the feedback current.

The feedback current and the reference current are determined by the expressions:

$$I_{fb} = \frac{U_{ref}}{R1}; \quad I_{ref} = I_{fb} \frac{R5}{R3 + R5} \qquad [\mathrm{A}]. \qquad (14)$$

The clock unit *D1* will be connected to the output of the integrator through the threshold detector *A4*. The clock unit controls the current switch consisting of diodes *V4* and *V5* through interface transistor *V8*.

In the following the values of construction parameters are given for one possible version of the digital magnetovariation converter with integration for the case when the frequency of the clock pulses is $F_{ref} = 32768$ Hz and the conversion period is $T_{conv} = 1$ s; $M = 5 \cdot 10^{-3}$ Am^2; $G_{fb} = 1.31 \cdot 10^{-3}$ T/A $K_{\Phi c} = 6 \cdot 10^{-3}$ A/rad; $W_1 = 1.25 \cdot 10^5$ rad/T ; $R3 = 910$ Ω; $\gamma_0 = 5.2 \cdot 10^{-3}$;

I_{fb}=5 ·10^{-3} A; $R2$=3.9 ·10^{5} Ω; $R4$=2 ·10^{4} Ω; $R5$=100 Ω;
W_{fb}=5 ·10^{9} pulse/T; W_M=4 ·10^{-8} Nm/rad; W_{EM}=7.66 ·10^{-6} Nm/rad

In negative feedback mode of operation the magnet of the variometer will be stabilized in the position where currents of photodiodes *V2* and *V3* are the same and the output voltage of the amplifier *A1* equals zero. In order to establish the working point of the converter in this mode of operation an offsetting direct current I_{disp} will be connected to the input of the integrator; its amplitude is half of the discharging current and its polarity is opposite to the latter. Since the offsetting current essentially determines the initial working point of the converter, this current should be stabilized taking into account the required measuring accuracy.

5. Experimental test of the digital magnetovariation converter with integration

The digital magnetovariation station type CMVS-6 was developed on the basis of the digital magnetovariation converter with integration [AMIANTOV et al. 1990]. The temperature coefficient of the measuring channels of the station is not more than 0.1 nT/°C and that of the sensors for *D*, *H* and *Z* components is 0.3 - 0.5 nT/°C. The station type CMVS-6 has been operated experimentally since December 1987 on the Antarctic, at station Mirny A continuous series of digital geomagnetic data with 1 s resolution for the station Mirniy for the period from December 1987 to December 1989 has been collected in IZMIRAN [ZAITSEV et al. 1990]. Experiments show high stability and wide dynamic range of the station which allowed recording without distortion of the strong magnetic storm of 13-15th March 1989. At that time the total magnetic variation in component *Z* was more than 3500 nT while the speed of change exceeded 500 nT/min at certain times.

6. Conclusion

The suggested method for digitization of the signals involves the development of a digital magnetovariation converter with integration. Its dynamic range is more than 84 dB; the converter has proper protection from periodic and impulse-like noises and allows the integration the measured signals continuously for an arbitrary long period of time.

REFERENCES

AMIANTOV A. S., ZAITSEV A. N. and ODINTSOV V. I. 1990: The unmanned geophysical datacollection platform based on the digital magnetometer CMVS-6. Physics of the Earth and planetary interiors **59**, 1-2

KAURISTIE K., SUCKSDORFF C. and NEVANLINNA H. (eds.) 1989: Proceedings of the International Workshop on Geomagnetic Observatory Data Acquisition and Processing (Nurmijärvi, Finland May 15-25, 1989), Recording instruments: Summary of instruments for Continuous Recording, pp. 26-27

KIME R. C. Jr. 1973: The charge-balancing A-D converter: an alternative to dual-slope integration. Electronics

KLUIEV A. S. 1973: Automatic controlling. (in Russian) Publ. H. "Energia" Moscow, 391 p.

ODINTSOV V. I. 1991: A development of wide range low noise quartz torsion magnetometers. this issue.

ZAITSEV A. N. and ODINTSOV V. I. 1986: An Integrating Digital-Analogue Converter for Quartz Magnetometers. In: Hardware and software tools for automatization systems in scientific research. (in Russian) Publ. H. of the Kola filial of the Acad. Sci. of the USSR, Apatity, pp. 77-83

ZAITSEV A. N., ODINTSOV V. I. and PETROV V. G. 1990: Digital geomagnetic data and the results of the experimental work among expedition circumstances on the Antarctic, Murny Observatory.(in Russian) preprint No. 19. (904) IZMIRAN, Moscow, 27 p.

A TÖLTÉS KIEGYENLÍTŐ INTEGRÁTORRAL ELLÁTOTT DIGITÁLIS KVARC TORZIÓS MAGNETOMÉTER

V. I. ODINCOV

A szerző a kvarc torziós magnetométer kimenő jelfeszültségének újfajta digitál-analóg konverzióját írja le. Az eljárás a fotoelektronikus rendszerrel ellátott kvarc torziós variométer erős negatív visszacsatolási áramkörébe egy töltés-kiegyenlítő A/D átalakítót helyez be, ami a variométer mágneseinek kitérését elektromos feszültségváltozássá alakítja át. Az automatikus vezérlő áramköri egység átviteli függvényeinek és a magnetométer egészének átviteli függvényének főbb kifejezéseit vezeti le a szerző. A töltés-egyensúlyozó integrátorral ellátott digitális torziós magnetométerre alapozott CMVS-6 digitális mágneses változásokat mérő állomás kisérleti vizsgálatának eredményeit is bemutatja .

ЦИФРОВОЙ МАГНИТОВАРИАЦИОННЫЙ ПРЕОБРАЗОВАТЕЛЬ ИНТЕГРИРУЮЩЕГО ТИПА

ОДИНЦОВ В.И.

Предложен способ дискретизации сигналов оптико-механических кварцевых вариометров с оптико-электронными преобразователями угловых перемещений основанный на включении аналого-цифрового преобразователя с уравновешиванием заряда в цепь отрицательной обратной связи вариометра.

Dан вывод основных расчетных соотношений для передаточных характеристик звеньев структурной схемы и магнитометра в целом.

Приводятся результаты опытной эксплуатации цифровой магнитовариационной станции CMVS-6 на основе цифрового магнитовариационного преобразователя интегрирующего типа разработанного с использованием предложенного способа.

GEOPHYSICAL TRANSACTIONS 1991
Vol. 36. No. 3-4. pp. 227-237

NEW MODEL OF QUARTZ STATION 'SIGMA' AND FLUXGATE MAGNETOMETER FM-2

V. S. BUKREEV*, V. N. KNYAZEV*, A. I. IVANITSA*, A. A. ZAROUTSKIJ*, B. S. PERUNOV*, V. E. KOLESNIK*
and N. Y. BAGDASAROVA*

The paper presents the SIGMA microprocessor-based geophysical measuring system and FM-2 three-component fluxgate magnetometer developed at the authors' workplace. It describes all relevant technical specifications and the operation of each unit.

Keywords: quartz magnetic variometer, microprocessor-based data-acquisition, three-component fluxgate magnetometer

A. Autonomous geophysical measuring station SIGMA

1. Introduction

SIGMA is a microprocessor-based system for measuring the variation of magnetic induction components *Z, H, D* of the Earth's electromagnetic field and other geophysical information in observatory and in a field conditions *(Fig.1)*. The system contain a quartz sensor block, a measurement block, and a data operation block (minimal model). The quartz sensor

* Physics Intrumentation Center, Institute of General Physics, USSR Academy of Sciences

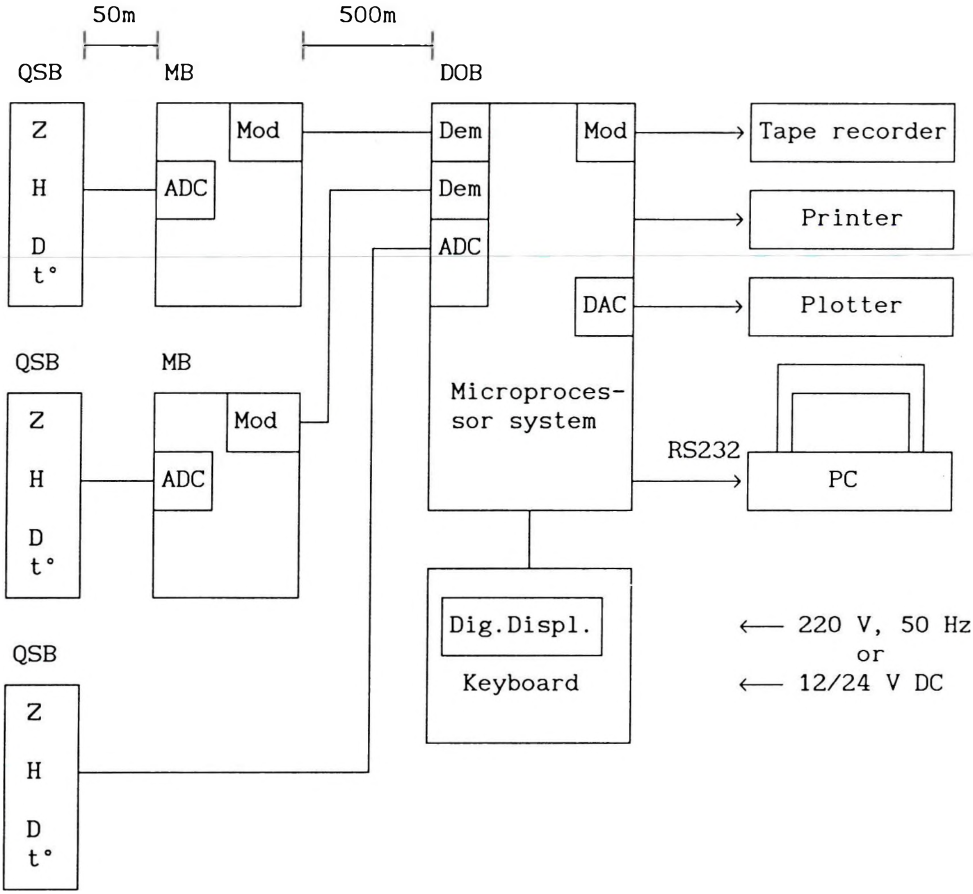

Fig.1. Diagram of the SIGMA system
QSB—quartz sensor block; MB—measurement block; DOB—data operation block

1.ábra. A SIGMA rendszer blokkvázlata
QSB—kvarc érzékelő blokk; MB—mérő blokk; DOB—műveleti blokk

Рис. 1. Диаграмма системы
QSB—узел кварцевых датчиков; MB—узел измерений; DOB—узел операций с данными

block is equipped with a temperature sensor; the data operation block is equipped with a keyboard and a digital display. The system has the following advantages:

— extended measuring range,

— capability of measuring the Earth's electromagnetic field gradients employing two measuring units,

— capability of measuring and registering the temperature of the quartz sensor block with correction of measurement results during subsequent processing,

— capability of effective monitoring of information recorded on a magnetic tape during output on the LCD under field conditions or on a TV set, recorder or printer in the observatory.

Testing and setting up the mode of operation are carried out through the built-in keybord. The system can run either built-in programs or custom programs loaded form an external carrier (e.g. tape recorder).

2. Specifications

Instrument name	Autonomous geophysical measuring station
Type	SIGMA
Supplier	Physics Instrumentation Center Institute of General Physics USSR Academy of Sciences
Reliability	MTBF 2 years MTTR electronic - 1 day sensors - 1 month
Protected	Lightning. Yes Humidity. Yes Radio freq. interference. Yes
Power	20 W (max) Uninterruptible. Yes
Export	Restrictions. No
Cost	$ U.S. 10000
3 Components	Yes

Sensor construction		Orthogonal within ±30'
Resolution		0.1 nT
Dynamic range		±3200 nT, ±8 V
Stability		<1 nT/mo
Passband		d.c. -1 Hz. (-0.5 dB), 2-pole
Noise		0.004 nT rms in passband
Linearity		0.1 % of full scale for sensor, 0.1 % of full scale for ADC
Timebase		±1 s /day (a.c. line ? No)
Sample rate		10 Hz
Measurement rate		1 s and averaging for 60 s time interval
Storage		for measure. rate 60 s in RAM in tape recorder
	4 channels	32 h 17 week
	8 channels	17 h 9 week
	12 channels	11 h 6 week
Temperature coefficient		Sensor block -0.5 nT/°C with temperature corrections -0.1 nT/°C Console 0.1 nT/°C
Temperature range		Sensor block -30 to +40° C Console: MB -10 to +40° C DOB +5 to +40 °C
Temperature recording		Resolution 0.1 °C
Tilt sensor		No (Two tilt indicators)
Azimuth sensor		No

3. Sensor block

The sensor block consists of three quartz sensors *Z*, *H* and *D*. The sensor block contains a quartz frame with a sensitivity element and a reflecting mirror, a photoconvertor, compensation and tuning magnets. The photoconvertor has a temperature coefficient of less than 0.005 nT/°C as a result of the choice of temperature parameters of the photodetectors. The compensation magnet provides a temperature coefficient of 0.2 - 0.3 n /°C. The installation of a compensating magnet on the quartz frame and of the tuning magnet in the quartz tube stabilizes their distance to the sensitivity element, excluding the action of the temperature on the sensor's construction. The sensitivity element thread on the quartz frame is made in the anti-seismic variant: it provides the low self noise of the sensor. The sensor is provided with a feedback winding and a calibrating winding. The temperature coefficient of the windings is less than 0.002 %/°C. All the three quartz sensors are fixed on the platform, which is equipped with three adjusting screws and two tilt indicators.

4. Electronics

The analog signals from the quartz sensor and the temperature sensor are filtered in a 1 Hz band are transmitted through the multiplexer to the input of a 12 bit ADC, which provides measurements with an interval of 0.1 s. The received information is transmitted by the tonal modulator via a two-wire communication line (with a maximum length of about 500 m) to the data operation block.

The data operation block is a system for collecting, processing and registering data of three measurement flows in four channels in each flow. The data operation block is controlled by a microprocessor (analog INTEL 8080).

The information from the measurement block is transformed in the demodulator from sequential to parallel form and is stored in the 35 kbit RAM processor. Depending on selected operation mode (1 or 60 s) the information is stored in RAM without processing or is averaged over 60 s. After RAM overflow the information is dumped to the tape recorder at a rate of 3200 bit/s (57 s), or is transmitted via a standard RS232 at a rate of

4800 bit/s to the computer input. Besides information storage in the RAM all the 12 channels and the current time are indicated on the LCD, and any two channels can be recorded on the plotter.

The data operation block allows one to monitor the information registered on the tape recorder by output on the printer, plotter or LCD. Testing and setting of the station operation mode is carried out via the in-built keyboard. The station is capable of running built-in programs (ROM-4 kB), and also customer programs loaded from external media, e.g. from the tape recorder. The possibility of extending the ROM processor to 20 kB is available by installing the following programs: assembler (4 kB), Basic (8 kB), and service programs (4 kB).

The data operation block can be used as a personal computer to process geophysical information and to solve customer problems provided that a monitor computer keyboard are connected.

B. Fluxgate magnetometer FM-2

1. Introduction

FM-2 was development for space exploration, and can also be used for other purposes, including measuring of absolute values and variations of three components of the Earth's magnetic induction under observatory conditions. FM-2 consists of three blocks: (*Fig. 2.*):

— sensor block
— electronic block
— componensation block.

FM-2 is equipped with a control-test console for magnetometer operation in ground conditions. The device is produced in small series.

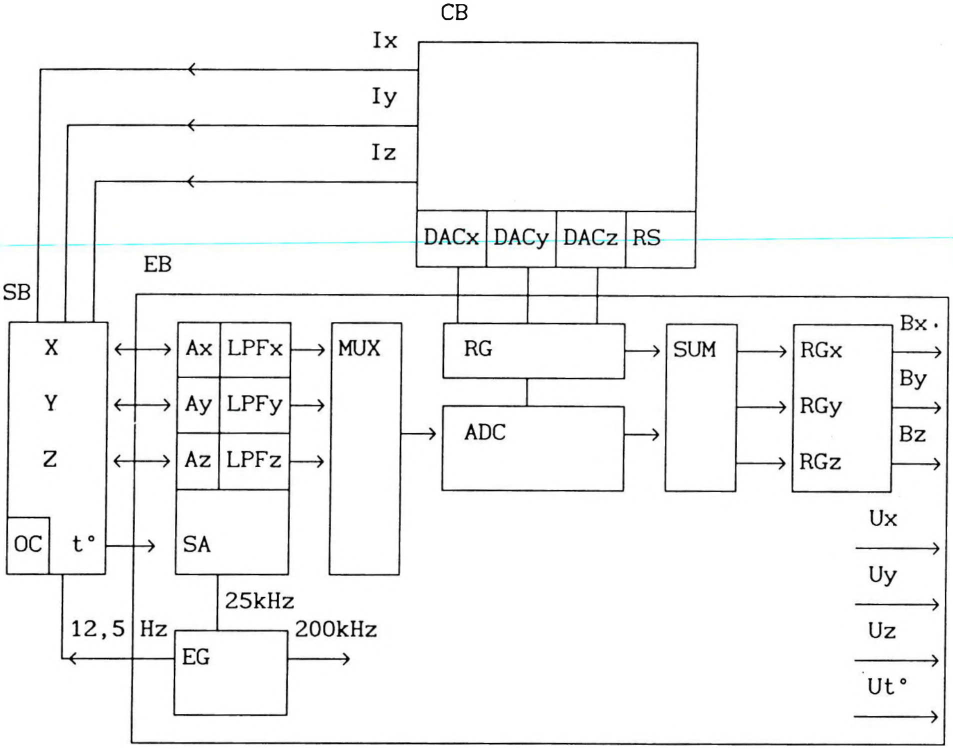

Fig. 2. Diagram of the FM-2 magnetometer
SB—sensor block; EB—electronic block; CB—compensation block

2.ábra. Az FM-2 magnetométer blokkvázlata
SB—érzékelő blokk; EB—elektronikai blokk; CB—kompenzáló blokk

Рис.2. Блок-схема магнитометра FM-2
SB—узел датчиков; EB—узел электроники; CB—узел компенсации

2. Specifications

Instrument name	Fluxgate magnetometer
Type	FM-2

Supplier	Physics Instrumentation Center Institute of General Physics USSR Academy of Sciences
Reliability	MTFB 5 years MTTR electronic - 1 day sensors - 1 month
Protected	Lightning. Yes Humidity. Yes Radio freq. interference. Yes
Power	12 W(max), 8W(standard) Uninterruptible. Yes
Export	Restrictions. No
Cost	$ U.S.10000
3 Components	Yes
Sensor construction	Orthogonal within ±30' Stable to 1.5 " / mo 0.5 " / °C
Resolution	1 nT (dig.output) 0.05 nT (analog output)
Dynamic range	±1000 nT, ±5 V (analog output ±65000 nT (dig. output)
Stability	<1 nT/mo
Passband	d.c. -1 Hz. (-0.5 dB), 2-pole
Noise	0.02 nT rms in passband
Linearity	0.01 % of full scale for sensor (analog output) 0.002% of full scale for ADC
Timebase	±1 s/day (a.c. line? No)
Sample rate	5 Hz
Measurement rate	1 s, 10 s, 60 s

Temperature coefficient	Sensor block -8 ppm/°C with temperature corrections -0.1nT/°C Electronic block 0.05 nT/°C
Temperature range	Sensor block -60 to +60 °C Electronic blocks +5 to +40° C
Temperature recording	Resolution 0.1 °C
Tilt sensor	No
Azimuth sensor	No

2. Sensor block

Three identical one-component sensors *X*, *Y*, and *Z*, which are spaced on the common base, are used in the sensor block of FM-2. Each sensor includes a ring core, an exciting winding, (forming a magnet-sensing element MSE), an element fixing MSE in the sensor body, a signal winding, a compensation winding and a feedback winding, all of copper wire. The ring core is made of permalloy tape, wound on the carrier frame and is protected by another frame. The one-layer compensation winding is placed between the carrier frame and a swinging frame, stabilizing their characteristics. The signal and the feedback windings are sectioned and placed in slots of the swinging frame. All the components of the sensor block are made of machine-processable glass ceramic with the purpose of reaching the characteristics reproducibility and reducing the dependence of the construction's hysteresis effects on temperature. The temperature sensor and the optic cube (20x20x20 mm) are installed on a common base, the non-orthogonality of the faces does not exceed 2″. We can consider any temperature change detected by the temperature sensor to eliminate the temperature effects on the magnetic data. The cable from the sensor block is 10 m long.

3. Electronic block

The electronic block includes an exciting generator of 12.5 kHz, three signal amplifiers with lowpass filters, a multiplexer, ADC, a register controlling the compensation block, a digital summator, and memory registers of output information. The signal amplifier on each channel separates and amplifies signals of the second harmonic of excitation frequency of 25 kHz, measures and carries them to the analog output through the lowpass filter.

4. Compensation block

The compensation block includes three 7 bit DAC, and a reference voltage source. Temperature dependent electronic components are placed into an active thermostat at a temperature 54 °C. The compensation block has ±63 compensation steps of 1024 nT each. The temperature coefficient is not more than ±2 ppm/°C.

The control-test console provides the FM-2 power supply in field conditions from 220 V, 50 Hz current, allowing parameter monitoring, visual indication of components and time, and analog information recording.

The data operation block of SIGMA may be used to record information from the FM-2 in the observatory.

ÚJ TÍPUSÚ SIGMA KVARC BERENDEZÉS ÉS FM-2 FLUXGATE MAGNETOMÉTER

V. S. BUKREEV, V. N. KNYAZEV, A. I. IVANITSA, A. A. ZAROUTSKIJ, B. S. PERUNOV, V. E. KOLESNIK and N. Y. BAGDASAROVA

A cikk ismerteti a szerzők munkahelyén kifejlesztett SIGMA mikroprocesszorbázisú geofizikai mérőrendszert. Leírja az egyes egységek működését és a fontosabb technikai jellemzőket. Ugyancsak ismerteti az FM-2 háromkomponensű fluxgate magnetométert.

НОВАЯ КВАРЦЕВАЯ АППАРАТУРА ТИПА И МАГНИТОМЕТР ФЛЮКСГЕЙТ FM-2

БУКРЕЕВ В.С., КНЯЗЕВ В.Н., ВАНИЦА А. И., ЗАРУЦКИЙ Б.С., ПЕРУНОВ В.Е., БАГДАСАРОВА Н.Ю.

В статье дается характеристика геофизической измерительной аппаратуры SIGMA, разработанной в организации, где работают авторы. Описываются основные технические параметры и действие отдельных узлов. Дается также характеристика трехкомпонентного магнитометра флюксгейт FM-2.

GEOPHYSICAL TRANSACTIONS 1991
Vol. 36. No. 3-4. pp. 239-259

RECENT DEVELOPMENTS OF THE INSTRUMENTATION IN FRENCH ANTARCTIC MAGNETIC OBSERVATORIES

J.M. CANTIN*, J. BITTERLY*, J. BURDIN*, J. FOLQUES*, R. PILLET*, M. BITTERLY*, D. GILBERT**, M. MENVIELLE**
G. CLERC***

Full details are given of the four stations of the antarctic and subantarctic Magnetic Observatories Network. The paper also gives information on the four stations of the French Antarctic and Subantarctic Observatories. Observatory instruments and methods involving both hardware and software are presented together with a portable digital recording field variometer constructed for magnetic repeat stations.

Keywords: magnetic observatories, fluxgate magnetometers, declination, inclination

1. Introduction

The French antarctic and subantarctic Magnetic Observatories Network consists of 4 permanent observatories operated by the Institut de Physique du Globe de Strasbourg. Several magnetic repeat stations are regularly reoccupied. All observatories record three orthogonal elements (*H, D, Z* or *X, Y, Z*) and the total field intensity (*F*). The instrumentation (absolute measurements, variometer and digital recording system) are identical at all observatories. The location of these observatories is given in *Table I*.

* Institut de Physique du Globe, Université Louis Pasteur 5, Rue René Descartes, 67084 Strasbourg Cedex, France
** Institut de Physique du Globe, Université P. Et M. Curie Tour 14-2 a, Place Jussieu, 75252 Paris Cedex 05, France
*** Centre de Recherches Géophysiques, Garchy 58150 Pouilly sur Loire, France

Dumont d'Urville (TERRE ADELIE)	DUM	66° 40'S,	140°01'E	1957
Port-aux-Français (KERGUELEN)	KGL	49° 21'S,	70°12'E	1957
Port Alfred (CROZET)	CZT	46° 28'S,	51°52'E	1974
Martin de Viviés (AMSTERDAM Island)	AMS	37° 59'S,	77°34'E	1980

The operation of the high latitude French observatories is the responsibility of the Territoire des Terres Australes et Antarctiques Françaises (T.A.A.F.).

Table. I. French antarctic and subantarctic magnetic observatories

I. Táblázat. Francia déli-sarki és szubantarktikus mágneses obszervatűroimok

Таблица I. Французские обсерватории на южном полюсе и в близантарктических районах

2. Digital magnetic observatory system (1989)

Digital recording of magnetic data at French antarctic observatories was introduced in 1972. Continuous recording of variations in the Earth's magnetic field is carried out in these observatories with a triaxial fluxgate variometer and a proton precession magnetometer. The new acquisition system described here has been operating continually since 1989 in the Crozet, Kerguelen, Amsterdam Island and Dumont d'Urville observatories.

2.1 The sensors

The VFO 31 triaxial fluxgate variometer, developed in collaboration with THOMSON SINTRA D.A.S.M. Corporation is a parallel type sensor with two saturated mumetal cores. The functioning and the performances of this variometer were analysed in a previous paper [BITTERLY et al. 1988]. The principal characteristics of the variometer VFO 31 are summarized in *Table II.*

1. THREE AXIS MAGNETOMETER SENSOR (construction).

- misalignment between magnetic axis and physical axis: less than 5' angular.
- orthogonality error between sensors: less than 10' angular.
- sensor: length 100 mm, diameter 20 mm.

2. ELECTRICAL SPECIFICATIONS

- excitation frequency: 2 kHz.
- excitation current: 120 mA peak to peak.
- amplitude of the second harmonic: 10μV RMS/nT
- output sensitivity: 5 mV/nT.
- output dynamic range: ±1000 nT from baseline (± 5V)
- frequency response within 3 dB from dc to 0.5 Hz.
- power requirements: 3 W (250 mA/12 V).

3. PERFORMANCE PARAMETERS.

- fluxgate sensor offset: less than 10 nT.
- range: ±79900 nT
- linearity better than 10^{-4}
- noise: 0.1 nT c.c (from dc to 0.5 Hz).
- temperature sensitivity of the sensing head: 0.05 to 0.15 nT/°C for 50000 nT compensated field.
- temperature sensitivity of the electronic housing: 0.01 to 0.08 nT/°C for 50000 nT compensated field.
- long term stability (drift): 1 nT per month.

Table II.. Characteristics of the fluxgate variometer VFO 31

II. Táblázat. A VFO 31 fluxgate variométer jellemzői

Таблица II. Параметры вариометра VFO 31 флюксгейт

A proton precession magnetometer completes the system and measures *F* with a resolution of 0.25 nT. The VFO 31 fluxgate variometer and the proton magnetometer are installed in a thermostatically controlled housing (± 2°C).

It should be observed that the performances of the VFO 31 variometer remain comparable with the characteristics of the other fluxgate instruments recently developed . In particular the excellent long-term stability of VFO 31 has been demonstrated and its resolution (0.1 nT) is consistent with the accuracy of the better absolute measurements. For these reasons, we consider that the VFO 31 characteristics are good enough for us to continue to use this variometer in our magnetic observatories. To upgrade the data acquisition, the IPGS has developed and constructed a new digital recording system based on a portable PC XT computer .

2.2 The Data Acquisition System: description and operation:

The electronics assembly contains all electronic circuit functions: power supply, Ad-on card with real time clock, serial and parallel I/O port and three A/D converter (16 bits). The A/D converter circuits are 100x160 mm Eurocards and the electronic console is 19″ standard rack (3U height). The acquisition system receives the signals delivered by the triaxial variometer (analog inputs) and by the proton magnetometer (digital input). The analog signals from the fluxgate variometer are transformed into digital information by three independent dual slope integrating converters. The three components are sampled simultaneously. The proton magnetometer is triggered by a command generated by the acquisition system at the end of each *HDZ* or *XYZ* sampling (once per minute). The basic instrument system is shown in *Fig. 1*.

2.3 Characteristics of the Data Acquisition System:

— Number of input channels:
  - 8 differential channels by converter
  - 1 channel for proton magnetometer
— Real time clock
— Analog-digital converter
  - 3 dual slope integrating converters (16 bits)
  - converter integrating time: 100 ms
— Sampling rate: software flexible from 1 mn to 2Hz
— RS 232 serial output
— Power requirements 15W-24V
— Power supply 24V-6Ah, internal battery
— Weight of electronic console: 14 Kg
— External battery charger
— Microcomputer: portable PC XT EPSON and control printer

2.4 Data and format:

Minute values (*H, D, Z, F* or *X, Y, Z, F*) are recorded on 3.5″ floppy disc (720 Kbytes) in ASCII storage.

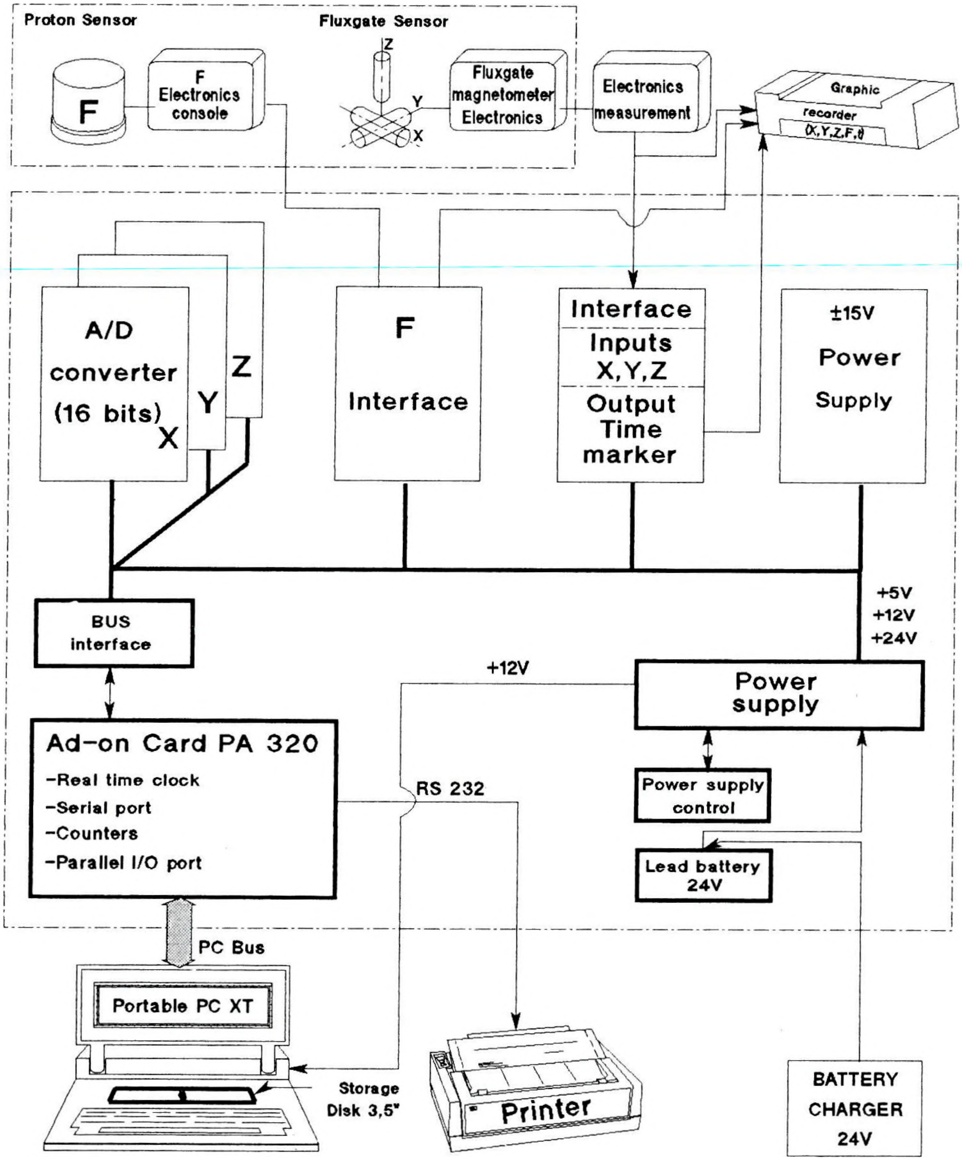

Fig. 1. Block diagram of the digital magnetic observatory system of the Institute de Physique du Globe de Strasbourg

1. ábra. Digitális mágneses obszervatórium-rendszer blokkvázlata

Рис. 1. Блок-схема системы цифровых магнитных обсерваторий

2.5 *Tests and software:*

The data acquisition software is written in assembly language, the data storage and test software in compiled basic. The autonomy with a sampling rate of 1 minute is 12 days per floppy disc (720 Kbytes) in ASCII storage.

For each group of 20 measurements the 'one minute values' of variation field *(H, D, Z* or *X, Y, Z)* are visualized on the PC display with the corresponding date and time. The differences between the instantaneous values of the total field reconstituted from three elements (to take into consideration the baseline references) and the total field values measured with the proton precession magnetometer are calculated every minute. These differences are also visualized on the PC display. For each hour a control message gives the hourly mean value of the differences.

The 1989 data have been processed with the usual observatory software. It is important to note that the percentage of missing one minute values is quasi null. The flexibility of the acquisition software will allow us to take into consideration the INTERMAGNET specifications concerning the sampling rate and the filtering algorithm. In 1991 we expect the magnetic observatory of Port Alfred (Crozet) to join the INTERMAGNET Network by using the METEOSAT geostationary satellite.

3. Magnetic and telluric digital recording system

The Institut de Physique du Globe de Paris (IPGP) and the Institut de Physique du Globe de Strasbourg (IPGS) are developing a programme of telluric observatories. The objective of this program is the study of the conductivity in the crust and upper mantle and its lateral variations on scale.

In the frame of this programme, permanent recordings of the Earth's potential variations started in February 1989 at Port aux Français observatory. The installation was carried out by D. GILBERT (IPGP) and J. BITTERLY (IPGS). The electric potentials are measured with Pb-Pb Cl_2 electrodes made by PETIAU and DUPIS [1980]. We use two perpendicular 400 meters long lines. At low frequencies the electrodes noise is low (1.2μV at 0.001 Hz). The magnetic variations are taken from the triaxial fluxgate variometer VFO 31 of the magnetic observatory.

3.1 Magnetic and Telluric Data Acquisition System:

For this application we have adapted the data acquisition system described in the previous section. A 12 bits A/D converter measures the voltage input for each channel (five filtered components: three magnetic and two electric) every 0.2 seconds. A simple average of 300 instantaneous data, centred on the minute, is sufficient to prevent aliasing. For optimum resolution the signal is conditioned by an automatic 11 levels gain amplifier before the A/D conversion. The block diagram of complete Magnetic and Telluric Digital Recording System is shown in *Fig. 2*

3.2 Specific characteristics of the Magnetic and Telluric Data Acquisition System:

— Input low-pass filters: cut off period 10 seconds, 24 db/octave
— Number of input analogic channels: 16 differential
— Gain amplifier: 2^0 to 2^{10} (11 levels)
— Analog Digital Converter: ±10 V/12 bits
— Sampling rate: software flexible from 0.5 s to 1 min
— RS 232 serial output
— Micro-computer: portable EPSON PC XT (MS-DOS) with printer

3.3 Data and Format:

Minute mean values (*X*, *Y*, *Z* magnetic, *NS* and *EW* telluric) are recorded on a 3.5″ floppy disc, these data are encoded on 16 bits words (4 bits for the gain and 12 for the mantissa). Telluric and magnetic data are put in separate files. A record begins with 24 bytes address followed by 900 words (300 minutes mean values for three components in the case of magnetic files). The autonomy with a sampling rate of 1 minute is 36 days per floppy disc (720 Kbytes) with binary storage.

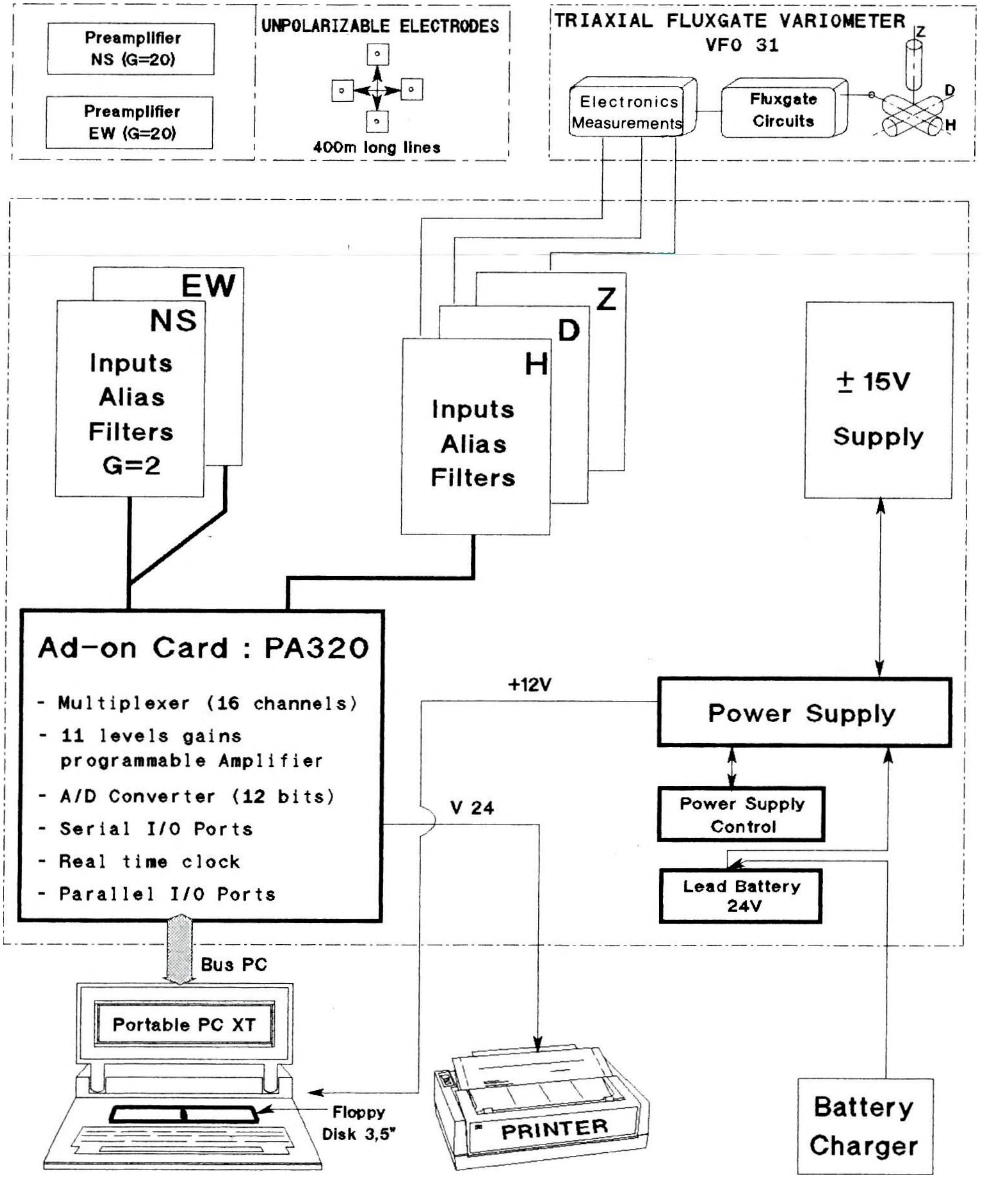

Fig. 2. Block diagram of magnetic and telluric digital recording system in the Ecole et Observatoire de Physique du Globe de Strasbourg

2. ábra. A mágneses és tellurikus digitális regisztráló rendszer blokkdiagramja

Рис. 2. Блок-схема магнитной и теллурической цифровой регистрирующей системы

3.4 Tests and Software

The control system operates in two modes: the automatic mode allows regular control messages on a printer (log book mode); the operator can select a "graphic mode" in order to plot minute averaged data on the computer screen or for quick-look in semi-graphic format on the printer. The running parameters can be checked or modified with the PC keyboard.

This equipment was tested under field operating conditions in 1989 at Port aux Français Observatory. An example of the data acquired at Port aux Français and plotted after processing is shown in *Fig. 3.*

Formatting data software and data processing software (conversion, plotting data storage minute values and mean values) were written in FORTRAN language. The transfer functions were processed for periods ranging from 20 seconds to some hours using both a robust and a non robust method. We have recently presented an analysis of a one year data set [JOUANNE et al. 1990].

4. Absolute instruments: the portable fluxgate declinometer-inclinometer D-I MAG 88

The absolute instruments in use throughout the French magnetic observatories are proton magnetometers (GEOMETRICS G816, ELSEC 870, ELSEC 820M3, Overhauser magnetometer GSM-10 GEM Systems) for measuring total field intensity and two versions of the IPGS portable Fluxgate Magnetometer Theodolite measuring declination and inclination.

The first version of the 'Portable Fluxgate Magnetometer Theodolite with Fluxgate Sensor for Earth's magnetic field component measurements' has been described in two previous papers [BITTERLY et al. 1984 and GILBERT et al. 1988]. This instrument allows direct intensity measurements (X, Y, Z components), it is used regularly at DUMONT D'URVILLE observatory in Antarctica. Indeed the conventional measurements of D and I are difficult at the latitude of this observatory on account of the low value of horizontal intensity (1300 nT).

The prototype of the Declinometer-Inclinometer D-I MAG 88 was presented at the Workshop in Nurmijärvi. The discussion and the results are given in the Proceedings of this Workshop [GILBERT 1990b].

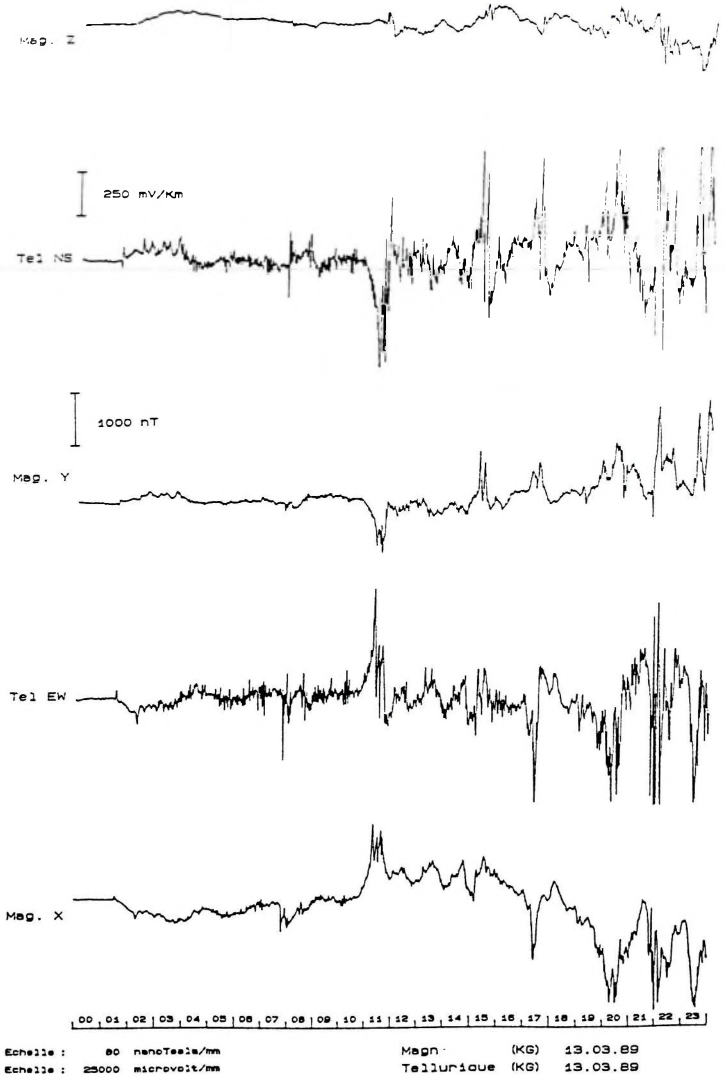

Fig. 3. The strong magnetic storm on March 13-14 1989. For 400 m long telluric line the amplitude of diurnal telluric variation at Kerquelen is about 20 mV/km. Corresponding amplitude of diurnal magnetic variation of horizontal components is about 70 nT

3. ábra. Az 1989. március 13-14-i erős mágneses vihar. A 400 km hosszú tellurikus vonalra a kétnapos tellurikus változás amplitudója Kerquelennél 20 mV/km. A kétnapi mágneses variáció horizontális komponensének megfelelő amplitudó kb. 70 nT

Рис. 3. Сильная магнитная буря 13-14-го марта 1989 г. Амплитуда двухдневного теллурического изменения по теллурической линии длиной 400 м у Кергелен составляет 20 мв/км. Амплитуда горизонтальной компоненты двухдневной магнитной вариации составляет примерно 70 нт

With these instruments we know that 'it is possible to measure, even absolutely, with an accuracy less than one nT' [LAURIDSEN 1990]. After a short recall of the description and technical specifications of D-I MAG 88 we will discuss the recent improvements of this instrument and of the observational procedures.

4.1 Description and technical specifications of D-I MAG 88

4.1.1 Description:

This portable magnetometer theodolite was produced using a fluxgate sensor mounted on the telescope of a one-second non-magnetic theodolite ZEISS JENA 010B.

The fluxgate sensor is of the 'parallel' type with two amorphous cores. The electronics, built by the Institut de Physique du Globe de Strasbourg (IPGS), is housed in a carrying case. The noise of the whole apparatus is less than 0.15 nT peak to peak, the linearity of the magnetometer circuit is better than 0.1% and the temperature coefficient is of the order 0.2 nT/°C.

The precision is better than 5 seconds of arc for D and I measurements. Direct approximate determination of any component of the geomagnetic field is possible by means of auto-ranging from 1-70000 nT. The calibration accuracy is of 0.1 % for the range 2000 to 90000 nT and of 0.15 % for the range 20000 to 90000 nT.

4.1.2 Technical specifications of D-I MAG 88:

Theodolite: ZEISS JENA 010B .

- Mean error: ±1 second of arc
- Special carrying case

Fluxgate sensor: developed by THOMSON SINTRA D.A.S.M. Corporation

- Single axis sensor, 'parallel' type, with two amorphous cores. length: 80 mm, diameter: 18 mm
- Temperature sensitivity of sensing head: less than 0.2 nT/°C in zero magnetic field
- Constant of sensor: 8.8 micro Ampere for 100 nT
- Fluxgate sensor offset: less than 2 nT
- Noise: less than 0.15 nT peak to peak from dc to 0.7 Hz

— Temperature sensitivity of sensing head: less than 0.2 nT/°C in zero magnetic field
— Resolution: 0.1 nT range ±2,000 nT
1 nT range ±20,000 nT
10 nT range ±100,000 nT
— Power requirements: internal, with Pb sealed battery 12 V/6 Ah, external battery charger
— Connecting cable: length 5 m standard

Electronics unit:

— Auto-ranging from 0 to 90,000nT
— Display: 4 1/2 digit standard LCD or LED (option)
-- Output sensitivity: 1mV/nT (range ±,2000 nT)
— Resolution: 0.1 nT range ±2,000 nT
1 nT range ±20,000 nT
10 nT range ±100,000 nT
— Bandwidth: -3dB at 2Hz
— Linearity: 0.1%
— Analog output: ±2 volts full scale
— Power requirements: internal, with Pb sealed battery 12 V/6 Ah, external battery charger
— Consumption: 100 mA/12 V (LCD display)
— Temperature range: -5 to 40 °C
— Carrying case: 21x17x28cm, weight 6kg (together with battery)

Accessories

— Sensor support (aluminium and Noryl)
— Counter-weight in Arcap
— External battery charger
— Operation and service manual (in French language)

The schematic for the measurement electronics is shown in *Fig. 4.*

4.2 Choice of fluxgate sensor for D-I MAG 88

The sensors are of the 'parallel' type with two saturable cores mounted in a quartz chuck. Since 1986 THOMSON SINTRA has delivered sensors with cores in amorphous alloy. The noise performance of these new sensors is improved. The spectral noise density of an old sensor (with mumetal cores) and of a new sensor (with amorphous cores) are given in *Fig.5*. The

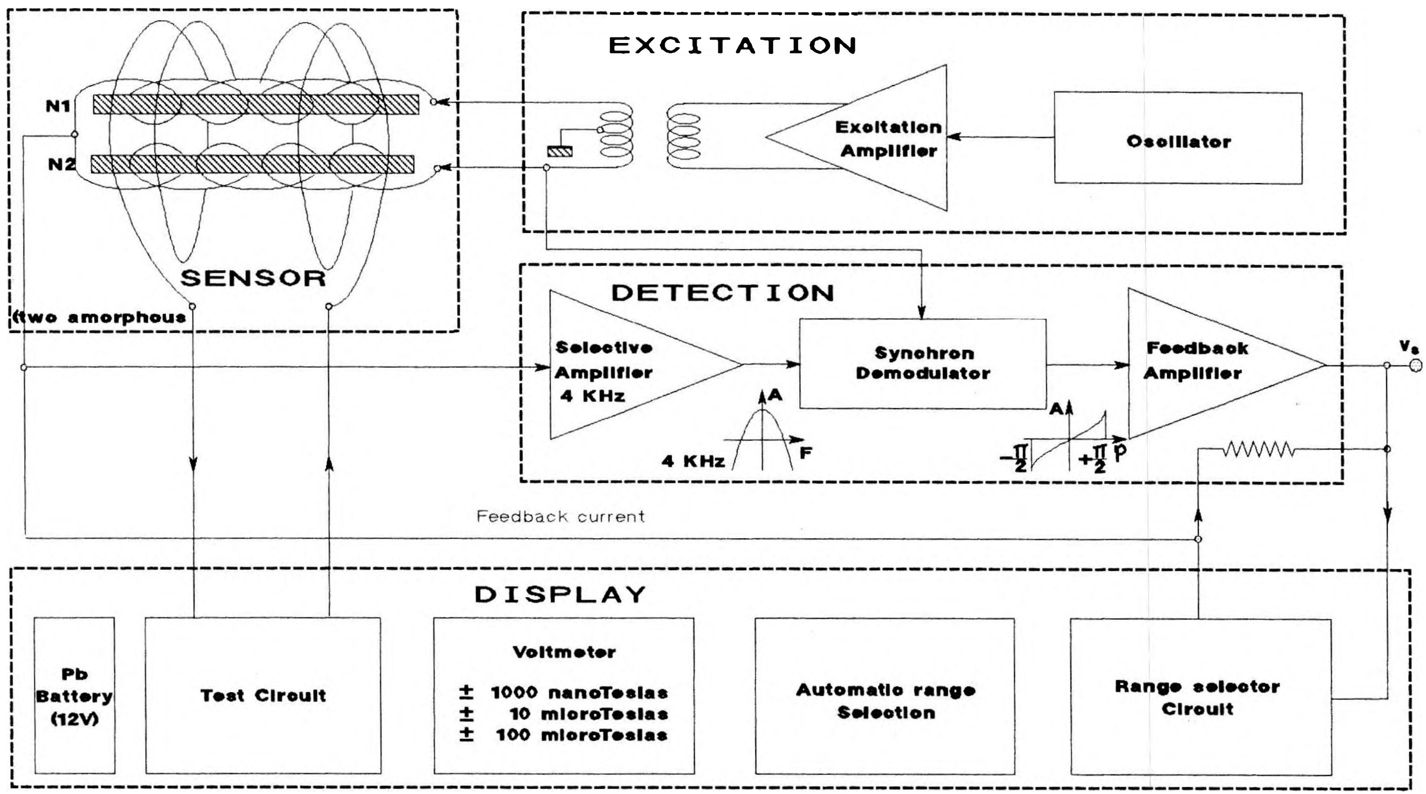

Fig. 4. Portable fluxgate declinometer-inclinometer.Schematic diagram of D-I MAG88. (Ecole et Observatoire de Physique du Globe de Strasbourg)

4. ábra. Hordozható fluxgate deklináció-inklináció mérő.A D-I MAG88 sematikus vázlata

Рис. 4. Портативный прибор флюксгейт для измерения склонения и наклонения

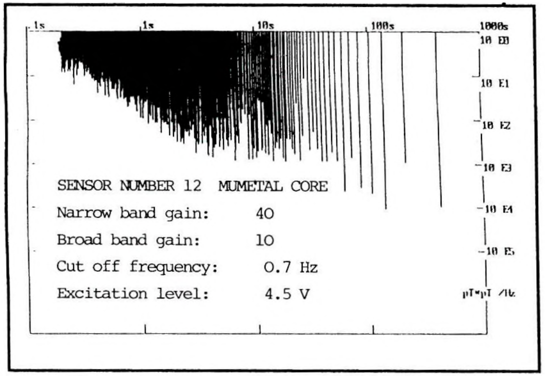

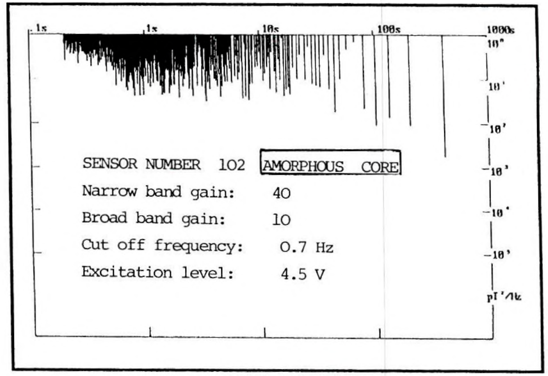

The noise of electronic circuits is less than 0.07 nT p–p

THOMSON CSF FLUXGATE SENSOR I

"Parallel" type

two mumetal cores

Noise power at 1s: 160 $nT^2 Hz^{-1}$

The noise is less than 0.35 nT p–p

THOMSON CSF FLUXGATE SENSOR II

"Parallel" type

two amorphous cores

Noise power at 1s: 80 $nT^2 Hz^{-1}$

The noise is less than 0.15 nT p–p

Fig. 5. Magnetometer D-I MAG 88: Noise spectra (1 to 1,000 seconds). The noise of electronic circuits is less than 0,07 nT_{p-p}

5. ábra. D-I MAG 88 magnetométer zajspektruma (1-től 1000 s-ig). Az elektronikus körök zaja 0,07 nT_{p-p} alatt van

Рис. 5. Спектр шумов магнитометра D-I MAG 88 (от до 100 с) Шум от электронных цепей ниже 0,0 нт $_{p-p}$

limit of resolution of the new sensors is thus between 0.1 and 0.2 nT, a value quite compatible with the resolution of observatory variometers.

4.3 Measurement electronics of D-I MAG 88

We have undertaken to redesign and upgrade the electronic measurement of the first series of the IPGS portable Magnetometer Theodolite. The magnetometer circuit is basically the same but we have added an automatic range selection and a protection circuit against over-discharge of the battery. The dimensions of the electronics box have been greatly reduced.

4.4 Observational procedures in French observatories

—The 'Nulled' method: This method is employed for absolute *D* and *I* measurements. For each classical sensor position a null was obtained at the time at which the observatory magnetometer sampled the field (every minute)

—The 'Residue' method proposed by [GILBERT 1990a]: This procedure is adapted from the method described by LAURIDSEN [1985]. On a *D* measurement the axis of the fluxgate sensor will be close to the perpendicular to the magnetic meridian. On an *I* measurement it will be close to the perpendicular to the total force *F*. The observer does not null the instrument simultaneously with the magnetometer sampling, but reads the displayed value (*R*) of the residual field (in nT with the sign).

The levelled sensor will take four positions :

The first one is the *Lr1* reading on grades and 1/10 of Grades (ggg,d000), corresponding to an approaching null (chosen to be less than 20 nT). The position of the theodolite micrometer is 000 throughout the measurements. On a *D* measurement the following three positions are defined by :

Lr2 = *Lr1* (by rotation around the horizontal axis of the theodolite)
Lr3 = *Lr1* ±200 (by rotation around the vertical axis of the theodolite)
Lr4 = Lr3

On an *I* measurement the following three positions are defined by :

Lr2 = *Lr1* +200 Grades
Lr3 = 600 Grades-Lr2
Lr4 = *Lr3*-200 Grades

As already written the position of the theodolite micrometer is 000 during the measurement. The residual readings (*R*) for the four positions

(*Lr1*, *Lr2*, *Lr3* and *Lr4*) are done on the minute, i.e. at the time at which the observatory magnetometers sample the field. The declination and the inclination may be calculated with the Lauridsen formulae. We may also come down to the 'null' method, introducing the theoretical reading *Lr0* corresponding to a null display.

On a D measurement: $L0 = Lr$ arcsin (R/H)

On an I measurement : $L0 = Lr$ arcsin (R/F)

It is important to note that this method is a 'pseudo-absolute' measurement one. As a matter of fact, the electronics must be ultra linear and have to be calibrated in order to know (or read) exactly the residual values (R) in nanotesla.

Even so, the 'residue' method offers actual advantages:

— It is faster and easier than the 'null' method.

— The 'residue' reading on the minute is easy to do; this is greatly appreciated in disturbed magnetic conditions (auroral zone).

The measurements made with the D-I MAG 88 at Chambon-la-Forêt and at the observatories of the TAAF confirm the perfect agreement of the results obtained with the two methods: The variometer baseline values computed are strictly identical. Since January 1989 the portable Declinometer-Inclinometer D-I MAG 88 has been used as a reference apparatus for the French antarctic and subantarctic observatories and repeat stations.

5. Portable digital recording field variometer

In the southern hemisphere, France has at its disposal a chain of magnetic stations spanning a latitude range of 45° from La Réunion Island to Dumont d'Urville and a longitude range of 89° from Crozet Archipelago to Dumont d'Urville. Various geophysical programs have been developed in this region and it was necessary to provide a portable digital recording field magnetometer for the following applications: magnetic repeat stations, geomagnetic deep sounding, reference station for the study of volcanomagnetic variations (La Réunion) and for the study of the coast effect (Kerguelen Island). The IPGS digital recording field variometer is designed for temporary installations. The instrument is able to monitor the three components and the total field at a rate of 10 samples per minute. The unit may be powered from any 12V DC source.

The equipment comprises 4 sub-systems (sensor, magnetometer electronics 'MAGTER', acquisition system 'STATER', and portable PC XT). The functional block diagram is shown in *Fig. 6*.

5.1 Description of the three components fluxgate magnetometer

5.1.1 Probe assembly

The three axis variometer is based on the THOMSON SINTRA D.A.S.M. fluxgate sensor (two amorphous core) already described in paragraph 3.2. The fluxgate elements are placed in grooves in a granite cube of 10 cm edge length mounted on a marble cylindrical base. Granite and marble have been selected for their low expansion coefficient and the facility for being able to machine the mechanical parts (for the mounting block the orthogonality of the grooves is better than 2 minutes of arc).

Two accurate level bubbles are fixed directly on the granite cube. The rotating plate of the mounting base is in ARCAP non-magnetic alloy . The sensor head is housed in its isolated box. Since this realization (1987) we know that it is preferable to use a suspended system [LAURIDSEN 1988].

5.1.2 The electronics assembly of the magnetometer

The electronics assembly contains all boards housed in a standard rack unit. This rack is enclosed in a fibreglass isolated and water resistant case. We use the same magnetometer cards as for the D-I MAG 88. The compensation generator current, as described in GILBERT [1990b], has a thermal stability better than 1 ppm/°C and linearity better than 10^{-5}.

5.2 Data Acquisition System

The output analog signals of the magnetometer are converted by a data logging system which also receives data from the proton magnetometer. Each minute, the data are stored in a temporary RAM and sent to 'Static Recorder' or to portable PC XT 3.5″ floppy disc. All electronic circuits are packaged in a fibreglass carrying case.

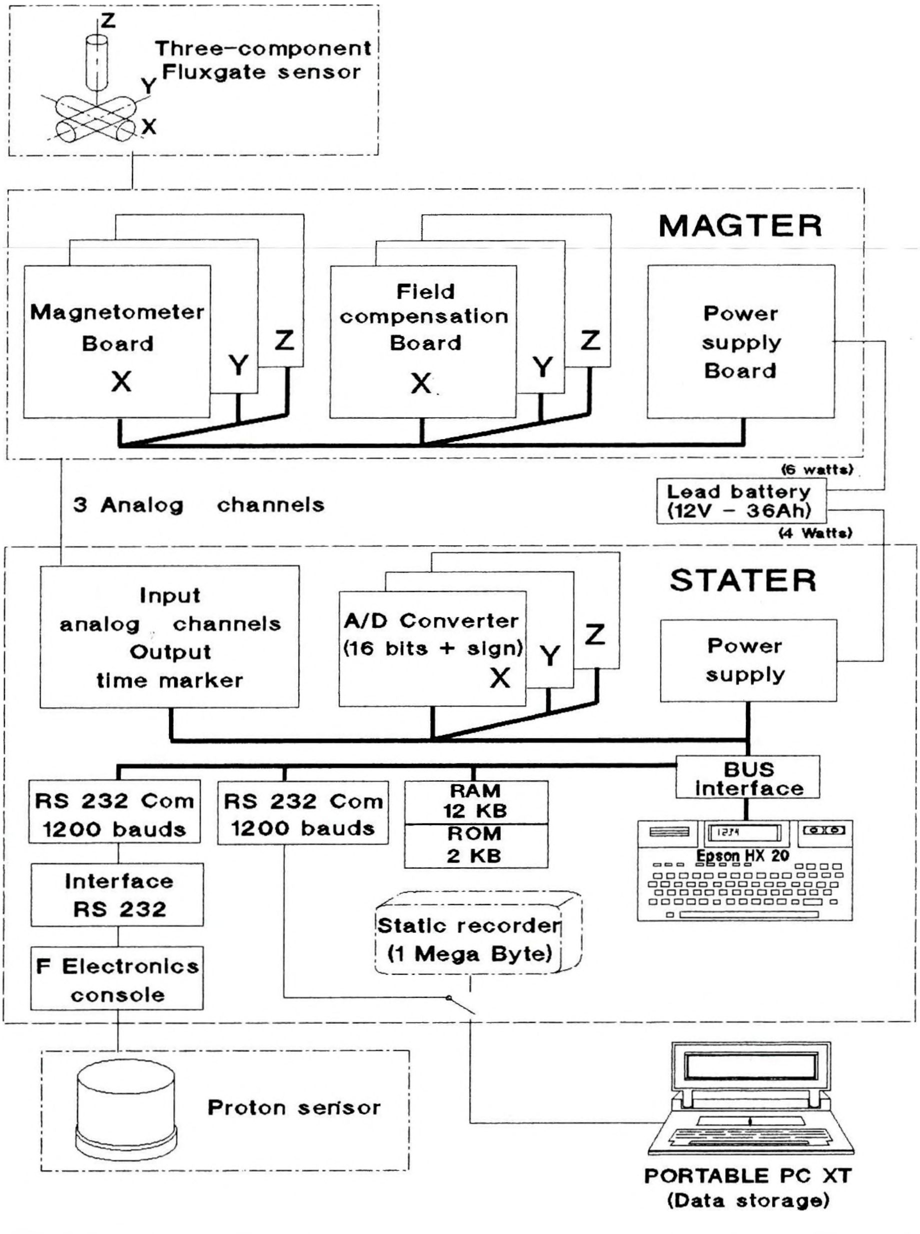

Fig. 6. Digital recording field variometer (portable equipment). Institute de Physique du Globe de Strasbourg

6. ábra. Digitális regisztrálású terepi variométer

Рис. 6. Полевой вариометр с цифровой записью

The different parts of data acquisition are:

5.2.1 Power supply

This card includes three parts:

— supply +5 V for numerical circuits (switching regulator)
— supply ±15 V for analog circuits (DC/DC converter)
— charging unit for HX 20

5.2.2 A/D converter

We use three identical ADC cards to convert the field components. It is a 16 bit integrating converter with separated sign. Its effective range is ±4095.9 nT with 1/16 nT resolution

5.2.3 Analog channels input

— Input signals connectors
— Interface circuit for external use (time marker event)
— Opto-isolated circuit to synchronize the 'real time clock' of the HX 20 micro-computer.

5.2.4 RS 232 communication and interface

— Synchronous serial link with selectable speed between 50 and 9600 Bauds by a strap.
— Specific module enables a serial communication with the electronics console of the proton magnetometer (GEOMETRICS G816)

5.2.5 HX 20 EPSON micro-computer

It is an all-in-one type miniature portable computer with a liquid crystal display, a keyboard, a micro-printer and a micro-cassette. We use it to control the whole external electronic cards with connection to an expansion connector. An extension ROM card contains a part of the user program. The software is written in BASIC language loadable from micro-cassette.

Since 1988 five campaigns have been carried out with the IPGS digital recording field variometer.

REFERENCES

BITTERLY J., CANTIN J. M., BURDIN J., SCHLICH R., FOLQUES J. and GILBERT D. 1988: Digital recording of variations in the Earth's magnetic field in French observatories: description of equipment and results for the period 1972-86. Geological Survey of Canada, Paper 88-17, Geomagnetic series **32**, pp.75-71.

BITTERLY J., CANTIN J. M., SCHLICH R., FOLQUES J. and GILBERT D. 1984: Portable magnetometer theodolite with fluxgate sensor for Earth's magnetic field component measurements. Geophysical Surveys **6**, pp. 233-239.

GILBERT D. 1990a: Nouvelle methodologie pour les mesures absolues magnetiques a partir d'un appareillage D-1 flux. Proc. of the internat. workshop on geomagnetic observatory data acquisition and processing. Nurmijärvi 15-25. May 1989. Geophysical publication of Finnish meteorol. inst. **15**, pp. 67-68

GILBERT D. 1990b: Magnetometre theodolite portable a vanne de flux pour la mesure de la declinaison et de l'inclinaison du champ magnetique terrestre. Geophysical publication of Finnish meteorol. inst. **15**, pp. 69-71

GILBERT D., CANTIN J. M., BITTERLY J., SCHLICH R. and FOLQUES J. 1988: Absolute measurements of the Earth's magnetic field in French observatories: result obtained with the portable fluxgate magnetometer for the period 1979-86. Geological Survey of Canada, Paper 88-17, Geomagnetic series **32**, pp. 59-66.

JOUANNE V., BITTERLY J., MENVIELLE M. and TARITS P. 1990: One year of permanent magnetotelluric recording at Port-aux-Français Observatory. Oral presentation at X. Workshop on Electromagnetic Induction in the Earth, Ensenada, Mexico

LAURIDSEN E. K. 1985: Experiences with DI fluxgate magnetometer. Geophysical Papers R71 pp.1-23.

LAURIDSEN E. K. 1988: Development at Danish Geomagnetic Observatories in recent years. Dt. Hydrogr. Z 41, H. 3-6 pp.131-144.

LAURIDSEN E. K. 1990: Experiences with modern absolute instruments. Geophysical publication of Finnish meteorol. inst. **15**, pp. 72-75

PETIAU G. and DUPIS A. 1980: Noise temperature coefficient and long time stability of electrodes for telluric observations. Geophysical Prospecting **28**, pp.792-804.

AZ ÉSZAKI SARKI FRANCIA MÁGNESES OBSZERVATÓRIUMOK MŰSZEREZETTSÉGÉNEK LEGUTÓBBI FEJLESZTÉSEI

J. M. CANTIN, J. BITTERLY, J.BURDIN, J. FOLQUES, R. PILLET, M. BITTERLY, D. GILBERT, M. MENVIELLE, G. CLERC

A szerzők részletesen ismertetik a négy obszervatóriumból álló hálózat elemeit. Ismertetik az obszervatóriumokban használt műszereket és mérési eljárásokat, részletes hardver és szoftver leírást adva. Bemutatják a mágneses állomások számára készített hordozható regisztráló variométert.

НОВЕЙШИЕ РАЗРАБОТКИ В ОБЛАСТИ АППАРАТУРЫ ФРАНЦУЗСКОЙ МАГНИТНОЙ ОБСЕРВАТОРИИ НА ЮЖНОМ ПОЛЮСЕ

КАНТЭН Ж. М., БИТТЕРЛЫ Ж., БУРДИН Й.,ФОЛОКЕС Ж., ПИЛЛЕ Р., БИТТЕРЛЫ М., ЖИЛЬБЕРТ Д., МЕНВЬЕЛ М., КЛЕРК Ж.

В статье детально рассматриваются звенья сети, состоящей из четырех обсерваторий, а также аппаратура и способы измерений. Дается детальная характеристика технического и программного обеспечения. Представлен портативный регистрирующий магнитометр, сконструированный для магнитных обсерваторий.

GEOPHYSICAL TRANSACTIONS 1991
Vol. 36. No. 3-4. pp. 261-269

TILT-COMPENSATION OF FLUXGATE MAGNETOMETERS

Ole RASMUSSEN*

The disturbing effect of tilting of the piers on the recorded field components in the magnetic observatories is dealt with. In unfavourable conditions tilting may cause a change in the baseline of some 10 nT within a short time. The paper presents the results achieved by a suspended fluxgate magnetometer constructed for tilt compensation; the results approximate to the appointed 2 nT/year.

Keywords: magnetometer, observatories

1. Introduction

Even in the days when we ran the La Cour photographic recorders, we realized that the tilting of the instrument pier could be a serious problem. Of course we didn't have to worry about the two horizontal components since these were measured with suspended magnets and therefore almost unaffected by tilt. Only the La Cour *Z*-variometers suffered from tilting of the piers, which has been described by several authors.

Today it is different. When operating fluxgate sensors in northern Europe or at higher latitudes the two horizontal elements are the ones most sensitive to tilt, so that a tilt of only 5″ of the supporting pier will show up as a change of the baseline of approx. 1 nT.

I know that some observatories have avoided tilting by building their observatories deep in the ground, as is the case with some Japanese observatories. But for most other observatories I think that tilting can be

* Danish Meteorological Institute, Lyngbyvej 100, DK-2100 Copenhagen, Denmark

observed as, for example, a seasonal variation of the baseline values or maybe as small fluctuations of the baselines.

At some observatories like the ones we are operating in the Arctic, tilting can be a real problem causing baseline drift of several tens of nT or more during a very short time in the summer when the permafrozen soil becomes soft.

Figure 1. shows an example of this kind of tilt. Here we have plotted baseline values for the two horizontal sensors together with the recorded tilt of the sensor pier. One can observe a very good correlation between tilt and baseline drift. The scale value of the H-level (LNS) is 0.64 min per full line (i.e.,2 divisions), corresponding to 10.5 nT at Thule. The scale value of the D-level (LEW) is 0.73 per full line (2 divisions), corresponding to 10.5 min at Thule.

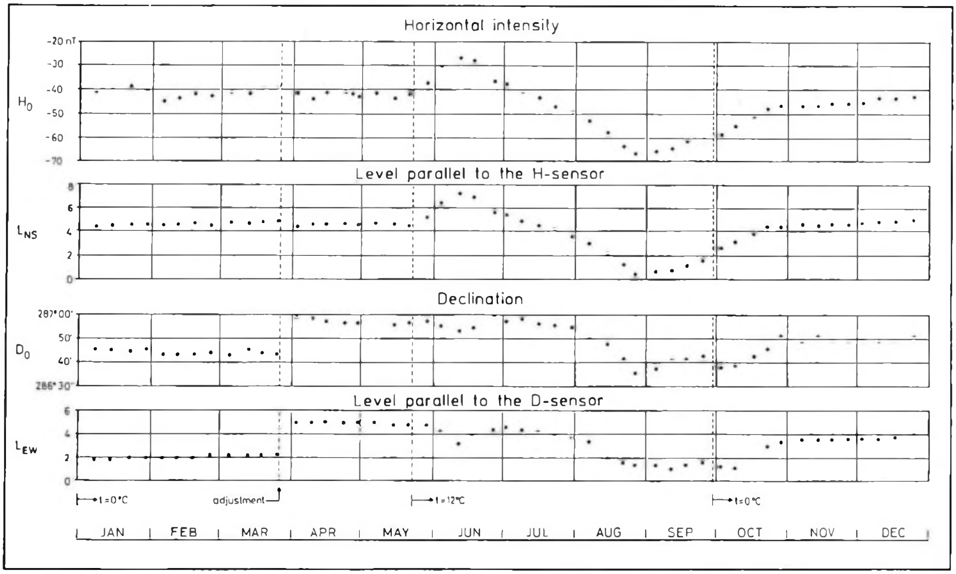

Fig.1. Baseline values and level readings. Thule 1985. Digital fluxgate magnetograph

1. ábra. Bázisvonal értéke és a pillérek dőlésének nagysága

Рис. 1. Значение опорной линии и величина наклонения столба

2. The suspended fluxgate magnetometer at Brorfelde

In an attempt to overcome the tilt problem some years ago we decided to build a suspended fluxgate magnetometer to compensate the tilt. I think it was one of the direct results of the discussions we had during the first instrument workshops in Ottawa. The principle of our suspended magnetometer is shown in *Fig. 2.* It consists of three fluxgate sensors mounted in grooves in a marble cube, the cube being suspended by two orthogonal Phosphor-bronze strips. Pictures of the instrument were published by Lauridsen [LAURIDSEN 1988].

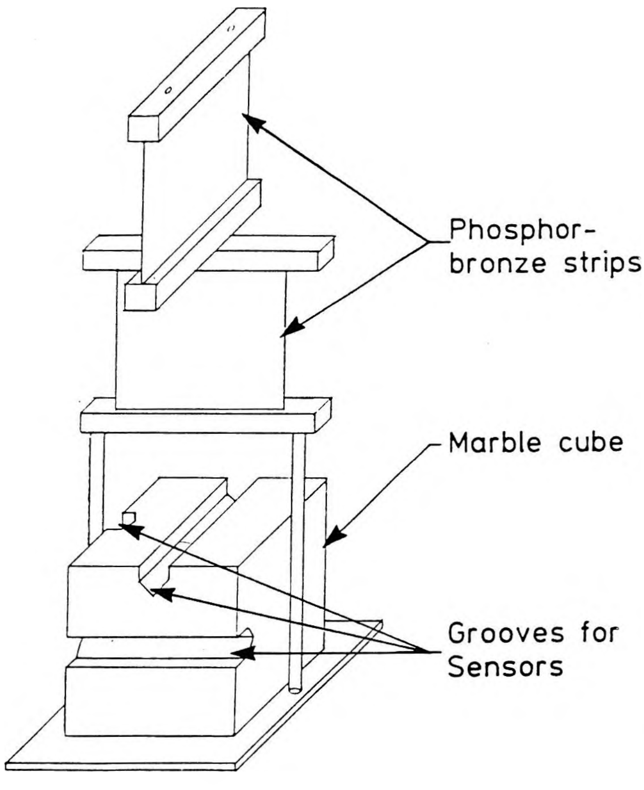

Fig.2. Principle of suspended magnetometer

2. ábra. Felfüggesztett magnetométer elvi rajza

Рис. 2. Принципиальная схема подвешенного магнитометра

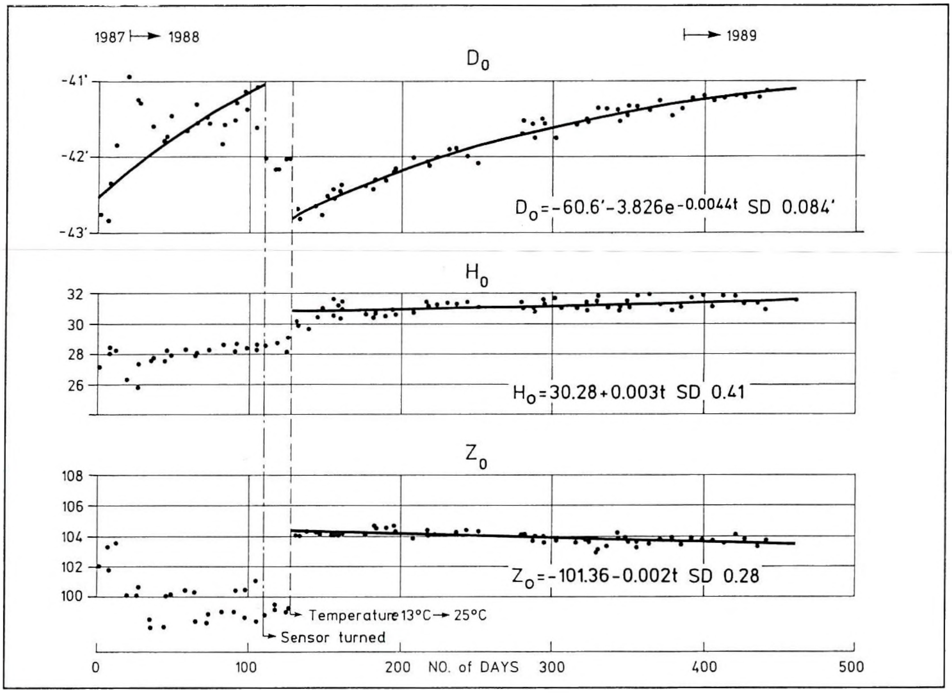

Fig. 3. Long-term stability of suspended system

3. ábra Felfüggesztéses rendszer hosszúidejű stabilitása

Рис. 3. Влияние изменения температуры на датчики

At the workshop in Nurmijärvi, we showed the results [RASMUSSEN 1990] of our first long-term test of the suspended system. It was tested for approximately one year and some of the results are shown in *Fig. 3*. During the first three months we had some problems which were associated with the data collecting system. After that we have had 11 months of undisturbed testing.

The main results are that the H- and Z-sensors show a drift of approx. 1 nT/year, while the D-sensor shows a drift which decays exponentially, so that after one year the drift is down to 3 nT/year.

We think that this rather large drift in the D-component may be caused by a too weak mechanical construction or may be due to improper annealing of the mechanical parts of the instruments.

The temperature drift of the sensors is also illustrated in Fig. 3. The values measured were somewhat higher than those measured before suspending the sensors and we therefore wondered if the higher temperature coefficient could be due to magnetic contamination of the mechanical parts of the magnetometers.

It was therefore decided to take down the instrument in order to test it for magnetic impurities. It did, in fact, show up to be quite magnetic, especially the bottom plate, which was made of brass.

After changing the magnetic parts and also building a new non-magnetic pier for the instrument, the magnetometer was once again set into operation, ready for a new long-term test.

The results for the first 7 months are shown in *Fig. 4*. During the first month some changes can be seen in the baselines, for which we have no good explanation, but some of the drift may have been caused by artificial disturbances as the sensor house was not completely undisturbed during

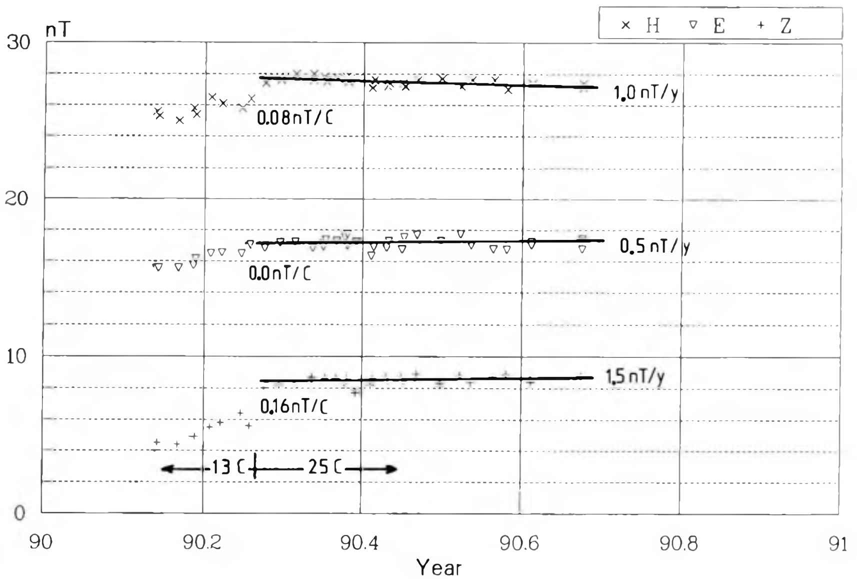

Fig.4. Baseline drift of suspended sensors. Brorfelde 1990

4. ábra. Felfüggesztett magnetométer bázisváltozása Brorfeldben 1990-ben

Рис. 4. Изменение базиса магнитометра в Брорфельде в 1990 г.

this period. The temperature was then raised by 12 °C and we found the temperature coefficients to be within the range expected (< 0.2 nT/°C).

The long-term stability is also very good now being less than 2 nT/year for all three components. I should maybe emphasize that the drift is the total drift of the instrument including, of course, the electronics.

3. Suspended magnetometers in the Arctic

During the last year we have also operated two suspended instruments at the observatory in Thule, where we have had the most serious tilt problems, as already indicated in the introduction. In the last 6 months these instruments were left completely undisturbed giving us an opportunity to measure long-term drift.

The baseline values for the supplementary magnetometer are shown in *Fig. 5.* As can be seen from the figure, we did have a small accident early

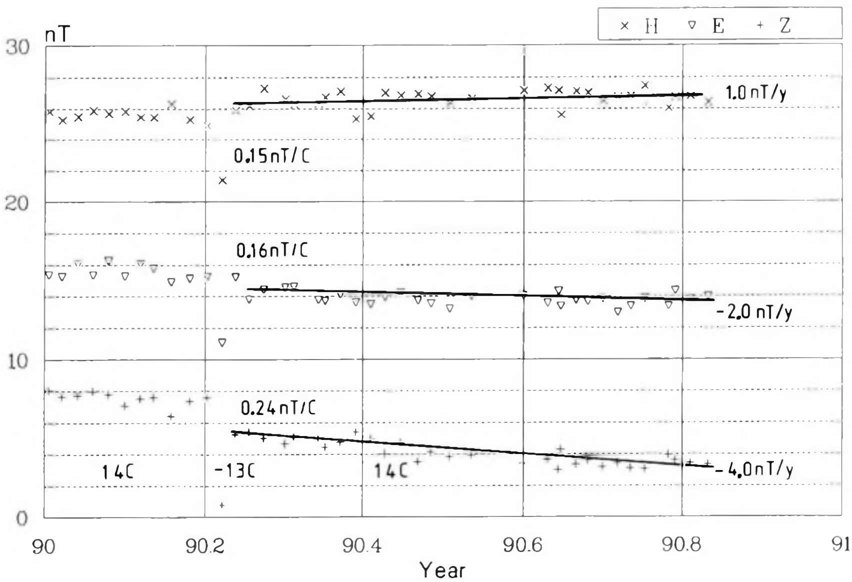

Fig. 5. Baseline drift of suspended sensors. Thule 1989-90. Supplementary magnetometer

5. ábra. Felfüggesztett magnetométer bázisváltozása Thule-ben 1989-90-ben (kisegítő műszer)

Рис. 5. Изменение базиса магнитометра в Туле в 1990 г. (вспомогательный прибор) in 1990, when the heating element in the variometer hut broke down so that the temperature for a few days went down to -13°C. This gave us the possibility to measure the temperature coefficients of the sensors. The temperature coefficients are approximately the same as for the sensors used in Brorfelde.

The long-term stability is also very good, less than 2 nT/year for *H*- and *E(D)*, while the drift for the *Z*-sensor is as high as -4 nT/year. *Figure 6* shows the baselines for the other magnetometer at Thule. The temperature coefficients are approximately the same as for the other suspended magnetometers. And the long-term drift is very good too. Only the *D*-sensor shows a somewhat larger drift.

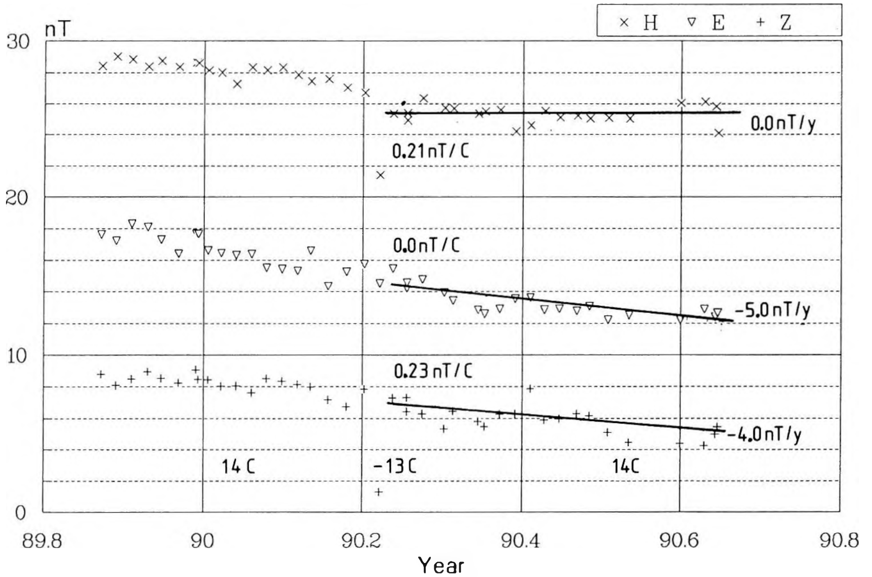

Fig. 6. Baseline drift of suspended sensors. Thule 1989-90 . Primary magnetometer

6. ábra . Felfüggesztett magnetométer bázisváltozása Thule-ben 1989-90-ben (főműszer)

Рис. 6. Изменение базиса магнитометра в Туле в 1989 г. (основной прибор)

4. Summary

In summary I must say that it was our aim to build an instrument with drifts of no more than 2 nT/year in all elements. Unfortunately this was not completely achieved as, for example, the two *Z*-sensors in Thule show a drift of -4 nT/year. As the *Z*-component in Thule is almost parallel to the main field *F*, we have the possibility to investigate this 'large' drift in detail by comparing the protonmagnetometer output with the *Z*-sensor output. I hope such an investigation will give us an idea of what can be the cause of the drift so that the drift can be reduced in future instruments.

Finally I would mention that this year we are installing two more suspended fluxgate magnetometers at variometer stations where we have very serious tilt problems. We are also constructing a portable version of the suspended magnetometer to be used in repeat station work.

REFERENCES

LAURIDSEN E. K. 1988: Development at Danish Geomagnetic Observatories in Recent Years. Deutsche Hydrographische Zeitschrift **41**, pp. 131-144.

RASMUSSEN O. 1990: Improvements in Fluxgate Magnetometers at Danish Meteorological Institute's Magnetic Observatories. Proceedings of International Workshop on Geomagnetic Observatory Data Acquisition and Processing., Finnish Meteorological Institute pp. 93-102.

FLUXGATE MAGNETOMÉTER DŐLÉSKOMPENZÁCIÓJA

Ole RASMUSSEN

A cikk ismerteti az obszervatóriumokban a regisztrálásra használt pillérek elmozdulásának zavaró hatását a mérési eredményekre. Ennek nagysága kedvezőtlen esetben néhányszor tíz nT bázisvonalváltozást is okozhat rövid idő alatt. Bemutatja azokat az eredményeket, melyeket a dőlés kompenzálására konstruált felfüggesztett fluxgate magnetométerrel lehet elérni, és amely megközelíti a kitűzött 2 nT/év értéket.

КОМПЕНСАЦИЯ НАКЛОНЕНИЯ МАГНИТОМЕТРА ФЛЮКСГЕЙТ

Оле РАСМУССЕН

В статье рассматриваются помехи в результатах измерений, возникающие от смещения столба, применяемого в обсерваториях при записях. Величина этих помех в неблагоприятном случае может обусловить изменения в несколько десятков нт по опорной линии. Представлены результаты, достигаемые подвешенным магнитометром флюксгейт, сконструированным для компенсации наклона, и приближающиеся к желаемому значению в 2 нт/год.

GEOPHYSICAL TRANSACTIONS 1991
Vol. 36. No. 3-4. pp. 271-288

THE STANDARD OF WINGST GEOMAGNETIC OBSERVATORY (ERDMAGNETISCHES OBSERVATORIUM WINGST) - ITS IMPROVEMENT AND PRESERVATION, DEMONSTRATED BY EXAMPLES

Günter SCHULZ*

The continuous measurement of the secular variation (SV) of the Earth's magnetic field is a task of highest priority at the Wingst Geomagnetic Observatory of the Bundesamt für Seeschiffahrt und Hydrographie (former Deutsches Hydrographisches Institut). As, by nature, SV progresses very slowly, the devices — i.e. the base-line instruments and, logically, those variometers the base-lines of which are determined by the measurements of the base-line instruments — have to keep their magnetic standards over several decades. Moreover, modern developments in the field of instrument construction have to be utilized in order to improve and/or ensure the standards. This paper describes by means of some examples, where priorities have been placed in the last few years. Problems which have arisen in this connection show where the limits of the measurement accuracy are set.

Keywords: observatory standards, pier tilt, secular variation, fluxgate magnetometer

1. Introduction

When Wingst Geomagnetic Observatory was inaugurated in 1938 it was possible to fall back upon a set of classic devices which had previously been procured for the predecessor station Wilhelmshaven in 1928: a magnetic station theodolite together with an oscillation box, an earth

* Bundesamt für Seeschiffahrt und HydrographieErdmagnetisches Observatorium Am Olymp 13 D-2177 Wingst
Previously published in Dt. hydrogr. Z. 41, 1988. H. 3-6; this version contains measurement data obtained since then

inductor, as well as a photographic variometer system, all designed by G. Schulze, Potsdam [VOPPEL, 1988].

It is remarkable that the station theodolite has been operating as the main base-line instrument for the declination (*D*) until the present day; the photographic recorder — the variometer for the vertical component (*Z*) has been replaced in the meantime by a Lacour balance (which, contrary to the Schulze type, is completely sealed against humidity changes) — is no longer used as the main system for deriving hourly mean values, but renders an indispensable service as a reliable back-up. It is true for both devices — the base-line instrument as well as the variometer — that the accuracy of the readings or the stability of the recording, respectively, is hardly attained by modern instruments.

Similar statements are not true for the earth inductor. Its insufficiency becomes obvious when considering the results of measurements with the first proton magnetometer (PRM), procured in 1960. *Fig. 1* shows a detail of the Schulze system base-lines' original display and, therefore, supplies

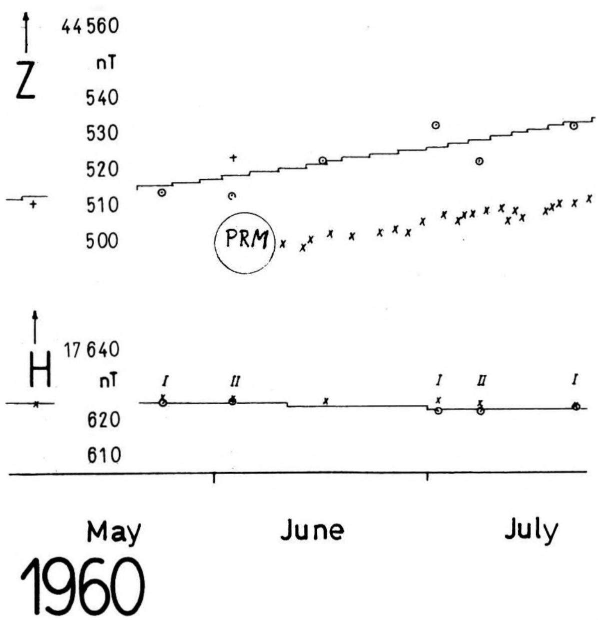

documentation of the Observatory's instrument history. The upper part shows the Z base-line of the Schulze balance. Circles and vertical crosses mean base-line values calculated from the horizontal intensity (H) and the inclination (I), the latter measured by the earth inductor. The wide scatter of these values around the smoothed base-line catches the eye; deviations of some 10 nT are not exceptional. H is shown below; it runs extremely stably.

Starting from the middle of June, the first measurements with the PRM (diagonal crosses) impressively confirm that the scatter has to be entirely attributed to the earth inductor. (The step of some 20 nT between both time series is due to pier differences and deviations between the observatory standard and the International Magnetic Standard, IMS.) From then onwards, the PRM has operated as the primary standard, and the earth inductor has taken second place. That is a classic example for the exchange of standards making use of instrumental innovations.

Fig. 1. Detail of SCHULZE system's H and Z base-line (lower or upper trace, respectively) of 1960, demonstrating the first measurements with the proton magnetometer (PRM) of the type VARIAN 4931 starting on June 09
H base-line:circles denote values measured with the magnetic theodolite according to Lamont's method, where I and II are the numbers of the deflection magnets used; diagonal crosses are values measured with three QHMs (Quartz Horizontal Magnetometer)
Z base-line: circles denote values derived from the smoothed H base-line and I values measured with the earth inductor; vertical crosses are values measured with a BMZ (Balance Magnetique Zero); diagonal crosses denote Z values derived from the smoothed H base-line and F values measured with the PRM

1. ábra. A Schulze rendszer 1960-as H (lent) és Z (fent) bázisvonalainak egy része a VARIAN 4931 típusú proton magnetométerrel (PRM) végzett június 9-én kezdődött első mérésekkel
H bázisvonal: a körök a Lamont módszer szerinti mágneses teodolittal végzett mérések eredményeit, I és II a mérésnél használt kitérítő mágneseket jelölik. Az ikszek 3 db kvarc horizontális magnetométerrel (QHM) végzett mérések értékeit jelölik
Z bázisvonal: a körök a simított H bázisvonalból és a föld-induktorral mért I értékekből számított Z bázisértékeket, a keresztek a BMZ-vel (Balance Magnetique Zero) mért értékeket, az ikszek a simított H bázisvonalból és a PRM-mel mért F értékekből levezetett Z értékeket jelölik

Рис. 1. Часть опорных линий H (внизу) и Z (вверху) 1960-го года системы Шульце с обозначением первых измерений выполненных протонным магнитометром (PRM) типа Вариан 4931 начиная с 9-го июня
Опорная линия H: кружками обозначены результаты измерений магнитными теодолитами по способу Ламонта, I и II обозначены магниты-уклонители применявшиеся при измерениях. Иксами обозначены результаты измерений выполненных тремя горизонтальными кварцевыми магнитометрами (QHM)
Опорная линия Z: кружками обозначены значения базисов Z рассчитанных по сглаженной опорной линии H и значениям I измеренным земным индуктором, крестиками - значения Z выведенные из сглаженной опорной линии H и значений F, измеренными PRM

The introduction of the digitally operating fluxgate magnetometer in 1980 [SCHULZ, 1983] means a complete change, not only from the standpoint of measuring technique but also from that of evaluation methodology. The new system renders improvements as far as linearity and certainty of the scale values, dynamic range, resolution, and cross-talk are concerned; in return for that, concessions have to be made to the stability of the fluxgates. Chapter 2 deals with this item.

As the fluxgates are mounted stationarily, they need not follow the SV — as is necessary with magnets of the classic type. What is more, statements with regard to technical disturbances of spontaneous (or statistical) type (outliers) or systematic type (drifts, cross-talk, and uncertainties of scale values) can be made by means of the simultaneous recording of the total intensity (F). The single components contribute to such a degree in so far as they contribute to the closing error (details are given in Chapter 3).

Whereas the quality of the recording system can be extensively controlled by internal observatory routines, the base-line instruments can only be checked by comparing them with those of other observatories: on the one hand, this can be accomplished by the momentary value comparison with nearby stations [SCHULZ and VOPPEL 1981]; on the other hand, if absolute standards are concerned, direct comparison measurements have to be carried out. Referring again to the station theodolite, it represents the Observatory's absolute D standard. Chapter 4 shows what kind of efforts have been made in order to track down the remaining permeable impurities and to meet the requirements for a connection measurement providing the check as to whether or not the IMS is fulfilled.

Chapter 5 gives an idea of how far pier differences can affect comparison measurements. Not only the instruments themselves have to be carefully preserved but also their environment has to be regularly checked so far as disturbing magnetic fields are concerned.

2. The base-line of the Z fluxgate

In the late 'seventies, the digital recording system was installed. Its main feature is a permanent over-determination, because F is recorded by means of a PRM as well. *Fig.* 2 shows the fluxgate magnetometer's Z

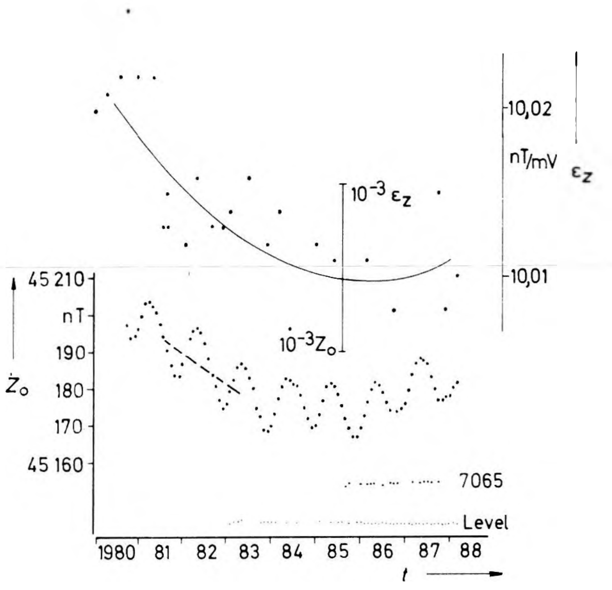

Fig. 2. Lower part: monthly means of the fluxgate magnetometer's *Z* base-line values (left-hand scale) since 1980; upper part: the fluxgate magnetometer's *Z* scale values (right-hand scale), measured galvanically, for the same period.The scales are matched in such a way that equal relative fluctuations of either quantity give the same amount (see the scale in the middle). The small dashed line indicates the part previously shown in [SCHULZ 1983]. For the traces marked by '7065' and 'Level' see the text

2. ábra. Lent: A fluxgate magnetométer Z bázisvonal-értékeinek havi átlagai (bal oldali skála) 1980-tól. Fent: A fluxgate magnetométer *Z*-re vonatkozó skála-értékei (jobb oldali skála), galvanikusan mérve, ugyanerre az időszakra. A skálák úgy vannak összehangolva, hogy mindkét mennyiség egyenlő relatív fluktuációi azonos nagyságúak (lásd a középső skálát). A pontozott vonal a korábban már [SCHULZ 1983]-ban bemutatott részt jelöli. A '7065'-tel és 'Level'-lel jelölt vonalak jelentését lásd a szövegben

Рис. 2. Внизу по-месячные средние (шкала слева из значений по опорной линии *Z* магнитометра флюксгейт начиная с 1980 г. Вверху значения шкал (шкала справа) магнитометра флюксгейт относящиеся к *Z* измеренные гальваническим способом, по тому же периоду. Шкалы увязаны между собой таким образом, что относительные флюктуации обеих величин равны между собой (см. шкалу на середине). Пунктирной линией обозначен участок уже представленный ранее (Шульц (SCHULZ 1983)) Смысл линий, обозначенных '7065' и 'Level', см. в тексте base-line. Monthly mean values of half-weekly measurements cover a period from 1980 to date. A long term trend is superimposed by an annual period, the amplitude of which attains almost 10 nT. As was shown earlier [SCHULZ 1983], the seasonal fluctuation runs with the variation of the humidity inside the variometer house. The point where the humidity penetrates into the system is not yet known.

Let us now have a look at the long term trend. It is the point in question: additionally, in the upper part of Fig. 2, the scale values were drawn in such a way that their relative scatter matches the relative fluctuations of the base-line. The scale values can be determined galvanically with an absolute accuracy of $5 \cdot 10^{-4}$ by means of the Observatory's magnetic field generating and electrical standards.The line smooths the individual values.

A parallel course of both quantities is quite obvious. This means that tilting and any deformation of the fluxgates can be ruled out as a cause of the base-line's trend, the former being confirmed by the level readings (marked 'Level'). Instability of the digital voltmeter within the feedback circuit does not play a role either, as can be seen below (marked '7065').

Two mechanisms are conceivable: fluctuations of the precision resistor and/or the compensation coil's factor, both parts within the feedback loop of the fluxgate.

3. Turning the horizontal fluxgates

Until May 1984, the horizontal fluxgates were aligned towards the geographic co-ordinates X (North component) and Y (East component), respectively. Then the fluxgates were turned counter-clockwise by 45° within the horizontal plain *(Fig. 3)*. As the orthogonal configuration was preserved, the base-line of F could be checked later on by the usual routine.

Y had not contributed to the closing error S until then, owing to the negligible coefficient of the linear term of the series expansion valid for Wingst:

$$S = F_m - F = \delta F_m - \delta F$$

$$\delta F = 0.37\,\delta X + 6.5 \cdot 10^{-3}\,\delta Y + 0.93\,\delta Z$$

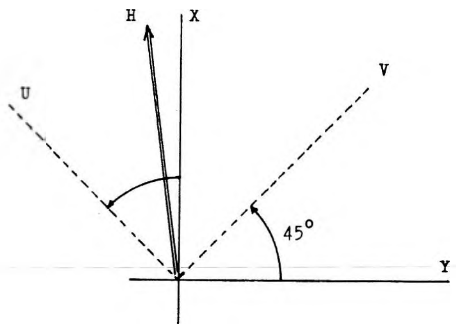

Fig.3. Turning of the horizontal fluxgates counter-clockwise by 45° from (X,Y) to (U,V) within the horizontal plane

3. ábra. A horizontális fluxgate-ek 45°-kal az óramutató járásával ellentétes irányba forgatva (X,Y)-tól (U,V) felé a horizontális síkban

Рис. 3. Горизонтальные флюксгейты повернутые на 45° ж против часовой стрелки от (X,Y) к (U,V) в горизонтальной плоскости

F means the readings of the PRM. Therefore, outliers and short term base-line fluctuations of Y had eluded the check. After the turning, the weight of X was allocated equally to both new components U and V:

$$\delta F = 0.27\ \delta U + 0.26\ \delta V + 0{,}93\ \delta Z$$

This is due to the fact that D almost vanishes at Wingst. From then onwards, D — calculated from U and V — has been included in the permanent check of the F base-line. The recording system has become more secure. *Fig. 4* shows the Z fluxgate in the foreground and those of the horizontal components in the background. One can recognize their directions easily by means of the Helmholtz coils with which the scale values are checked.

A recording sample of 1984, (4th September) from 10 to 20 UTC (*Fig.5*), i.e., three months after turning the fluxgates, where H and D were computed from U and V, demonstrates the efficiency of the over-determined system. A fairly strong disturbance is shown — F and Z each increase by more than 200 nT within two hours. H fluctuates within comparable limits.

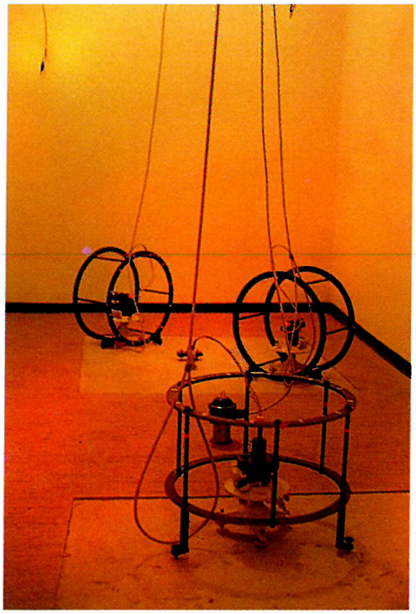

Fig. 4. View of the fluxgates mounted separately on levelled bases, after turning them by 45° (see Fig.3). The components to be recorded can be recognized by the orientations of the Helmholtz coils. *U* and *V* are positioned in the background. For the configuration before that, see Fig.3 in [SCHULZ 1983].

4. ábra. A *Z, U* és *V* műszerek külön-külön szintezett talpakon felállítva, a 45 °-os elfordítás után (ld. 3. ábra). A regisztrálandó komponenseket a Helmholtz tekercs helyzetéből lehet megállapítani. Az *U* és *V* komponenseket regisztráló műszerek a háttérben láthatók. Az ezt megelőző felállást ld. [SCHULZ 1983] 3. ábráján

Рис. 4. Приборы *Z, U* и *V*, установленные на отдельно нивелированных опорах после поворота на 45° (см. рис. 3). Компоненты подлежащие регистрации определяются по положению катушки Гельмгольца. Приборы по регистрации компонент *U* и *V* видны на заднем плане. Предшествовавшую ситуацию см. на рис. Шульц (SCHULZ 1983)

The essential point in this Figure is the run of the base-line *F*, the resolution of which is fifty times higher than that of the components. It can easily be seen that the fluctuation of *F* corresponds to that of *H*. This fact points clearly to cross-talk, because the scale values of *U* and *V* are certain within $5 \cdot 10^{-4}$.

A multiple regression of this recording proved the cross-talk — referred to *F* — to be relatively high for both *U* and *V*:

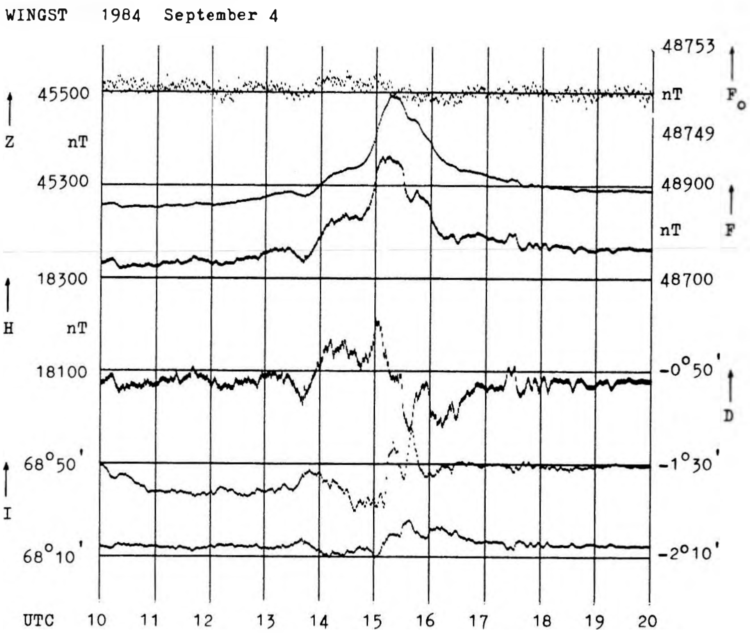

Fig.5. Plotted minute values as a function of UTC. The components *Z*, *H*, and *I* are scaled on the left, *F* and *D* on the right. Top: scatter of base-line *F* scaled on the right. A relationship between *H* and *F* can be recognized.

5. ábra. UTC függvényében ábrázolt perces értékek. A *Z, H* és *I* komponensek a bal oldali skálán, az *F* és *D* komponensek a jobb oldali skálán vannak. Fent: Az F alapvonal szórása. H és F között összefüggés figyelhető meg

Рис. 5. Минутные значения изображенные в зависимости от UTC. Компоненты *Z, H* и *I* находятся на левой, а компоненты *F* и *D* - на правой шкале. Вверху: разброс по опорной линии F. Наблюдется зависимость между *H* и *F*

$$F_0 = C + 10^{-3}\,(3.36\,U + 2.83\,V - 0.64\,Z),$$

where *C* denotes a constant value without any physical significance. 'Referred to *F*' means that only deviations from the orthogonality of the triple as a whole could have been picked up. That is why *F* does not contain any information about the triple's orientation within the reference coordinate system. The coefficients of *U* and *V* can be interpreted as follows: they are caused by a deviation from orthogonality either of the horizontal fluxgates to each other or of the vertical fluxgate against the perpendicular on the plane spanned by the horizontal fluxgates.

Fig. 6 — a check of the *Z* fluxgate's alignment — indeed revealed a tilting towards the South by some 15'. The Figure shows the reception characteristic of the fluxgate projected into the horizontal plain. The characteristic was obtained by turning the fluxgate round the axis of the tripod, plotting the readings azimuthal against their mean. The outcome of the multiple regression resulted in portions for *U* and *V* according to the two circles. They fit well the coefficients of *Z* — indicated by dots.

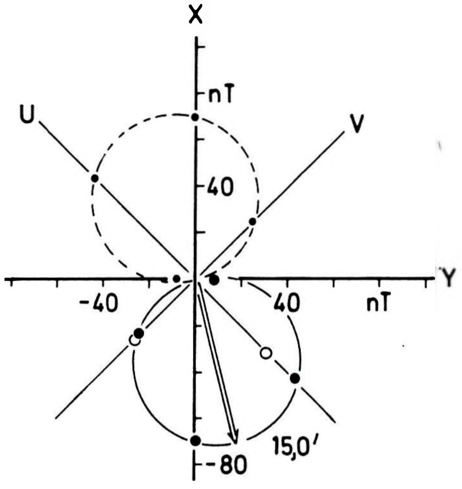

Fig.6. Reception characteristic of the *Z* fluxgate, projected into the horizontal plane, before adjustment. Dots: readings of *Z* referred to their mean value by turning the fluxgate around the tripod's axis; circles: values expected from the result of the multiple regression mentioned in the text. The arrow denotes the direction towards which the fluxgate was tilted.

6. ábra. A *Z* fluxgate vételi tulajdonsága a függőleges síkra vetítve, beállítás előtt. Pontok: A *Z* leolvasási értékei a fluxgate tripód tengely körüli elfordításakor az adatok középértékeire vonatkoztatva. Körök: a szövegben emlitett többszörös regresszió eredményéből várt értékek. A nyíl a fluxgate dőlési irányát jelzi.

Рис. 6. Приемные свойства флюксгейта *Z* в проекции на вертиакльную плоскость перед установкой. Точки: значения отсчета *Z* при повороте флюксгейта вокруг оси треноги, приведенные к средним значениям данных. Кружки: значения ожидаемые по многократной регрессии упомянутой в тексте. Стрелкой обозначено направление наклона флюксгейта

We came to the conclusion that the fluxgate must have been tilted by mistake while the horizontal ones were rotated in May of the same year. The coefficients for *Z* can be used as correction terms in order to cancel the effect of cross-talk when evaluating the recordings.

4. The station theodolite

It has been shown that the base-line stability of *Z* is far from being satisfactory. This problem can be overcome by carrying out base-line measurements more frequently. On the other hand, the variations are recorded with high accuracy due to the fact that the scale values are well known and the alignment of the fluxgates can be monitored and, if necessary, adjusted to within 3' [SCHULZ 1983].

What about the base-line instruments' accuracy? Do they represent IMS? *Table I* shows the result of absolute comparisons between Wingst (WNG) and the observatories Niemegk (NGK), Fürstenfeldbruck (FUR), Witteveen (WIT), Rude Skov (RSV), Brorfelde (BFE), Grocka (GCK), Nurmijärvi (NUR), Belsk (BEL), Hel (HEL) and Tihany (THY) carried out since 1980. It is noteworthy that the difference of *D* shows a systematic portion. The value of some 0.5' towards E (respectively 2 nT) is fairly high.

In November 1987, the difference between the connection measurement pier (SW) and the *D* pier (NE) was checked by the station theodolite itself. Previous results, attained by means of the same method (April 1981 and October 1984), were confirmed. That fact was sufficient motivation for subjecting the theodolite to a thorough investigation.

In the early 'sixties, iron impurities had already been found and were removed within the inserting and revolving device, i.e., rather close to the magnet (Deutsches Hydrographisches Institut, [1965]). In order to trace further possible impurities, a fluxgate was installed in a stationary manner very close to the magnet housing. Then the theodolite was turned around its vertical axis.

Fig. 7 shows the vertical component picked up by the fluxgate (diagonal crosses, left-hand scale). Drawn against the azimuth it clearly shows a double amplitude of some 7 nT.

Measurement			WNG	D	I	F	H	Z		
when		where	minus			nT	nT	nT		
1980	Jun	NGK	NGK	+0.63		-0.1	+2.9		QHM,	PRM
		NGK	RSV	(+0.6)			(-0.6)			
1982	Mar	FUR	FUR	+0.2	+0.1	-1	(-1.7)	(-0.3)	DIF,	PRM
	Jul	WNG	BFE	+0.2			-0.6		QHM	
	Nov	WNG	FUR	+0.21	+0.05	-0.2	(-0.7)	(+0.1)	DIF	PRM
1983	Sep	WNG	FUR						DIF,	PRM
	Dec	WNG	GCK			+0.7			HTM,	PRM
1984	Oct	WNG	WIT	+0.56	+0.06	-1.5	(-1.3)	(-1.1)	DIF,	PRM
1987	Oct	FUR	FUR	+0.40	+0.05	-0.4	(-0.8)	(-0.1)	DIF,	
									PRM	
1988	Apr	WNG	BFE	+0.74	-0.11	-1.0	+1.9	+0.7	DIF,	PRM
		WNG	NGK						PVM	
1989	Feb	FUR	FUR	+0.50	+0.05	+1.5	(0.0)	(+1.7)	DIF,	PRM
	May	NUR	NUR	+0.43	-0.03	+0.4	(+0.5)	(+0.3)	DIF,	PRM
1990	Apr	NGK	NGK	+0.14	-0.38	+1.8	(+5.6)	(-0.4)	DIF,	PRM
		BEL	BEL	+0.49	-0.01	+0.5	(+0.3)	(+0.4)	DIF,	PRM
	May	HEL	HEL	+2.20	+0.35	+3.4	(-3.3)	(+5.0)	DIF,	PRM
	Sep	THY	THY	+0.59	+0.14	-13.1	(-7.6)	(-10.8)	DIF,	PRM *
		FUR	FUR	+0.15	+0.28	-1.9	(-4.3)	(0.0)	DIF,	PRM
		NGK	NGK	+0.45	-0.41	+0.5	(+5.6)	(-1.6)	DIF,	PRM *
1991	Mar	FUR	FUR	+0.58					DIF	*
		BFE	BFE	+0.78					DIF	*
	Apr	BFE	BFE	+0.72					DIF	*

QHM: Quartz Horizontal Magnetometer, PRM: Proton Magnetometer, DIF: Probe Theodolite. Values in parentheses are derived.
Results of comaprison measurements (* preliminary)

Table I. Results of absolute comparison measurements between Wingst (WNG) and the observatories Niemegk (NGK), Rude Sjov (RSV), Brorfelde (BFE), Fürstenfeldbruck (FUR) Witteveen (WIT), Grocka (GCK), Nurmijärvi (NUR), Bels k (BEL), Hel (HEL) and Tihany (THY)

I.Táblázat. A Wingst (WNG), Niemegk (NGK), Rude Sjov (RSV), Brorfelde (BFE), Fürstenfeldbruck (FUR) Witteveen (WIT), Grocka (GCK), Nurmijärvi (NUR), Bels k (BEL), Hel (HEL) és Tihany (THY) obszervatóriumai közti abszolút összehasonlító mérések eredményei

*Таблица I.*_ Результаты абсолютных сравнительных измерений между обсерваториями Уингст (WNG) Нимегк (NGK) Руде Съов (RSV) Брорфельде (BFE) Фюрстенфельдбрук (FUR) Виттевен (WIT) Гроцка (GCK), Нурмиярви (NUR), Бельск (BEL), Гель (HEL) и Тихань (THY)

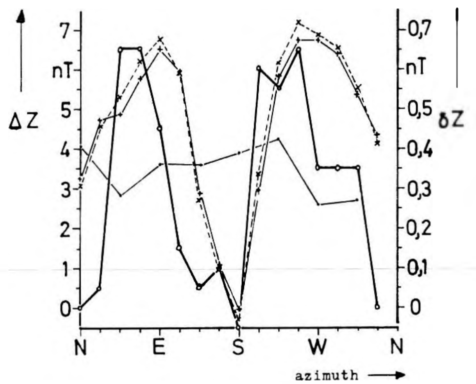

Fig. 7. Fluctuations of the *Z* component close to the station theodolite's magnet housing picked up while turning the instrument around its vertical axis (azimuth). Diagonal crosses (left-hand scale): without an additional field; vertical crosses (left-hand scale): the same procedure after having over-compensated the *Z* component by its own amount (–*Z*), via a Helmholtz coil; circles (right-hand scale): difference between both curves in the sense '–*Z* minus *Z*'; dots (left-hand scale): the same procedure as denoted in the first case after having removed permeable magnetic impurities (see text)

7. ábra. Az állomás mágneses teodolitja melletti *Z* komponens fluktuáció, melyet a műszer függőleges tengelye (azimuth) körüli elforgatásakor vettünk fel. Ikszek (bal oldali skála): kiegészítő mező nélkül; keresztek (bal oldali skála): ugyanaz az eljárás a *Z* komponens saját összegével való (–*Z*) kompenzálása után, Helmholtz tekercs segítségével; körök (jobb oldali skála): a két görbe közti különbség '–*Z* minus *Z*' irányban; pontok (bal oldali skála): ugyanaz az eljárás, mint az első esetben, a permeábilis mágneses szennyeződés eltávolítása után (lásd a szövegben)

Рис. 7. Флюктуация компоненты *Z* близ магнитного теодолита станции записанная во время поворота прибора вокруг вертикальной (азимутальной) оси. Иксы (шкала слева): без дополнительного поля. Крестики (шкала слева): то же, после компенсации компоненты *Z* собственной суммой (–*Z*) с помощью катушки Гельмгольца; кружки (шкала справа): разность между двумя кривыми в направлении '–*Z* минус *Z*'; точки (шкала слева): то же как и в первом случае после удаления проницаемого магнитного загрязнения (см. в тексте

When over-compensating the geomagnetic *Z* component by its own amount (–*Z*), the second curve was obtained (vertical crosses, left-hand scale). The field was generated by means of a Helmholtz coil connected to a highly stable DC source. The difference of both curves in the sense '–*Z* minus *Z*', indicated by the strong line (circles), is referred to the right-hand scale. Its peak-to-peak variation is just 0.7 nT and can be interpreted as the induced part of magnetism within the magnet housing. This is the only part that matters, because the permanent portion can be averaged away by observing in different positions of the telescope (Deutsches Hydrographisches Institut, [1965]).

The curve in the middle of Fig. 7 (dots) again refers to the left-hand scale and demonstrates the result after removing several parts of the housing and replacing them by new ones, where necessary.

Surprisingly, check measurements with the old parts and the new ones, do not show any significant difference, i.e., the alteration did not cause any shift of the *D* level (*Table II*). The differences in the sense 'telescope South minus North' do not differ significantly from each other either.

1985 July 9			Do	telescope South minus North
with	new	parts	-1 ° 29.08'	-0.06'
	old		29.03'	-0.11'
	new		28.96'	-0.12'
new	minus	old	+0.01'	+0.02'

Table. II. Magnetic Theodolite Schulze 75, comparison of measurements with old and new parts, respectively (see text).

II. Táblázat. Schulze 75 mágneses teodolit a mérések összehasonlítása régi és új részekkel (ld. szöveg.)

Таблица II. Сопоставление измерений магнитным теодолитом Шульце 75 с прежними и новыми частями (см. в тексте)

The results are interpreted as follows: the impurities discovered within the housing — in their combined effect — had been negligible in such a way that they had not falsified the *D* measurements at any time. That means that the instrument is now virtually free of iron and may — at least in this sense — represent IMS. The reason for the deviation towards the East when comparing with neighbouring observatories is to be considered elsewhere.

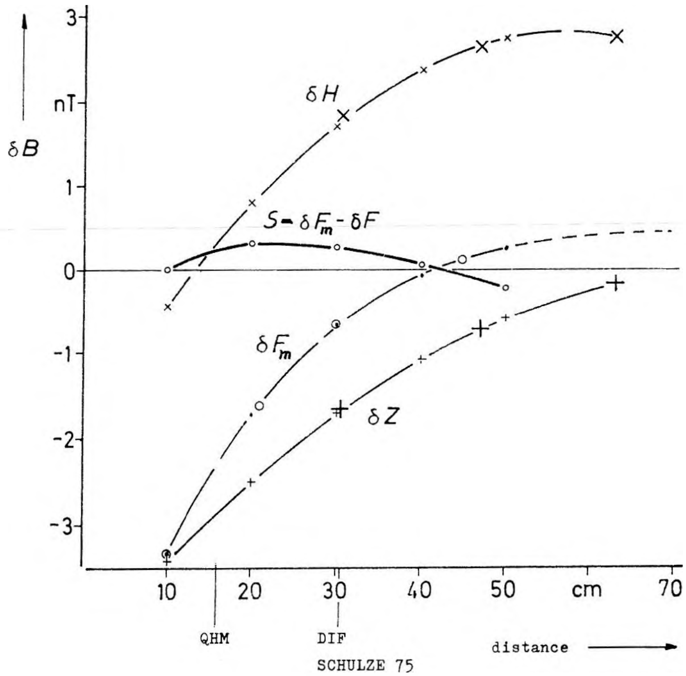

Fig.8. Gradients of pier differences above the connection pier SW in the sense 'NW minus SW'. Enlarged symbols: measured values; small symbols: calculated values. *S* (bold line) denotes the closing error within the magnetic meridian (see text); QHM and SCHULZE 75 mark the positions of the comparison instrument's magnets (quartz horizontal magnetometer or station theodolite, respectively); DIF marks the position of the probe theodolite's fluxgate

8. ábra. Pillérkülönbségek gradiensei a DNy-i kapcsoló pillér fölött 'ÉNy minusz DNy' irányban. Nagy jelek: mért értékek. Kis jelek: számított értékek *S* (vastag vonal) a mágneses meridiánon belüli zárási hibát jelöli (ld. szöveg). QHM (quartz horizontális magnetométer) és Schulze 75 (állomás-teodolit) az összehasonlító műszerek mágneseinek, DIF a próba teodolit fluxgate-jének elhelyezkedését mutatja

Рис. 8. Градиенты разностей между столбами в направлении 'СЗ минус ЮЗ' над юго-западным соединительным столбом. Крупные значки: измеренные значения. Малые значки: расчетные значения. *S* (жирная линия): ошибка при замыкании контура в пределах магнитного меридиана (см. в тексте) 'QHM' (кварцевый горизонтальный магнитометр и 'Schulze 75' (станционный теодолит отмечают положение магнитов сопоставляемых приборов а 'DIF' - флюксгейта пробного теодолита

5. Pier differences

Vertical gradients in D above the connection measurement pier can be ruled out as a cause of the deviation discussed in Chapter 4 because the magnet of the station theodolite and the fluxgate of the probe theodolite, i.e., the instrument the standard was transported with, are positioned at the same distance above the pier. On the other hand, gradients are quite possible, as *Fig. 8* shows. The diagram shows the correction for H, Z, and F as functions of the distance above the pier's cover plate, obtained from a set of different measurements. They were carried out by means of a PRM and a probe theodolite.

Within the range of interest, the closing error

$$S = \delta F_m - \delta F$$

$$\text{with} \quad \delta F = 0.37\, \delta H + 0.93\, \delta Z$$

does not become greater than 0.3 nT. As the difference in F was measured very accurately, the error must be attributed to H and/or Z.

6. Conclusion

The examples make it clear that - besides the routine work — considerable effort is necessary in order to preserve the Observatory's standard and, if possible, to improve it. This means that, apart from any considerations, one has to keep pace with the rapid instrumental development.

At Wingst Geomagnetic Observatory (and, of course, at other observatories as well) the introduction of the PRM and its improvements [Schulz, Carstens 1979] and its development to the proton vector magnetometer [Voppel 1969], [Voppel 1972] and [Schulz 1981] represents an important milestone.

On the other hand, the declination standard, i.e. the station theodolite, was already put into operation in 1928 — four years before the Second International Polar Year — and has not been replaced since. A non-magnetic theodolite of the Zeiss type (DI-flux) may be an alternative.

The introduction of the digital technique in connection with the fluxgate principle resulted in a change of the recording system. However, the base-lines of the modern system do not reach the stability of those of the old photographic apparatus. This is an example showing the need for compromises within the interplay of priorities.

REFERENCES

SCHULZ G. and U. CARSTENS 1979: A period measuring proton magnetometer with a direct readout. Dt.hydrogr. Z. **32**, pp. 119-125.

SCHULZ G., 1981: Base-line measurements of the declination, by means of a proton vector magnetometer, at the Wingst Geomagnetic Observatory (Erdmagnetisches Observatorium Wingst) Dt.hydrogr. Z.**34**, pp. 26-37

SCHULZ G. and D. VOPPEL 1981: A comparison of momentary values between 22 European geomagnetic observatories continued over many years. Manuscript presented at the 4th IAGA Scientific Assembly, Edinburgh, Aug.3-15, 1981

SCHULZ G.1983: Experience with a digital recording magnetometer system at Wingst Geomagnetic Observatory (Erdmagnetisches Observatorium Wingst). Dt.hydrogr.Z.**36**, pp. 173-190

Deutsches Hydrographisches Institut, 1965: Preface in: Ergebnisse der erdmagnetischen Beobachtungen im Observatorium Wingst in den Jahren 1961 und 1962. Deutsches Hydrographisches Institut. Erdmagn.Jahrb. **13**, Hamburg

VOPPEL D. 1969: Ein Spulentheodolit zur Messung der erdmagnetischen Komponenten mit dem Protonenmagnetometer. Z. Geophys. **35**, pp. 151-159.

VOPPEL D.1972: The proton vector magnetometer at Wingst Observatory. Deutsches Hydrographisches Institut. Erdmagn.Jahrb. **17**, pp. 133-149, Hamburg

VOPPEL D. 1988: Some remarks on the history of Wingst Geomagnetic Observatory during the first 50 years. Dt.hydrogr.Z.**41**, pp. 109-117

A WINGSTI MÁGNESES OBSZERVATÓRIUM ÁLLANDÓI - TÖKÉLETESÍTÉSÜK ÉS MEGŐRZÉSÜK NÉHÁNY PÉLDÁN BEMUTATVA

Günter SCHULZ

A földi mágneses tér szekuláris variációjának folyamatos mérése a Bundesamt für Seeschiffahrt und Hydrographie (korábban Deutsches Hydrographisches Institut) wingst-i geomágneses obszervatóriumának legfontosabb feladata. Mivel természeténél fogva a szekuláris mágneses variáció igen lassú folyamat, a mérőeszközöknek - nevezetesen az abszolút-műszereknek és természetesen azoknak a variométereknek, melyeknek bázisait ezen műszerek mérései alapján határozzák meg - több évtizeden keresztül meg kell

őrizniük minőségüket. Másfelől, a műszerfejlesztés eredményeit fel kell használni a minőség megtartásának ill. javításának érdekében. Jelen dolgozat néhány példán keresztül bemutatja, mely területek kaptak jelentőséget az elmúlt években. Az ezzel kapcsolatban felmerült problémák jelzik, hova helyeződtek a mérési pontosság határai.

ПАРАМЕТРЫ МАГНИТНОЙ ОБСЕРВАТОРИИ В УИНГСТЕ ИХ УСОВЕРШЕНСТВОВАНИЕ И СОХРАНЕНИЕ ИЛЛЮСТРИРОВАННОЕ НА НЕКОТОРЫХ ПРИМЕРАХ

Г. ШУЛЬЦ

Задача Магнитной обсерватории в Уингсте заключается в наблюдении вековых изменений магнитного поля. Фундаментальным требованием обсерватории является постоянство (или хотя бы известность) аппаратурных параметров в течении нескольких десятилетий. Наряду с этим имеются значительные достижения в разработке новых видов магнитной аппаратуры. Автором дается характеристика процесса введения новых видов аппаратуры в Обсерватории Уингст с иллюстрациями на примерах.

GEOPHYSICAL TRANSACTIONS 1991
Vol. 36. No. 3-4. pp. 289-302

A MAGNETIC OBSERVATORY / INTERMAGNET INTERFACE

Gerrit JANSEN VAN BEEK*

The paper gives some useful recommendations for observatories when changing the former instrumentation to a new one that is compatible with INTERMAGNET. Proposals for data acquisition (hardware) and for processing (software) are included. It briefly presents the procedures for processing magnetic data and for data validity checking, and describes the way in which one can obtain data measured by other members of the net and one can be given other pieces of information derived from these data.

Keywords: magnetic observatory, INTERMAGNET

1. Introduction

The Canadian Magnetic Observatory Unit has edited digital data since the installation of the first AMOS MK I at St. John's in 1969. Since that time, there have been 2 major observatory hardware changes and at least 4 major data computer mainframe or operating system changes. With the introduction of the CANMOS/INTERMAGNET instrument configuration, extensive modification of the data processing procedures are again in progress. This paper presents some recommendations which may be useful when changing to observatory instrumentation compatible with INTERMAGNET. The discussion also concerns data stored at the observatory and real-time data collected at a Geomagnetic Information Node (GIN) from the INTERMAGNET net.

* Geological Survey of Canada, Geophysics Division, Observatory Crescent, Ottawa, Canada K1A 0Y3

2. Hardware

An INTERMAGNET compatible magnetic observatory consists of a digital 3-component magnetometer and a digital absolute *F* magnetometer. *Figure 1* illustrates such an arrangement of instruments around a central

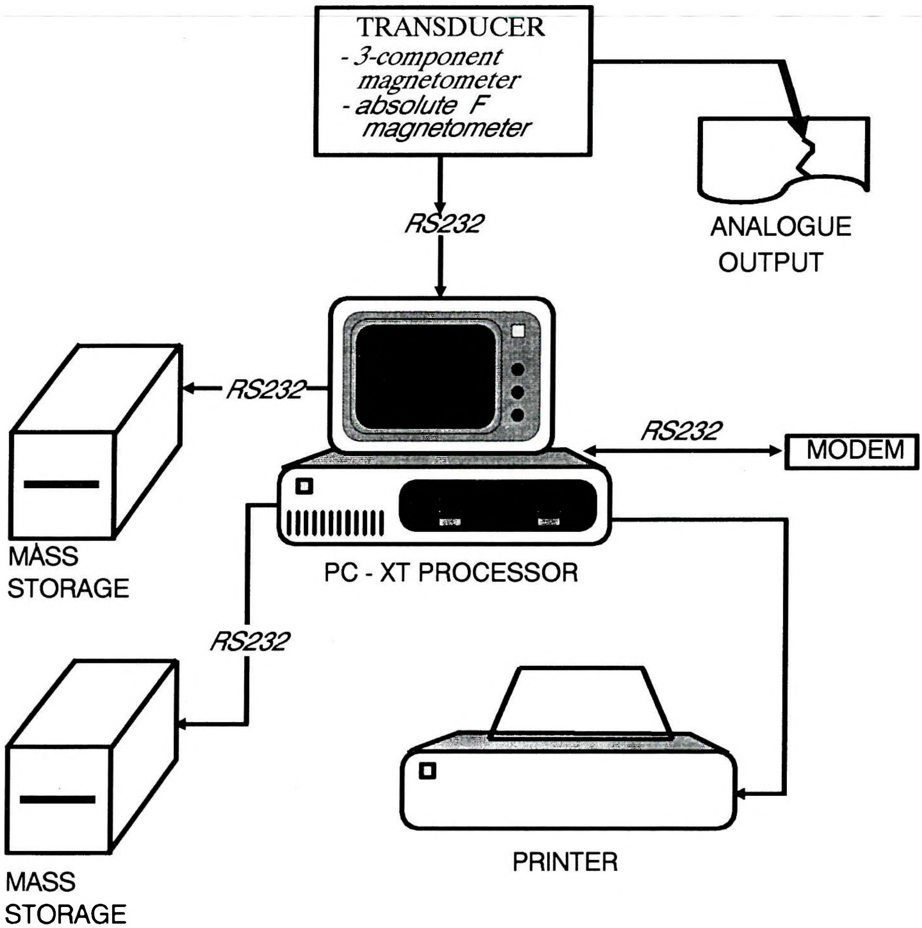

Fig. 1. Data collecting platform

1. ábra. Adatmérő és gyűjtőhely

Рис. 1. Пункт производства измерений и сбора данных controller capable of communicating with a wide area network. The heart of the system is a personal computer which acts as a controller of all the peripherals. By the use of the standard communication protocol RS232 up to eight serial devices can be attached to the PC serial ports. One of these ports may be attached to an INTERMAGNET satellite radio transmitter. In addition, by the use of a Small Computer System Interface (S.C.S.I.) board, numbers of S.C.S.I. mass storage devices may be serially linked to each other. This provides considerable flexibility in the on-site storage of data.

The personal computer will allow both DOS and UNIX operating systems. In turn, these operating systems are able to use BASIC, FORTRAN and C compilers. BASIC and C are able to handle interrupt-driven tasks. If the PC is an 80386 operating in UNIX, then any number of tasks can be run at different priorities at the same time without resorting to such memory hungry software as WINDOWS.

For ease in later editing of the stored data in case the INTERMAGNET net fails, the following suggestions with respect to data storage should be kept in mind:

— Do not pack the data by the use of non-standard binary values or character packing routines as recovery from storage medium failure may be impossible. For unattended operation then, 1.2 or 1.4 Mb floppies are not recommended because of the limited data storage capacity.
— If at all possible use ASCII code for ease in resolving hardware problems.
— Allow enough numbers to define the dynamic range of the geomagnetic field (+/- 3500 nT should be a minimum).
— Terminate records with a carriage return/line feed pair as this is recognized by BASIC, FORTRAN and C.
— Keep records to a length which when in ASCII code can be accepted by full screen text editors (usually 500 to 600 characters).
— All recording media can develop a bad spot in the middle of the file. Therefore, use recording/reading devices that will allow one to read past these spots.
— Embedding signposts in the record (+ or - signs or a sequence of special characters) allows one to recover data from within a record which has become jumbled or to regain position in a stream type file.

Traditionally, observatory data were recorded at one site and processed in some other place. *Figure 2* illustrates an assembly of equipment with which to process the stored data. This equipment will also serve to produce backup data in case the INTERMAGNET communication link fails. The final product is a file of magnetic data suitable for merging into the INTERMAGNET data file.

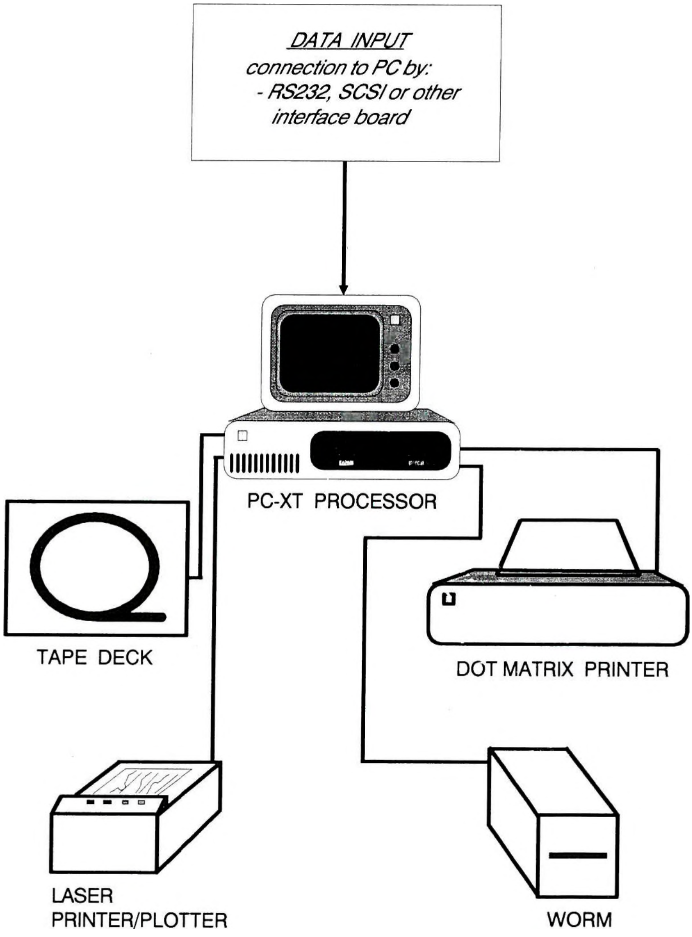

Fig. 2. Simple data processing centre

2. *ábra.* Egyszerű adatfeldolgozó központ

Рис. 2. Простой центр обработки данных

WORM (Write Once, Read Many) storage can be attached to PCs whenever permanent on-line storage of processed data is desired. The optical disks used in these devices have an expected life time in excess of 10 years and can contain as much as 1000 Megabytes of data. The use of tapes or tape cartridges for permanent storage is not encouraged. Tapes in any form are liable to print-through, signal fading and tape stretching. However, a standard 1 inch tape deck is included as this is still an acceptable method for the interchange of large amounts of data.

A laser printer/plotter can display the data for quality checking or microfilming. One-minute magnetic data can be displayed at the rate of 10 mm of plotted trace per data hour. The quality is superior to photographic magnetograms and more than adequate for quick-look searches for special events. The plots themselves can be placed on micro-fiche at the rate of one data month per fiche. There is enough spare space on the fiche for repeat plots at lower sensitivities when there is a crossover of traces due to magnetic activity.

The dot matrix printer allows a listing from the data processing programs for further analysis of extraordinary errors, or diagnostic messages.

Figure 3 shows desirable hardware requirements. One cannot stress the importance of well documented hardware. It is difficult enough to diagnose and debug data errors without struggling with undocumented processor peculiarities as well.

3. Software

Let us now consider some elemental requirements for the programming language needed for the data collecting platforms as well as the data processing hardware.

The requirements in *Figure 4* were learned by experience but now these can easily be read about in any of the numerous self help books that are available. As well, many of the documents supplied with the compilers also include a section on how to make the code transferable to a multitude of machines.

The code compilers available for PCs are powerful and can compete successfully with compilers found on large computers. Furthermore, as

- USE PROCESSORS THAT HAVE A PROVEN RECORD
  - e.g. - for P.C.'s: INTEL 8X86, IBM with Phoenic BIOS, etc.
    - for mainframes: DEC, IBM, CONTROL DATA, etc.
- USE PROCESSORS THAT HAVE STANDARD COMPILERS
  - e.g. - FORTRAN 77, ANSI C, etc.
- USE HARDWARE THAT CAN BE EXPANDED
  - e.g. - extra hard disks, tape drives, WORMS, CDROMS
    - extra output devices:
      - e.g. - line printers
        - rasterizing plotters
        - analogue plotters
- USE HARDWARE THAT HAS A WELL DOCUMENTED OPERATING SYSTEM
  - e.g. - VAX VMS
    - IBM OS
    - PC or MS DOS

Fig. 3. Hardware requirements

3. ábra. Hardver követelmények

Рис. 3. Требования к программному обеспечению

- PORTABLE
  - using FORTRAN 77, ANSI C, or BASIC compilers made by such well known companies as Microsoft allow code to migrate from P.C. to mainframes with only minor alterations,
- RELEVANT
  - within reason use the latest "safe" versions of of the compilers and file management software
- UTILIZE WELL KNOWN OR STANDARD TECHNIQUES
  - there are ANSI and IEEE standards as to binary files; use them
  - don't become hardware/software dependent, e.g. record blocking
- MODULAR
  - for ease of modifying and comprehension

long as all of the compilers are of the same manufacturer, it has become possible to cross-link or mix subroutines compiled in BASIC, FORTRAN and C. This gives one the advantage of building a program where character manipulation and serial port input/output is in BASIC, file handling and memory allocation is in C and complex mathematical calculations are in FORTRAN.

4. A suite of data editing programs

Figure 5 displays a family of programs adequate for processing magnetic data. This basic set will most certainly expand to meet one-of-a-kind data problems, which is the reason for the insistence on modularity in the data processing.

- FIRST PASS EDITING
- LISTING PROGRAMS
- DATA VALIDATION PROGRAMS
  - despikers
  - quality checkers
- PLOTTING PROGRAMS
- DATA REDUCTION PROGRAMS

Fig. 5. A suite of data editing programs

5. ábra. Adatszerkesztő kódok fajtái

Рис. 5. Типы програм, редактирующих данные

4.1. A simple edit procedure

Figure 6 describes a traditional editing procedure for the raw data as it first comes from the observatory on some sort of storage medium. The 'Edit Program' reads the raw data and builds ASCII files. Records which are of the correct length and in the correct time sequence are placed in the 'Passed Records' file. If the records are of the correct length and have 'signposts' in their proper places but contain embedded non-numeric characters, then that particular data value can easily be replaced by a null

Fig. 4. Basic code requirements

4. ábra. Alapvető adatkódolási követelmények

Рис. 4. Основные требования к кодированию данных

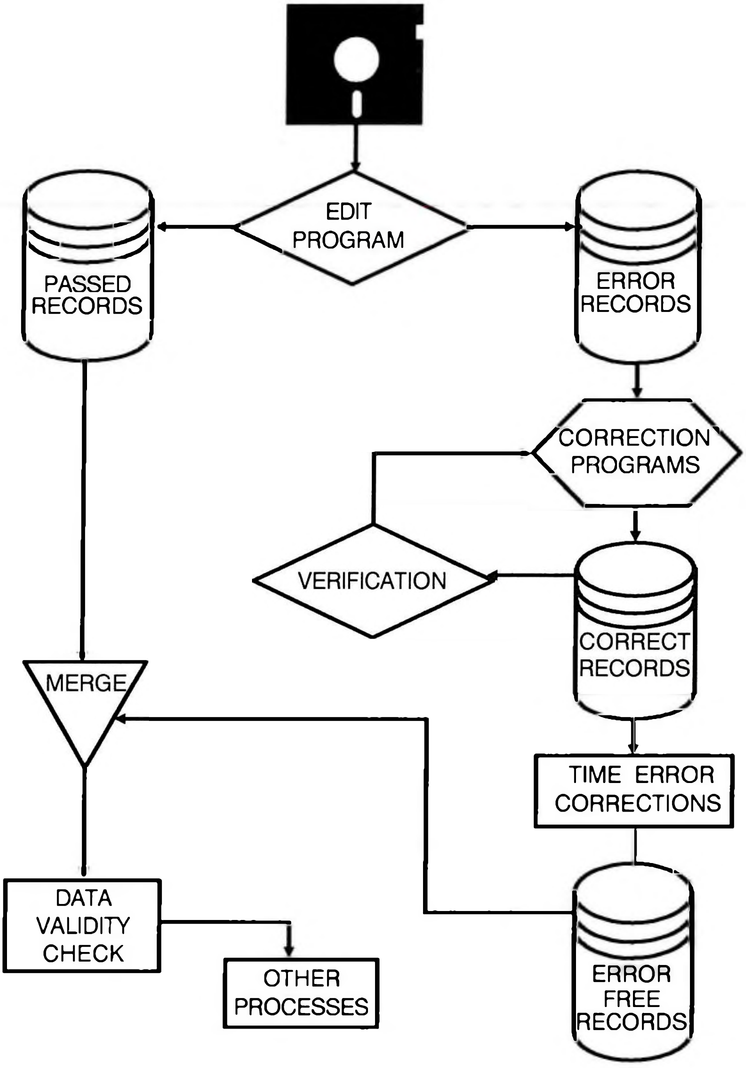

Fig. 6. A simple EDIT process

6. ábra. Egyszerű adatszerkesztési folyamat

Рис. 6. Простой процесс редактирования данных value. If the record contains errors which the program cannot fix, then that record is placed in the 'Error Records' file for later correction. If a time sequence error (e.g. time reversal) has been detected, then all subsequent records are placed in the 'Error Records' file. Various correction programs are then run on the error file. At present in the Observatory Unit, most of these batch oriented programs have been replaced by full screen text editors (hence the need for ASCII files). These editors can be run on either PCs or mainframes. A verification pass is made over the error file to make sure that everything is as it should be. Timing errors are sorted out and correction programs are applied. The two files 'Passed Records' and 'Error Free Records' are merged. A data validity checking program can then be passed over the merged file. With slight modification of the 'Error Record' stream, the stored data can just as easily be the input into or the output from an INTERMAGNET network.

Data validity checking programs require an understanding of the behaviour and characteristics of the geomagnetic field. The most common check is the sequential difference check. This check can be run 'blind' on magnetic data. That is, if the sequential differences are allowed to be as large as several hundred nTs per minute for subauroral observatories, then most data spikes are removed. In auroral zones, these differences have to be increased to about 1,000 nT. Care has to be taken during auroral substorms or magnetic storms as these rates of change are too small and will remove valid data. If a plot of the raw data exists, then the sequential difference check for stored data can be limited to the time interval in which the spike occurs. The allowable rate of change can then be substantially reduced. The only other despiking procedure which is as effective and simple is 'Bullard's Sieve'. [BULLARD 1960]

Another check is the calculation of the total force (F^*) from component measurements which is then matched against an independently measured F from a P.P.M. The difference $(F-F^*)$ should be constant but may slowly change with some magnetometers. If the component data has been properly despiked, then it has short-term stability and can be used to eliminate erroneous data from the F measurements. Variations in the $F-F^*$ then indicate possible anomalous behaviour of the component data.

4.2. Format correction programs

On PCs it is convenient when programming in C or BASIC to think of a data file in terms of a string of characters. This long string can easily be read one character at a time. Thus files which have been recorded on a damaged medium or have missing record terminators can be processed by looking for the sign posts which were so thoughtfully placed in the data. Mainframes do not always allow this to take place easily as they tend to impose their own record structures and file descriptors onto files.

4.3. Plotting programs

Figure 7 is a plot of the magnetic data suitable for quick searches of events or data errors. The display in analogue form of the data has to be an integral part of any data processing. No matter how clever one has been in correcting anticipated errors, an error will always either creep through or mutate into another form. Plotting the data is a fast convenient check and has the added advantage of having the viewer become familiar with the displayed phenomena. Finally, it is an easy way to answer a request for the time and date of magnetic activity as these magnetograms may easily be sent by facsimile to the user.

4.4. Data reduction programs

At this stage the data should now be cleaned up so that they can be read under format control with no possibility of error. Data quality has also been verified and the data is ready to be reduced to absolute values by the addition of baseline corrections. The process of establishing absolute corrections is similar to the ones in use for the past century for photographic records. However, digital data now allow corrections to be added with as much precision as the basic time increment and data sensitivity. For this purpose it is convenient to think in terms of the minute of the year and correction increments in fractions of a nanotesla. After all, there are only some 527 thousand minutes in a leap year and most computers are capable of working in 8 significant digits.

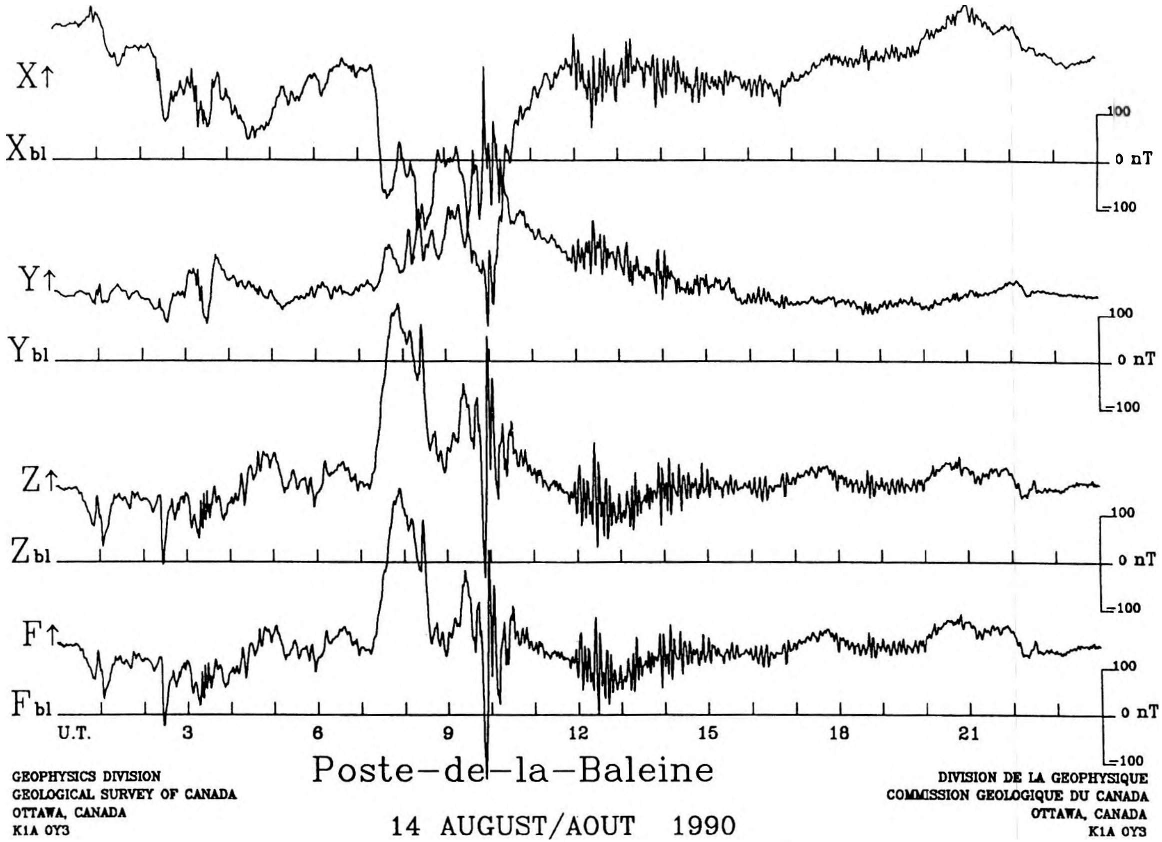

Fig. 7. Sample plot of magnetic data for quick searches of events or data errors

7. ábra. Minta digitális adatok rajzolására gyors hibakereséshez

Рис. 7. Пример вывода цифровых данных на экран с целью быстрого обнаружения ошибок

5. Observatory/INTERMAGNET relationship

The discussion given so far has focused on the instrumentation and data processing as it applies to a modern magnetic observatory. Hopefully, it has also become apparent that the instrumentation can be successfully adapted to make use of the newest observatory enhancement, INTERMAGNET. Furthermore, the data editing procedures previously discussed can be adapted to run on the INTERMAGNET data as it is received.

INTERMAGNET allows the routing of magnetic data to a Geomagnetic Information Node (GIN). It is in the GIN that the data from large observatory nets are processed in near real-time. The results are :

— 'real' time magnetic activity indices for use by:
centres reponsible for navigation satellite orbits,
geodetic surveys at high latitudes,
electric power utility companies with long power lines;

— 'real' time modelling of ionospheric current systems;

— the early anticipation of auroral substorms that have developed to the east of a site;

— other advantages as outlined in INTERMAGNET documentation.

6. A geomagnetic information node (GIN)

Figure 8 shows a possible PC net used to process the INTERMAGNET data. The PC labelled 'DECODER' is placed near the satellite receiver. It decodes the special binary data received from the satellite, provides a few days of backup storage of the data and forwards the translated data to 'LISTENER' and 'BROWSER'. Data safety and security are ensured by redundant storage of data in the PCs labelled 'BROWSER' and 'LISTENER'. 'LISTENER' is protected and will not allow itself to be used for any other purpose but to store INTERMAGNET data in a data base and to display it. 'BROWSER' will allow itself to be utilized by other tasks running on other PCs and allow access to past INTERMAGNET data. All of the PCs are connected by a real-time operating system which can deal with multi-tasks and multi-users on one or all of the machines in the net. Other functions such as the addition of solar information, the merging of backup data, the reduction of data by the use of absolute observations and

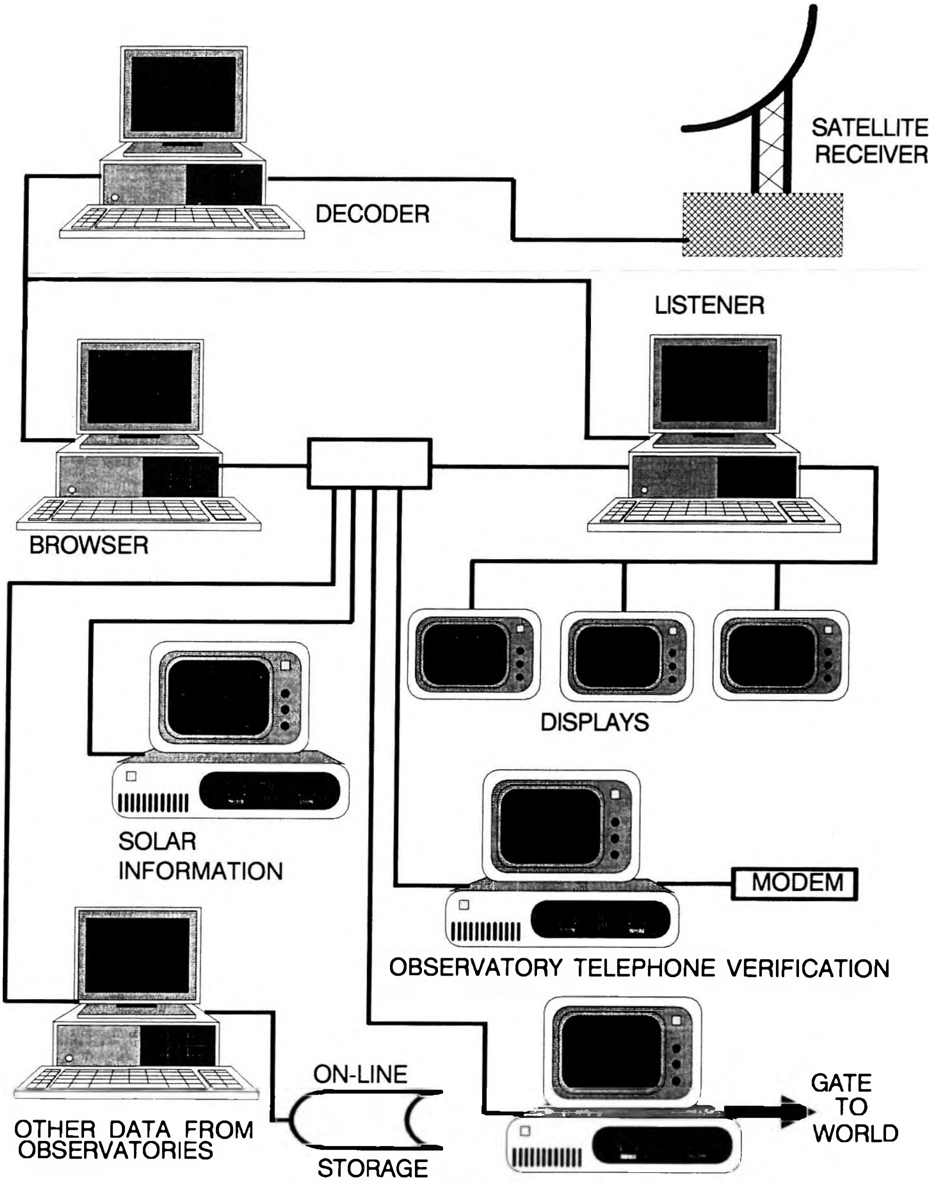

Fig. 8. Distributive geomagnetic data processing

8. ábra. Szétosztás céljára szolgáló adatfeldolgozás

Рис. 8. Обработка данных с целью расклада communication to such world-wide data exchange nets as INTERNET can then be added easily to the GIN as the need arises or as equipment becomes available.

7. Summary

A modern type of digital magnetic observatory and its associated data processing stream can be easily adapted to fit into the INTERMAGNET net with all of its advantages.

REFERENCES

BULLARD E. C. 1960 : The automatic reduction of geophysical data. Geophysical Journal RAS, **3** (2), pp. 237-243

EGY MÁGNESES OBSZERVATÓRIUM MINT INTERMAGNET ÁLLOMÁS

Gerrit JANSEN VAN BEEK

A szerző az INTERMAGNET digitális mágneses obszervatóriumi műholdas világhálózat elvárásainak megfelelő berendezésre (hardver és szoftver) való átállás kapcsán felmerülő problémákra tesz javaslatot. Röviden ismerteti a nyers mérési adatok ellenőrzésének és előfeldolgozásának menetét és bemutatja, hogyan juthatunk hozzá a hálózat tagjai által mért és továbbított adatokhoz illetve az azokból előállított egyes további információhoz.

МАГНИТНАЯ ОБСЕРВАТОРИЯ КАК СТАНЦИЯ INTERMAGNET

Геррит ЙАНСЕН ВАН БЕК

В статье рассматриваются рекомендации по техническому и программному обеспечению аппаратуры, соответствующей требованиям всемирной спутниковой сети магнитных обсерваторий INTERMAGNET.

GEOPHYSICAL TRANSACTIONS 1991
Vol. 36. No. 3-4. pp. 303-312

SOME THOUGHTS CONCERNING NEW DIGITAL MAGNETIC INDICES

Richard L. COLES* and Michel MENVIELLE **

The paper presents several problems of computer calculation of K-indices and of the methods that are suggested for solving this task. It recalls previous tests of sampling rate, the result of which is that 1 minute sampling rate is inadequate even when the methods are being tested. The paper calls attention to the questions of K-indices in connection with INTERMAGNET.

Keywords: digital magnetic indices, *K*-indices

1. Introduction

This brief note is concerned with the determination of K-indices and other indices from digital data, and with new, purely digital indices. We do not set out to define yet more algorithms but rather to add some points that may have been overlooked.

2. Digital representation of the K-index

There have been, for several years now, several algorithms in existence that claim to derive K-indices from digital data. One such algorithm [WALKER 1987] has been used routinely for several years for determining the published K-indices for three Canadian observatories; there may be

* Geophysics Division, Geological Survey of Canada, Ottawa, Canada K1A 0Y3
** Geomagnetisme, Institut de Physique du Globe, 4 Place Jussieu, 75252 Paris Cedex 05, France

others. Some of the algorithms are simple and straightforward, others are quite complex, involving Fourier-type analysis and pattern recognition, or data-adaptive techniques [including RANGARAJAN and MURTY 1980, RIDDICK and STUART 1984, HOPGOOD 1986, GOLOVKOV et al. 1989, WILSON 1987, WALKER 1987, JANKOWSKI et al. 1988, PIRJOLA et al. 1989, HATINGH et al. 1988]. All are concerned with the production of the so-called 'regular variation', the S_R curve for each day, that is to be removed from the data to provide the residuals to be scaled in three-hour segments to obtain the ranges that are converted to the K scale for that particular observatory. This is not an insignificant task—the definition of the 'regular variation' is itself not conducive to clear analytical description, let alone the determination of it on a daily basis from data at a single observing point. Nonetheless, several recent algorithms do seem to have made reasonable attempts at modelling the S_R for some observatories. These algorithms are at the present time being submitted to a test, by using them on a one-year data set from twelve observatories [see MENVIELLE and SUCKSDORFF, in this proceedings]. The indices derived from these algorithms are compared with the K-indices that have been handscaled from the data in the traditional way. Some of these results are presented at this Workshop (PAPITASHVILI et al. and WILSON and GREEN).

Such a test is fine, so long as the digital data and the handscaling are good quality. However, one observation from the comparisons so far presented using this test data set, both here and elsewhere, is that none of the algorithms seem to result in better than about 85% agreement with hand-scaled indices, and often much worse. To those of us who are concerned about the maintenance of the quality of the long series of K-indices, this is disturbing. Is this difference simply a result of a basic 'slackness' in the definition of the K-index itself? Some years ago, in the early days of 'digital K', opponents to the early algorithms pointed out that 'well-trained hand-scalers agreed within 2 or 3%', and that computer methods should achieve the same degree of agreement. More recently, it is interesting to find that some comparisons are now showing that hand-scalers more typically can disagree by as much as 15%. This may be a result of the loss of a central figurehead who was very concerned with training of handscalers.

In interpreting these statistics, however, we need to take into account the borderline cases. A level of disagreement between 5 and 10% can be obtained by not including the borderline cases, whereas the level of disagreement increases to 15% when the borderline cases are included. A degree of agreement of the order of 85% between computer and handscaled indices may be acceptable, provided the differences do not exceed 1 unit and they are distributed at random.

There is, however, one other point that has been overlooked by most people since its introduction in 1983. That is the question of digital sampling rate. NIBLETT et al. [1984] compared K-indices that were hand-scaled from photographic Ruska magnetograms at some Canadian observatories with K-indices that were handscaled from computer plots of digital data recorded at those same observatories. The digital data were available at 5 seconds intervals, although the magnetometer was sampling internally at 1 second intervals. Plots were produced using spot data samples at 5 seconds, 20 seconds, 30 seconds, 40 seconds and 60 seconds, by simple data point skipping. In addition, the 1 second data were filtered twice to produce samples at 1 minute intervals. The frequency responses of the filters were published in the paper. The frequency response of the Ruska magnetometer was determined experimentally to be flat between periods of 10 seconds and at least several hours. The results of this comparison clearly showed that sampling rates are important for the proper determination of K-indices *(Fig. 1)*. Plots from data at 1-minute samples, filtered or not, did not produce accurate K-indices. It must be emphasized that this is a result of sampling rate—not the choice of S_R curve—the same S_R curve was used for the different plots and the analogue magnetogram.

Subsequent to this, WALKER [1987], in his paper describing his K-algorithm, provide a similar test result. In his case he used his algorithm to produce an S_R curve, and then applied the same S_R curve to data sets sampled at 10 seconds, 30 seconds, 60 seconds, 90 seconds and 120 seconds. Again, the results clearly showed the effect of inadequate sampling rate on the actual values of K-indices — relative to a given S_R curve *(Fig. 2)*.

This raises several serious points. If, as we argue, the sampling rate that is being used in the present K test data set (i.e. 1 minute) is inadequate, are the comparisons valid? Practically speaking, to our knowledge, there is only one observatory network (Canadian) that at the moment routinely samples at a rate that could improve on the 1 minute sampling rate. (In fact, the Canadian K-indices are routinely derived from 10 second data). If we, as a community, are able to choose an algorithm for S_R should it be

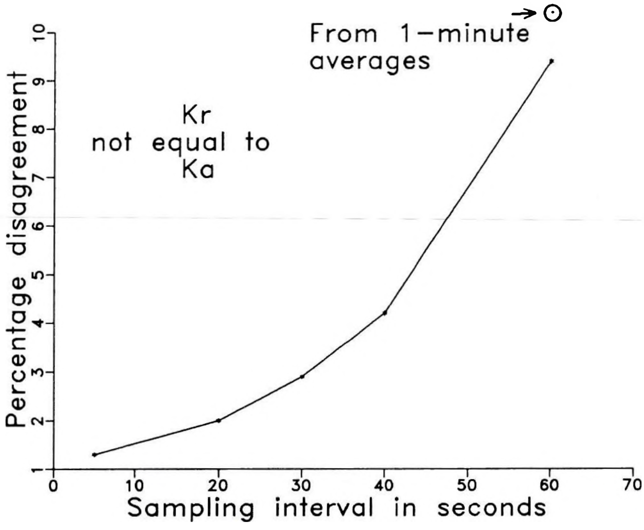

Fig. 1. The percentage disagreement between *K*-indices derived from Ruska magnetograms *(Kr)* and those from computer plots derived from digital data at various sampling rates *(Ka)* [after NIBLETT et al. 1984]

1. ábra. A Ruska magnetogramokból (*Kr*) és a digitális regisztrátumokból kirajzolt magnetogramokból (*Ka*) levezetett *K*-indexek közötti százalékos eltérés különböző mintavételi frekvenciákra [NIBLETT és mások 1984 után]

Рис. 1. Расхождения в процентах между индексами *K*, выводимыми из магнитограмм Руска (*Kr*) и магнитограмм, вычерченных по цифровым записям (*Ka*) при различных частотах наблюдений [по NIBLETT et al.1984]

subjected to tests with data at faster sampling rates, so that we know what we are missing by staying with 1 minute data? If, as we expect, there will be a resultant degradation in the *K*-indices, are we prepared to accept what amounts to a degradation in the quality of the long series of published *K*-indices?

The potential degradation of the *K*-index by the introduction of 'defective' computer-derived S_R curves has generated a great deal of emotional debate. Yet, the question of sampling rate has been ignored. As we move into the era of INTERMAGNET, which promises rapid determination of indices, we must face this question— because by the nature of the limitations on data transmissions, INTERMAGNET observatories will only transmit data sampled at 1 minute intervals. Are we, de facto, committed to a degradation of the quality of the *K*-index? Or, are we going to

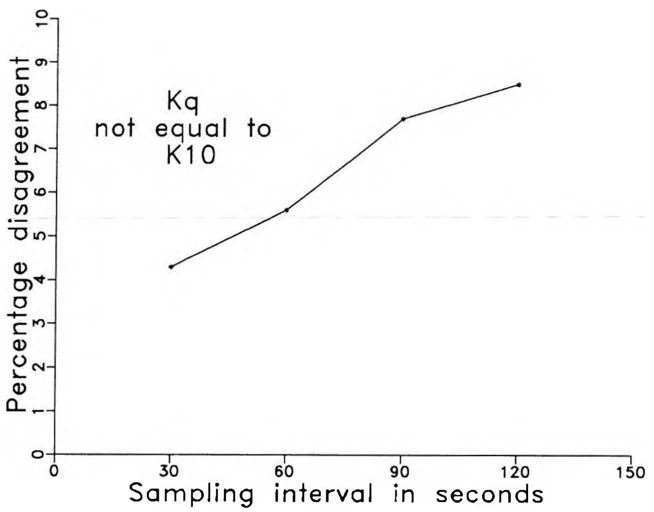

Fig. 2. The percentage disagreement between *K*-indices derived from 19 second data *(K10)* and data sampled at lower rates *(Kq)* [after WALKER 1987].

2. ábra. *K* indexek százalékos eltérése 19 másodperces (*K10*) és alacsonyabb mintavételi frekvenciájú (*Kq*) alakból számítva [WALKER 1987 után]

Рис. 2. Расхождение в процентах между инсдексами К, рассчитанными по форматам 19 с (*K10*) и более низких частот наблюдений [по WALKER 1987]

insist that the algorithm for S_R production be sufficiently simple that it can be automatically derived in the (unmanned) observatory computer so that the *K*-indices are computed at the (often-remote) observatory from data that is sampled at a higher rate but not transmitted? Or, are we going to accept the status-quo—that *K*-indices are not near-real-time, but delayed in production? We must be clear on what is required, because considerable cost is involved, both in instrumentation and in person-time.

In effect, it is becoming essential that we clearly distinguish between the users of the true *K*-index, and those who use *K* because it happens to be closest to what they believe they need. In most, if not all cases, the latter group's needs can be met by one or more near-real-time indices that are approximations to the 'true, traditional *K*'.

The previous argument points very strongly to the derivation of new indices that take advantage of the capabilities of digital data, available in near-real-time, but that are not constrained by a need to be scrupulously close to the traditional *K*-index. Some proposals for such indices already exist [Stuart and Green 1987].

3. Digital representation of other indices

Much of the concern over the application of digital data to the production of indices has centred around the controversy of the *K*-index, and has to some extent overshadowed the concerns for other indices such as the *AE*, *AL*, *AU* series. These indices, though more clearly defined, still have problems associated with a subjective choice of reference level. But more important, at present, is the need to assemble data rapidly from a group of stations, some of which are not yet producing digital data in a timely fashion. The situation ranges from no digital data at all, through poor data, to good data but delayed by weeks or months. The promise of INTERMAGNET again is to provide timely data. The challenge then is to process the data to produce the indices in a correspondingly timely way. In similar vein, the *Dst* index can also benefit from timely digital data.

The International Service of Geomagnetic Indices is investigating the possibility of deriving the present IAGA indices (*aa*, *Kp*, *Dst*, *AE*, *AU*, *AL*, *am*, *an*, *as*) using INTERMAGNET data. *K*-derived indices would be computed in Europe (Orsay/St. Maur, France, and Göttingen, Germany) in close liaison with the Paris INTERMAGNET Geomagnetic Information Node; the *AU*, *AL*, *AE*, and *Dst* indices would be computed in Japan. This implies that the observatories involved in the derivation of IAGA indices be active in the INTERMAGNET network as soon as possible (see IAGA Bulletin no. 32, or Menvielle [1990], for lists of these observatories). It is worth noting that the 'IAGA indices observatories' provide us with relevant descriptions of the magnetic transient variations on a planetary scale, except for polar phenomena. These 'IAGA indices observatories' would therefore provide a useful skeleton for the INTERMAGNET network, from the transient variation standpoint.

However, no matter what kind of amplitude-dependent index is used, it will be affected by sampling rate and filtering. The 1-minute sampling rate fits with the present requirements for *Dst*, *AU*, *AL*, and *AE* derivation. On the contrary, the filtering process used in the derivation scheme for these indices (2.5 minute or 1 hour averages) could be improved to take advantage of the availability of the 1-minute digital data. More generally, the filtering will always reduce amplitudes, and the selection of the filter used when processing geomagnetio data (observatory data as well as indices) should also be discussed in the near future, with clear recommendations made.

4. New concepts for digital indices

The results obtained with *K*-derived indices in solar-terrestrial and magnetospheric physics clearly show the relevance of indices based upon *K* indices from subauroral-latitude observatories in describing the global status of the magnetosphere. The computation of an index according to the same scheme as that for the *am* index, but with 3-hour intervals shifted by successive 12 or 15 minute intervals, would provide a relevant monitoring of the magnetospheric energy. Preliminary values of this index could be computed with only a short delay using the INTERMAGNET 1-minute data. Definitive indices could be computed later with 10 second values. Such an index is an extrapolation of the existing *am* index, and one can therefore easily foresee its effectiveness.

In tandem with digital determination of *K*, *AE* and *Dst* indices, and with the introduction of digitally conceived indices that mimic to some degree the *K*-index [e.g. STUART and GREEN [1987], there exists the challenge to create new, very different types of index, possible now through the use of microcomputers and rapidly sampled, good-quality digital data.

For example, such indices may take the form of spectral indicators, as suggested by GREEN and WILSON at this Tihany workshop. Or, through the aegis of INTERMAGNET, data from many observatories may be combined in an INTERMAGNET node to compute a regional index from a modelling procedure such as proposed by WALKER [1989]. There are many possibilities.

Further, there is also a need for warning, or alert, indicators. These do not necessarily meet the rather stringent requirements that apply to indices such as *K*, *AE* and so on, but rather they are designed specifically for a particular user group. These indicators will be developed in collaboration with the users, whether in the electric power industry, communications, exploration, or elsewhere, and they may be quite local in their applicability. One simple indicator for possible application with the power industry, for example, has been proposed by JANSEN van BEEK (private communication).

5. Summary

At the IAGA Scientific Assembly in Exeter 1989, it was agreed that a decision on the future determination of *K*-indices by computer must be taken at the Vienna 1991 Assembly —enough effort will have been spent, and other matters must come to occupy our working time. To do this, the comparison of proposed algorithms must be completed, and a recommendation made for the future. The question of the significance of sampling rate must be resolved and an acknowledgement of the consequences of the ensuing action must be accepted.

Other existing indices can only benefit from the digitalization of the observatory network. New innovative indices and warning indicators are sought, and proposals are welcomed. The authors of this note form a joint subcommittee of IAGA Working Group V-5 and INTERMAGNET to receive such proposals for consideration, and scientists are encouraged to submit proposals to us.

REFERENCES

GOLOVKOV V. P., PAPITASHVILI V. O. and PAPITASHVILI N. E. 1989: Automatic calculation of *K*-index using the method of natural orthogonal components. Geomagn. Aeron. **29**, pp. 667-670

HATTINGH M., NAGTEGAAL D. and LOUBSER L. 1988: The estimation of *K*-indices by computer using a data-adaptive filtering technique. Annal. Geophys. **6**, pp. 611-618

HOPGOOD P. A. 1986: On the computer generation of geomagnetic *K*-indices from digital data. J. Geomag. Geoelectr. **38**, pp. 861-871

JANKOWSKI J. A., ERNST T., SUCKSDORFF C., PIRJOLA R. and RYNO J. 1988: Experiences of a filter method for determining *K*-indices. Annal. Geophys. **6**, pp. 589-594

MENVIELLE M. 1990: About the derivation of geomagnetic indices from digital data. *in*: K. Kauristie, C. Sucksdorff, and H. Nevanlinna (Eds.), Proceedings of the International Workshop on Geomagnetic Observatory Data Acquisition and

Processing, Finnish Meteorological Institute, Geophysical Publication No. **15**, Helsinki, pp. 117-126

NIBLETT E. R., LOOMER E. I., COLES R. L. and JANSEN VAN BEEK G. 1984: Derivation of *K*-indices using magnetograms constructed from digital data. Geophys. Surv. **6**, pp. 431-437

PIRJOLA R., RYNO J. and SUCKSDORFF C. 1989: Computer production of *K*-indices by a simple method based on linear elimination. *in*: K. Kauristie, C. Sucksdorff, and H. Nevanlinna (Eds.), Proceedings of the International Workshop on Geomagnetic Observatory Data Acquisition and Processing, Finnish Meteorological Institute, Geophysical Publication No. **15**, Helsinki, pp. 136-146

RANGARAJAN G. K. and MURTY A. V. S. 1980: Scaling of *K*-indices without subjectivity. IAGA News **19**, pp. 112-118

RIDDICK J. C. and STUART W. F. 1984: The generation of *K*-indices from digitally recorded magnetic data. Geophys. Surv. **6**, pp. 439-456

STUART W. F. and GREEN A. W. Jr. 1987: Real time range indices of geomagnetic activity. IAGA News **26**, pp. 94-97

WALKER J. K. 1987: Adaptive separation of regular and irregular magnetic activity for *K*-indices. J. Atmos. Terrestr. Phys. **49**, pp. 1017-1025

WALKER J. K. 1989: Spherical cap harmonic modelling of high latitude magnetic activity and equivalent sources with sparse observations. J. Atmos.Terrestr. Phys. **51**, pp. 67-80

WILSON L. R. 1987: An evaluation of digitally derived *K*-indices. J. Geomagn. Geoelectr. **39**, pp. 97-109

NÉHÁNY GONDOLAT AZ ÚJ DIGITÁLIS MÁGNESES INDEXEKKEL KAPCSOLATBAN

Richard L. COLES és Michel MENVIELLE

A cikk a *K*- indexek gépi számításának illetve ezen feladat néhány javasolt megoldási módjának gondjait ismerteti. Emlékeztet a mintavételi frekvenciák megválasztásával kapcsolatos vizsgálatokra, melyek szerint a perces mintavételnél nagyobb felbontás szükséges már a módszerek tesztelésénél is. Felhívja a figyelmet az indexek kérdésével kapcsolatos eldöntendő problémára az INTERMAGNET-tel kapcsolatban

НЕКОТОРЫЕ ИДЕИ ОТНОСЯЩИЕСЯ К ИНДЕКСАМ К СОЗДАВАЕМЫМ ИЗ ЦИФРОВЫХ ДАННЫХ

Р. Л. КОЛС и М. МЕНВЬЕЛ

В статье рассматриваются затруднения, связанные с рассчетом индексов *K* на компъютерах и с некоторыми предлагаемыми способами решения этой задачи. Напоминаются исследования, связанные с выбором частот для производства наблюдений, в соответствии с результатами которых уже при тестировке методов разрешение должно быть больше, нежели при минутных измерениях. Обращается внимание на проблему, которая должна быть решена в связи с вопросом индексов в связи с INTERMAGNET.

GEOPHYSICAL TRANSACTION 1991
Vol. 36. No. 3-4. pp. 313-320

EVALUATION OF ALGORITHMS FOR COMPUTER PRODUCTION OF *K*-INDICES

Michel MENVIELLE*

The paper explains why computer production of *K*-indices was introduced and it summarizes the methods of computer- and traditional handscale production of *K*-indices. It shows the necessity for and the mode of comparing hand-scaled and computed *K*-values.

Keywords: geomagnetic indices, *K*-index, algorithmus

1. Introduction

The derivation of geomagnetic indices from digital data was discussed during the Second Workshop, at Nurmijärvi [MENVIELLE 1990]. According to the IAGA regulations, the *K*-indices are to be handscaled from analog magnetograms. In the case of digital observatories, it implies the production of computer plots of digital data with scale values similar to those of photographic magnetograms (about 2 cm/h and 5 nT/mm). *K*-handscaling thus induces delays and *K*-indices are generally circulated some weeks after the end of a month. Computation and circulation of IAGA *K*-derived indices within a short time clearly require computer derivation of the *K*-indices.

A lot of algorithms that claim to derive *K*-indices from digital data have been proposed for several years now [VAN WIJK and NAGTEGAAL 1977, RIDDICK and STUART 1984, HOPGOOD 1986, WALKER 1987, WILSON 1985,

* International Service of Geomagnetic Indices and Laboratoire de Géomagnétisme, Institut de Physique du Globe de Paris
now at: International Service of Geomagnetic Indices and Laboratorie de Géophysique, Batiment 504, University de PARIS SUD F-91405 ORSAY CEDEX

HATTINGH et al. 1988, GOLOVKOV et al. 1989, PIRJOLA et al. 1990]. These algorithms have been tested with different data sets, and using different statistical tests. It is therefore almost impossible to compare them and decide which algorithm is relevant.

It was thus decided during the Vancouver and Exeter meetings to organize a comparison between these algorithms with a common data set and using the same statistical tests. It was also decided that the comparison be completed before the 1991 IAGA General Assembly, in Vienna, where a recommendation should be made for the future. This short note briefly presents the data set and statistical tests to be used for this comparison.

2. The *K*-index

The *K*-index was designed by BARTELS et al. [1939] to provide objective monitoring of the irregular variations observed at a given station. It was extensively analysed and discussed in Mayaud's Atlas of *K*-indices [MAYAUD 1967] and by MAYAUD [1980]. A short review of its basic characteristics is given by MENVIELLE and BERTHELIER [1991].

An individual *K*-index is a code characterizing the activity during a Greenwich Universal Time (UT) three hour interval. During each 3-hour interval, the range in the two horizontal magnetic components is measured after eliminating the so-called 'non-*K* variations'. MAYAUD [1967] established morphological rules as guidelines to estimate the non-*K* variations (see Appendix 1). According to these rules, one retains as non-*K* variations the simplest and least speculative curve which correspond to a possible S_R variation. In practice, it should be estimated from the quiet parts of the records.

Ten classes of ranges are defined according to the corrected geomagnetic latitude of the station. The limits of the classes are proportional to those defined by BARTELS at the Niemegk observatory (*Table I*). The 3-hour *K*-index is the integer between 0 and 9 corresponding to the class containing the larger of the two ranges measured in the horizontal components.

Table I.

K value	0	1	2	3	4	5	6	7	8	9
range (nT)	0	5	10	20	40	70	120	200	330	500

The K-indices are to be handscaled on analog magnetograms. They thus depend to a given extent on the observer, and the subjectivity of K-indices was a matter of debate [e.g. RANGARAJAN and MURTY 1980, MENVIELLE 1981]. It is at present agreed that the measurements made by two well trained observers differ by about 8% if the border cases are neglected, and by 15% to 20% otherwise. The differences never exceed one unit and they are randomly distributed [MAYAUD 1980, MAYAUD and MENVIELLE 1980, SUCKSDORFF et al. 1991].

3. The tests

Computer K-methods will be tested using the magnetic data of the period March 1985 to February 1986 from the observatories listed in *Table II.* These digital data together with digital hand-scaled K-values are available on request from the Finnish Meteorological Institute.

The tests are based upon the comparison between computed K-values and hand-scaled K-values. The results should be presented as histograms of the differences $\Delta K = K(\text{computed}) - K(\text{hand-scaled})$. A list of the histograms is given in Appendix 2. According to the results from comparison between handscalings made by different observers, full agreement of about 85% is satisfactory, provided the differences never exceed one unit and are randomly distributed.

The tests also include a comparison between magnetograms and computer estimated regular S_R curves. Magnetograms of the X and Y (or H and D) components with the computer estimated S_R curve should therefore also be plotted for a selected set of 30 days (July 5 to 14, September 1 to 10, December 22 to 31, 1985). The horizontal time scale in the magnetograms is 6 mm/hour, and the vertical scale is 2 nT/mm, except for July 12, December 28 and December 30 for which it is 5 nT/mm.

Table II.

Station	Geographic		Corrected	K = 9 Lower Limit	
	lat.	long.	Geomag.lat.	Computed	Used
ARGENTINE ISL.	-65.12	295.42	-49.7	490	500
BELSK	51.83	20.80		480	450
CANBERRA	-32.39	149.30	-45.2	420	450
CROZET	-46.26	51.52	-52.4	500	500
HARTLAND	50.59	355.31	50.0	530	500
HERMANUS	-34.25	19.14	-41.1	300	300
MEMAMBETSU	43.54	114.12	37.4	340	350
NEWPORT	48.16	242.53	54.8	700	700
NURMIJRÄVI	60.52	24.65		750	750
OTTAWA	45.24	284.27	58.9	790	750
P.AUX FRANCAIS	-49.21	70.12	-52.4	760	750
SODANKYLA	67.37	26.63	63.9	1540	1500

Observatories used in the test of computer K-methods. The computed lower limit for K=9 is estimated with respect to the angular distance to the closest point of the auroral zone (see Mayaud 1980, or Menvielle and Berthelier 1991 for further details). The used K=9 lower limit is generally rounded to the nearest fifty or hundred; it should be used for the computer K-derivation.

The tests take into account both the experimental results from comparisons between well trained observers and the morphological basis of the S_R estimation. We therefore expect that the computer derived K-index will have the same statistical properties as the original ones, thus ensuring the homogeneity of the *aa*, *am*, *an*, *as* and *Kp* time series.

Acknowledgements

The data used for these tests were kindly provided by the observatories. Chris Sucksdorff and his team (Geophysical Department, Finnish Meteorological Institute, Helsinki, Finland) took care of gathering, checking and circulating the test data set. I am pleased to thank them for their efficient contribution which made these tests possible.

REFERENCES

BARTELS J., HECK N.H. and JOHNSTON H.F. 1939: The three-hour-range index measuring geomagnetic activity. Terr. Magn. Atmos. Elec., **44**, 411 p.

GOLOVKOV V. P., PAPITASHVILI V.O. and PAPITASHVILI N.E. 1989: Automatic calculation of *K*-indices using the method of natural orthogonal components. Geomagn. Aeron. **29**, 667 p.

HATTINGH M.D., NAGTEGAAL D. and. LOUBSTER L. 1989: The estimation of *K*-indices by computer using a data adaptative filter technique. Annales Geophysicae **6**, 589 p.

HOPGOOD P. A. 1986: On the computer generation of geomagnetic *K*-indices from digital data. J. Geomagn. Geoelectr. **38**, 861 p.

MAYAUD P. N. 1967: Atlas des Indices *K*. IAGA Bull. 21, IUGG Publ. Office, Paris

MAYAUD P. N. 1980: Derivation, Meaning and Use of Geomagnetic Indices. Geophysical Monograph **22**, American Geophysical Union, Washington D.C.

MAYAUD P. N. and MENVIELLE M. 1980: A report on *Km* observatories visit. *in:* IAGA Bull. 32i, p. 113, IUGG Publ. Office, Paris

MENVIELLE M. 1981: About the scaling of *K*-indices. IAGA News N20, 110 p.

MENVIELLE M. 1990: About the derivation of geomagnetic indices from digital data. *in*: Proceedings of the International Workshop on Observatory Data Acquisition and Processing, ed. by K. Kauristie, C. Sucksdorff and H. Nevanlinna, Finnish Meteorological Institute, Geophysical Publications 15, p.117

MENVIELLE M. and BERTHELIER A. 1991: The *K*-derived planetary indices : description and availability. Reviews Geophys. Space Phys., submitted

PIRJOLA R., RYNÖ J. and SUCKSDORFF C. 1990: Computer production of *K*-indices by a simple method based on linear elimination. *in:* Proceedings of the International Workshop on Observatory Data Acquisition and Processing, ed. by K. Kauristie, C. Sucksdorff and H. Nevanlinna, Finnish Meteorological Institute, Geophysical Publications **15**, p.128

RANGARAJAN G. K. and MURTY A.V. S. 1980: Scaling *K*-indices without subjectivity. IAGA News N19, 112 p.

RIDDICK J. C. and STUART W. F 1984: The generation of *K*-indices from digitally recorded magnetic data. Geophysical Surveys **6**, 439 p.

SUCKSDORFF C., PIRJOLA R. and HÄKKINEN L. 1991: Computer production of *K*-values based on linear elimination. these proceedings

VAN WIJK A. M. and NAGTEGAAL D. 1977: *K* measurements by computer. J. Atmos. Terr. Phys. **39**, 1447 p.

WALKER J. K. 1987: Adaptative separation of regular and irregular magnetic activity for *K* indices. J. Atmos. Terr. Phys. **49**, 1017 p.

WILSON L. R. 1985: An evaluation of digitally derived *K*-indices. J. Geomagn. Geoelectr. **39**

APPENDIX 1

Mayaud's rules for scaling K-indices

1. The observer should carry out, by following the smooth variations, smoothing of the record such that it corresponds to a possible form of the S_R The quiet parts of the records, presenting little or no sudden variations, will guide this smoothing. However, the observer must be conscious of the possible existence of smooth (or moderately smooth) K-variations in order to eliminate them, as far as possible, from this smoothing.

2. The possibility of such smoothing, and its practical usefulness from the point of view of the measurements, diminishes rapidly as the agitation level increases. Often it will be sufficient to make it only for certain parts of the records.

3. On days following a storm, the general aspect of the H-curve can be profoundly different from the normal S_R, particularly at low latitudes. The smoothing should be carried out however without departing too much from the observed H-curve.

4. In cases where smoothing seems wholly or partly useless, the following procedure will often be practical :

— make a first measurement of the index as if there were no non-K variations;

— estimate whether the measure thus obtained is sufficiently remote from a borderline so that any hypothetical non-K variation be negligible;

— if the measurement is near a borderline, lower or raise by one unit the first value obtained as a prudent and reasonable estimation of the possible non-K variation suggests.

5. When, with respect to the level of the agitation, the smoothing carried out for the S_R identification seems useful but remains uncertain (this fact will probably occur at stations where S_R may contain more or less complex secondary movements), and if the various possible solutions lead to different values of the index, the interpretation retained should always be the simplest and least speculative.

6. If a secondary movement of the curve, which presents a smooth aspect and does not contain, in particular, any sudden change at its beginning or at its end, resembles a secondary movement which S_R can produce,

the observer should always interpret it as belonging to S_R without asking himself whether a comparison with a record of another observatory would show that it is a K-variation.

7. If a smooth secondary movement occurs during night hours so that one can assume that it is very probably a K-variation although its beginning is indiscernable in the end of the S_R (or its end in the beginning of the S_R), it must be interpreted as being a K-variation, by taking as a reference the simplest possible form of S_R in the given interval or intervals.

APPENDIX 2

The results obtained by different K-methods should be presented as histograms of the differences $\Delta K = K$(computed) - K(hand-scaled) in the following 'formats' :

a) histogram of all results (Mar 85 ... Feb 86)
histogram of results of Nov 85 ... Feb 86 (Winter)
histogram of results of May 85 ... Aug 85 (Summer)
histogram of results of Mar 85 Apr 85 and Sep 85 Oct 85 (Equinox)
histograms of results of the selected 30 days (Jul 5 ... 14, Sep 1 ... 10, Dec 22 ... 31, 1985).

The vertical scale is in % with 100% = 100 mm; the width of one column is 5 mm (columns : 0, -1, +1, -2, +2, ...)

b) for each three seasons, histograms of all results (Mar 85 ... Feb 86) as functions of the time of the day, i.e. 8 different histograms according to the three hour intervals (UT 00-03, 03-06, ...). The vertical scale is in % with 100% = 100 mm; the width of one column is 3 mm, and the space between zero-columns of two adjacent histograms is 24 mm.

c) histograms of all results (Mar 85 ... Feb 86) as functions of the hand-scaled K values, i.e. 9 different histograms. The scale, width and space information is the same as in case b).

SZÁMÍTÓGÉPPEL KÉSZÍTETT K-INDEXEK ALGORITMUSAINAK ÉRTÉKELÉSE

M. MENVIELLE

A cikk ismerteti a gépi számítási indexek bevezetésének okát, és utal a *K*-indexek hagyományos és gépi számításának módjaira. Magyarázza a kétféle eljárással készült indexek összehasonlításának szükségességét és részletesen ismerteti az összehasonlítás módját.

ОЦЕНКА АЛГОРИТМОВ ИНДЕКСОВ К, СОЗДАННЫХ НА КОМПЪЮТЕРАХ

М. МЕНВЬЕЛ

В статье рассматривается причина введения индексов, рассчитываемых на компъютерах, и дается ссылка на традиционные и компъютеризированные способы расчета индексов К. Объясняется необходимость сопоставления индексов, полученных двумя различными способами, и детально излагаются способы сопоставлений.

GEOPHYSICAL TRANSACTIONS 1991
Vol 36. No. 3-4. pp. 321-331

SOME NUMERICAL TESTS OF *AS* METHOD FOR COMPUTER DERIVATION OF *K*-INDICES

Krzysztof NOWOZYNSKI, Tomasz ERNST, Jerzy JANKOWSKI*

A procedure is presented for determining *K*-indices simulating hand-scaling determination, with the help of which *K*-indices can be derived by computer calculation as well. It describes the tests of the adaptive smoothing (AS) method on 36 hour event data of Belsk Observatory for 5 different cases and supposes that the AS method can be applied without modification by observatories at different latitudes.

Keywords: AS-method, *K*-index

1. Introduction

During the last decade many algorithms have been developed for computer calculation of *K*-indices [e.g., RIDDICK and STUART 1984, JANKOWSKI et al. 1988, HATTINGH et al.,1989]. Many methods are used for this purpose, e.g., maximum-minimum method, linear detrending, mean S_q curve, harmonic synthesized S_q, natural orthogonal synthesized S_q, filter method, standard curve method.

The difficulty in the subtraction of the S_R part from the original data is the lack of a clear definition of S_R. In this paper the algorithm is shortly described. Some numerical tests are made using the Belsk Observatory data. The interested reader can find details of the algorithm in the paper: 'Adaptive smoothing method for computer derivation of *K*-indices' NOWOZYNSKI et al. [1990].

* Institute of Geophysics, Polish Academy of Sciences, Ks. Janusza 64. 01-452 Warsaw, Poland

2. Theory

For the determination of the K-indices it is necessary to remove the regular S_R part from the record. For the S_R estimation we do not use any physical assumptions. Our algorithm tries to simulate the hand-scaling procedure. The main features of the method are the following:

— least squares procedure is used,
— second derivatives are limited,
— weight factors are introduced.

Let us assume that the recordings are represented by a vector $\vec{x}$, composed of one-minute values. The output is a vector $\vec{y}$ estimating S_R.

We minimize the expression:

$$\min_{y_1,\dots,y_n} \left(\sum_{i=1}^{n} \lambda_i^2 (y_i - x_i)^2 + \sum_{i=2}^{n-1} \delta^2 \left(\frac{y_{i+1} - 2y_i + y_{i-1}}{h}\right)^2 \right) \tag{1}$$

where:
δ—smoothing coefficient,
$\vec{\lambda} = (\lambda_1,\dots,\lambda_n)$—weighting factors,
$\vec{x} = (x_1,\dots,x_n)$
$\vec{y} = (y_1,\dots,y_n)$
$h=1$, because the effect of h can be included in δ.

Using the matrix formulation we have:

$$\min_{y_1,\dots,y_n} \left\| \begin{array}{c} \\ \\ n \\ \\ \\ \\ \\ n-2 \\ \\ \end{array} \begin{bmatrix} \lambda_1 & & & & & \\ & \lambda_2 & & & & \\ & & \ddots & & & \\ & & & \ddots & & \\ & & & & \ddots & \\ & & & & & \lambda_n \\ 1 & -2 & 1 & & & \\ & 1 & -2 & 1 & & \\ & & & \ddots & & \\ & & & 1 & -2 & 1 \end{bmatrix} \begin{bmatrix} y_1 \\ y_2 \\ \vdots \\ y_n \end{bmatrix} - \begin{bmatrix} \lambda_1 x_1 \\ \lambda_2 x_2 \\ \vdots \\ \lambda_n x_n \\ 0 \\ \vdots \\ 0 \end{bmatrix} \right\|^2 \tag{2}$$

where:

$$\lambda_i^{'} = \frac{\lambda_i}{\delta}$$

The linear least squares method gives the system of normal equations:

$$(\Lambda^2 + D^T D)\vec{y} = \Lambda \vec{x} \tag{3}$$

where:

$$\Lambda = \begin{bmatrix} \lambda_1^{'} & & & \\ & \lambda_2^{'} & & \\ & & \cdots & \lambda_n^{'} \end{bmatrix} \qquad D = \begin{bmatrix} 1 & -2 & 1 & & & \\ & 1 & -2 & 1 & & \\ & & & \cdots & & \\ & & & 1 & -2 & 1 \end{bmatrix} \tag{4}$$

The smoothing coefficient δ is introduced to achieve a smooth curve to represent S_R. The weighting factors λ_i are introduced in order to make the influence of the quiet period larger than that of the disturbed one. Thus λ_i has to be inversely proportional to the variations. After numerical tests we decided to define λ_i in a very simple way as follows. The procedure has two steps: first $\lambda_i = 1$ for i = 1,... , 2160, and $\delta = \delta_1$. For the numerical calculation we used data series which represent one day extended by twelve hours added from neighbouring days. Solving (3) the vector $\vec{y}$ is calculated giving the first approximation of S_R. For every hour, differences between maximum and minimum values of $\vec{x} - \vec{y}$ are calculated, which we denote by V_j ($j = 1,...,36$).

In the second step the procedure is used once more with the weights defined as follows:

$$\lambda_i = \exp\left(1 - \frac{V_j}{M}\right) \tag{5}$$

where: $i = 60\,(j-1) + 1,...,60\,j \qquad j = 1,...,36$

Solving (3) with the new parameters and removing the new vector $\vec{y}$ from the data series $\vec{x}$ the final K-indices are obtained.

The free parameters δ, M must be determined individually for each observatory to achieve the best agreement with the hand-scaling method.

Because the procedure has two steps, and the weighting factors depend on the data, we call it Adaptive Smoothing (*AS*).

3. Results

We made the computations and compared the results with hand scaling data from the Belsk Observatory. The data for the whole year, beginning on March 1 1985, were used. At the beginning of the computation we normalized the data series for the Observatory to receive the upper limit of K-index equal to 500. In the normalized units the limit for $K = 3$ is 20. In our calculation we adopted for M one third of this value, because the same weights are defined for one hour ($M = 20/3$). The other parameter, δ, was established after some numerical tests. The value of these parameters for Belsk Observatory is $\delta = 10^{-6}$. To show how the procedure works we presents some figures. *Figure 1* illustrates the influence of the weights (lower part of the figures) on the S_R curve. One can see that after introducing weights the estimated S_R curve corresponds better to that used in hand scaling. The next two figures, *Figs. 2, 3*, show how S_R is eliminated from the horizontal components recorded at Belsk Observatory using different values of δ. Each figure displays the recorded horizontal components, S_R curves and the differences. The values of hand-scaled and computer generated K-indices are also included. The vertical scale is in normalized units, with their values given on the right side of the figures. The values of amplitudes used for determining K-indices are also presented. *Figures 4* and *5* show how S_R is eliminated using modified weights for the night period. We made this modification because some authors believe that during the night the S_R curve should be much smoother. We can achieve it in the AS method in a very simple way, by dividing the night's values by 10. The total agreement with hand scaled values was 82 %, and the percentage of the differences bigger than one unit was less than 0.3 %. In our calculation we have used one minute values for 36-hour events. The same algorithm can be used based on the 24-hour data series with an accuracy less than about 2 %.

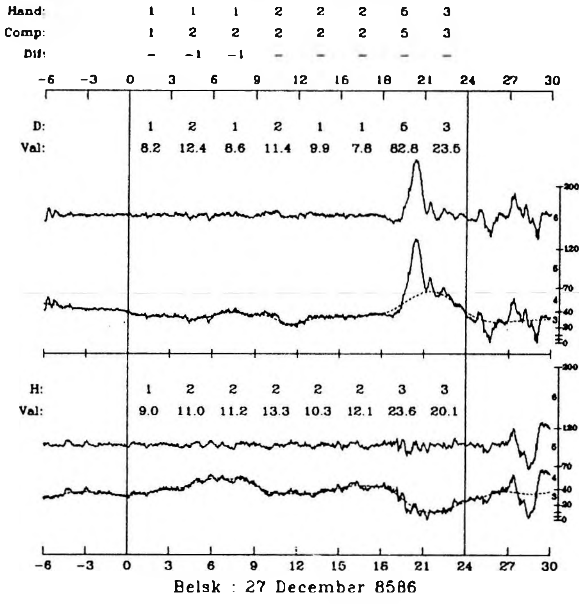

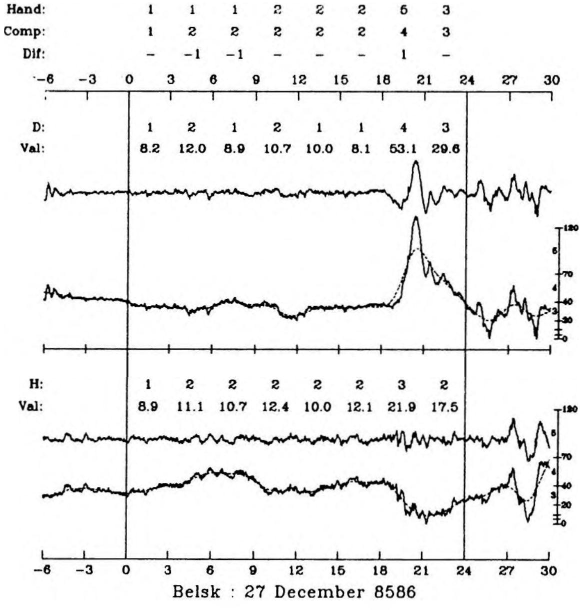

Fig. 1. Influence of the weights on S_R curve

1. ábra. Súlyfüggvény hatása az S_R görbére (ugyanazon szakasz fent súlyfüggvény nélkül, lent súlyfüggvénnyel)

Рис. 1. Влияние весовой функции на кривую S_R (тот же интервал, вверху — без весовой функции, внизу — с весовой функцией)

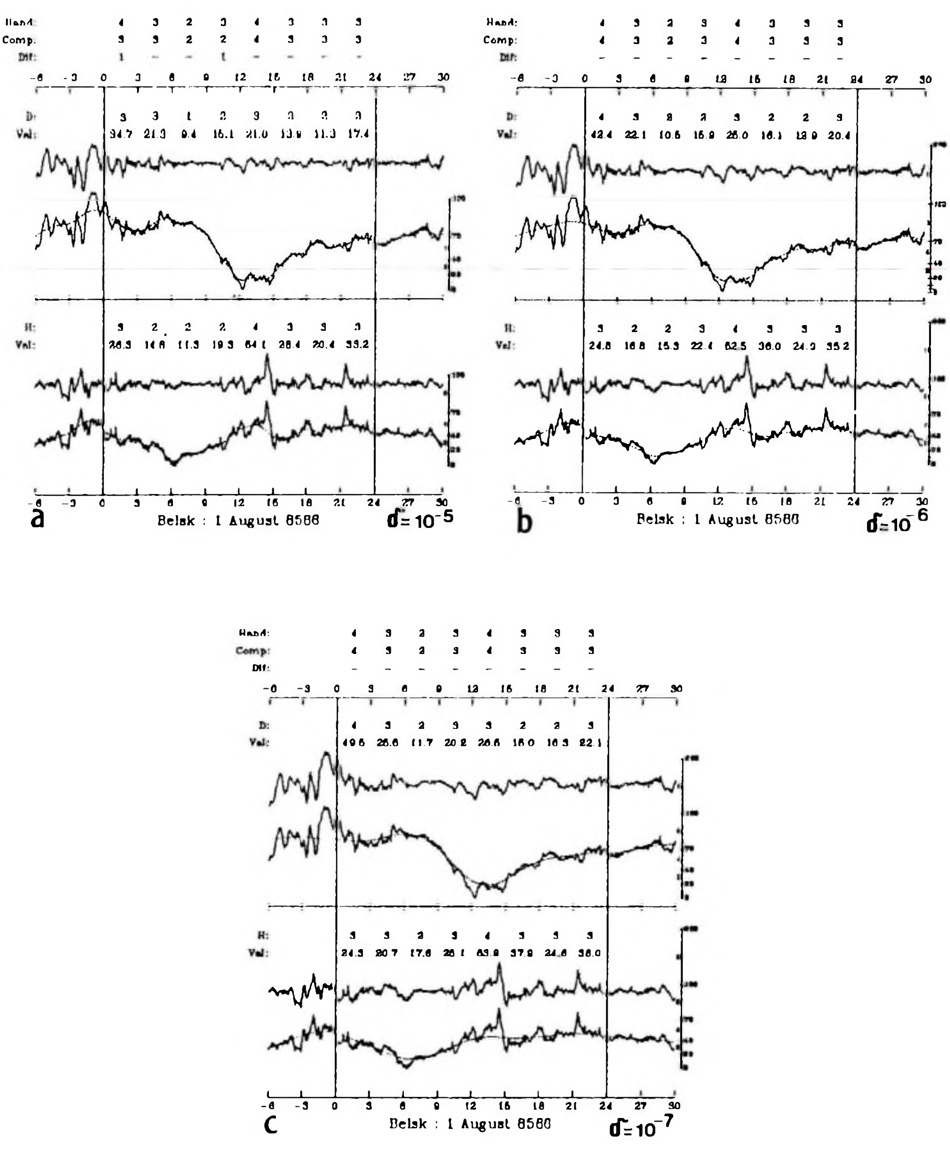

Fig. 2. Elimination of S_R from the horizontal components recorded at Belsk on 1th August using different values of δ.)

2. ábra. Különböző súlyfüggvények hatása az S_R görbe eliminálására a Belski Obszervatórium *H* görbéjén augusztus 1-én

Рис. 2 . Влияние различных весовых функций на элиминацию кривой S_R на кривой *H* Бельской обсерватории

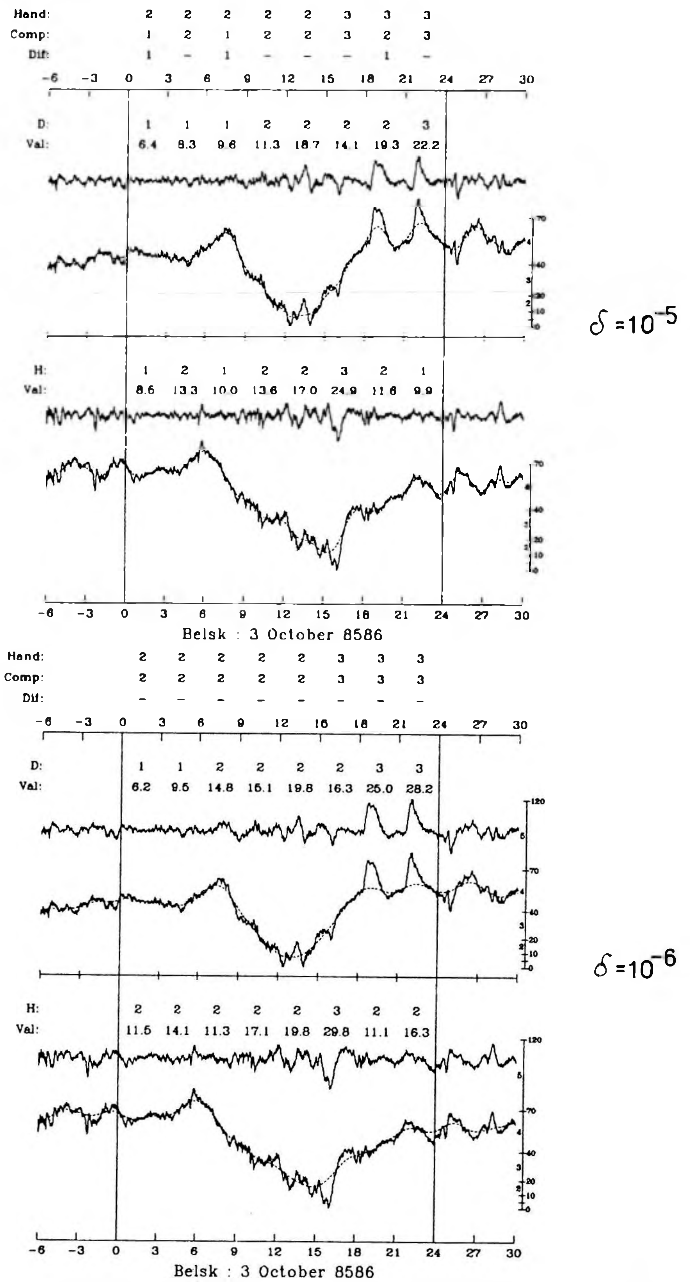

Fig. 3. Elimination of S_R from the horizontal components recorded at Belsk on 3rd October using different values of δ

3. ábra. Különböző súlyfüggvények hatása az S_R görbe eliminálására a Belski Obszervatórium *H* görbéjén október 3-án

Рис. 3. Влияние различных весовых функций на элиминацию кривой S_R на криво *H* Бельской обсерватории

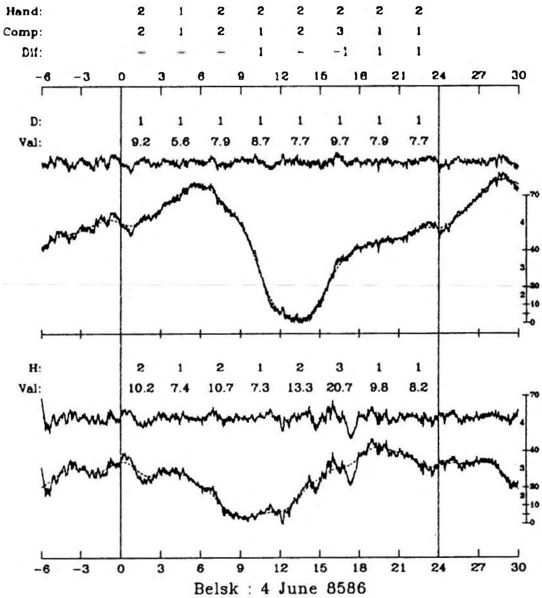

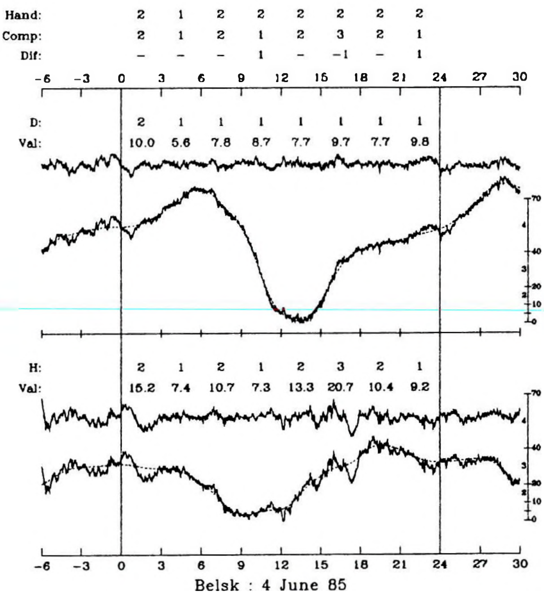

Fig. 4. Elimination of S_R using modified weights for the right period on 4th June

4. ábra. S_R eliminálása az éjszakai időszakra módosított súlyfüggvényekkel június 4-én

Рис. 4 . Элиминация S_R весовыми функциями, модифицированными для использования в ночное время

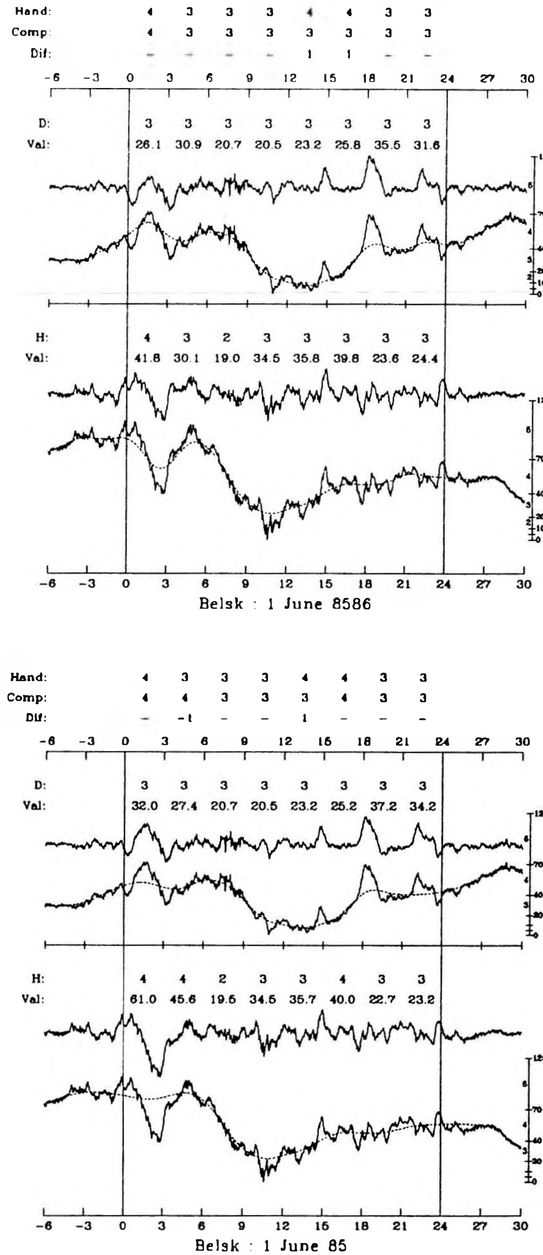

Fig. 5. Elimination of S_R using modified weights for the right period on 1st June

5. ábra. S_R eliminálása az éjszakai időszakra módosított súlyfüggvényekkel június 1-én

Рис. 5. Элиминация S_R весовыми функциями, модифицированными для использования в ночное время

4. Conclusions

The developed algorithm is based on statistical treatment of one-minute values of the horizontal components of the magnetic field without any physical criteria. It simulates the hand-scaling procedure well enough to give 82 % agreement. It is reasonable to believe that the developed method is suitable for all Observatories at different latitudes.

LITERATURE

HATTINGH M., LOUBSER L. and NAGTEGAAL D. 1989: Computer K-index estimation by a new linear-phase, robust, nonlinear smoothing method. Geophs. J. Int. **99**, pp. 533-547

JANKOWSKI J. A., ERNST T., SUCKSDORFF C., PIRJOLA R., RYNO J. 1988: Experiences of a filter method and a standard curve method for determining K-indices. Ann. Geophys. **6**, pp. 589-594

LOOMER E. I. 1984: Derivation of K-indices using magnetograms constructed from digital data. IAGA News. **22**, pp. 87-90

NOWOZYNSKI K., ERNST T., JANKOWSKI J. 1990: Adaptive smoothing method for computer derivation of K-indices. Geophys. J. Int. 103 (in press)

RIDDICK J. C. and STUART W. F. 1984: The generation of K-indices from digitally recorded magnetic data. Geophys. Surveys **6**, pp. 439-456

WALKER J. K. 1987: Adaptive separation of regular and irregular magnetic activity for K-indices. J. atmos terr. Phys. **49**, pp. 1017-1025

WILSON I. R. 1987: An evaluation of digitally derived K-indices. J. Geomagn. Geoelectr. **39**, pp. 97-109

AS ADAPTIV SIMÍTÁS MÓDSZERÉNEK ALKALMAZÁSA *K*-INDEXEK SZÁMITÓGÉPES ELŐÁLLITÁSÁBAN

Krzysztof NOWOZYNSKI, Tomasz ERNST, Jerzy JANKOWSKI

A szerzők a kézi K-index meghatározási eljárást szimuláló módszert ismertet, melynek segítségével az indexek gépi úton is meghatározhatók. Az adaptív simítás (AS) módszerének próbáját mutatja be a Belski Obszervatórium 36 órányi adatán 5 különböző

esetre és feltételezi, hogy az eljárás módosítás nélkül használható más különböző szélességi fokon elhelyezkedő obszervatóriumok esetében is.

ПРИМЕНЕНИЕ МЕТОДА АДАПТИВНОГО СГЛАЖИВАНИЯ В СОЗДАНИИ ИНДЕКСОВ К НА КОМПЪЮТЕРЕ

К. НОВОЗЫНСКИЙ, Т. ЕРНСТ, Й. ЙАНКОВСКИЙ

В статье излагается метод, симулирующий способ определения индексов *K* вручную, с помощью которого индексы могут быть определены и на компъютере. Представлено испытание метода адаптивного сглаживания (*AS*) по материалам Бельской обсерватории за 36 часов для 5 различных случаев, и предполагается, что данный способ может использоваться без изменений и в обсерваториях, расположенных на иных географических широтах.

GEOPHYSICAL TRANSACTIONS 1991
Vol. 36. No. 3-4. pp. 333-345

COMPUTER PRODUCTION OF *K*-INDICES BASED ON LINEAR ELIMINATION

C. SUCKSDORFF*, R. PIRJOLA* and L. HÄKKINEN*

The paper presents a method of computer production of *K*- indices that can be applied without modification for data sets in observatories at different latitudes and that can be run on PCs. It describes several results of the computations made by the 'FMI' method (method of linear elimination) for a one-year test period at different observatories. It is concluded that computer production of *K*-indices gives roughly the same agreement as can be expected from the differences between observers.

Keywords: *K*-index, linear elimination, magnetic observatory, FMI method

1. Introduction

In search for a method of computer production of *K*-indices [MAYAUD 1967, 1980] we have tried to follow the main criterion: The values produced have to be as close as possible to the hand-scaled *K*-indices.

Also the following requirements were kept in mind:

— The method should be valid at all times at a given observatory.

— The same method should be usable at different observatories, if possible without changing coefficients, which means that the same program is valid everywhere.

— Only a short time delay should be needed for the production of *K*-values, say about one day.

— The program should be simple enough to run on PC's.

— The program should be able to cope with small gaps in data.

* Geophysics Dept., Finnish Meteorological Institute, Box 503, SF-00101 Helsinki, Finland

An additional criterion having a practical value at high latitudes for the production of A_E indices might be the requirement for the correct shape of the S_R curve. The methods presented by JANKOWSKY et al. [1988] or GOLOVKOV et al. [1990] very closely fulfil this requirement. In the present paper, however, a common method suitable for all latitudes is sought for.

2. What can be expected from a machine *K*-method

To find out how well different experienced geomagneticians agree on scaling *K*-indices, we let two persons scale the same magnetograms which had previously been scaled by the observer in charge at the Nurmijärvi Observatory. The test months were June and July 1985. The test showed that the three observers agreed in slightly less than 80 % of the cases. No values differed by more than one unit. When comparing the results of the two new observers, their values agreed to 84 %.

We also studied how many values are so close to the borderline of two *K*-values that it is difficult to say which is the right one. A very small tilting of the scaling glass would make the difference. By putting a + sign after a lower choice, which could as well be a higher one, and a - sign after a higher choice, which could as well be the lower one, we could count as many as 8.5 % such cases. At low latitudes where limits for the different *K*-values are lower, the figure would probably be even higher than 8.5 %.

The conclusion from the percentages presented above is: the highest agreement to be expected between hand-scaled and computer-produced value is 91 %. If we accept the same level of agreement which experienced *K*-scaling can reach, the highest agreement between hand-scaled and machine production should be around 80 %. No values can be accepted to differ by more than one unit.

3. Method of linear elimination, the 'FMI Method'

The method developed at the Geophysics Department of the Finnish Meteorological Institute (FMI) is based on simple mean values of the observed one-minute or denser data. For each hour the mean is calculated from the data of that hour and of the data $m+n$ minutes outside both ends of the hour m is fixed for each three-hour period in local time so that during the day it is 0 minutes, from 3 to 6 and from 18 to 21 it is 60 minutes and during the local night 120 minutes. The time n depends on the magnetic activity so that $n = K^{3.3}$ minutes, where K is a preliminary value (see below). The value used for an hour in producing the S_R curve is the mean of all the datapoints inside the hour and $(m + n)$ minutes on both sides of the hour, which is the same as the middlepoint of a line fitted to the values in question.

The program is run in two steps. In the first step the preliminary K-values used for the calculation of n are simply determined from differences maximum minus minimum. The S_R curve is then produced by performing a 5^{th} degree harmonic fit to the middle points of each hour. In the second step the K-indices produced in the first run are used to determine n, and the final S_R curve is then produced by performing a 5^{th}-degree harmonic fit to the middle points of each hour now having slightly different values.

The program is applied to the test period of one year (March 1, 1985 - February 28, 1986) chosen by the IAGA Working Group V5, Magnetic Indices, for testing different methods of machine K-index production. The observatories used in the test are listed in *Table I.*

4. Results

The method described above is able to produce different kinds of S_R curves making them follow the original data points very closely or smoothing more. The smoothing can be regulated by changing the values of m and n. n varies by changing the exponent of K. If one chooses a higher degree in the Fourier analysis it also makes the S_R curve to follow the data points more closely. In this study we tried to find the values of n and m so that the same values could be used at all test observatories. It was easy to see that in the hand-scaling some observatories had followed the original recorded curve more closely than some others, so that by changing the constans it would have been possible to improve the agreement between hand-scaling and computer production of K-indices.

We believe, however, that the choice of the constants in the way we have done it produces S_R curves which are not very far from the right ones.

		lat.	long.	0	1	2	3	4	5	6	7	8	9
KGL	Kergueklen	-57.4	70.2		7.5	15	30	60	105	180	300	495	750
AIA	Argentine I.	-54.1	295.7		5	10	20	40	70	120	200	330	500
CZT	Crozet	-51.5	51.9		5	10	20	40	70	120	200	330	500
CAN	Canberra	-43.4	149.4		4.5	9	18	36	63	108	180	297	450
HER	Hermanus	-33.7	19.2		3	6	12	24	42	72	120	198	300
MMB	Memambetsu	+34.5	144.2		3.5	7	14	28	49	84	140	231	350
BEL	Belsk	+50.2	20.8		4.5	9	18	36	63	108	180	297	450
HAD	Hartland	+54.2	355.5		5	10	20	40	70	120	200	330	500
NEW	Newport	+55.2	242.9		7	14	28	56	98	168	280	462	700
OTT	Ottawa	+56.6	284.5		7.5	15	30	60	105	180	300	495	750
NUR	Nurmijärvi	+57.7	24.7		7.5	15	30	60	105	180	300	495	750
SOD	Sodankylä	+63.6	26.6		15	30	60	120	210	360	600	990	1500

Table I. Amplitude ranges for K-indices at the observatories used for testing computer-produced K-indices. The latitude is geomagnetic, the lonfitude geographic. K=9 as given by the observatories

I.Táblázat. K-index amplitudó tartományok a számítógéppel előállított K-indexek teszteléséhez használt obszervatóriumokra. A szélesség geomágneses szélesség, a hosszúság földrajzi. K=9 az obszervatóriumok által szolgáltatott adatok alapján

Табл. 1. Диапазоны амплитуд индексов K по обсерваториям, по которым выполнялась тестировка индексов K. Широта - геомагнитная, долгота - географическая. K=9, по данным, полученным от обсерваторий

So we have used for all observatories the constans given above (see Method of linear elimination, the 'FMI Method').

Figures 1-6 give some examples of S_R curves at different latitudes. *Figures 1* and *2* depicting the situation at Hartland during a disturbed and during a quiet day show how the S_R curves have almost similar shapes during both days. In the X component in the middle of the day the disturbance has slightly distorted the shape. However, this had no remarkable effect on the K-indices.

The same conclusion can be drawn from the curves of Memambetsu (*Figures 3* and *4*). Also here the shapes of the S_R curves remain roughly the same regardless the level of magnetic activity, although not as well as at Hartland. At both observatories the S_R curve is rather smooth during the

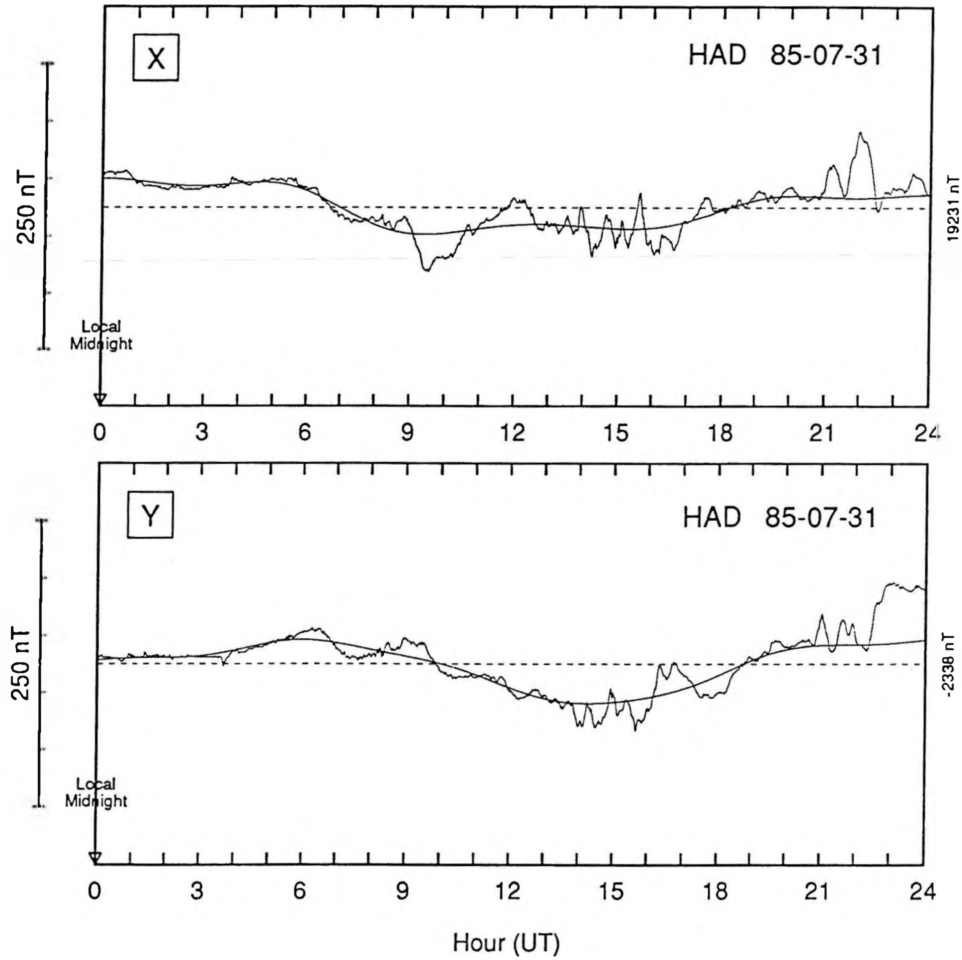

Fig. 1. Magnetograms and S_R curves at the middle-latitude observatory Hartland during a disturbed day

1. ábra. Magnetogramok és S_R görbék Hartland közepes szélességű obszervatóriumra háborgatott napon

Рис. 1. Магнитограммы и кривые S_R по обсерватории Хартланд в средних широтах в день с магнитными возмущениями

night, which shows that the smoothing procedure used, m=120 minutes during the local night, works as planned.

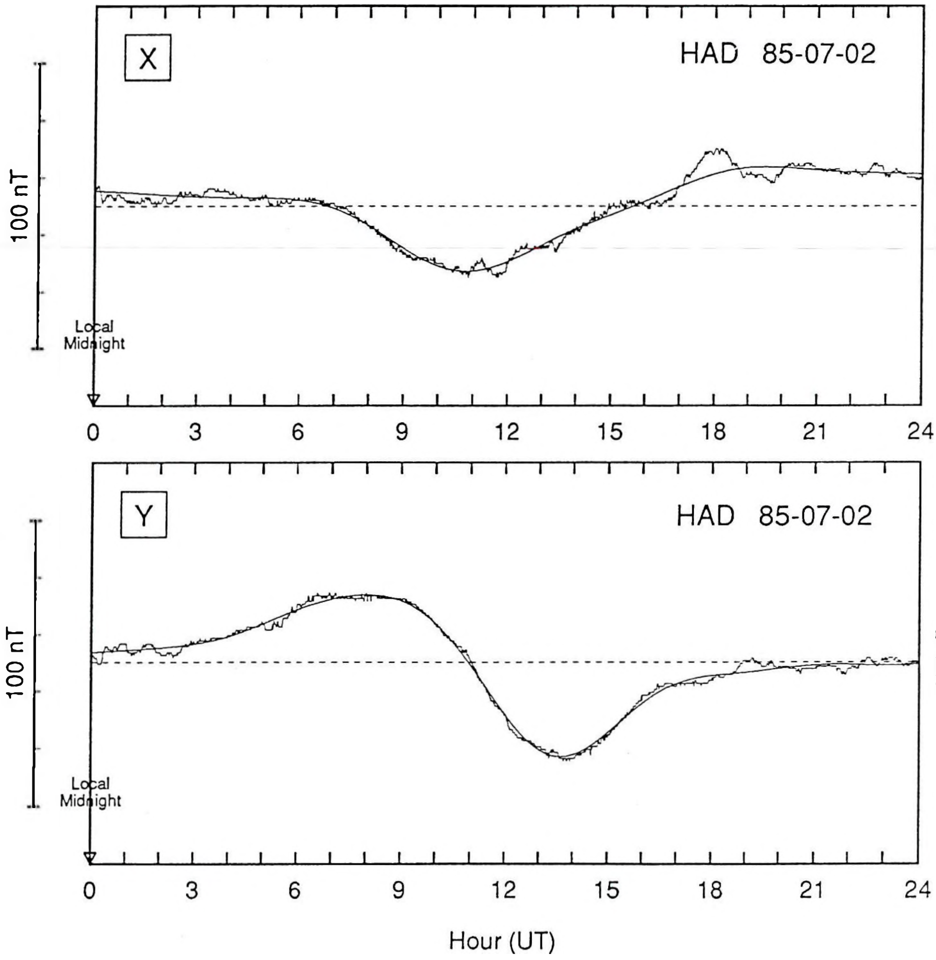

Fig. 2. Magnetograms and S_R curves at the middle-latitude observatory Hartland during a quiet day

2. ábra. Magnetogramok és S_R görbék Hartland közepes szélességű obszervatóriuma nyugodt napon

Рис. 2. Магнитограммы и кривые S_R по обсерватории Хартланд в средних широтах в спокойный день

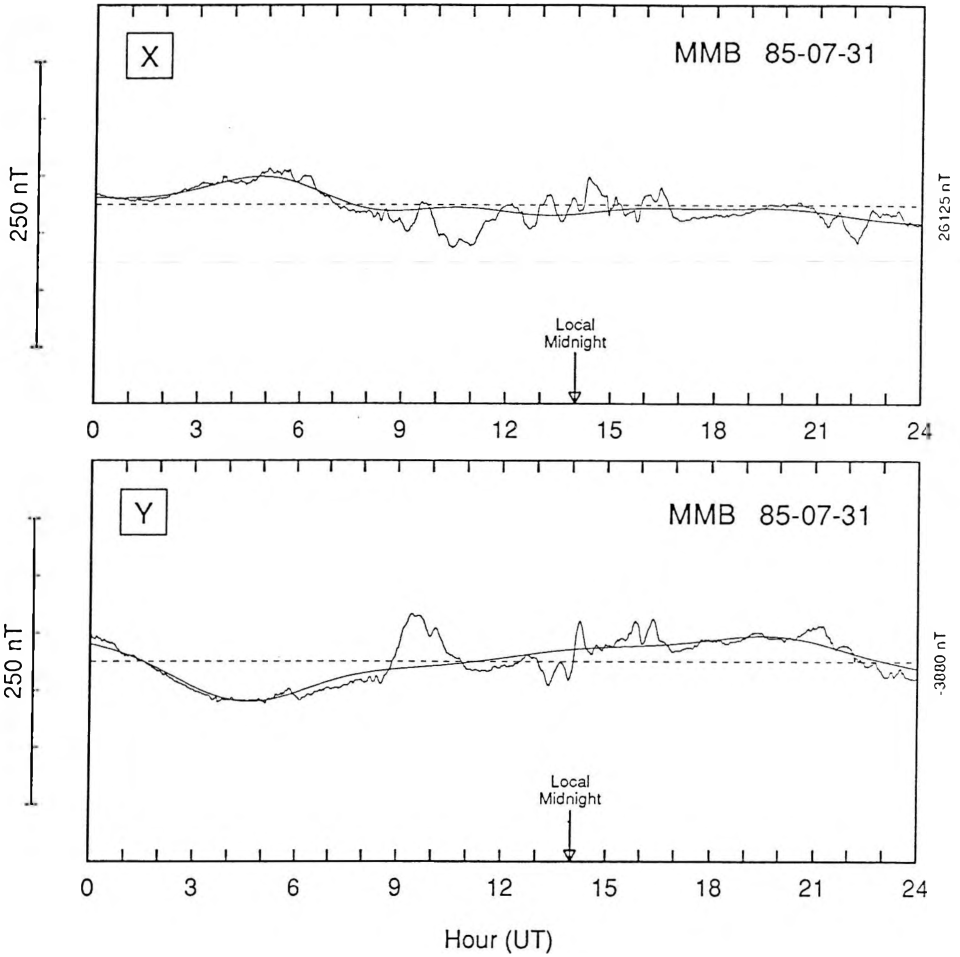

Fig. 3. Magnetograms and S_R curves at the low-latitude observatory Memambetsu during a disturbed day

3. ábra. Magnetogramok és S_R görbék Memambetsu alacsony szélességű obszervatóriumra háborgatott napon

Рис. 3. Магнитограммы и кривые SR по обсерватории Мемамбецу в низких широтах в день с магнитными возмущениями

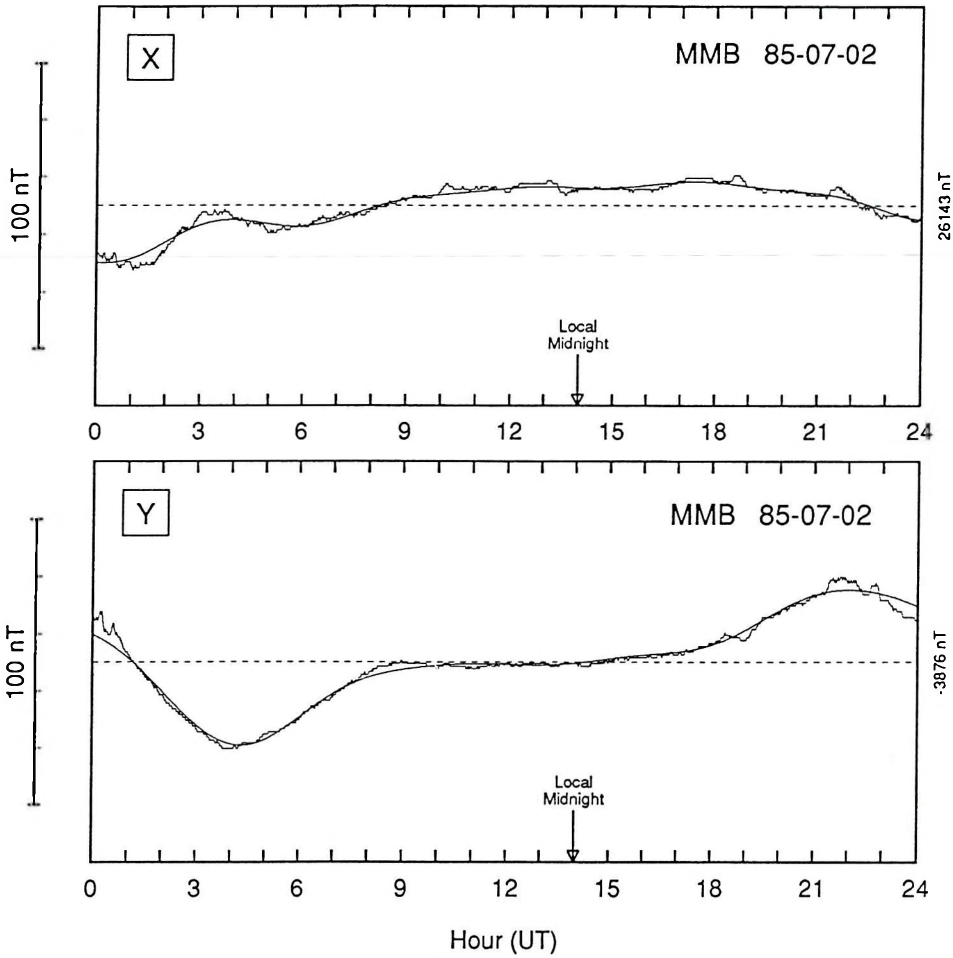

Fig. 4. Magnetograms and S_R curves at the low-latitude observatory Memambetsu during a quiet day

4. ábra. Magnetogramok és S_R görbék Memambetsu alacsony szélességű obszervatóriumra nyugodt napon

Рис. 4. Магнитограммы и кривые SR по обсерватории Мемамбецу в низких широтах в спокойный день

The situation is not as good at Sodankylä during disturbed periods, as can be seen from *Figures 5* and *6*. Here the same disturbed day and quite day as shown in Figures 1-4 for Hartland and Memambetsu are presented on a slightly smaller scale. In Sodankylä there are very often disturbances during the night, and in spite of the rather long line fitted to the disturbed night hours there seems to be some non-desired curvature in the S_R during that period. The day, July 31, is rather disturbed at Sodankylä as can be seen from the scale used (1000 nT compared to the 100 nT used for quiet days).

Figure 7. shows histograms of the differences between the hand-scaled and computer-produced *K*-values at all the test observatories in July 1985.

5. Conclusions

Looking at the histograms, it is obvious that at most high- and middle-latitude observatories this simple method gives roughly the same agreement as can be expected from the differences between two observers. A positive surprise is Memambetsu, a low-latitude observatory, where the agreement is very good — especially compared with Hermanus, another observatory at almost the same latitude. The difference between handscaled and computed values in Hermanus is highly asymmetric showing higher computed values. A higher K=9 limit would improve the situation, so would a higher Fourier degree, but not essentially.

Some details in the histograms reveal obvious differences in *K*-hand-scalings: NUR and OTT are somewhat asymmetric, but not to the same side in spite of nearly the same geomagnetic latitude. This means that in the hand-scaling at Nurmijärvi the curve has been followed more closely than the computer does, and the situation is opposite for Ottawa. The differences of -2 (2%) for Ottawa are rather surprising. The difference between BEL and CAN, which have the same K=9 limit, is also interesting and needs further study.

The S_R curves presented in Figures 1-6 show some clear defects in our method, although these defects do not influence the produced *K*-values very much because they appear during larger disturbances: during disturbances the produced S_R follows the curve too well. The same is true during the night, again with a minor effect on the value of the *K*-indices computed:

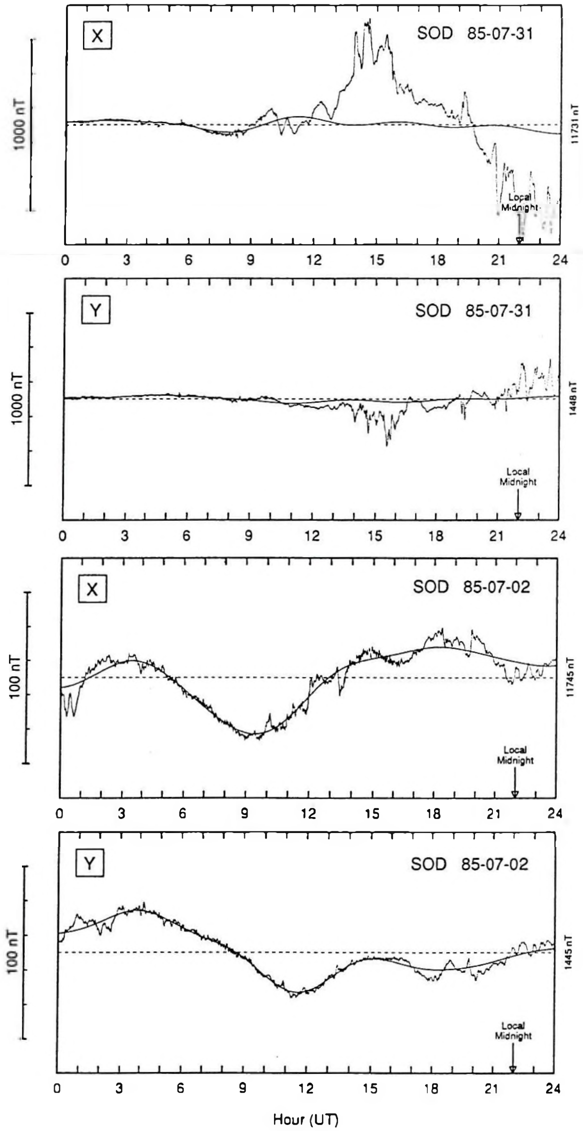

Figs. 5–6. Magnetograms and S_R curves at Sodankylä Observatory, which is situated at high latitude close to the auroral electrojet. Upper part: X and Y at a disturbed day. Lower part: X and Y at a quiet day

5., 6. ábra. Magnetogramok és S_R görbék a Sodankylä nagy szélességen fekvő obszervatóriumra, mely az aurora electrojet-hez közeli helyen van. A felső részben háborgatott napi X és Y, az alsó részben nyugodt napi X és Y van ábrázolva

Рис. 5 и *6.* Магнитограммы и кривые S_R по обсерватории Соданкыла в высоких широтах близ авроры электройет. Вверху- X и Y в день с магнитными возмущениями, внизу X и Y в спокойный день

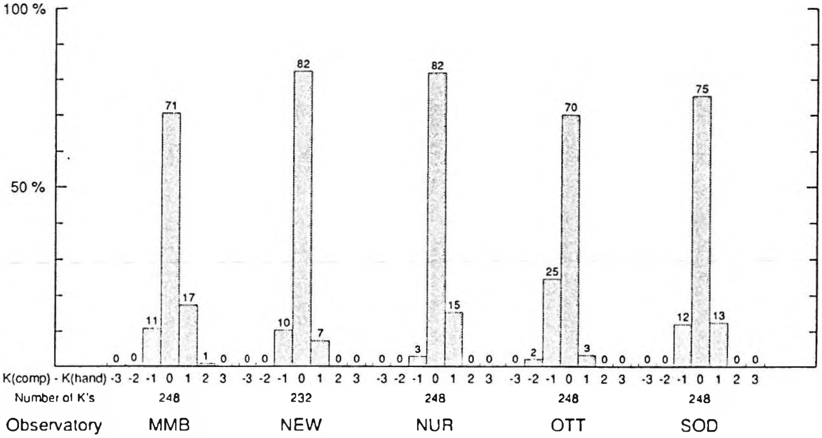

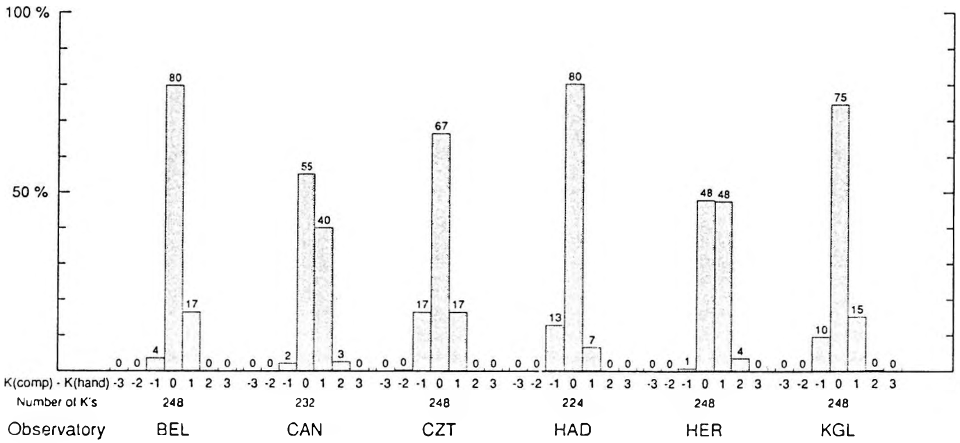

Fig. 7. Histograms for July 1985 of the differences between computed and hand-scaled *K* values at eleven test observatories

7. ábra. Géppel és kézzel számolt *K*- indexek közötti eltérések 1985 júliusára hisztogrammokon ábrázolva 11 teszt obszervatóriumra

Рис. 7. Расхождения между индексами K, рассчитанными вручную и на компьютере за июль 1985 г. в виде гистограмм по 11 обсерваториям, по которым была выполнена тестировка

The S_R curve produced is not in good agreement with the original definiton by BARTELS et al. [1939] if there are disturbances during the night. So this is one clear point where the method still needs development. The few stations showing poor results need closer examination, perhaps applying different methods. In any case, comparison of different methods with explanations of detected differences would be both interesting and useful for further developing the machine production of *K*-indices.

REFERENCES

BARTELS J., HECK N. H., JOHNSTON H. F. 1939: The three-hour-range index measuring geomagnetic activity. Terr. Magn. Atm. Electr. **44**. 411 p.

GOLOVKOV V. P., PAPITASHVILI V. O. and PAPITASHVILI N. E. 1990: Automated calculation of *K*-index using the method of natural orthogonal components. *in*: Proceedings of the international workshop on geomagnetic observatory data acquisition and processing, editors K. Kauristie, C. Sucksdorff and H. Nevanlinna. Finnish Meteorological Institute, Geophysical Publications **15**, pp. 128–135.

JANKOWSKI J. A., ERNST T., SUCKSDORFF C., PIRJOLA R. and RYNÖ J.,1988: Experiences of a filter method and a standard curve method for determining *K*-indices. Annales Geophysicae **6**, pp. 589-593

MAYAUD P. N. 1967: Atlas of Indices *K*. IAGA Bulletin No.21. 113 p.

MAYAUD P. N. 1980: Derivation, meaning and use of geomagnetic indices. Geophys. Monogr. **22**, 154 p., AGU, Washington DC.

LINEÁRIS ELIMINÁCIÓN ALAPULÓ SZÁMITÓGÉPES *K*-INDEX MEGHATÁROZÁS

C. SUCKSDORFF , R. PIRJOLA és L. HÄKKINEN

A szerzők olyan *K*-index előállítási eljárást ismertetnek, mely változtatás nélkül használható a különböző helyeken fekvő obszervatóriumok mérési adatsoraira és amely PC-vel elvégezhető. Bemutatják az 'FMI' módszerrel (lineáris elimináció módszere) egyéves tesztidőszakra és különböző obszervatóriumokra végzett számítások néhány eredményét. Megállapítják, hogy az eltérések a kézi módszerrel készített K-indexhez viszonyítva általában nem haladják meg a két kiértékelő által meghatározott értékek közötti különbséget.

СОЗДАНИЕ ИНДЕКСОВ К НА КОМПЪЮТЕРЕ В МЕТЕОРОЛОГИЧЕСКОМ ИНСТИТУТЕ ФИНЛЯНДИИ

Ц. СУКСДОРФ, Р. ПИРЙОЛА и Л. ХАККИНЕН

В статъе излагается способ создания индексов *K*, который без изменений может применяться к сериям данных, получаемым в обсерваториях различного географического положения, причем задача может быть выполнена на персональном компъютере. Представлены некоторые результаты расчетов по различным обсерваториям с применением метода 'FMI' (линейной элиминации) в течении годового периода тестировок. Делается вывод о том, что расхождения по сравнению с индексом *K*, полученным ручным способом, обычно не превышают таковые между значениями, полученными двумя разными интерпретаторами.

GEOPHYSICAL TRANSACTIONS 1991
Vol. 36. No. 3-4. pp. 347-353

SYNERGETIC ASPECTS OF GEOMAGNETIC INDICES

Zoltán VÖRÖS *

On the basis of nonlinear time series analysis new merits of the re/distribution of energy, information, mass and impulse are examined. Special emphasis is placed on the relationship between nonlinear macroscopic dynamics of the magnetosphere-ionosphere system and the new indices of geomagnetic activity.

Keywords: time series analysis, magnetosphere, ionosphere, geomagnetic indices

1. Introduction

The appearance of digital geomagnetic stations equipped with highly improved electronics opens new vistas for more precise and rapid data storage, exchange and processing. The expectations of both the observers and the users of geomagnetic data are basically common: new techniques perhaps allow us to determine 'classical' geomagnetic indices (e.g. K, D_{St}, AE etc.) in an up-to-date manner and in real time.

On the other hand the time is ripe for introducing new kinds of geomagnetic indices which correspond better to our recent knowledge about the solar wind — magnetosphere-ionosphere coupling and global, nonlinear dynamics. The essence of our nonlinear approach to this problem is based on the fact that the Earth's magnetosphere-ionosphere system is a macroscopic, nonlinear, open and dissipative system with a characteristic permanent ordered and/or turbulent state far from thermal equilibrium. As has been demonstrated by various authors turbulent and ordered structures (spatial, spatiotemporal as well as functional ones) arise from the same sort

* Geomagnetic Observatory, 947 01 Hurbanovo, CSFR

of nonlinear laws [HAKEN 1978, HAKEN 1983, GAPONOV-GREKHOV – RABINOVICH 1990]. So, nonlinear analysis is required if we want to find some measure which would characterize these nonlinear structures. Nowadays there already exists a theory of nonlinear pattern formation developed and denominated as synergetics by HAKEN [1978,1983]. Techniques for nonlinear, chaotic time series analysis are also widely used in other fields of science [ECKMANN — RUELLE 1985, RUELLE – TAKENS 1971]. These numerical methods render it possible to obtain new information about the nonlinear macroscopic magnetosphere and about the re/distribution of energy, information, mass and momentum within the magnetosphere-ionosphere system. So a close connection with the question of indices is given.

In this paper we propose three ways based on nonlinear analysis which enable us to drag more characteristic information out of a disturbed geomagnetic signal. We shall shortly discuss the 'new approach—new index' relationship.

2. Fractal analysis applied to *H*-component during geomagnetic storms

The Hausdorff-Besicovitch or fractal dimension D was introduced as a measure of both irregularity and self-similarity of a curve in the regular as well as in the statistical sense of the word [MANDELBROT 1982].

To measure the fractal dimension of geomagnetic storms we have applied the ruler method [VÖRÖS 1990]. This method uses dividers with a ruler of length ε_j , to measure along the continuous storm curve in a sequence of steps: The number of steps multiplied by the ruler length ε_j , yields the total measured length $L_i(\varepsilon_j)$. The relation of the divider size ε_j , to the measured length $L_i(\varepsilon_j)$ is given by

$$L_i(\varepsilon_j) = F\,\varepsilon_j^{1-D} \tag{1}$$

where D is the fractal dimension and F is a constant. We have analysed 15 geomagnetic storms (*H*-components recorded at the Hurbanovo Geomagnetic Observatory) and have computed the fractal dimensions of these curves using the method described (*Table I*) [VÖRÖS 1990].

No.	SSC						D ($\pm s.d.$)	K
	Start, UT			End, UT				
1	07.06.1972	13	10	19.06.1972	10	00	1.20 ±0.03	5.13
2	11.05.1980	01	36	12.05.1980	23	00	1.03±0.01	3.44
3	25.07.1980	11	11	27.07.1980	15	00	1.07±0.03	3.76
4	16.08.1980	12	42	18.08.1980	13	00	1.04±0.02	3.11
5	03.09.1980	13	35	04.09.1980	21	00	1.008±0.002	2.73
6	30.10.1980	15	19	01.11.1980	18	00	1.006±0.002	3.29
7	11.12.1980	10	06	12.12.1980	23	00	1.05±0.03	3.23
8	07.06.1981	17	48	08.06.1981	21	00	1.08±0.03	3.95
9	11.11.1981	12	40	12.11.1981	15	00	1.17±0.03	4.78
10	05.09.1982	22	48	08.09.1982	02	00	1.40±0.04	7.76
11	21.09.1982	03	40	23.09.1982	21	00	1.34±0.03	6.05
12	25.09.1982	20	29	28.09.1982	09	00	1.16±0.05	4.38
13	06.02.1986	13	10	09.02.1986	08	00	1.25±0.02	5.78
14	03.11.1986	23	55	05.11.1986	12	00	1.08±0.03	4.67
15	24.11.1986	09	20	26.11.1986	01	20	1.14±0.03	4.28

Table I. Fractal dimension and mean three-hour range K-indices for the given geomagnetic storms

I. Táblázat. A vizsgált geomágneses viharok három órás K-indexei és fraktális dimenziói

*Таблица I.*_ Фрактальные размерности и индексы K трехчасового порядка по данным геомагнитным бурям

We have shown that there are self-similar fractal curves. We made a comparison between the obtained fractal dimensions and the mean three-hour range K-indices (K) and found a linear dependence in the form:

$$D = 0.086\,K + 0.755 \qquad \text{for } K > 2.5 \qquad (2)$$

with correlation coefficient $r\,(D,K) = 0.95$.

3. The correlation dimension

Starting from the time series of a single, scalar variable ($H(t)$) we are able to reconstruct the corresponding phase space portrait in an m dimensional phase space using the time delay method [ECKMANN — RUELLE 1985, RUELLE — TAKENS 1971, GRASSBERGER — PROCACCIA 1983b].

A set of N points on the phase portrait (attractor A) is reconstructed as

$$H_{i,\, i=1\ldots N} = H(t_i), H(t_i+\tau), \ldots, H(t_i+(m-1)\,\tau)\,, \qquad H_i \in A \subset R^m \quad (3)$$

where τ is the time delay. More detailed discussion is to be found in [SIMM et al. 1987, VÖRÖS in press]. A suitable quantity which characterizes an attractor as a metric structure is its correlation dimension D_c, defined as in Ref. [GRASSBERGER — PROCCACIA 1983b].

$$C_m(r) = \lim_{\substack{K\to\infty \\ r\to 0}} \frac{1}{N_{ref}} \sum_{j=1}^{N_{ref}} \frac{1}{K} \sum_{i=1}^{K} \theta\,(\,r - \|\,H_i^{(m)} - H_j^{(m)}\|\,) = r^{D_c^{(m)}} \quad (4)$$

where N_{ref} - is the number of reference points,
θ - is the Heaviside step function,
$C_m(r)$ - is the correlation function in m dimensional phase space.
Then

$$\log D_c^{(m)} = \log C_m(r)/\log r\,. \quad (5)$$

If $\lim_{m\to\infty} D_c^{(m)} = D_c$ (finite) then the signal is deterministic or corresponds to the low dimensional coloured noise [LINHUA SHAN et al. 1991]. For a stochastic signal it holds that $D_c^{(m)} \to \infty$ for $m \to \infty$.

A finite correlation dimension for deterministic signals provides the minimum number of variables necessary for modelling the behaviour represented by an attractor in the phase space on a given time scale.

We have analysed a geomagnetic storm on the substorm time scale (0.5 - 1.5 h) from 13.3.1989 (Hurbanovo geom.data [PODSKLAN — BRUNNER unpubl.]). The correlation dimension obtained is: 2.3 ± 0.1. Physically the correlation dimension is a measure of the complexity of the internal dynamics of the magnetosphere-ionosphere system on the given time scale.

4. Entropy

When the dynamics of a system is represented by a low-dimensional attractor in the phase space, even erratic, chaotic motion is possible; this is known as deterministic chaos. In this case the attractor is chaotic, and the phase trajectories on the attractor are unstable in the sense of Lyapunov. Chaotic systems are characterized by at least one positive Lyapunov exponent λ_i [ECKMANN–RUELLE 1985, RUELLE — TAKENS 1971, GRASSBERGER — PROCACCIA 1983b, SIMM et al. 1987]. To estimate the sum of all positive exponents λ_i^+ we introduce the 2nd order Rényi entropy K_2 [GRASSBERGER — PROCACCIA 1983a], which can be estimated from the measured signal using the same type of correlation function as in Eq. (4)

$$K_2 = \lim_{m \to \infty} \lim_{r \to 0} \frac{1}{\tau} \ln \frac{C_m(r)}{C_{m+1}(r)} \tag{6}$$

The K_2 entropy has the following properties:

1. $K_2 \geq 0$,
2. $K_2 \leq \sum_i \lambda_i^+$,
3. K_2 is infinite for random systems,
4. $K_2 \neq 0$ for chaotic systems

So, $0 < K_2 << \infty$ is a sufficient condition for deterministic chaos.

We have computed the K_2 entropy for a geomagnetic storm. The obtained K_2 entropy is positive: 0.03 ± 0.01. It means that the observed geophysical phenomenon—geomagnetic storm on substorm time scale — should be described by non-linear systems in a 3 dimensional phase space which is capable of deterministic chaos.

5. Conclusions

The storm curve's fractal dimension can easily be extracted from geomagnetic data. The geometric self-similarity feature of field variations could perhaps be useful for the automatic digital treatment of observatory data. On the other hand the linear dependence of fractal dimensions on mean three-hour range K-indices ensures a continuity and some compatibility between the old and new indices.

The computation of the correlation dimension and K_2 entropy is much more problematic and computer-time consuming [for detailed information see VÖRÖS in prep.]. However, this kind of nonlinear analysis is a necessary condition for understanding the global dynamics of the magnetosphere-ionosphere system. We believe, the new geomagnetic indices should involve such information about the macroscopic, nonlinear system.

The description of global geomagnetic storm activity utilizing this point of view is still in its infancy and should be continued by further careful analysis. Our view is that on such a basis it will be possible to decide whether the language of chaotic attractors is relevant to observed macroscopic nonlinear dynamics and whether the dynamic invariants (dimensions, entropies, etc.) could serve as a new measure—index—for energy, information, mass, impulse re/distribution within the magnetosphere-ionosphere system.

Acknowledgements

The author expresses his thanks to the staff of Tihany Geophysical Observatory for wide-ranging support during the workshop, and to colleagues from the University of Iowa for allowing us to see their unpublished results .

In addition the author would like to express his appreciation to R. Szlizs (Galanta) for many fruitful discussions, and for help in editing and manuscript preparation.

REFERENCES

ECKMANN J. P., RUELLE D. 1985: Ergodic theory of chaos and strange attractors. Rev. Mod. Phys **57**, pp. 617-656

GAPONOV-GREKHOV A. V., RABINOVICH M. I. 1990: Disorder, dynamical chaos and structures. Physics Today July, pp. 30-38

GRASSBERGER P., PROCACCIA I. 1983a: Estimation of the Kolmogorv entropy from a chaotic signal. Phys. Rev. A **28**, pp. 2591-2593

GRASSBERGER P., PROCACCIA I. 1983b: Characterization of strange attractors. Phys. Rev. Letters **50**, pp. 346-349

HAKEN H. 1978: Synergetics. Berlin-Heidelberg-New York, Springer Verlag 371 p.

HAKEN H. 1983: Advanced Synergetics. Berlin-Heidelberg- New York, Springer Velag,

LINHUA SHAN, HANSEN P., GOERTZ C.K., SMITH R. A. 1991: Chaotic Appearance of the AE index. Geophys. Res. Lett. 18, pp 147 -163

MANDELBROT B. B. 1982: The fractal geometry of nature. Freeman, San Francisco, p.465

PODSKLAN J., BRUNNER J. 1989 unpublished mat.

RUELLE D., TAKENS F. 1971: On the nature of turbulence. Commun. Math. Phys. **20**, pp. 167-192

SIMM C. W., SAWLEY M. L., SKIFF F., POCHELON A. 1987: On the analysis of experimental signals for evidence of deterministic chaos. Helvetica Physica Acta **60**, pp. 510-597

VÖRÖS Z. 1990: Fractal analysis applied to some geomagnetic storms observed at the Hurbanovo geomagnetic observatory. Ann. Geophys. **8**, pp. 191-194

VÖRÖS Z. The magnetosphere as a nonlinear system. (In press)

K-INDEXEK ÉRTELMEZÉSE SINERGETIKUS SZEMPONTBÓL

VÖRÖS Zoltán

A szerző azt vizsgálja, hogy új matematikai módszerekkel, fraktál-analízissel, mágneses komponensek idősorának nonlineáris dinamikus elemzésével milyen fizikai ismeret-többletre tehetünk szert.

АНАЛИЗ ИНДЕКСОВ *К* С СИНЕРГЕТИЧЕСКОЙ ТОЧКИ ЗРЕНИЯ

З. ВЕРЕШ

Автором рассматриваются возможности увеличения физической информативности при введении новых математических методов, фрактального анализа и нелинейной динамической интерпретации временных рядов магнитных компонент.

APPENDIX

List of Participants

ABONYI Magda
Hungarian Astronautical Society
Fő u. 68. H-1027 Budapest , Hungary

ACZÉL Etelka
Eötvös Loránd Geophysical Institute of Hungary
P.O.B. 35. H-1440 Budapest, Hungary
Telephone : (36-1) 163 7256
Telex: 226194 elgi h   Fax: (36-1) 163 7256

ALEXANDRESCU Mioara
Inst. de Geologie si Geofizica
Strada Caransebes Nr.1. 78344 Bucuresti, Romania
Telephone : 657530

AUSTER JR Hans-Ulrich
Institut für Kosmosforschung Ber. 8. Rudower Chaussee 5 O-1199 Berlin, GERMANY
Telephone : 6745054
Telex : 11-3132 ife dd

AUSTER SR. Volker
Heinrich-Hertz-Institute, Observatorium Niemegk
Lindenstr. 7, O-1821 Niemegk, Germany
Telephone : 295
Telex : 157528

BAGDASAROVA N.Y.
Physics Instrumentation Centre of General Physics Inst. of USSR Academy of Sciences, Moscow region
SU-142092 Troitsk USSR
Telephone : 334 09 94

BELOV B. A.
IZMIRAN, Moscow region
SU-142092 Troitsk, USSR
Telephone : (7-95) 334-02-86
Telex : 412623 scstp su

BERGER Jozef
Central Institute for Meteorology and Geodynamics Department of Geophysics
P.O.Box 342. Hohe Warte 38. A-1191 Wien, Austria
Telephone : (43) 1364453/2502
Telex: 131837 a metw a Fax : (43) 1 364570

BICSKEI Tamás
Geomagnetski Institut
YU-11306 Grocka,Yugoslavia
Telephone : (38-11) 326767

BITTERLY Jacques
Institut de Physique du Globe de Strasbourg
5 rue René Descartes, 67084 Strasbourg Cedex France, France
Telephone : (33) 88416367
Telex: 890518 F Fax: (33) 88616747

BLAHA Jiri
Geofyzika s.p. Brno, dept. Praha
Geologická 2 15200 Praha, Czechoslovakia
Telephone : (42) 590619

BOURTEMBOURG Andre
Institute Royal Meteorologique Centre de Physique du Globe
B-6381 Dourbes, Belgique
Telephone : 060/399312
Fax : 060/399421

BRUNNER Juraj
Geomagnetic Observatory
CS-94701 Hurbanovo , Czechoslovakia
Telephone : (42) 818 2211

BURTSEV Yu. A.
IZMIRAN, Moscow region
SU-142092 Troitsk, USSR
Telephone : (7-095) 334-02-96
Telex: 412 623 scstp su

CANTIN Jean-Michel
Institut de Physiqe du Globe de Strasbourg
5 rue René Descartes, 67084 Strasbourg Cedex France ,France
Telephone : (33) 88416361
Telex : 890518 F Fax: (33) 88616747

COLES Richard
Geological Survey of Canada, Observatory Crescent
KIA 0Y3 Ottawa, Ont. Canada
Telephone : 1 613 995 5487
Telex: 053 3117 Fax: 1 613 952 9088

DEUTSCH Judit
Eötvös Loránd Geophysical Institute of Hungary
P.O.B. 35. H-1440 Budapest, Hungary
Telephone : (36-1) 163-7256
Telex : 226194 elgi h Fax: (36-1) 163-7256

DIANISKA László
Eötvös Loránd Geophysical Institute of Hungary
P.O.B. 35. H-1440 Budapest, Hungary
Telephone : (36-1) 163-7256
Telex : 226194 elgi h Fax : (36-1) 163-7256

ERNST Tomasz
Polish Academy of Sciences, Institute of Geophysics
Ks. Janusza 64. 01-452 Warsaw, Poland
Telephone : 361901 w 314

FARKAS László
Geophysical Observatory
Kossuth Lajos u. 91-93. H-8237 Tihany, Hungary
Telephone : (36-86) 48 501
Telex: 32294 geoty h

GILBERT Daniel
Institut de Physique du Globe de Paris, Department de Geomagnetisme
4 Place Jussieu F-67084 Paris Cedex 05, France
Telephone : (33) 144274927
Telex: 202810 Fax: (33) 144273373

GREEN Arthur W.
US Geological Survey
MS968 Box 25046 Federal Centre 80225 Denver , CO USA
Telephone : 303 236 1363
Telex: 5106014123 ESL UD Fax: 303 236 1519

HÄKKINEN Lasse
Finnish Meteorological Institute
P.O.B. 503. SF-00101 Helsinki, Finland
Telephone : (358) 0 1929508
Telex: 124436 EFKL SF Fax: (358) 0 1929539

HASKIC Alija
Geomagnetski Institut
YU-11306 Grocka , Yugoslavia
Telephone : (38-11) 326767
Fax: (38-11) 894151

HEGYMEGI László
Eötvös Loránd Geophysical Institute of Hungary
P.O.B. 35. H-1440 Budapest, Hungary
Telephone : (36-1) 163 7256
Telex: 226194 elgi h Fax : (36-1) 163 7256

HRVOIC Ivan
GEM Systems, Inc.
52W. Beaver Creek Road,14, L4B IL9 Richmond Hill, Ont. Canada
Telephone : (416) 764 8008
Telex: 06 964749 Fax: (416) 764 9329

IVANITZA A. I.
Physics Instrumentation Bureau of General Physics Inst., Moscow region
142092 Troitsk, USSR
Telephone : 334 02 06
Telex: 411074 - LIMEN SU.

JANSEN VAN BEEK Gerrit
Geophysics Division, Geological Survey of Canada
1 Observatory Crescent K1A OY3 Ottawa, Ont. Canada
Telephone : 613 995 5457
Telex : 0533117 Fax: 613 952 9088

JOVANOVIC Prvoslav
Geomagnetski Institut
YU-11306 Grocka, Yugoslavia
Telephone : (38-11) 326767

KISS János
Geomagnetic Observatory
CS-97401 Hurbanovo , Czechoslovakia
Telephone : (42) 818 2211

KNIJZEV V.N.
Physics Instrumentation Bureau of General Physics Inst., Moscow region
142092 Troitsk, USSR

Telephone : 334 02 14
Telex: 411074 limen su

KOLESNIC B. E.
Physics Instrumentation Bureau of General Physics Inst., Moscow region
142092 Troitsk, USSR
Telephone : 334 09 94
Telex: 411074 limen su

KÖRMENDI Alpár
Geophysical Observatory
Kossuth Lajos u. 91-93. H-8237 Tihany, Hungary
Telephone : (36-86) 48-501
Telex: 32294 geoty h

KÖVESI Gábor
Eötvös Loránd Geophysical Institute of Hungary
P.O.B. 35. H-1440 Budapest, Hungary
Telephone : (36-1) 163 7256
Telex: 226194 elgi h Fax: (36-1) 163 7256

KULTIMA Johannes
Geophysical Observatory
SF-99600 Sodankyla, Finland
Telephone : (358-693) 12228/26
Fax : (358-693) 14158

LALANNE Francois-Xavier
Institut de Physique du Globe de Paris, Department de Geomagnetisme
4 Place Jussieu F-75252 Paris Cedex 05, France
Telephone : (33) 1 44274927
Telex: 202810 Fax: (33) 1 44273373

LICHOPOJ Alexander
Heinrich-Hertz-Institute, Observatorium Niemegk
Lindenstr. 7. O-1824 Niemegk , Germany
Telephone : 295
Telex: 157528

MARIANIUK Janusz
Polish Academy of Sciences, Institute of Geophysics
Pl-05-622 Belsk, Poland
Telephone : 364764
Telex: 817582 pl

MELICHAR Peter
Central Institute for Meteorology and Geodynamics, Departement of Geophysics
P.O.Box 342. Hohe Warte 38. A-1191 Wien, Austria
Telephone : (43) 1364453/2502
Telex: 131837 a metw a   Fax: (43) 1364570

MENVIELLE Michel
Institut de Physique du Globe de Paris, Department de Geomagnetisme
4 Place Jussieu F-75252 Paris Cedex 05, France
Telephone : (33) 1 44 274935
Telex: 202810   Fax: (33) 1 44 273373

PAJUNPAA Kari
Finnish Meteorological Inst. Nurmijärvi Geophysical Observatory
SF-05100 Röykka ,Finland
Telephone : 3580 2765820
Telex: 124436 EFKL SF   Fax: 3580 2765820

PALANGIO Paolo
Instituto Nazionale di Geofisica Via di Villa Ricotti, 42
I-00161 Roma, Italy
Telephone : (39) 6 4210200
Telex: 620246-625335   Fax : (39) 6 429040

PAPITASHVILI V. O.
IZMIRAN, Moscow Region
SU-142092 Troitsk , USSR
Telephone : (7-095) 334 02 86
Telex: 412623 scstp su

PETERSEN Jan Raagaard
Department of Electrophysics, Techn. Univ. Dan.
Building 322, DK-2800 Lungbyvej, Denmark
Telephone : 45 42881188
Telex: 37529 OTHOIA DK   Fax : 45 42882239

PODSKLAN Jozef
Geomagnetic Observatory
CS-97401 Hurbanovo, Czechoslovakia
Telephone : (42) 818 2211

PRIHODA Karel
Geofyzika s. p. Brno, dept. Praha
Geologická 2, 15200 Praha, Czechoslovakia
Telephone : (42) 59 06 19

RASMUSSEN Ole
Danish Meteorological Institute
Lyngbyvej 100, DK-2100 Copenhagen, Denmark
Telephone : (45) 31 292100
Fax: (45) 31 293400

RASSON Jean
Royal Meteorological Ins. Centre de Physique du Globe
B-6381 Dourbes, Belgique
Telephone : 060/399 312
Telex: 51239 / GEOPHY Fax: 060/399 421

REDA Jan
Obserwatorium Geofizyczne
PL-05-622 Belsk, Poland

REZNIKOV A. E
IZMIRAN, Moscow region
SU-142092 Troitsk, USSR
Telephone : (7-095) 334-01-21
Telex: 412623 scstp su

SÁRHIDAI Attila
Eötvös Loránd Geophysical Institute of Hungary
P.O.B. 35. H-1440 Budapest, Hungary
Telephone : (36-1) 163 7256
Telex: 226194 elgi h Fax: (36-1) 163 7256

SCHULZ Günter
Erdmagnetisches Observatorium Am Olymp 13
D-2177 Wingst, Germany
Telephone : 4778/306

STOMFAI Róbert
Eötvös Loránd Geophysical Institute of Hungary
P.O.B. 35. H-1440 Budapest, Hungary
Telephone : (36-1) 163-7256
Telex: 226194 elgi h Fax: (36-1) 163-7256

SUCKSDORFF Christian
GEO/Finnish Meteorological Institute
P.O.Box-503 SF-00101 Helsinki, Finland
Telephone : (3580) 19 291
Telex: 12 44 36 EFKL Fax: (3580) 1929539

SZABÓ Zoltán
Eötvös Loránd Geophysical Institute
Columbus utca 17-23. H-1145 Budapest, Hungary
Telephone : (36-1) 25-24-999
Telex: 226194 elgi h Fax: (36-1) 163-7256

TOSHKOV A. Dimitrov
Geophysical Institute, Bulgarian Academy of Sciences
Acad. G. Bontchev str. Bl. 3., 1113 Sofia, Bulgaria
Telephone : 3592 700 128
Telex: 22632 Fax: 3592 700 226

VÁCZY Magdolna
Geomagnetic Observatory
CS-94701 Hurbanovo, Czechoslovakia
Telephone : (42) 818 2211

VERŐ József
Geodetic and Geophysical Research Inst.
Múzeum u. 6-8. H-9400 Sopron, Hungary
Telephone : (36-99) 14290
Telex : 127445

WESZTERGOM Viktor
Geodetic and Geophysical Research Inst.
Múzeum u 6-8. H-9400 Sopron, Hungary
Telephone : (36-99) 14290
Telex: 127445

VÕRÖS Zoltán
Geomagnetic Observatory
CS-97401 Hurbanovo, Czechoslovakia
Telephone : (42) 818 2211

WALLNER Ákos
Geodetic and Geophysical Research Inst.
Múzeum u 6-8. H-9400 Sopron, Hungary
Telephone : (36-99) 14290
Telex: 127445

ZAROUTSKIJ A.A.
Physics Instrumentation Bureau of General Physics Inst., Moscow region
SU-142092 Troitsk, USSR
Telephone : 334 02 06
Telex: 411074 limen su

The proven technology to help you reduce risk and increase your success rate – worldwide.

HGS

Halliburton Geophysical Services

6909 Southwest Freeway Houston, TX 77074 Ph: (713) 774-7561 FAX: (713) 778-3487/Telex: 76-2781

A Halliburton Company


Strike oil
by advertising
with us

This page is waiting for you!